Studies of post-Golgi syntaxins in GLUT4 trafficking of 3T3-L1 adipocytes

A thesis submitted to the
FACULTY OF BIOMEDICAL AND LIFE SCIENCES

For the degree of
DOCTOR OF PHILOSOPHY

By
Handunge Kumudu Irani Perera

Department of Biochemistry and Molecular Biology
University of Glasgow

November 2002

Abstract

Insulin stimulates glucose transport in fat and muscle tissues by increasing the translocation of the glucose transporter 4 (GLUT4) from intracellular storage compartments to the plasma membrane. In the basal state, GLUT4 is sequestered away from the constitutively recycling endosomal pathway into a specialised GLUT4 storage vesicle compartment (GSV). This sequestration is at the heart of the ability of insulin to increase plasma membrane GLUT4 levels by such large magnitudes. Studies have shown that the SNARE proteins syntaxin (STX) 4, VAMP2 and SNAP-23 mediate the fusion of GLUT4-containing vesicles with the plasma membrane. However, there are no reported studies of the role of SNAREs in intracellular GLUT4 trafficking pathway. The aim of this work was to characterise and identify the role of post-Golgi syntaxins in GLUT4 trafficking in 3T3-L1 adipocytes.

As the first step towards understanding post-Golgi syntaxins in GLUT4 trafficking, the extent of colocalisation of STX 6, 8, 12 and 16 with GLUT4 was determined. The results showed that STX 6 and STX 16 are extensively localised in immuno-purified GLUT4 vesicles and that they translocate to the plasma membrane in response to insulin, resulting in a large increase similar to GLUT4. Iodixanol gradient analysis showed that both STX 6 and 16 are present in the two major pools of intracellular GLUT4, GSV and endosomal/TGN pool. In contrast, STX 8 and 12 are localised in GLUT4 vesicles into a significantly lesser degree. Endosomal ablation studies demonstrated that about 50% of the STX 6, 8 and 12 are present in the early or recycling endosomal compartment. Furthermore, *in vivo* immunoprecipitation studies showed that STX 16 is a SNARE partner of STX 6 in 3T3-L1 adipocytes.

Recombinant adenovirus (AdV) over-expressing the cytosolic domains of STX 6, 8 and 12 were produced in order to study the function of these syntaxins in 3T3-L1 adipocytes. Overexpression of the STX 6 cytosolic domain significantly slowed down the resequestration of GLUT4 into intracellular compartments after insulin withdrawal. Furthermore, iodixanol gradient analysis revealed that STX 6 function is required to deliver GLUT4 into the GSV during this process. By contrast, expression of STX 8 and 12 cytosolic domains had no effect on the trafficking events examined.

The findings of this study strongly suggest that STX 6 is involved in trafficking of GLUT4 from the recycling pathway to the GSVs. Further studies are required to identify the precise intracellular location where STX 6 functions to move GLUT4 into the GSV, and to identify the other SNARE proteins involved. Data of this study suggests that STX 16 could be the Qa-SNARE of this event.

Experiments were performed to understand the biogenesis of the GSV in 3T3-L1 cells. The data suggests that an insulin-responsive compartment which sequesters insulin responsive aminopeptidase, exists by day 4 post-differentiation of 3T3-L1 fibroblasts into adipocytes. The expression pattern of syntaxins during differentiation showed that STX 6 expression followed a very similar pattern to GLUT4.

Declaration

I declare that the work described in this thesis has been carried out by myself unless otherwise cited or acknowledged. It is entirely of my own composition and has not, in whole or in part, been submitted for any other degree.

..

Handunge Kumudu Irani Perera

November 2002

Dedication

To my ever loving father and mother who have educated me,
To my beloved husband, for his patience and support,
and
To my darling sons Varuna and Yasiru who enriched
my family with love and happiness

Acknowledgements

First and foremost I would like to thank my supervisor Prof. Gwyn Gould for all his support throughout my Ph.D. work, helpful discussions and comments on the thesis and being always there whenever I needed advice. I have learned a lot during the stay in his lab. I am grateful to the Association of Commonwealth Universities, UK and the British Council for funding my studies and the stay in UK.

Many thanks to all the present and past members of Gould lab members for always being nice and helpful. I would like to thank specially to Drs. Luke Chamberlain, Ian Salt, Declan James and Gilles Hickson for their support and advice with various aspects of the work presented in this thesis and to Ms Claire Millar for technical support. I wish to thank Drs. Tim Palmer, Billy Sands and Andy Baker for their advice and support on adenoviral work.

My deepest thanks go to my parents for all their support and encouragement over the years. Most importantly a very big thank to my husband Vajira for his patience, support and encouragement.

Table of contents

List of Tables and Figures

Tables

Figures

Chapter 1

Chapter 3

Abbreviations

AdV	Adenovirus
CCVs	Clathrin-coated vesicles
EE	Early endosomes
GLUT	Glucose transporter
GSV	GLUT4 storage vesicles
HDM	High-density microsomes
IRAP	Insulin responsive aminopeptidase
LDL	Low-density lipoprotein
LDM	Low-density microsomes
LE	Late endosomes
M6PR	Mannose 6 phosphate receptor
PM	Plasma membrane
RE	Recycling endosomes
SDS-PAGE	Sodium dodecyl sulphate-polyacrylamide gel electrophoresis
SNAP-25	Synaptosomal-associated protein of 25 kD
SNARE	Soluble *N*-ethylmaleimide attachment protein receptor
STX	Syntaxin
TfR	Transferrin receptor
TGN	*trans*-Golgi network
TM	Transmembrane
VAMP	Vesicle associated membrane protein

Chapter 1

Introduction

1 Introduction

1.1 Glucose transport in mammalian cells

Glucose transport into mammalian cells is of fundamental importance, as glucose is the main energy source in most tissues and is the sole source of energy in some cells such as red blood cells. Transport of glucose across membranes is mediated by two distinct families of glucose transporters. The family of facilitative glucose transporters transport glucose down a concentration gradient and do not use energy. The other family is the Na^+ dependent glucose transporters (Bell *et al.*, 1993), which move glucose into cells against a concentration gradient using a Na^+ gradient to energise transport (e.g. intestinal mucosal cells, renal epithelial cells). This latter family is not discussed here.

Facilitated transport of glucose is mediated by a family of highly related glucose transporters (GLUTs). In addition to providing glucose to cells they have a role in blood glucose homeostasis. Thirteen members of the GLUT family have been identified to date, however only four GLUTs (GLUT1, 2, 3 and 4) are described and documented to function as authentic glucose transporters (Pessin *et al.*, 1999). GLUTs 5, 7, 9 and 11 are fructose transporters. GLUTs 6, 8, 10,12 and HMIT 1 (H^+/myo-inositol co-transporter) are structurally atypical and are poorly defined at present (reviewed in Bryant *et al.*, 2002; Joost *et al.*, 2002). The overall structure and sequence of these GLUTs are broadly similar.

GLUTs are integral proteins with 12 predicted amphipathic helices spanning the membrane (Figure 1.1). The human isoforms are about 500 amino acids in length, with both the N- and C-termini of the protein being cytosolic. About 50% of the protein is transmembrane which is highly conserved within the family (Lachaal *et al.*, 1996). Isoform-specific amino acid sequences are located almost exclusively at the cytoplasmic and exoplasmic domains of GLUTs, which might mediate tissue-specific functions (Lachaal *et al.*, 1996). There are large connecting loops between helices 1 and 2 and 6 and 7 and the latter divides the GLUT structure into two halves (reviewed in Gould and Holman, 1993). All the GLUTs are post-translationally glycosylated on an asparagine residue of the exofacial loop between helices 1 and 2. It is suggested that the 12 helices accommodate an aqueous channel for glucose movement and

provide hydroxyl and amide hydrogens for hydrogen bond formation with glucose (Lachaal *et al.*, 1996). The binding of glucose induces a conformational change(s) in the transporter that results in the movement of the glucose through the aqueous channel and subsequent release on the other side of the membrane (Barrett *et al.*, 1999).

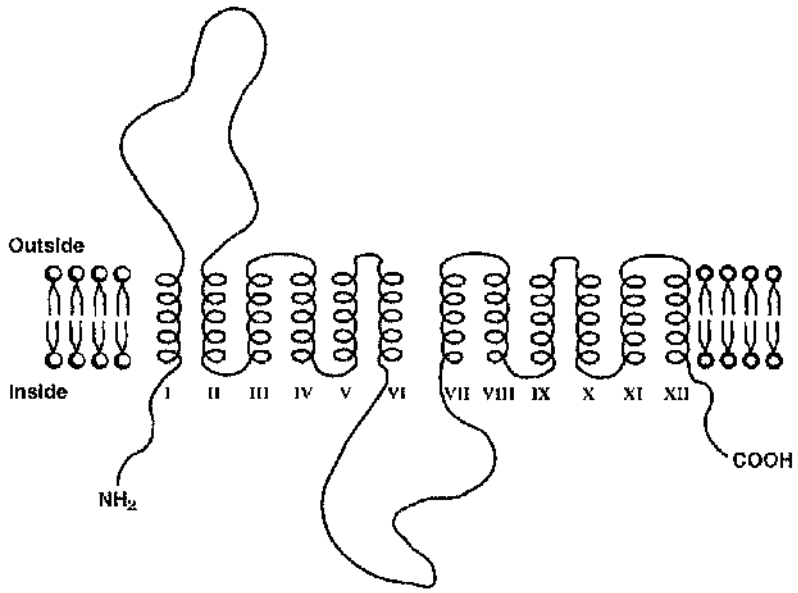

Figure 1.1 Structure of the glucose transporter (adapted from Barrett *et al.*, 1999)

The figure depicts the proposed organisation of glucose transporter structure. The structure of all the glucose transporters is thought to consist of 12 transmembrane helices with cytosolic N- and C-termini. Helices 1 and 2, and 6 and 7 are connected by large loops. See text for details.

Each of the glucose transporters is derived from a separate gene. They differ in their tissue distribution and kinetic properties, which have specific functions in maintaining glucose homeostasis. GLUT1 is expressed in many tissues with a high expression in brain and red blood cells. GLUT1 facilitates basal glucose transport and its relatively low K_m value enables cells to take up glucose even at low blood glucose concentrations (Gould, 1997). GLUT2 is predominantly expressed in liver, intestine, kidney and pancreatic β-cells. It is a low affinity isoform with a high capacity, which

allows glucose uptake at high blood glucose concentrations (e.g. in the post absorptive state) (Gould, 1997). GLUT3 facilitates glucose transport in brain and neurons. The K_m value of GLUT3 is lower than that of GLUT1 and thus ensures glucose uptake into neuronal tissues under hypoglycaemic conditions (Gould, 1997). Virtually all GLUT isoforms other than GLUT4 constitutively reside at the PM to optimise the transport of extracellular glucose into the cell. GLUT4 is primarily expressed in insulin-sensitive tissues, adipose tissue, skeletal muscle and cardiac muscle and is responsible for increased glucose uptake into these tissues under insulin-stimulation (reviewed in Gould and Holman, 1993; Gould, 1997). GLUT4 is the transporter which is studied in this thesis.

1.2 GLUT4

In 1980, two independent groups reported that insulin stimulates the movement of a GLUT in rat adipocytes into the plasma membrane (PM) from an intracellular site (Suzuki and Kono, 1980; Cushman and Wardzala, 1980). The suggestion that insulin-responsive tissues such as fat and muscle express a distinct GLUT isoform led to cloning and sequencing of GLUT4 in 1989 (Garcia and Birnbaum, 1989; Charron *et al.*, 1989; Kaestner *et al.*, 1989; James *et al.*, 1989). GLUT4 is the major glucose transporter in insulin sensitive tissues (fat and muscle). It is unique among the GLUTs due to its ability to remain localised extensively in intracellular vesicles in the absence of insulin and its 10 to 40-fold increase at the PM in response to insulin. Among the diverse actions of insulin, one of its most important functions is glucose homeostasis. Insulin facilitates glucose uptake into muscle and adipose tissue via translocation of GLUT4 from an intracellular store to the cell surface. Several observations have indicated that GLUT4 has a crucial role in glucose homeostasis in the body. These include severe disruption of insulin-stimulated glucose transport in both fat and muscle tissues in non-insulin dependent diabetes mellitus (NIDDM), development of insulin resistance in mice upon disruption of GLUT4 expression and improvement of glucose tolerance in db/db mice with diabetes upon overexpression of GLUT4 (reviewed in Bryant *et al.*, 2002).

1.3 Intracellular GLUT4 compartments

Several studies have attempted to understand the intracellular location of GLUT4 as this may hold the key to its intense responsiveness to insulin. Morphological studies have been made difficult due to the compressed nature of the cytoplasm of fat and muscle cells due to presence of either lipid droplets or myofibrils. Despite these difficulties many studies have provided information on the sites of the intracellular storage of GLUT4 using immunoelectron microscopy, and subcellular fractionation with subsequent immunoblotting (Slot *et al.*, 1991b; Malide *et al.*, 2000; Martin *et al.*, 2000a). These findings were supported by three-dimensional electron microscopic imaging of GLUT4 vesicles in thin rim sections from rat adipocytes (Ramm *et al.*, 2000). Approximately 95% of the GLUT4 in basal adipocytes is found to localise in the intracellular tubular vesicular network, which is connected to the endosomal-TGN system (reviewed in Bryant *et al.*, 2002).

Immunoelectron microscopic studies have provided the best evidence on the presence of GLUT4 in multiple intracellular compartments. These studies demonstrated that in the basal state GLUT4 is predominantly localised in small vesicles and tubular vesicular structures clustered around early or late endosomes, *trans* Golgi network (TGN) and close to the PM. In addition GLUT4 is localised to the TGN, clathrin coated vesicles, early and recycling endosomes (Slot *et al.*, 1991b; Gould, 1997). A small fraction (~5%) of GLUT4 is localised to the PM in the absence of insulin. The different types of GLUT4 vesicles identified include AP1 positive vesicles (budding from the TGN or endosomes), AP2 positive vesicles (budding from the PM), or discrete population of GLUT4-enriched vesicles that are highly responsive to insulin (Simpson *et al.*, 2001). Figure 1.2 shows the relative distribution of GLUT4 in different organelles of adipocytes under basal and insulin stimulated states.

Immunoadsorption and subcellular fractionation studies have shown a considerable co-distribution of GLUT4 with well-established markers of the endosomal recycling pathway such as transferrin receptor (TfR), mannose 6 phosphate receptor (M6PR) and also with GLUT1 (Rea and James, 1997). I shall return to this point below.

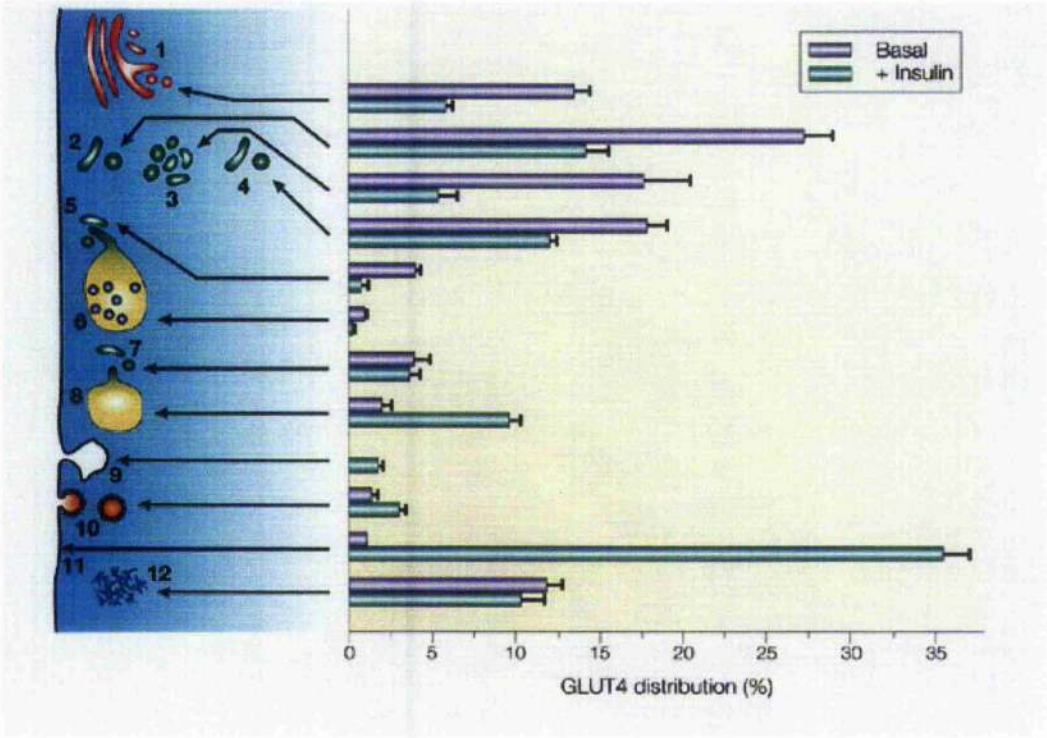

Figure 1.2 Relative distribution of GLUT4 in different membrane compartments of adipose tissue in basal and insulin-stimulated state (adapted from Bryant *et al.*, 2002)

The amount of GLUT4 in different compartments was quantified using immunoelectron microscopy. (1) *trans*-Golgi network (TGN); (2) tubulo-vesicular (TV) elements located underneath PM; (3) clusters of TV elements; (4) TV elements distributed throughout the cytoplasm; (5) TV elements connected or close to late endosomes; (6) late endosomes; (7) TV elements connected to early endosomes; (8) early endosomes; (9) non-coated pits of plasma membrane (PM); (10) coated pits and vesicles; (11) PM; (12) cytoplasm.

The graph shows the relative distribution of GLUT4 within these organelles under basal and insulin-stimulated (+insulin) states.

1.3.1 Specialised GLUT4 storage vesicles (GSV)

Even though it was difficult to distinguish the GLUT4 compartment from other elements of the constitutively recycling pathway, several observations suggested that there is a unique compartment of GLUT4 (Rea and James, 1997). Double labelled immunofluorescence microscopy in 3T3-L1 adipocytes showed differential targeting of GLUT1 and GLUT4 (Haney *et al.*, 1991). Endosomes can be chemically ablated by internalisation of HRP-conjugated transferrin and this procedure has been used to determine the proportion of protein localised to endosomes. Using this approach it is recognised that only about 40% of GLUT4 is localised to endosomes in basal state and the majority was found in ablation resistant compartments (Livingstone *et al.*, 1996). It was also found that endosomal ablation does not prevent insulin-stimulated GLUT4 translocation in adipocytes (Martin *et al.*, 1998). Furthermore, vesicle immunoadsorption studies have revealed two sets of GLUT4 vesicles, with only one set enriched in endosomal markers such as TfR (Livingstone *et al.*, 1996). Similarly, recently conducted quantitative immunoelectron microscopic studies revealed that GLUT4 resides in an apparently unique compartment devoid of other recycling proteins (Malide *et al.*, 2000).

Further evidence for the presence of a separate GLUT4 storage vesicle compartment (GSV) comes from the identification of differential regulatory mechanisms of GLUT4 compartment trafficking in adipocytes (Millar *et al.*, 1999). In this study it was shown that while insulin could stimulate translocation from both GSV and endosomes, GTPγS stimulates only the pathway derived from endosomal system. It is also known that in muscle, exercise recruits GLUT4 from a TfR-positive compartment, presumably endosomes (Ploug *et al.*, 1998). Further support for the concept of a distinct insulin-sensitive compartment is provided by the observation that under insulin stimulation, PM levels of GLUT1 and constitutively recycling proteins such as TfR increases only by 2-3 fold, whereas GLUT4 increases by 10-40 fold (Shepherd and Kahn, 1999). Such data argue that GLUT4 is present in endosomes and GSV, but that GSV are the main site of insulin action. The colocalisation of some other proteins such as insulin-responsive amino peptidase (IRAP) and vesicle-associated membrane protein 2 (VAMP2) with GLUT4 in fat and muscle cells supports the idea of the GSV compartment being a separate entity which might be analogous to well defined synaptic vesicles in neurons (reviewed in Rea and James, 1997). Figure 1.3 (p12)

shows the two distinct GLUT4 compartments identified by various biochemical studies.

Support for the concept of a unique GLUT4 storage compartment was recently provided by iodixanol sedimentation analysis to resolve GSV and the endosomal GLUT4 compartment. Hashiramoto and James separated GLUT4 from a low-density microsome (LDM) fraction into two distinct peaks using a self-generating iodixanol gradient (Hashiramoto and James, 2000). They showed that the denser peak 1 represents a subpopulation of GLUT4 vesicles that is highly insulin-regulatable and enriched in GLUT4, but depleted in endocytic markers. Experiments such as transferrin internalisation and endosomal ablation show that the lighter peak 2, is enriched in endosomes. Immunoblotting with antibodies against various membrane protein markers revealed that the second peak also contains TGN proteins such as sortilin and syntaxin 6 (Hashiramoto and James, 2000). The greater insulin responsiveness of peak 1 suggested that peak 1 contains the GSV (Hashiramoto and James, 2000; Maier and Gould, 2000).

The basis of the remarkable regulation of GLUT4 by insulin may reflect the biogenesis of this specific GSV compartment and the correct targeting of GLUT4 into it. However, the precise nature of this GLUT4 compartment is not yet known. An important finding in this regard was the identification of an insulin-responsive aminopeptidase (IRAP) as a component of GSVs which traffics in a similarly insulin-responsive manner to GLUT4. However it is not yet clear whether the GSV represents a specialised secretory organelle, homologous to synaptic vesicles in brain and unique to adipose and muscle cells, or whether insulin sensitivity has been applied to a pre-existing pathway during differentiation or whether this ablation resistant compartment is a subdomain of the TGN (Gould, 1997; El Jack *et al.*, 1999, Hashiramoto and James, 2000). One of the aims of this thesis is to resolve this issue.

1.4 GLUT4 trafficking

Numerous integral membrane proteins recycle continuously between the PM and specific intracellular locations by a series of discontinuous tubular and vesicular structures collectively referred to as the endosomal compartment (Rea and James, 1997). GLUT4 continuously internalises and recycles in both basal and insulin-

stimulated states (Yang and Holman, 1993). GLUT4 targeting is unique because of its predominant (~95%) intracellular localisation in the basal state. In contrast, as much as 30% of the total TfR is present in the PM despite the presence of a very efficient internalisation signal in TfR (Jing *et al.*, 1990). Internalisation studies have consistently shown that the rate of internalisation of GLUT4 from the PM is similar to that of constitutively recycling proteins such as TfR and GLUT1, which seems to occur through a common clathrin-mediated pathway. Therefore it is proposed that the effective exclusion of GLUT4 from the PM in the basal state is due to extensive retention in intracellular vesicles (reviewed in Gould, 1997; Holman and Sandoval, 2001). This selective retention of GLUT4 provides an intracellular pool of GLUT4 which can be moved rapidly into the PM in response to insulin. Insulin stimulates the rate of exocytosis of GLUT4 vesicles by about 5-fold while slowing the rate of endocytosis by ~2-fold, resulting in a 10 to 40-fold elevation of GLUT4 levels at the PM, rapidly redistributing up to about 50% of total GLUT4 to the PM (reviewed in Simpson *et al.*, 2001).

The identification of another major protein, IRAP, from GLUT4 vesicles which translocates to the PM in a similar insulin-responsive manner suggested that there is a specialised pool of vesicles which can fuse directly with the PM. Observation of GLUT4 clustered in tubulo-vesicular elements adjacent to early (sorting) endosomes and the TGN by electron microscopy provided strong evidence for the idea that GLUT4 is internalised first into the endosomal system, and then sorted into a specialised compartment from endosomes or the TGN (Gould, 1997; Rea and James, 1997). However, the presence of GLUT4 in multiple compartments such as the TGN and endosomal system and in several classes of carrier vesicles has made the identification of the exact trafficking pathway of GLUT4 difficult. Several models are reviewed to describe GLUT4 trafficking and the biogenesis of the intracellular GLUT4 compartment (Rea and James, 1997). One model suggests that GLUT4 may constantly move between two compartments in the basal state in such a way that the majority of GLUT4 is excluded from the recycling pathway directed to the PM. Another model suggests that in the basal state GLUT4 is sequestered within a topologically continuous subdomain of the endosomal system. No specialised vesicular fusion machinery is required to mediate GLUT4 trafficking in this model (reviewed in Bryant *et al.*, 2002). The model which is more widely accepted suggests that GLUT4 is sorted and packed

into regulated storage vesicles at some stage during transit through the endosomal recycling system. These vesicles may be stored in the cytoplasm until insulin stimulates their exocytosis. The important feature of this model is that once formed, these vesicles have the ability to dock and fuse directly with the PM independently of the endocytic recycling system in a similar manner to the small synaptic vesicles of neurons and secretory granules. A recently described model amalgamated features from previously described models, and proposes that GLUT4 trafficking is controlled by retention, dynamic sorting and storage into a more stationary compartment (Bryant *et al.*, 2002). This model includes an intracellular store of GLUT4 that represents a slowly recycling pool trafficking between the TGN and endosomes. Furthermore, this model suggests that this TGN associated GLUT4 pool can fuse with endosomes in the absence of insulin and with the PM in the presence of insulin (Bryant *et al.*, 2002; Zeigerer *et al.*, 2002).

1.4.1 Role of the TGN in GLUT4 trafficking

Around 10-20% of GLUT4 in basal adipocytes and myocytes is localised to the TGN, independently of newly synthesised protein (Slot *et al.*, 1991a; Slot *et al.*, 1991b; Rodnick *et al.*, 1992). There is data to show that GLUT4 enters the TGN via a recycling pathway independent of the biosynthetic pathway which suggest a role of TGN in GLUT4 trafficking. These include the localisation of GLUT4 to secretory granules containing atrial natriuretic factor in atrial cardiomyocytes even when protein synthesis is blocked (Slot *et al.*, 1997). In addition, it has been demonstrated that there is a significant decline of GLUT4 level in the TGN upon insulin stimulation of adipocytes and cardiac myocytes (Slot *et al.*, 1991a; Slot *et al.*, 1991b). Furthermore, GLUT4 in adipocytes was shown to localise with AP-1 positive clathrin-coated vesicles in the vicinity of TGN (Martin *et al.*, 2000b). In support of a role for the TGN in GLUT4 recycling, it was also shown that GLUT4 internalising from the PM of adipocytes is transported through endosomes into a perinuclear compartment that differs from recycling endosomes (Palacios *et al.*, 2001). This perinuclear compartment appears to represent a subdomain of the TGN due to the presence of syntaxin 6 and syntaxin 16, which are predominantly localised to the TGN (Shewan *et al.*, unpublished observation). Taken together, it is feasible that the TGN plays a role in targeting of GLUT4 to GSV (Figure 1.3).

1.4.2 Trafficking signals of GLUT4

The distribution of GLUT4 is remarkably different from GLUT1, despite the amino acid sequence of these transporters being 65% identical. GLUT4 is retained intracellularly, even when expressed in fibroblasts or other non-native cells such as CHO, COS-7, PC12 and HepG2 (reviewed in Gould, 1997). These findings suggested that GLUT4 might harbour intrinsic targeting signals for efficient sequestration within the cell. Even though the results of these studies are at times conflicting, several studies support a role for putative signal sequences located in N- and C- termini of GLUT4 for efficient internalisation of GLUT4 (reviewed in Watson and Pessin, 2001). Two sequences were identified by studying the distribution of chimeric, truncated or point-mutated transporters. They are the phenylalanine based sequence (FQQI) in position 5 of the N-terminus and the di-leucine (LL) motif at the 489/490 position of the C-terminus. These sequences are believed to function in both the internalisation and sorting between intracellular compartments (Garippa *et al.*, 1996; reviewed in Holman and Sandoval, 2001). The phenylalanine motif was shown to bind to adaptor proteins, implicating this motif in targeting of GLUT4 to clathrin-coated vesicles (Garippa *et al.*, 1994; Al Hasani *et al.*, 2002) and sorting GLUT4 away from the endosomal system (Melvin *et al.*, 1999). Mutation of the FQQI motif inhibited the recycling of endocytosed GLUT4 to the GSV compartment and resulted in its transport to late endosomes/lysosomes where it is rapidly degraded (Palacios *et al.*, 2001). Similarly, the di-leucine based signal appears to be important in sorting GLUT4 between the TGN and GSV (Melvin *et al.*, 1999; Martinez-Arca *et al.*, 2000).

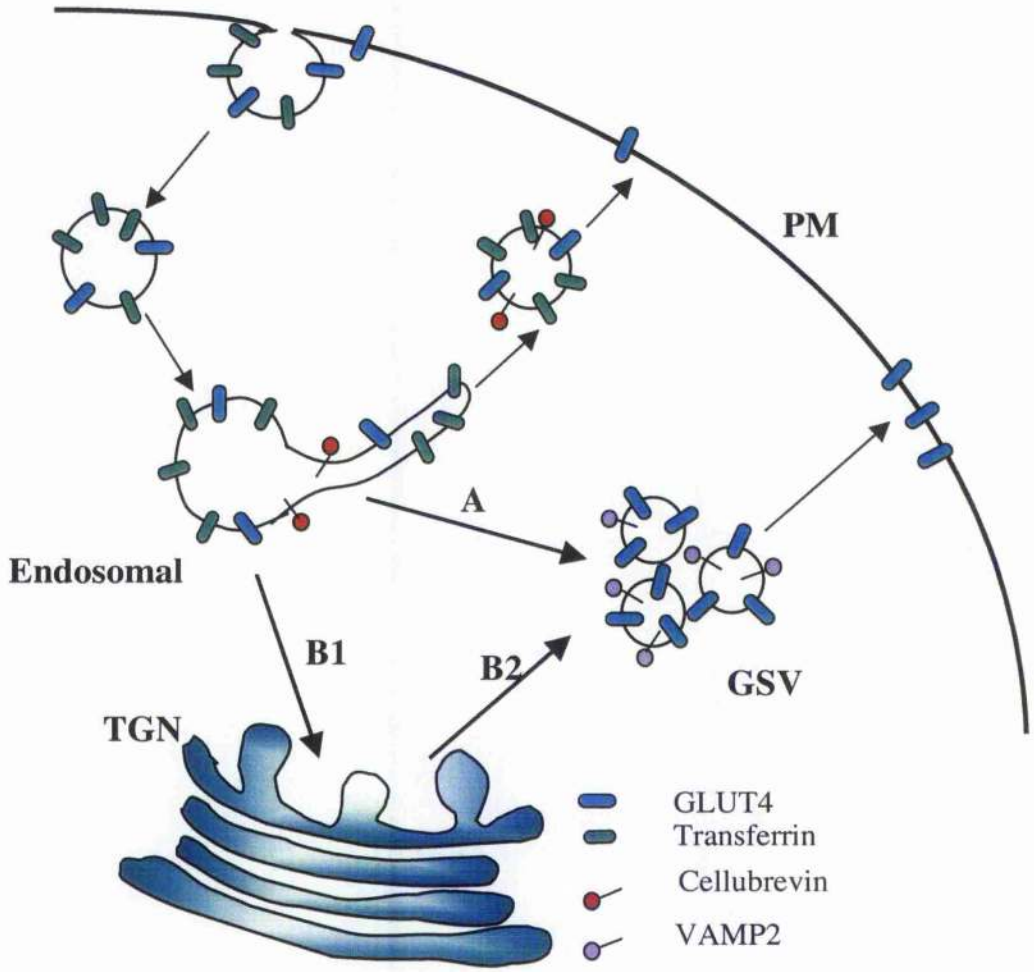

Figure 1.3 A model to represent GLUT4 trafficking

The figure shows the trafficking of GLUT4 and TfR. Both proteins are internalised from PM and move into early endosomes. The majority of TfR and a small proportion of GLUT4 recycle back to the PM. The majority of GLUT4 is sorted into a VAMP2-positive GSV compartment which could arise from endosomes (cellubrevin positive) (A), TGN (B1 and B2) or both. Insulin stimulates the exocytosis of the GSV compartment, which is responsible for the marked increase in GLUT4 at the PM.

1.5 IRAP, the only known protein to traffic identically to GLUT4

IRAP (or vp165) is a membrane aminopeptidase of 165 kD, that is extensively colocalised with GLUT4 in rat adipocytes, 3T3-L1 adipocytes and rat skeletal muscle (Kandror and Pilch, 1994; Malide *et al.*, 1997; Ross *et al.*, 1996; Aledo *et al.*, 1997). Over 90% colocalisation between IRAP and GLUT4 has been demonstrated by isolating vesicles from purified LDM fractions of 3T3-L1 adipocytes with anti-IRAP or anti-GLUT4 antibodies (Ross *et al.*, 1996). Similarly use of confocal microscopy with double labelling showed that about 85% of IRAP in rat adipocytes colocalised with GLUT4 (Malide *et al.*, 1997), and 70-90% colocalisation was found in a study using immuno-electron microscopy (Martin *et al.*, 1997). In addition to the identical distribution, IRAP is found to traffic like GLUT4 in basal and insulin-stimulated states in 3T3-L1 adipocytes (Ross *et al.*, 1996; Martin *et al.*, 1997; Ross *et al.*, 1998; Garza and Birnbaum, 2000) as well as in rat adipocytes (Malide *et al.*, 1997). Using cell surface biotinylation of IRAP Ross and co-workers (1996) demonstrated that the PM level of IRAP was increased extensively in response to insulin in 3T3-L1 adipocytes. In another study using cell surface biotinylation it was shown that IRAP is endocytosed rapidly in the absence and presence of insulin and the rates of endocytosis and exocytosis are similar to that of GLUT4 (Garza and Birnbaum, 2000). These authors found that IRAP and GLUT4 translocate to the same degree, using biotinylation and PM lawn assays which are more sensitive methods to study translocation than subcellular fractionation. Furthermore, using subcellular fractionation they showed that insulin elicits a dramatic redistribution of IRAP from the LDM to the PM in a manner similar to GLUT4. Although many other proteins have been identified within GLUT4 vesicles, IRAP is the only protein found to translocate to a similar degree to GLUT4 in response to insulin.

Despite identical subcellular distribution and trafficking in insulin-sensitive cells, the tissue distribution of IRAP differs markedly from GLUT4. IRAP is expressed in many tissues including 3T3-L1 fibroblasts where GLUT4 is not expressed. The function of this protein is not known, however it has been suggested to function in hormonal modulation of vasoactive peptides such as vasopressin (Herbst *et al.*, 1997). If this is the case, the pathogenesis of diabetic complications such as peripheral vascular disease and hypertension may have a link to impaired translocation of IRAP (Garza and Birnbaum, 2000).

1.6 TfR a well characterised marker of constitutive trafficking

The TfR is an 80 kD integral protein that mediates cellular iron uptake by binding, to the iron-carrying protein transferrin. The TfR is considered a model receptor of choice to study the early/ recycling endosomal pathway. It has been used as a valuable tool to follow the endocytic pathway as its ligand, holotransferrin, can be easily labelled and monitored. TfR carrying the ligand is internalised via clathrin-coated pits to the early endosomes where iron is released in the acidic environment of the compartment. From early endosomes, iron free transferrin is carried back to the PM by TfR with a half-time of about two to three minutes (Mayor *et al.*, 1993). A proportion of TfR reaches the recycling endosomal compartment through early endosomes and recycles back to PM with a half-time of about five to ten minutes (Daro *et al.*, 1996). The TfR is recycled 100-200 times during the life time of TfR (Rutledge *et al.*, 1998). In the basal state, the exocytosis of TfR is about 10-fold faster than that of GLUT4 (Tanner and Lienhard, 1987). Around 30% of TfR is present in PM at a given time and around 70% is localised intracellulary in recycling endosomes (Jing *et al.*, 1990).

1.7 Insulin signalling

Insulin is the major hormone that regulates glucose transport and serves as a prototypic molecule for the studies of cell signalling pathways. The insulin receptor is a ubiquitously expressed $\alpha_2\beta_2$ heterotetramer with intrinsic tyrosine kinase activity. Insulin binds to the α subunits and activates the intracellular tyrosine kinase domain of the β subunit (reviewed in Holman and Kasuga, 1997). The activated insulin receptor phosphorylates several intracellular substrates that serve as docking sites for effector proteins. e.g. insulin receptor substrate (IRS) 1 to 4, Cbl, Gab-1, Shc. Tyrosine phosphorylation of these intracellular substrates creates recognition sites for downstream effector proteins that contain Src homology 2 (SH2) domain and phosphotyrosine-binding (PTB) domains. Adjacent Pleckstrin homology (PH) domains on some substrate proteins also have a role in receptor binding and phosphorylation (Czech and Corvera, 1999). The participation of IRS proteins in insulin signal transduction is well documented (White, 1998).

Phosphorylated IRS proteins act as docking sites for the SH2 domain of the p85 regulatory subunits of class 1a, p85/p110-type phosphatidylinositol (PI) 3-kinase,

which brings this enzyme in to close proximity of its major substrates phosphoinositides (PI), localised to the PM lipid bilayer. PI3-kinase is a major switch element of insulin receptor signalling. Studies have shown strong evidence for the involvement of p85/p110-type PI3-kinase as a key element in GLUT4 translocation. Such evidence includes complete inhibition of insulin action on glucose transport by microinjection or expression of an inhibitory construct of the p85 subunit of PI3-kinase (reviewed in Czech and Corvera, 1999). The activation of PI3-kinase is followed by an increased level of phosphatidylinositol triphosphate (PIP_3) which stimulates downstream kinases such as PDK, which activates serine/threonine kinases Akt (PKB) and atypical PKC isoforms PKCλ and PKCζ (reviewed in Watson and Pessin, 2001). Pathways activating Akt appear to be responsible for most of cellular actions of insulin, including GLUT4 translocation into the PM (Cheatham, 2000). However, activation of PI3-kinase activity alone was shown to be insufficient for insulin-stimulated glucose uptake (Pessin and Saltiel, 2000). An additional pathway leading to phosphorylation of Cbl via its recruitment to the insulin receptor by the adaptor CAP is also necessary for insulin-stimulated glucose transport by insulin (Watson and Pessin, 2001).

1.7.1 Phosphatidylinosoitol 3-kinase (PI3-kinase)

The PI3-kinase family of proteins has been shown to regulate the endocytic trafficking of various proteins (reviewed in Mukherjee *et al.*, 1997). This enzyme has kinase activity and phosphorylates the membrane phospholipid, phosphoinositide (PI) forming PI-3-P, PI-3,4-P_2 and PI-3,4,5-P_3. PIP_3 is apparently the most important product of PI3-kinase. PIP_3 specifically interacts with FYVE domain and PX domain containing membrane proteins (Corvera *et al.*, 1999), many of which have been implicated in vesicle trafficking processes, and which involve calcium and lipid binding domains and GTPase activating proteins that control the GTPase activity of Arf. Inhibition of PI3-kinase by wortmannin (a fungal metabolite) has been shown to inhibit levels of PM TfR and insulin stimulated GLUT4 translocation (reviewed in Mellman, 1996). In addition, inhibition of PI3-kinase by wortmannin or LY294002 (another PI3-kinase inhibitor) induces the secretion of newly synthesised cathepsin D in mammalian cells suggesting involvement of PI3-kinase in sorting of M6PR into lysososmes (Brown *et al.*, 1995; Davidson, 1995). The mechanism of action of PI3-kinase in the regulation of endocytosis is poorly understood.

1.8 Insulin resistance

Insulin resistance is defined as a condition in which a normal concentration of insulin fails to bring about its normal physiological effects. The primary physiological role of insulin is associated with glucose homeostasis (Cheatham, 2000). Insulin resistance is a key factor in the pathogenesis of non-insulin dependent diabetes mellitus (NIDDM/ type 2 diabetes), which accounts for ~90% of all cases of diabetes (Reaven, 1995). Insulin resistance also increases the risk of heart disease and stroke by 2-4 times and is a leading cause of end stage renal disease, blindness and non-traumatic limb amputation. The total medical costs involved annually involve 100s of billions of pounds.

There is an alarming increase in the prevalence of NIDDM worldwide. The estimated number of individuals affected in 1985 was 30 million. By the year 2000 this figure had risen to over 150 million. Recent estimates predict that if the current trend continues the number affected with diabetes will be around 300 million in 2025 (Fujimoto, 2000).

NIDDM is characterised by hyperglycaemia and hyperinsulinaemia in the post-absorptive state. Hyperglycaemia is a consequence of the inability of insulin to stimulate glucose uptake in both skeletal muscle (Dohm *et al.*, 1988) and adipose tissue (Ciaraldi *et al.*, 1982).

1.9 Defects of GLUT4 trafficking in insulin resistance

Insulin stimulates glucose transport via translocation of GLUT4 proteins from an intracellular store to the cell surface in fat and muscle tissues, an exceptionally important event in maintaining blood glucose homeostasis. GLUT4 expression in fat cells is markedly reduced in NIDDM and obesity (Garvey *et al.*, 1988; Garvey *et al.*, 1991). In contrast, the normal levels of GLUT4 found in skeletal muscle under a variety of insulin resistance states (NIDDM, obesity, gestational diabetes, impaired glucose tolerance) (Garvey *et al.*, 1991) has suggested that insulin resistance in muscle is caused by defects in GLUT4 translocation to the PM (Pedersen *et al.*, 1990; Garvey *et al.*, 1992). This hypothesis was supported by several investigations, indicating that translocation of GLUT4 in skeletal muscle is impaired in many forms of insulin resistance (Klip *et al.*, 1990; King *et al.*, 1992; Kelley *et al.*, 1996; Zierath *et al.*, 1996;

Garvey *et al.*, 1998). A similar defect in translocation was observed in adipocytes collected from women with gestational diabetes (Maianu *et al.*, 2001), in addition to the reduction in total GLUT4 level. In these cells GLUT4 translocation was impaired with a redistribution of GLUT4 to dense membrane vesicles under basal conditions (Maianu *et al.*, 2001). Even though adipocytes collected from NIDDM patients under basal conditions had a normal level of IRAP, the redistribution of IRAP away from LDM with more recovery of IRAP in HDM and PM was evident (Maianu *et al.*, 2001). Therefore failure of targeting GLUT4 into its normal compartment as supported by these studies may be a cause of insulin resistance.

Further to defects in translocation, defects in signal transduction (e.g. tyrosine kinase activity of insulin receptor, IRS1 phosphorylation and PI3-kinase activation) have been observed in skeletal muscle under insulin resistance (Goodyear *et al.*, 1995). These will not be discussed further here.

1.10 Intracellular protein trafficking

The endocytic and exocytic pathways of eukaryotic cells are organised into several functionally distinct membrane compartments connected by vesicle budding and fusion events. Vesicle trafficking between the compartments permits the transport of soluble and membrane components from one compartment to another while maintaining the composition, size and the polarity of the membrane. Communication between biosynthetic and endocytic pathways occurs by vesicle trafficking between the Golgi complex and endosomes.

1.10.1 Endocytosis

Eukaryotic cells take up extracellular or cell surface material by a variety of mechanisms, which are collectively called endocytosis. Endocytosis serves several functions in cells. Basically, it is essential to maintain cellular homeostasis by recovering membrane components targeted to the PM by secretory activity. Furthermore, endocytosis is essential to maintain cellular communication, for the uptake of nutrients and defence mechanisms (reviewed in Mellman, 1996; Gruenberg and Maxfield, 1995). Uptake of extracellular fluid, ligands and receptors occurs in every cell to varying degrees. Many PM proteins are subjected to endocytosis and recycle back to the PM escaping the lysosomal pathway. It is estimated that some PM

receptors participate in as many as 10 rounds of ligand uptake per hour (Mellman, 1996).

1.10.1.1 Clathrin-mediated vesicle budding

The biogenesis of transport vesicles is initiated by the recruitment of large multi subunit proteins called coats. The assembly of coat proteins is important in the selection of cargo and deforming the lipid bilayer into a budding vesicle. Clathrin-mediated endocytosis is the best characterised and the principal pathway for receptor-mediated endocytosis (Kirchhausen, 2002). Clathrin-coated vesicles (CCVs) mediate vesicle biogenesis at the PM and TGN and selective transport of membrane-bound proteins to endosomes. Furthermore, CCVs have been shown to localise to vesicles budding from endosomes (Stoorvogel *et al.*, 1996). During formation of CCV, soluble clathrin from the cytoplasm is recruited onto the PM or TGN and assembled into a lattice of haxagons and pentagons forming a cage-like structure around the membrane vesicle (Kirchhausen, 2002). This process is thought to help the membrane to form a vesicle bud by distortion.

Certain membrane proteins, especially receptors for extracelluar ligands such as transferrin, epidermal growth factor and low-density lipoprotein, are very efficiently concentrated in CCVs (Robinson *et al.*, 1996). The presence of tyrosine based and di-leucine internalisation sequences in the cytoplasmic domain of the membrane protein and their association with adaptors are associated with targeting of proteins to CCVs (Kirchhausen, 2002; Boehm and Bonifacino, 2002). In addition to a membrane cargo, coated vesicles are thought to include molecules which determine the destination and fusion of the vesicle e.g. Rab proteins and SNAREs (Kirchhausen, 2000). Dynamin, a GTPase is required for coated pits to pinch off as coated vesicles (reviewed in Kirchhausen, 2000). Budding of clathrin-coated vesicles from the TGN requires the GTP binding protein, ADP-ribosylation factor (Arf). CCVs carrying receptor bound ligands become uncoated by an ATP-dependent chaperone and auxilin and insitol-5 phosphatase within the cell and are delivered to early endosomes (reviewed in Lemmon, 2001).

1.10.1.2 Coat proteins (COPs)

In addition to clathrin, two other types of coats (COPI and COPII) are associated with intracellular trafficking. COPII is associated with vesicles targeting to the Golgi from the endoplasmic reticulum (ER). COPI is associated with retrogtrade traffic from the Golgi to the ER (reviewed in Barlowe, 2000). COPI was also found to associate with early endosomes. GTP loading of Arf or Sar 1 initiates the recruitment of pre-assembled cytosolic coat complexes of COPI and COPII respectively to the membranes (reviewed in Springer *et al.*, 1999). This recruitment of COPs plays an active role in cargo selection since coats interact directly with different cargo such as transmembrane proteins with the KKXX ER retrieval motif (Mellman, 1996). COPs may also be involved in the selection of v-SNAREs into vesicles (Matsuoka *et al.*, 1998).

1.10.1.3 Adaptors

CCVs are composed of adaptor proteins in addition to clathrin. Adaptors play a critical role in the attachment of clathrin to the membrane and in recruiting membrane proteins selectively (reviewed in Mellman, 1996; Huizing *et al.*, 2001; Robinson and Bonifacino, 2001; Boehm and Bonifacino, 2002). There are four types of adaptor complexes characterised to date (AP-1 to AP-4). They are heterotetramers consisting of four different subunits. AP-2 is localised in PM coated pits and AP-1 is in the TGN, which interact with proteins that exit the Golgi (Robinson and Bonifacino, 2001). AP-3 and AP-4 are suggested to function in the TGN by associating with non-clathrin coated vesicles (Simpson *et al.*, 1996; Hirst *et al.*, 1999 respectively) AP-3 is suggested to function in transport to lysosome-related organelles e.g. yeast vacuole, mammalian melanasomes, platelet dense bodies, lysosomes (Boehm and Bonifacino, 2002). The function of AP-4 is not definitely known to date (Boehm and Bonifacino, 2002). Some other adaptors identified recently include the monomeric GGAs (Golgi-localised, γ-ear containing, ARF binding proteins) and members of the β-arrestin family (Boehm and Bonifacino, 2001).

Studies have shown that tyrosine-based sequences are involved in many sorting events delivering material from the secretory pathway to the lysosomal pathway (Davis *et al.*, 1987), retrieval to the TGN (Bos *et al.*, 1993; Humphrey *et al.*, 1993) and transport

from early endosomes to the basolateral PM in polarised epithelial cells (Mellman, 1996). Involvement of di-leucine based sequences has been demonstrated in endocytosis and lysosomal delivery (Letourneur and Klausner, 1992) and sorting of Fc receptor into the basolateral PM of macrophage (Hunziker and Fumey, 1994).

1.10.1.4 Organisation of endosomes

Four classes of endocytic vesicles are typically distinguished, which are early endosomes (EE), recycling endosomes (RE), late endosomes (LE) and lysosomes (Mellman 1996) Figure 1.4 shows the basic organisation of the endocytic pathway. The organisation of the endocytic pathway is regulated by interaction with the cytoskeleton. Many of these interactions are based on the activity of motor proteins, which couple nucleotide hydrolysis to the movement of vesicles along the endocytic pathway (reviewed in Woodman, 2000).

1.10.1.5 Sorting in endosomes

Selective inclusion of receptors at the PM into coated pits is the initial sorting event in endocytosis. Further sorting events occur in the endosomes and the materials are targeted to a variety of destinations, depending on their ability to interact with a number of complex, ill-defined sorting events (Woodman, 2000). Endosomes mediate specific sorting events in addition to the basic functions such as discharge of internalised ligands from their receptors and subsequent transfer of ligands to lysosomes and receptors to the PM. These include targeting of membrane proteins to their correct PM domain in polarised epithelial cells, to a range of specialised endosomal-derived recycling or secretory vesicles and to the TGN.

Endosomal sorting depends on recognition between receptors and proteins, the pH of compartment, the regulation of fusion and vesicle formation by endosomes, and the molecular properties of ligands and receptors. But the exact mechanism involved in sorting is incompletely understood (reviewed in Mellman, 1996; Mukherjee *et al.*, 1997). Different parts of the endosomes have a characteristic pH essential for function. Several ligands including iron, insulin, epidermal growth factor and low-density lipoprotein dissociate from their ligands in the EE, probably due to a pH-dependent conformational change in the receptors (reviewed in Mukherjee *et al.*, 1997). Some ligands require a much lower pH to cause dissociation e.g. ligands of M6PR are

released at a pH of around 5.8. the acidity of the endosomes is maintained by an ATP-dependent proton pump (vacuolar H^+-ATPAase).

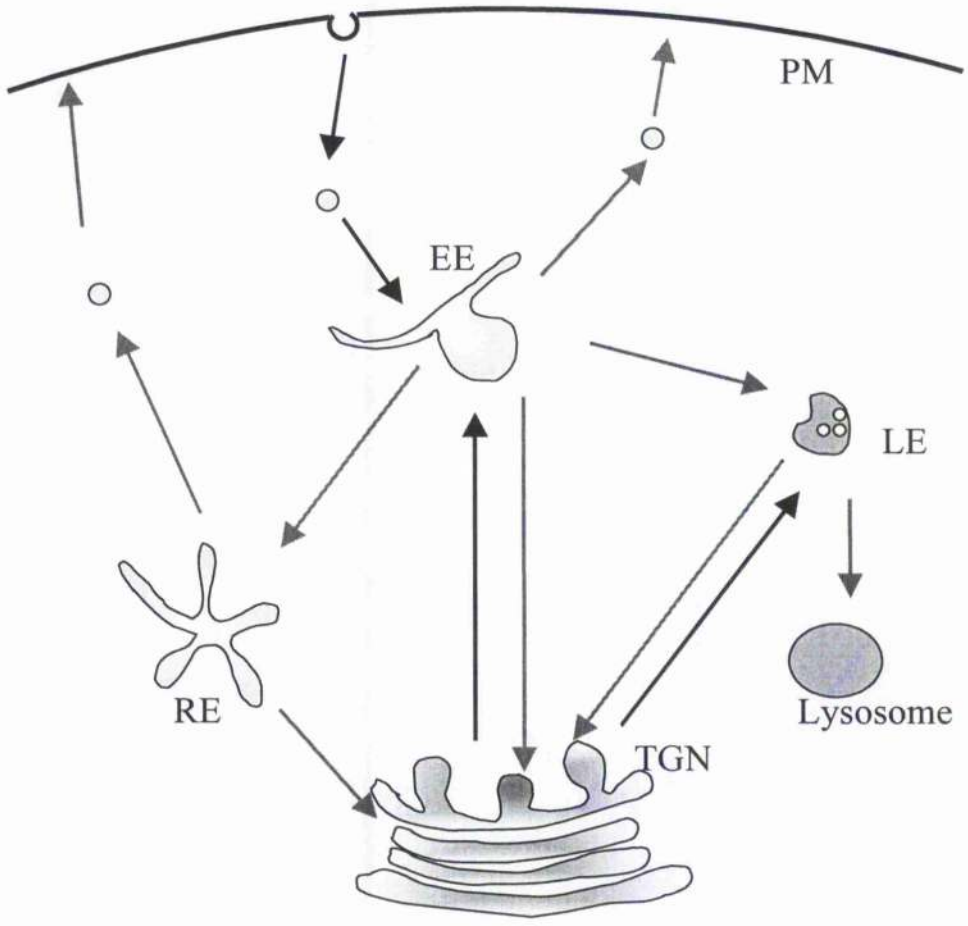

Figure 1.4 Organisation of the endosomal pathway

Receptor-ligand complexes enter the endocytic pathway as vesicles budding from specialised regions of the PM. The cargo reaches the EE where most of the recycling receptors are dissociated from ligands. This cargo is sorted and directed into various destinations from the EE. e.g. to the PM, RE, TGN and to specialised endosomal-derived recycling vesicles or secretory vesicles in cells with regulated trafficking or lysosomes by maturing into LE.

1.10.1.6 Early endosomes (sorting endosomes)

EEs represent a dynamic network of tubules and vesicles dispersed throughout the periphery of the cytoplasm (Mukherjee *et al.*, 1997). Morphologically this compartment is comprised of vacuoles, cisternae and tubules. The primary function of EEs is sorting membrane proteins, lipids and bound ligands which enter the EE following their internalisation from the PM. Transport from the PM to the EE is dependent upon the small G protein Rab5. EEs have a slightly acidic pH (6.3-6.8) where dissociation of some receptor-ligand complexes (particularly the rapidly recycling receptors) takes place (Mukherjee *et al.*, 1997). Generally this dissociation is followed by targeting of material to three general exit routes, (i) the degradation pathway through the LE (free ligands), (ii) the recycling pathway via the RE (free receptors) or (iii) directly to the PM (Woodman, 2000). When the recycling molecules are segregated into tubular extensions the material remaining within the central region will eventually mature into LE (Lemmon and Traub, 2000). In addition to these routes, proteins may be sorted out of the EE to the TGN and specialised compartments in certain cells (Lemmon and Traub, 2000). Some cells contain specialised endosome-derived storage compartments that allow their rapid delivery of proteins into PM in response to external stimuli. e.g. GSV in insulin-sensitive tissues, synaptic vesicles in neurons, water channel-containing vesicles in renal duct cells, H^+/K^+ ATPase vesicles in gastric epithelial cells (Keller and Simons, 1997). EEs also function to sort newly synthesised proteins arriving from the TGN to the lysosomal pathway e.g. lysosomal hydrolases bound to M6PR (Keller and Simons, 1997). Rab4, 5 and 11 are associated with distinct domains within the EE and are often used to biochemically define distinct compartments.

1.10.1.7 Recycling endosomes

Recycling vesicles accumulate closely apposed to the microtubular organisation centre and in perinuclear cytoplasm. Recycling vesicles contain recycling receptors, but they usually do not contain markers of LEs and lysosomes. The pH of the RE is less acidic than that of the EE (Mukherjee *et al.*, 1997).

1.10.1.8 Late endosomes

LEs accumulate and concentrate internalised material after sorting in the EE. LEs act as another sorting compartment before the lysosomes (Donaldson and Lippincott-

Schwartz, 2000; Lemmon and Traub, 2000). The internal pH of the LE is around 5.5. The LEs and lysosomes are enriched in highly glycosylated, conserved lysosomal membrane glycoproteins e.g. lysosomal membrane glycoproteins (lgps) and lysosomal associated membrane proteins (lamps). Rab7 and 9 are localised in the LE. Rab7 is required for progression of M6PR from the EE to LE (Hirst *et al.*, 1998). Retrograde transport of M6PR from LE appears to require Rab9 (Riederer *et al.*, 1994). Certain receptors such as the epidermal growth factor receptor and ligands such as low-density lipoprotein traffic to lysosomes via LEs. (reviewed in Mukherjee *et al.*, 1997). LEs undergo extensive vesicular traffic with the TGN to acquire newly synthesised lysosomal enzymes and to return M6PR back to the TGN (Mellman, 1996).

1.10.1.9 Lysosomes

Lysosomes are regarded as the terminal and major degradation compartment of the endocytic pathway. They also play an important role in phagocytosis, autophagy and proteolysis of some cytosolic proteins that are transported across the lysosomal membrane. The delivery of endocytosed molecules to lysosomes occurs by direct fusion of late endosomes with lysosomes (reviewed in Luzio *et al.*, 2001). They continuously pack lysosomal hydrolases, which are brought to the LE from the TGN with the aid of M6PR. Lysosomes are localised mainly to the perinuclear region of cells, and their internal pH is acidic (5-5.5). Lysosomal membranes play a vital role in maintaining acidic pH and their ability to fuse with other membrane organelles. Lysosomal membrane is resistant to degradation by lysosomal hydrolases (Fukuda, 1991). In mammalian cells lysosomes are ~5 μm in diameter and can make up 0.5-5% of the cell volume.

1.10.1.10 *Trans* Golgi network (TGN)

The TGN is the major sorting station for newly synthesised proteins and lipids in the biosynthetic pathway (Traub and Kornfeld, 1997). Many different constitutive and regulated routes emerge that deliver molecules, either to the cell surface or to a number of compartments such as the EE and LE of the endosomal system. The TGN also receives vesicles from EEs, REs and LEs connecting endocytic and biosynthetic pathways. The TGN is centred at the microtubular organising centre and maintained there by association with microtubules and microtubular motors (Donaldson and Lippincott-Schwartz, 2000). Adaptor proteins, AP-1 (in CCVs), AP-3 and AP-4 are

associated with the TGN in an Arf-dependent manner and are thought to participate in the sorting of cargo into the different vesicles which arise from the TGN. (Lemmon and Traub, 2000).

1.10.2 Exocytosis

Exocytosis is the process in which intracellular proteins and membrane-bound vesicles fuse with the PM of eukaryotic cells (reviewed in Lin and Scheller, 2000). This process allows incorporation of vesicle membrane proteins into the PM and release of the contents of the vesicle to the extracellular space. There are two mechanisms by which exocytosis takes place namely, constitutive and regulated. Constitutive exocytosis occurs in every eukaryotic cell and this pathway does not need the influence of external stimuli. Regulated exocytosis occurs in specialised cells, which perform specific functions. Regulated exocytosis plays diverse roles such as release (secretion) of neurotransmitters, hormones, enzymes and cytokines into extracellular environment. This pathway is also critical in regulating the levels of various lipids, receptors and the transporters in the PM, for example, the increase in GLUT4 content at the PM in response to insulin stimulation in fat and muscle cells.

The most extensively studied and characterised type of regulated exocytosis is synaptic vesicle exocytosis at the presynaptic PM. Homologues of most of the proteins involved in synaptic vesicle exocytosis (e.g. SNAREs) have been identified in other forms of regulated and constitutive exocytosis and also in intracellular trafficking events from diverse eukaryotic cells, including yeast (Lin and Scheller, 2000).

1.10.2.1 Secretion of proteins from adipocytes

Adipose tissue is an organ which secretes many physiologically important proteins collectively called "adipokines", which have autocrine, paracrine or endocrine effects. Some of these proteins have roles in lipid metabolism, insulin sensitivity, inflammatory response, complement system or vascular homeostasis. These secretory products include leptin, adipsin, adiponectin (the murine isoform, ACRP30-adipocyte complement related protein of 30 kD or adipoQ), lipoprotein lipase, tumor necrosis factor-α, resistin, metalothionein, interleukin 6, plasminogen activator inhibitor-1 and angiotensinogen (Trayhurn and Beattie, 2001).

Studies conducted both *in vivo* and *in vitro* recognised that these proteins are secreted from two compartments, which undergo constitutive or regulated secretion (Roh *et al.*, 2000). Insulin increases the secretion of many soluble proteins from adipocytes in addition to enhancing exocytosis of membrane proteins such as GLUT4, GLUT1 and TfR. These secreted proteins include leptin (Barr *et al.*, 1997), ACRP30 (Hu *et al.*, 1996) and adipsin (Kitagawa *et al.*, 1989; Rosen *et al.*, 1989; Peake *et al.*, 1997).

Adipsin is a serine protease with complement factor D activity constitutively secreted from adipose tissue. It was demonstrated that the pathway secreting adipsin is different from the pathways employed by GLUT4 and TfR to reach the PM in response to insulin (Millar *et al.*, 2000). Millar and co-workers showed that adipsin secretion is increased in response to insulin by a phospholipase D-dependent step, possibly a budding step at the TGN. ACRP30 seems to play an important role in energy homeostasis (Hu *et al.*, 1996). Decreased expression of ACRP30 was shown to be associated with insulin resistance in mice (Yamauchi *et al.*, 2001). Leptin has a critical role in maintaining energy balance (Trayhurn and Beattie, 2001). It was shown that ACRP30 (Bogan and Lodish, 1999) and leptin (Barr *et al.*, 1997); (Roh *et al.*, 2000) use regulated secretory pathway/s, different from the trafficking route of GLUT4. ACRP30 appears to reside in vesicles that are distinct from ER, TGN, endosomes and GLUT4 vesicles (Roh *et al.*, 2001). All together, these results suggest that at least some of these secretory proteins (e.g. adipsin, ACRP30 and leptin) use a regulated secretory pathway distinct from that of GLUT4.

1.11 SNAREs as key mediators of membrane fusion events

The transport of molecules to various destinations within the eukaryotic cell occurs by vesicle formation, trafficking and fusion with the correct membrane destination, while maintaining the membrane integrity of cellular compartments. Vesicular trafficking is essential for a variety of cellular functions including maintenance of compartments, cell division, secretion of proteins and hormones and regulated trafficking events. Among several protein families implicated in vesicular trafficking, SNAREs (soluble *N*-ethylmaleimide sensitive factor attachment protein receptors) are identified as central mediators of vesicle fusion with the target membrane. SNAREs are also considered to mediate the specificity of membrane fusion events with the aid of other proteins such as Rabs. SNARE proteins are now established as mediators of insulin-

stimulated GLUT4 translocation to the PM. (discussed later in section 1.14). NSF and SNAP are two proteins which have a general role in almost all of the fusion processes. The Sec/Munc family of proteins are also known to function in regulation of SNARE complex formation. These will be discussed further from 1.11.1 to 1.14.

1.11.1 SNAREs

Most if not all membrane fusion events in eukaryotic cells are mediated by a conserved group of proteins known as SNAREs. SNAREs serve as receptors for the cytosolic proteins, *N*-ethylmaleimide sensitive factor (NSF) and soluble NSF attachment protein (SNAP) (Rea and James, 1997). SNAREs represent an evolutionary conserved superfamily of membrane-associated proteins that are localised in different membranes of the cell (Jahn and Sudhof, 1999; Bock *et al.*, 2001). They have been identified as the core machinery involved in the vesicle fusion with its specific target membrane (Bennett *et al.*, 1993; Sollner *et al.*, 1993).

The cytosolic proteins, NSF and SNAP were known to play a general role in a number of membrane trafficking events before identification of SNARE proteins (Rea and James, 1997). The SNARE hypothesis originated with the observation that three membrane proteins from detergent extracts of brain complexed with α-SNAP and NSF (Sollner *et al.*, 1993; Rothman and Warren, 1994). These membrane proteins had been previously identified and characterised by groups studying synaptic transmission or protein trafficking in yeast (reviewed in Gerst, 1999). The SNARE hypothesis suggested that a unique set of proteins, anchored to vesicles, specifically recognise and interact with a unique receptor molecule found in target membranes (Sollner *et al.*, 1993). This hypothesis further suggested that unique interactions between different sets of cognate SNAREs provide the required specificity to ensure that a particular vesicle will dock and fuse with a particular target membrane.

Originally, SNAREs were classified as v- or t-SNAREs depending on their localisation, whether on the vesicle membrane or target membrane respectively (Sollner *et al.*, 1993). v-SNAREs are also known as vesicle associated membrane proteins (VAMPs) or synaptobrevins. v- and t-SNAREs were reclassified as R-SNAREs and Q-SNAREs respectively, on the basis of their most conserved residues, arginine or glutamine respectively which are involved in the formation of the central

layer of the SNARE complex (Fasshauer *et al.*, 1998). Q-SNAREs are of two types, syntaxins and synaptosome-associated protein of relative molecular mass 25 kD (SNAP-25) homologues. (SNAP-25 proteins are unrelated to NSF attachment protein (SNAP)). Recently Q-SNAREs were categorised as Qa (syntaxins), Qb (N-terminal helix of SNAP-25) and Qc (C-terminal domain of SNAP-25) based on resemblance to one of the helical domains of the SNARE complex (Bock *et al.*, 2001) Figure 1.5 shows the basic structure of three categories of SNAREs.

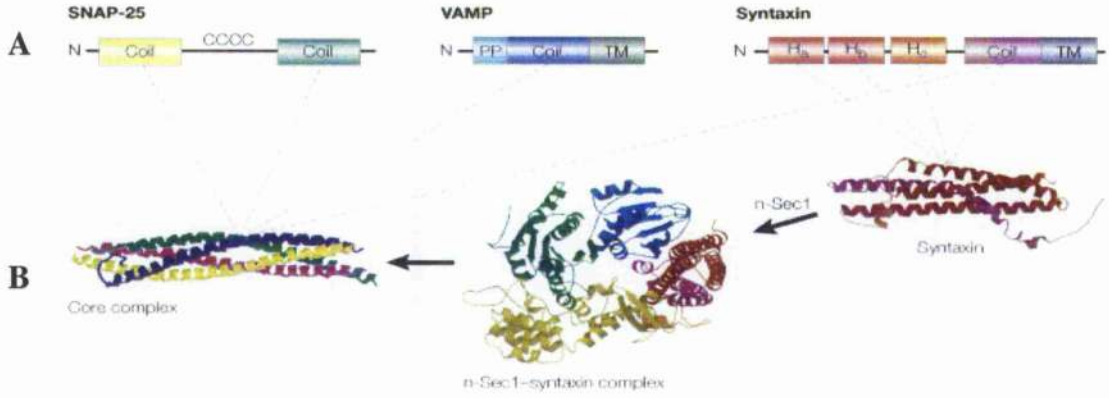

Figure 1.5 Members of the SNARE family (adapted from Chen and Scheller, 2001)

A Shown are the three members of the SNARE family, SNAP-25, VAMP and syntaxin. Both syntaxin and VAMP are associated with the membrane by a C-terminal transmembrane domain and they each contribute one SNARE domain to form the SNARE complex. SNAP-25 contributes two SNARE domains to form the complex and is associated with membranes by palmitoylation of the cysteine rich central region.

B The N-terminus of the syntaxin binds to its C-terminal SNARE domain forming the closed conformation (right), which is stabilised by n-Sec1 of the Sec/ Munc protein family (middle). Dissociation of n-Sec1 from syntaxin facilitates the formation of SNARE complex (left).

CCCC- cysteine rich region; Coil- SNARE domain; Ha-Hb-Hc- N-terminal coiled coil domains; PP- proline rich N-terminus

The best characterised members of the SNARE proteins are those involved in synaptic vesicle exocytosis. Recent investigations have characterised several SNAREs from a variety of membranes, based on association with known SNAREs or by sequence homology to known SNAREs (Bock *et al.*, 1996; Hay and Scheller, 1997; Advani *et al.*, 1998; Steegmaier *et al.*, 1998). So far 35 SNARE proteins have been identified in the human genome (Bock *et al.*, 2001) and over one hundred SNARE proteins in diverse organisms (Jahn and Sudhof, 1999). Table 1.1 shows a summary of mammalian SNAREs identified to date with their putative yeast homologues and the membrane localisation.

The identification of numerous SNARE proteins in a range of organisms and their localisation within specific cellular compartments (Jahn and Sudhof, 1999; Scales *et al.*, 2000) suggested that they are involved in specific membrane trafficking events (Bennett *et al.*, 1993; Ferro-Novick and Jahn, 1994). In support of this, it was shown that liposome fusion catalysed by purified recombinant SNAREs displayed significant specificity for cognate SNAREs (McNew *et al.*, 2000). A similar observation was made in a cracked PC12 cell system where cognate SNAREs competed more successfully for complex formation compared to non-cognate SNAREs (Scales *et al.*, 2000). However, some recent studies suggested that SNAREs mediate the fusion reaction but not the specificity of fusion. In support of this suggestion it was found that certain SNAREs function in several trafficking steps (von Mollard *et al.*, 1997; Gotte and von Mollard, 1998). Furthermore, it was observed that non-cognate SNAREs form SNARE complexes *in vitro*, albeit to a lesser degree than that of cognate SNAREs (McNew *et al.*, 2000). However, the *in vitro* studies conducted with the use of purified SNAREs, had the limitation that other docking and tethering mechanisms that act prior to SNAREs, which might influence the specificity are absent (Hay, 2001). Taken together, it is likely that the specificity of intracellular membrane transport is determined by SNARE proteins in concert with upstream targeting and tethering factors (Chen and Scheller, 2001). Proteins of the Rab and Sec 1 family may be some of these candidates (Scales *et al.*, 2000).

Mammalian SNARE	Yeast orthologue	Structural role	Localisation
STX 1a, 1b	Sso1, 2p	Qa	PM
STX 2		Qa	PM
STX 3		Qa	PM
STX 4		Qa	PM
STX 5	Sed5p	Qa	ER, Golgi
STX 7	Vam3p	Qa	Endosomes
STX 11		Qa	LE, TGN
STX 12/13	Pep12p	Qa	EE, RE
STX 16	Tlg2p	Qa	TGN
STX 17		Qa	SER
STX 18	Ufe1p	Qa	ER
vti1a	Vti1p	Qb	TGN
vti1b		Qb	Endosomes, Golgi
vti1c		Qb	Not characterised
vti1d		Qb	Not characterised
GOS-28	Gos1p	Qb	Golgi
Membrin	Bos1p	Qb	Golgi
STX 6	Tlg1p	Qc	TGN, endosomes, ISGs
STX 8	Vam7p	Qc	EE, LE
STX 10		Qc	Golgi, TGN
rbet1	Bet1p	Qc	ER
gs15	Sft1p	Qc	Golgi
SNAP-23	Sec9p	Qbc	PM
SNAP-25		Qbc	PM
SNAP-29	Spo20p	Qbc	Golgi and many organelles
VAMP1, 2	Snc1, 2p	R	SVs, SGs, RE
VAMP3		R	RE
VAMP4		R	TGN, ISGs
VAMP5		R	PM, peripheral vesicles
VAMP7	Nyv1p	R	LE, lysosmes, TGN
VAMP8		R	EE,LE
sec22b	Sec22p	R	ER
ykt6	Ykt6p	R	Golgi?
Tomosyn		R	Nerve terminals

Table 1.1 SNARE summary table (adapted from Hay, 2001)

For each mammalian SNARE the structural role and subcellular localisation and the putative yeast homologues are summarised. EE- early endosome; ISG- immature secretory granule; LE- late endosome; L- lysosome; RE- recycling endosome; SG- secretory granule; SV- synaptic vesicle

SNAREs share a homologous domain of ~60 amino acids which is referred to as a SNARE motif (Weimbs *et al.*, 1997). This motif mediates the association of SNAREs into core complexes. Syntaxins and VAMPs contain a single SNARE motif between a variable N-terminal region and a C-terminal transmembrane (TM) region. SNAP-25 and its homologue SNAP-23 contain two SNARE motifs that are separated by a cysteine rich sequence (Hess *et al.*, 1992). Intracellular membrane fusion is mediated by the formation of the core complex of four helical bundles comprised of four SNARE domains contributed by syntaxin (1 domain), VAMP (1 domain) and SNAP-25 (2 domains). In addition to the SNARE domain, SNAREs contain flanking regions that attach them to the membranes and mediate additional protein-protein interactions (Jahn and Sudhof, 1999). Both syntaxins and VAMPs are anchored to their respective membranes by C-terminal hydrophobic TM domains. The majority of these two types of proteins are exposed to the cytoplasm (type II integral proteins). On the other hand, SNAP-25 proteins associate with the membrane via palmitoylation of their cysteine rich region (Waters and Hughson, 2000; Wong *et al.*, 1998).

The SNARE complex formed between VAMP, syntaxin and SNAP-25 with 1:1:1 stoichiometry is extremely stable (Sollner *et al.*, 1993; Fasshauer *et al.*, 1998; Teng *et al.*, 2001) The best-studied SNARE complex is the one mediating fusion of small synaptic vesicles at the presynaptic PM, which is comprised of the Q-SNAREs syntaxin 1 and SNAP-25 and R-SNARE, VAMP (or synaptobrevin). Assembly of SNAREs occur spontaneously from unstructured monomers. Since four interacting SNARE motifs are aligned in parallel and these coils are just proximal to the membranes, the formation of this SNARE complex could bring opposing membranes into close proximity (Hay, 2001). In addition, the formation of extremely stable SNARE complex would release a large amount of free energy that would be available to drive the fusion of the two membranes overcoming the energy barrier caused by repulsive forces of two membranes. (Brunger, 2000; Hay, 2001). In support of this it has been shown that the SNARE core complex is sufficient to drive membrane fusion in artificial liposomes (Weber *et al.*, 1998).

SNARE motifs assemble into tight complexes of a 12 nm long twisted bundle formed by parallel alignment of four α-helices which interact by 16 layers (Fasshauer *et al.*,

1998) (Figure 1.6). The interacting layers of the four α-helices are formed by interacting side chains of highly conserved amino acids from each helix (Sutton *et al.*, 1998). The majority of these layers contain hydrophobic amino acids with an ionic layer at the centre. At this central layer each helix contributes a polar side chain: three glutamines (Q) from the Q-SNAREs and one arginine (R) from the R-SNARE. The precise function of the Q and R residues is uncertain. Functional studies conducted to date indicated that this layer provided by Q and R residues is not important for membrane fusion *per se* (Hay, 2001). It is assumed that they have a role in aligning the helices in the proper register during assembly of the SNARE complex and perhaps in the dissociation of complex (Scales *et al.*, 2001; Hay, 2001). Figure 1.6 shows the formation of the SNARE complex prior to membrane fusion and the interactions between the helices of the SNARE complex.

Major conformational changes take place during assembly of the SNARE complex, which converts these molecules from unstructured forms to helical forms (Fasshauer *et al.*, 1997). Complex formation proceeds from the membrane distal (N-terminal) end of SNARE domain, towards the membrane proximal C-terminus in a parallel manner (Fiebig *et al.*, 1999; Jahn and Sudhof, 1999). This process brings two membranes into close proximity and aids membrane fusion. Single amino acid substitutions in the core of bundle, have been shown to result in loss or severe impairment of SNARE function, indicating the functional significance of the core complex (Fasshauer *et al.*, 1998).

The TM domains of syntaxin and VAMP appear to be essential in membrane fusion (Grote *et al.*, 2000) and they are found to contribute to the overall stability of SNARE complex (Poirier *et al.*, 1998).

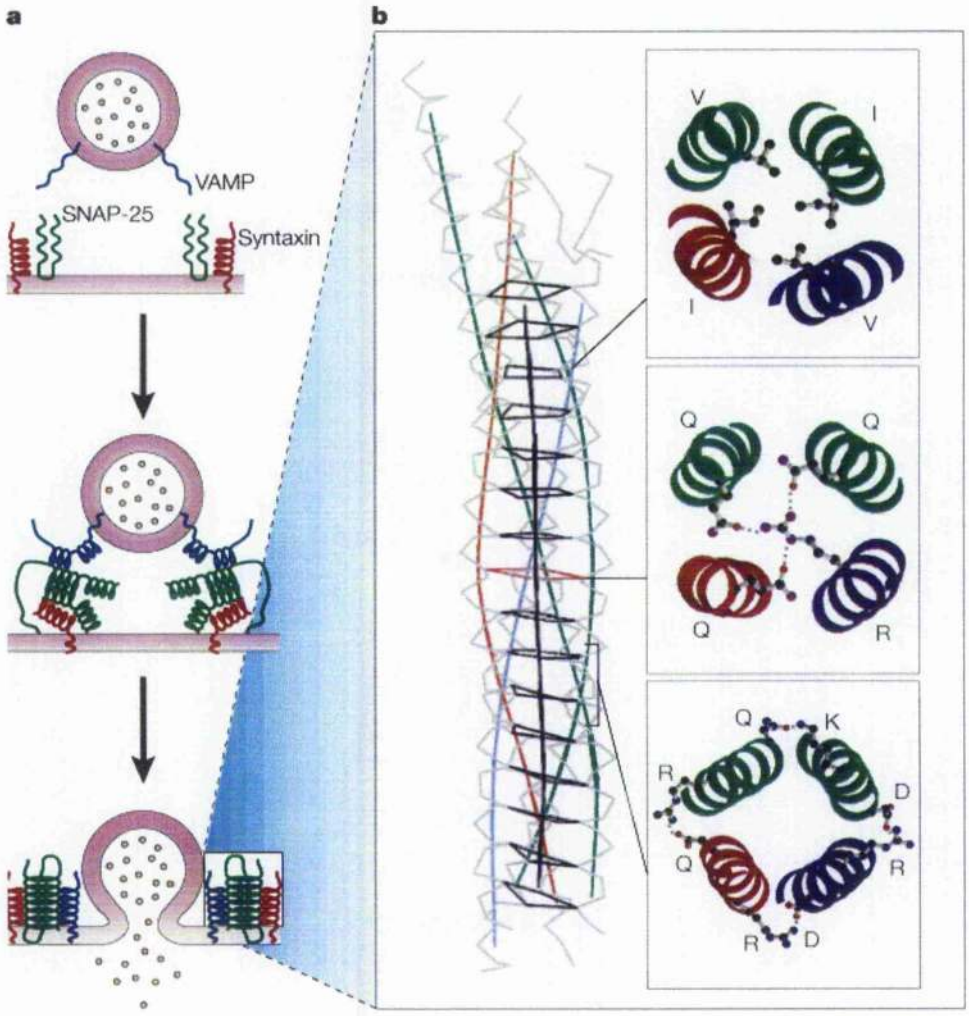

Figure 1.6 Schematic representation of vesicle fusion mediated by SNARE complex formation (adapted from Chen and Scheller, 2001)

(a) Vesicle R-SNARE VAMP (blue) associates with two Q-SNAREs of the target membrane syntaxin (red) and SNAP-25 (green).

(b) The structure of the SNARE complex with the central ionic layer (red) and 15 hydrophobic layers (black) that mediate the core interactions.

Top-bottom views of the side-chain interactions are shown on the right. Four SNARE helices are indicated by ribbon structures. Ball-and-stick structures represent the indicated amino acids. Hydrogen bonds or salt bridges are indicated by dotted lines.

SNARE complex can be reversibly disassembled by the ATPase activity of NSF with the aid of its adaptor, SNAP (Figure 1.7). Structural studies of three non-exocytic intracellular SNARE complexes demonstrated that their structure is remarkably similar to the well-studied neuronal exocotytic SNARE complex. However, four helices of these three SNARE complexes are contributed by four SNAREs instead of three in the case of neuronal exocytic SNARE. This difference is due to involvement of two SNAREs to contribute the Qb and Qc helices instead of one SNARE, which contributes both (Qbc). These intracellular SNARE complexes whose structure was determined include, a putative mammalian endosomal SNARE complex (STX 7, STX 8, Vti1b and VAMP 8) (Antonin *et al.*, 2002), a mammalian SNARE complex suggested to be involved in ER to Golgi transport (STX 5, membrin, rbet1 and sec22b) (Xu *et al.*, 2000) and a yeast complex presumably involved in homotypic vaculole fusion (Vam3p, Vti1p, Vam7p and Nyv1p) (Fukuda *et al.*, 2000).

Ternary SNARE complexes are resistant to SDS denaturation (Hayashi *et al.*, 1994) and protease digestion (Fasshauer *et al.*, 1998; Hayashi *et al.*, 1994). Even though uncomplexed SNARE proteins are targets for clostridial neurotoxins such as botulinum and tetanus toxins (Jahn and Niemann, 1994), the SNARE complex is resistant to clostridial neurotoxin cleavage (Hayashi *et al.*, 1994) and is heat stable up to about 90°C (Yang *et al.*, 1999).

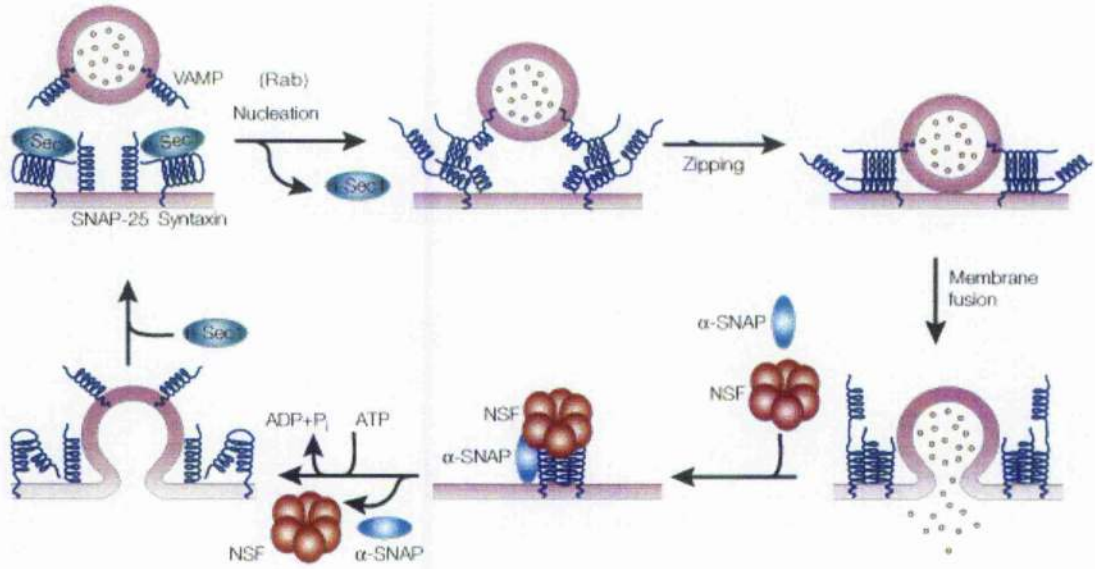

Figure 1.7 Involvement of Sec/ Munc proteins, NSF and α-SNAP in SNARE complex dynamics (adapted from Chen and Scheller, 2001)

The protein n-Sec1 of Sec/Munc family stabilises the closed conformation of syntaxin and regulates the SNARE complex formation. Rab proteins might facilitate the dissociation of n-Sec1 from syntaxin allowing subsequent association of SNAREs. α-SNAP and NSF mediate dissociation of cis-SNARE complex (post-fusion SNARE complex when both R- and Q-SNAREs are found in the same membrane) by hydrolysis of ATP and make them available for another round of fusion.

1.11.2 R-SNAREs (VAMPs)

VAMPs were first identified as components of synaptic vesicles (Trimble *et al.*, 1988). About ten different R-SNAREs have been identified to date from mammalian tissues (Steegmaier *et al.*, 1999). VAMPs have a proline rich N-terminal region of about 24 amino acids, in addition to a SNARE domain (Chen and Scheller, 2001).

VAMP1 and 2 are highly homologous and are localised to synaptic vesicles and secretory granules. VAMP3 is ubiquitously expressed and is associated with endocytic pathway (McMahon *et al.*, 1993). VAMP4 is expressed in variety of tissues and is localised to the TGN (Steegmaier *et al.*, 1999). VAMP5 has been demonstrated to

increase *in vitro* myogenesis and was localised to the PM (Zeng *et al.*, 1998). VAMP7 is localised to LEs (Advani *et al.*, 1998) and VAMP8 to EEs (Wong *et al.*, 1998). In addition to these, the VAMP homologue sec22b is associated with the ER (Hay and Scheller, 1997). The other VAMP homologues ERS-24 (Paek *et al.*, 1997) and Ykt6 (McNew *et al.*, 1997) are implicated in trafficking between the ER and the Golgi.

1.11.3 Syntaxins

Syntaxins were first identified as components of the PM of presynaptic terminals (Bennett *et al.*, 1992). Subsequently, a number of the members of syntaxin family were identified in a variety of membrane compartments of the exocytic and endocytic pathways of eukaryotic cells (Becherer *et al.*, 1996; Darsow *et al.*, 1997). There are 16 mammalian syntaxins described, making it the largest SNARE family identified so far (Gerst, 1999). Seven syntaxin genes have been identified in yeast, and there are other syntaxin-like sequences in all eukaryotes examined to date (Teng *et al.*, 2001). Typically syntaxins are proteins of about 300 amino acids.

STX 1, 2, 3 and 4 are predominantly localised to the PM and they mediate constitutive and regulated vesicle transport to the PM (Inoue *et al.*, 1992; Bennett *et al.*, 1993). STX 5 is localised to the Golgi (Dascher *et al.*, 1994). The majority of STX 6 (Bock *et al.*, 1997), 10 (Tang *et al.*, 1998b) 11 (Valdez *et al.*, 1999) and 16 (Tang *et al.*, 1998a) are localised to the TGN. (Recently, STX 6, STX 8 and STX 10 have been classified as Qc-SNAREs, rather than Qa-SNAREs based on a genome scale comparison of SNARE-motif sequences (Bock *et al.*, 2001). STX 7 (Wong *et al.*, 1998), STX 8 (Subramaniam *et al.*, 2000), STX 12 (Tang *et al.*, 1998c) and STX 13 (Prekeris *et al.*, 1999a) are localised in post-Golgi endosomal membranes. STX 17 is distributed in smooth endoplasmic reticulum (Steegmaier *et al.*, 2000) and STX 18 in the endoplasmic reticulum (Hatsuzawa *et al.*, 2000). Figure 1.8 shows the distribution of syntaxins in different cellular membranes.

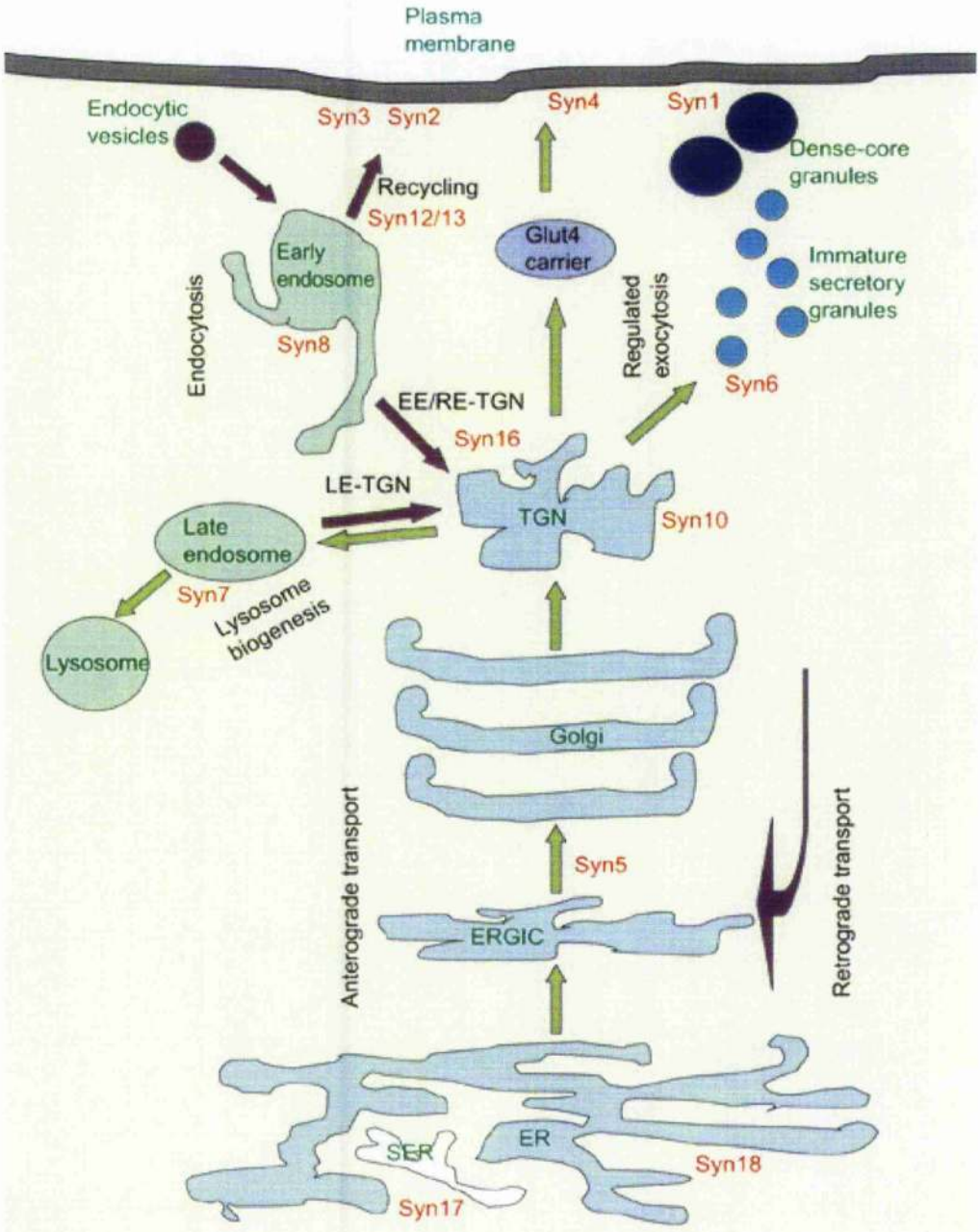

Figure 1.8 Distribution of syntaxins in different membranes of the cell (adapted from Teng *et al.*, 2001)

Figure 1.8 shows the subcellular localisation of the syntaxins (red) in relation to anterograde (exocytic) (green arrows) and retrograde (endocytic) (purple arrows) vesicle trafficking pathways and known transport steps (black).

ER- endoplasmic reticulum; ERGIC- ER-Golgi intermediate compartment; SER- smooth endoplasmic reticulum; Syn- syntaxins

All mammalian syntaxins except STX 11, are TM proteins anchored to the membrane by their C-terminal tail. Other than TM domains, there are several hydrophobic regions in syntaxin with the potential to form coiled-coil α-helical structures. Four such domains have been recognised from the majority of Qa-SNAREs. An approximately 60-residue long membrane proximal domain is the SNARE domain, which is characteristic of and conserved in all syntaxins. N-terminal domains of syntaxin are conserved between syntaxins that function in the same trafficking pathway. These domains were found to be different between syntaxins that function at different trafficking steps (Weimbs *et al.*, 1997). Uncomplexed syntaxins show a closed conformation and it switches to an open state upon binding to SNAP-25 (Fiebig *et al.*, 1999). In the closed conformation of syntaxin, N-terminal helices fold back to interact with the C-terminal SNARE motif. The TM tail anchor is essential for syntaxin membrane localisation, but in most cases it is not sufficient for targeting to specific membranes. Compartmental targeting signals, which are ill defined, reside in the targeting domains (Reviewed in Teng *et al.*, 2001).

Di-leucine motifs are identified as sorting signals present in endosomal/ lysosomal targeted proteins (Letourneur and Klausner, 1992) and have been found to bind to adapter complexes AP-1, AP-2 (Heilker *et al.*, 1996) and AP3 (Darsow *et al.*, 1998). Several members of the syntaxin family associated with the TGN and endosomes contain putative di-leucine signals, suggesting the involvement of these motifs in sorting of syntaxins. These include STX 6, 7, 8, 12 and 16 (Reviewed in Tang and Hong, 1999). These di-leucine motifs were not identified in STX 5, which resides in Golgi or STX 1-4, which reside in PM. Similar findings were obtained with the yeast homologues (Reviewed in Tang and Hong, 1999). The involvement of di-leucine motifs in the localisation of STX 7 and 8 has been demonstrated (Kasai and Akagawa, 2001). It was shown that the tyrosine-based (YGRL) motif of STX 6 in concert with its SNARE motif plays a major role in maintaining STX 6 in the TGN (Watson and Pessin, 2000). Although a role for the TM domain of STX 5 in its localisation to the Golgi is established a role for the TM domains of STX 6, 7 or 8 in sorting has not been identified (Kasai and Akagawa, 2001).

Syntaxins have been shown to interact with a range of other proteins as well as their SNARE partners. They are either components of vesicular transport machinery (vesicle

coat proteins, Rab GTPases and tethering factors) or proteins with no predicted function in vesicular transport. For example, STX 1A and STX 3 have been known to interact with sodium channels in epithelial cells, thereby regulating the intrinsic properties and cell-surface expression of the channels (reviewed in Teng *et al.*, 2001).

1.11.4 SNAP-25 family

In contrast to the large family of syntaxins only three members of mammalian SNAP-25 family (the other Q-SNARE family) are recognised to date. The first member identified was SNAP-25, which was characterised as a synaptosomal protein (Oyler *et al.*, 1989). SNAP-25 is a 206 amino acid protein expressed in neuronal tissues. SNAP-23 (or syndet) and SNAP-29 are ubiquitously expressed homologues of SNAP-25 (Hodel, 1998; Steegmaier *et al.*, 1998). The N- and C-terminal domains of the SNAP-25 family of proteins are highly conserved and are predicted to form coiled-coil structures. SNAP-25 and -23 associate with membranes through palmitoyl residues that are thioester linked to four adjacent cysteine residues located in the middle of the protein (Hodel, 1998). SNAP-29 lacks this cysteine rich palmitoylation site and is thought to be associated with membranes by interaction with other membrane proteins such as syntaxins (Steegmaier *et al.*, 1998). SNAP-25 and -23 are primarily localised to the PM while SNAP-29 is predominantly found in intracellular membranes. SNAP-29 is suggested to be involved in multiple transport steps, interacting with different syntaxins and VAMPs, which themselves are specifically localised to distinct membranes (Steegmaier *et al.*, 1998). These three SNAP-25 homologues are classified as Qbc-SNAREs due to their contribution of two helices in the SNARE complex formation (Table 1.1).

1.11.5 NSF and SNAP

Cells have evolved a specialised chaperone, NSF, and its adaptor, soluble NSF attachment protein (SNAP), to disassociate the highly stable SNARE complex. Both NSF and SNAPs are structurally and functionally conserved, and participate in virtually all intracellular trafficking steps (Rothman and Warren, 1994). NSF and α-SNAP act together to dissociate SNARE complexes (Figure 1.7), allowing SNAREs to recycle for another round of fusion. It was recently suggested that NSF/SNAP prime the docking step in SNARE assembly by dissociating preformed complexes allowing syntaxins to form into an active conformation (Gerst, 1999).

NSF is a hexamer with three subunits, one of which is crucial for its ATPase activity (Fleming *et al.*, 1998; Wilson *et al.*, 1989). There are three mammalian variants of SNAPs referred to as α-, β-, γ- (Clary *et al.*, 1990). The SNAP- interacting region of SNAREs overlap, with the SNARE complex forming region (Hayashi *et al.*, 1995). β-SNAP is brain specific and probably functionally equivalent to α-SNAP (Sudlow *et al.*, 1996). γ-SNAP enhances binding of α-SNAP to membranes (Whiteheart *et al.*, 1993).

1.12 Sec /Munc (SM) proteins

SM proteins are hydrophilic proteins of 60- 70 kD, originally identified by a genetic screen of *Caenorhabditis elegans* and yeast. All SM proteins interact tightly with syntaxins and play an essential role in membrane fusion (Pevsner *et al.*, 1994; Jahn and Sudhof, 1999). Four members of the Sec1 protein family (Sec1p, Slp1p, Vps45p, Sly1p) were identified in yeast. Sec1p related proteins have also been identified in the nervous tissue of *Caenorhabditis elegans* (UNC-180) and *Drosophila melanogaster* (Rop). In mammals, similar proteins known as Munc18, n-Sec1 and rbSec1 were identified as syntaxin binding proteins in brain tissue.

The neuronal Sec1 protein (n-Sec1) was shown to inhibit the association of STX 1 with SNAP-25, and, overexpression of (sec1 homologue) *Drosophila* Rop inhibits neurotransmitter release *in vivo*. In addition, the presence of Sec1 has been shown to inhibit membrane traffic *in vivo* (Dresbach *et al.*, 1998). On the other hand, lack of neuron specific Munc 18a has been associated with loss of synaptic transmission in mice (Verhage *et al.*, 2000). Similarly, null mutations of these genes have caused a dramatic reduction in vesicle exocytosis. Therefore these proteins are thought to play both negative and positive roles in membrane fusion events (Waters and Hughson, 2000). Munc 18 binds to the closed conformation of syntaxin and stabilises it, therefore preventing formation of SNARE complex causing a negative regulatory effect (Waters and Hughson, 2000). However this effect is known to prevent the reformation of cis-SNARE complex (association of SNAREs in the same membrane) after the membrane fusion event (Woodman, 2000). A positive role of *Drosophila* homologue Rop in neurotransmitter release was demonstrated in addition to its inhibitory role in neurotransmitter release (Wu *et al.*, 1998a). A positive role of Sec1

proteins has been suggested to involve a conformational change in syntaxin upon binding with Sec1 so that syntaxin can efficiently bind with its cognate SNAREs upon its release from Sec1. This area remains the subject of intense debate.

1.13 Rab protein family

This is a family of low molecular weight (20-25 kD) (Jahn and Sudhof, 1999), GTPases of about 200 amino acids which are homologous to the protooncogene Ras. They are implicated as a group of central regulators of vesicle budding, trafficking and fusion events (Stenmark and Olkkonen, 2001). It is estimated that human genome encodes for at least 60 different Rab family members (Bock *et al.*, 2001). Different members of Rab are localised in membranes of specific cellular organelles suggesting that they mediate specificity of vesicular transport. e.g. Rab4 is mainly found in the EE and Rab11 is predominant in the RE whereas Rab7 and 9 are primarily localised in the LE (reviewed in Mellman, 1996).

Rab proteins share the two conformations, which are common for all GTPases, GTP-bound and -unbound forms. The GTP-bound form is active and binds to specific membranes and interacts with its own set of downstream effectors (Zerial and McBride, 2001). The GDP-bound inactive form of Rab is maintained in the cytosol by Rab GDP-dissociation inhibitors (GDI). This activity prevents nonspecific binding of Rab to membranes. GDI is displaced by a GDI displacement factor upon binding to a specific membrane compartment. Rab is activated by converting GDP to GTP by guanine nucleotide exchange factors (GEFs). The active form is resistant to displacement from membranes by Rab GDI. GTP hydrolysis by intrinsic GTPase activity of Rab protein with the aid of GTPase-activating proteins (GAPs) displaces the Rab from membrane (Reviewed in Novick and Zerial, 1997; Brunger, 2001).

The Sec/Munc dependent block on syntaxins is suggested to be released by the action of Rab proteins (Woodman, 2000). Furthermore, Rabs are thought to drive the assembly of *trans* SNARE complex (association of the SNAREs in two different membranes) by recruiting tethering factors that draw the membranes together (reviewed in Woodman, 2000).

Rab4 and Rab11 regulate recycling from EE (de Wit *et al.*, 2001). Rab4 and has been implicated in GLUT4 vesicle trafficking (Bortoluzzi *et al.*, 1996). Rab 11 is also a component of GLUT4 vesicles (Al Hasani *et al.*, 2002). It is suggested that Rab proteins might displace Munc 18c from STX 4 (Misura *et al.*, 2000).

1.14 SNAREs and SNARE binding proteins involved in GLUT4 trafficking

The first implication of the participation of SNAREs in GLUT4 trafficking was the identification of a VAMP homologue in GLUT4 vesicles from rat adipocytes using an antibody to brain synaptobrevin (Cain *et al.*, 1992). It was subsequently shown that adipocytes and muscle express at least two R-SNAREs involved in endosomal recycling, cellubrevin (VAMP3) and VAMP2 (Volchuk *et al.*, 1994, Volchuk *et al.*, 1995). Both VAMP2 and cellubrevin undergo insulin-dependent movement to cell surface and both are expressed in numerous cell types (Martin *et al.*, 1996). VAMP2 and cellubrevin have been identified from immunopurified GLUT4 vesicles in insulin-responsive cells (Volchuk *et al.*, 1996; Martin *et al.*, 1996). Immuno electron microscopic examinations in isolated rat adipocytes revealed that a large fraction of VAMP2 was targeted to the GSV compartment whereas the majority of cellubrevin was observed in endosomal structures (Martin *et al.*, 1996; McMahon *et al.*, 1993). Q-SNAREs STX 2, 3, 4 (Timmers *et al.*, 1996; Volchuk *et al.*, 1996; Olson *et al.*, 1997) and SNAP-23 (Wang *et al.*, 1997; Wong *et al.*, 1997) have been identified in the PM of 3T3-L1 adipocytes.

The crucial function of VAMP2, STX 4 and SNAP-23 in insulin-stimulated GLUT4 translocation was demonstrated by several studies. Most of these studies used microinjection or overexpression of mutant or wild type protein or synthetic peptides, incubation of permeabilised cells with specific antibodies or microinjection of clostridial neurotoxins, which specifically cleave different SNAREs (see below).

STX 4 is largely located at the PM of fat and muscle cells (Volchuk *et al.*, 1996; Sumitani *et al.*, 1995). STX 4 was the first Q-SNARE investigated extensively in respect of the insulin-stimulated GLUT4 translocation process. STX 4 is resistant to cleavage by botulinum toxin C, even though it cleaves STX 1-3 (reviewed in Foster and Klip, 2000). Therefore use of other approaches such as microinjection of anti-STX 4 antibodies (Tellam *et al.*, 1997) or the cytosolic domain of STX 4 (Cheatham *et al.*,

1996; Olson *et al.*, 1997; Macaulay *et al.*, 1997) or overexpression of cytosoloic domain of STX 4 using vaccinia virus vector (Olson *et al.*, 1997) were used to inhibit cellular STX 4 function. These approaches resulted in an around 50% inhibition of insulin-dependent glucose transport in 3T3-L1 adipocytes (Cheatham *et al.*, 1996; Olson *et al.*, 1997; Tellam *et al.*, 1997) and primary rat adipocytes (Timmers *et al.*, 1996). It was also found that homozygous knockout of the STX 4 gene in mice cause early embryonic death and the heterozygous knockout mice develop insulin resistance in muscle (Yang *et al.*, 2001).

VAMP2 is known to function in regulated vesicle trafficking in several tissues. These include release of neurotransmitter in neural synapses, insulin-stimulated GLUT4 translocation in fat and muscle cells and aquaporin-2 translocation in renal collecting ducts (reviewed in Foster and Klip, 2000). VAMP2 was shown to be distributed in similar proportions in the PM and intracellular membranes (Martin *et al.*, 1996; Martin *et al.*, 1998). It has been shown that GLUT4 is primarily recruited to the PM in response to insulin by fusion of pre-existing VAMP2 positive vesicles using a novel immunocytochemical technique which enables high labelling efficiency and 3-D resolution of cytoplasmic rims isolated from rat adipocytes (Ramm *et al.*, 2000).

The functional importance of VAMP2 in insulin-stimulated GLUT4 translocation has been identified by several approaches. These evidences include around 50% inhibition of GLUT4 translocation by microinjection of clostridial neurotoxins (botulinum toxins B and D), which specifically cleave VAMP2 (Cheatham *et al.*, 1996; Macaulay *et al.*, 1997) or by introduction of the cytoplasmic domain of VAMP2 into permeabilised cells by microinjection or by expression using vaccinia virus (Cheatham *et al.*, 1996; Olson *et al.*, 1997). In addition, introduction of anti-VAMP2 antibodies also diminished GLUT4 level in the PM in response to insulin. Another study demonstrated that VAMP2 inhibited GLUT4 translocation, without affecting constitutive trafficking, using the cytosolic domain of VAMP2 in permeabilised 3T3-L1 adipocytes (Martin *et al.*, 1996) or peptides (Martin *et al.*, 1998).

SNAP-23 (syndet), is an ubiquitously expressed homologue of the neuronal SNARE SNAP-25. The involvement of SNAP-23 in GLUT4 translocation in rat adipose tissue has been identified (St Denis *et al.*, 1999). Immunoprecipitation of SNAP-23 showed

its association with VAMP2 and STX 4 (Foster *et al.*, 1998). It is reported that microinjection of anti-SNAP-23 antibodies and incubation of permeabilised cells with a C-terminal peptide of SNAP-23 significantly inhibited insulin stimulated GLUT4 translocation in 3T3-L1 adipocytes (Rea *et al.*, 1998), while the full-length protein stimulated translocation (Foster *et al.*, 1999). Several studies have shown that botulinum toxins A and E, which cleave SNAP-25 were less effective at cleaving SNAP-23 even though some studies reported inhibition of GLUT4 translocation by using these toxins (reviewed in Foster and Klip, 2000).

The interaction of these SNAREs, was found to be regulated by a range of SNARE binding proteins. Munc18-c and synip (syntaxin interacting protein) selectively interact with STX 4 and inhibit GLUT4 translocation in adipocytes (Min *et al.*, 1999; Nelson *et al.*, 2002). Cysteine string protein interacts with STX 4 in 3T3-L1 adipocytes and may regulate the conformation of STX 4 (Chamberlain *et al.*, 2001). VAMP-associated protein of 33 kD (VAP-33) is proposed to be a regulator of VAMP2 availability for GLUT4 traffic and other vesicle fusion events (Foster *et al.*, 2000). Pantophysin, a component of GLUT4 vesicle binds to VAMP2 and has been suggested to regulate the availability of VAMP2 (Brooks *et al.*, 2000). However, the mechanism by which these interactions are regulated and their role in GLUT4 vesicle fusion remains unclear at the present.

In mammals, Munc18a is expressed predominantly in neurons where it inhibits association of VAMP1 and SNAP25 with STX 1. Munc18b and c are expressed ubiquitously. Three different Sec1/Munc18 isoforms were recently cloned from 3T3-L1 adipocytes. Of these only Munc 18c exhibited a specific binding capacity to STX 4 and inhibited the in vitro binding of STX 4 to VAMP2. The subcellular localisation of Munc18c was almost identical to STX 4, both being enriched in the PM (Tellam *et al.*, 1997).

Overexpression of Munc18c (67 kD) in 3T3-L1 adipocytes by adenovirus mediated gene transfer resulted in inhibition of insulin-stimulated glucose transport in a dose-dependent manner (Tamori *et al.*, 1998; Thurmond *et al.*, 1998). In contrast, microinjection of Munc 18c antibody stimulated basal GLUT4 level in the PM in 3T3-L1 adipocytes (Macaulay *et al.*, 2002). Furthermore, inhibition of GLUT4

translocation into transverse tubules of skeletal muscle without affecting translocation to sarcolemma was observed when Munc 18c was overexpressed in transgenic mice (expressing GLUT4-EGFP) (Khan *et al.*, 2001). It was observed that overexpressed Munc 18c associates with STX 4 under basal state, which appeared to dissociate under insulin stimulation (Thurmond *et al.*, 1998). Munc 18c inhibited the *in vitro* binding of SNAP-23 to STX 4 (Araki *et al.*, 1997) and STX 4 with VAMP2 and VAMP3 (Tellam *et al.*, 1997). It was therefore suggested that insulin may de-repress the inhibitory function of Munc 18c on STX 4 (Thurmond *et al.*, 1998). This was supported by the observation of Fujita and co-workers who demonstrated the prevention of Munc 18a binding to STX 1 upon the phosphorylation of Munc 18a by protein kinase C, then allowing the association of VAMP1 with STX 1 (Fujita *et al.*, 1996).

Synip is expressed in insulin sensitive tissues (Min *et al.*, 1999) and binds specifically to STX 4 without interacting with the other PM syntaxins STX 1, 2 and 3. It was demonstrated that insulin causes dissociation of STX 4-Synip interaction *in vivo* and *in vitro* (Min *et al.*, 1999). Synip bears a PDZ domain, which has a role in the organisation of membrane signalling complexes, and coiled coil domains involved with the association with SNARE proteins (Min *et al.*, 1999). Synip is therefore proposed to be a candidate which might couple insulin signalling and the modulation of the SNARE complex (Cheatham, 2000). Figure 1.9 shows the involvement of SNAREs and SNARE binding proteins in insulin-stimulated GLU4 trafficking.

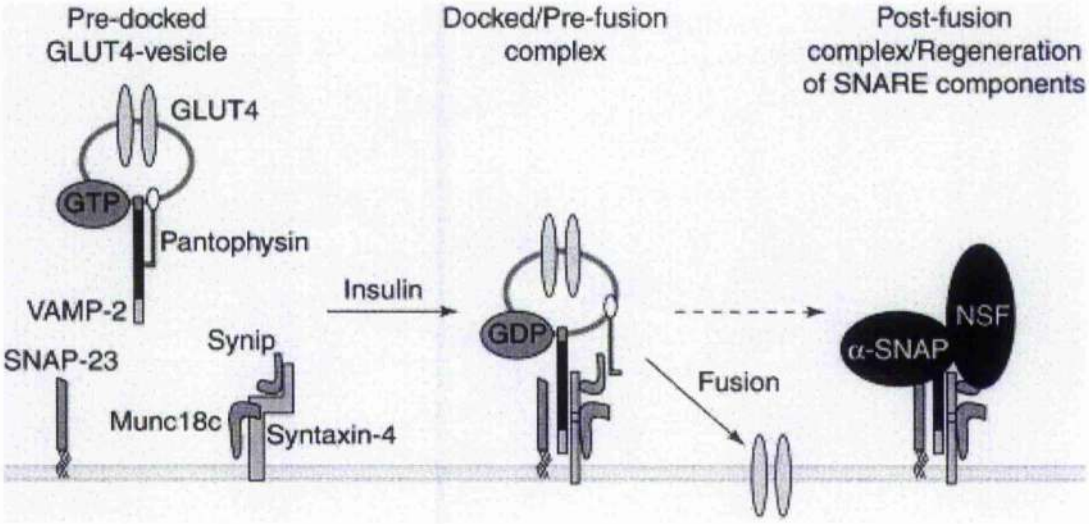

Figure 1.9 Role of SNAREs and SNARE associated proteins in GLUT4 translocation to PM in response to insulin (Adapted from Cheatham, 2000)

The R-SNARE VAMP2, which is a component of GLUT4 vesicles specifically interacts with Q-SNAREs STX 4 and SNAP-23 of the PM upon insulin stimulation. This interaction is known to be sufficient to drive the fusion of GLUT4 vesicles with the PM *in vitro*. Potential regulators of SNARE complex formation include the two STX 4 binding proteins, Munc18c and Synip and VAMP2 interacting protein pantophysin, which can modulate GLUT4 translocation. NSF and α-SNAP proteins dissociate the SNARE complex and allow regeneration of the SNAREs for another round of fusion.

1.15 Aims of the study

The role of SNARE proteins in insulin-stimulated GLUT4 translocation to the PM in fat and muscle tissues is well documented. However, to date there are no reports on the identification of SNAREs regulating the endocytic trafficking pathway of GLUT4 and more importantly on the SNARE involved in the traffic of GLUT4 into GSV.

The aim of this study was to study the distribution of STX 6, 8, 12 and 16 of 3T3-L1 adipocytes, and to identify their functional role in GLUT4 trafficking. Chapter 3 describes the distribution of the four post-Golgi sytaxins mentioned above, in relation to GLUT4. Chapter 4 describes the generation and use of recombinant adenoviruses in order to overexpress the cytosolic domain of sytaxins in 3T3-L1 adipocytes as a tool to use in functional studies. Chapter 5 describes the effect of inhibition of syntaxins 6, 8 and 12 on protein trafficking with main emphasis on GLUT4 trafficking. Finally, the biogenesis of insulin-responsive compartment during differentiation of 3T3-L1 cells was studied and is described in chapter 6.

Chapter 2

Materials and Methods

2.1 Materials

All materials used in this study were of high quality and were obtained from the following suppliers.

2.1.1 General reagents

Amersham Pharmacia Biotech, Little Chalfont, Buckinghamshire, UK

ECL Western blotting detection reagents

Horseradish peroxidase (HRP)-conjugated donkey anti-rabbit IgG antibody

Horseradish peroxidase (HRP)-conjugated sheep anti-mouse IgG antibody

Horseradish peroxidase (HRP)-conjugated protein A

Protein A Sepharose

Protein G Sepharose

Anachem Ltd., Luton, Bedfordshire, UK

30% acrylamide/bisacrylamide

Bio-rad Laboratories Ltd, Hemel Hempstead, Hertfordshire, UK

Bradford protein assay reagent

N,N,N',N'-tetramethylethylenediamine (TEMED)

Boehringer Mannheim, Germany

Brefeldin A

Isopropyl-thio-β-D-galactopyranoside (IPTG)

Protease inhibitor cocktail tablets: complete™ and complete mini™

Thesit (C12E8; Octaethylene glycol dodecyl ether)

CN Bioscience

Pansorbin cells (formaldehyde fixed *Staphylococus aureus* cells)

Fisher Scientific Ltd, Loughborough, Leicestershire, UK

Ammonium persulphate

Calcium chloride ($CaCl_2$)

Diaminoethanetetra-acetic acid, disodium salt (EDTA)

Disodium hydrogen orthophosphate (Na_2HPO_4)

D-Glucose

Glycerol

Glycine

N-2-hydroxyethylpiperizine-N'-2-ethanesulphonic acid (Hepes)

Hydrochloric acid (HCl)

Isopropanol

Magnesium sulphate ($MgSO_4$)

Methanol

Potassium chloride (KCl)

Potassium dihydrogen orthophosphate (KH_2PO_4)

Sodium chloride (NaCl)

Sodium dihydrogen orthophosphate dihydrate (NaH_2PO_4)

Sodium dodecyl sulphate (SDS)

Sodium hydrogen carbonate ($NaHCO_3$)

Sucrose

Tetra-sodium citrate ($Na_4C_6H_5O_7$)

Invitrogen, Groningen, The Netherlands

Electroporation cuvettes

pCRII-TOPO™ TA cloning kit

Konika Ltd, UK

X-Ray films

Life technologies, Paisley, Scotland, UK

Agarose

1kb DNA ladder

Merck Ltd (BDH), Lutterworth, Leicestershire, UK

Ethanolamine

Magnesium chloride ($MgCl_2$)

Tween 20

Zinc chloride ($ZnCl_2$)

Coverslips

Molecular probes, Oregon, USA

Alexa^{488}-conjugated donkey anti-mouse IgG secondary antibody

Alexa^{488}-conjugated donkey anti-rabbit IgG secondary antibody

3,3'-dioctadecylindocarbocyanine (DiI) LDL^{555}

Transferrin Oregon green^{488}

Transferrin Texas red^{595}

MWG-Biotech, Germany

All oligonucleotide primers

NEN Dupont (UK) Ltd, Stevanage, Hertfordshire, UK

^{3}H deoxy-Dglucose

$H_3{}^{32}PO_4$

^{125}I transferrin

New England Biolabs (UK) Ltd, Hitchin, Hertfordshire, UK

Pre-stained protein marker, broad range (6-175kDa)

Novo Nordisk, Denmark

Insulin (Porcine, monocomponent)

Nycomed, Norway

Optiprep^{TM} (Iodixanol)

Oxoid Ltd, Hampshire, UK

Bacteriological agar

Tryptone

Yeast extract

Pierce, Rockford, Illinois, USA

Slide-a-lyzer^{TM} dialysis cassettes

Streptavidin-HRP

Sulpho EZ-link NHC-LC biotin

Premier Brands UK, Knighton, Adbaston, Staffordshire, UK

Marvel powdered milk

Promega, Southampton, UK

All restriction enzymes

Calf intestinal alkaline phosphatase

Deoxynucleotide triphosphates (dNTPs)

Nuclease-free water

Pfu polymerase

Taq polymerase

Qiagen, Crawley, West Sussex, UK

Nickel NTA-agarose

QIAprep™ spin maxiprep kit

QIAprep™ spin miniprep kit

Qiagen gel purification kit

Schleicher & Schell, Dassel, Germany

Nitrocellulose membrane (pore size: 0.45μM)

Shandon, Pittsburgh, PA, USA

Immu-mount™ mounting medium

Whatman International Ltd, Maidstone, UK

Whatman No.1 filter paper

Whatman No.3 filter paper

Whatman 3 mm filter paper

All other chemicals used were supplied from Sigma Chemical Company Ltd, Poole, Dorset, UK unless otherwise mentioned.

2.1.2 Cell culture material

American Type Culture Collection, Rockville, USA

3T3-L1 fibroblasts

HEK 293 cells

HeLa cells were generous gifts from Dr. Pam Scott (University of Glasgow).

AS Nunc, DK Roskilde, Denmark

50 ml centrifuge tubes

13.5 ml centrifuge tubes

Bibby-Sterlin, Staffordshire, UK

Iwaki tissue culture plasticware, 6-well plates,75 cm2 flasks, 150 cm2 flasks

Graduated disposable pipettes

Gibco BRL, Paisley, Lanarkshire, UK

Dulbecco's modified Eagle's medium (with 4500mg/L glucose, without sodium pyruvate) (DMEM)

Foetal bovine serum (FBS) (USA)

Foetal bovine serum (ECU)

L-Glutamine

Lipofectamine reagent

Modified Eagle's medium (MEM)

Newborn calf serum (NCS)

Non-essential amino acids

Opti-MEM

Penicillin (10000 U/ml)/ Streptomycin (10000 U/ml) (P/S)

Trypsin/EDTA solution

Falcon tissue culture plastic ware, Fred Barer, UK

10 cm dishes

6-well plates

12-well plates

2.1.3 Primary antibodies

Anti-GLUT4 was generated by Dr. Alison Brant in this laboratory and is described in (Brant *et al.*, 1993).

Monoclonal anti-IRAP was the gift of Prof. Morris J. Birnbaum (University of Pennsylvania). A rabbit polyclonal IRAP was also used in some experiment, this was the gift of Prof. Paul F. Pilch, Boston University.

Monoclonal TfR antibody was from Zymed laboratories, Cambrige, UK.

SNAP-23 (Syndet) antibody was from synaptic systems.

Anti-syntaxin 4, anti-VAMP2 and anti cellubrevin were kind gifts from Prof. David James, University of Queensland, Australia.

Monoclonal anti-syntaxin 6 was from Transduction Laboratories, Lexington, KY.

Monoclonal anti-syntaxin 13 was from Bioquote Limited, York, UK.

Anti-syntaxin 8, 12 and 16 were a kind gift of Dr. Wanjin Hong, Institute of Molecular Cell Physiology, University of Singapore. These anti-syntaxin 8 and anti-syntaxin 12 antibodies were used for the initial experiments performed to identify the distribution of STX 8 and 12 in 3T3-L1 adipocytes.

2.1.4 *Escherichia coli* strains

DH5α

BJ5183

M15

2.1.5 General solutions

Citrate buffer	150 mM NaCl, 20 mM sodium citrate, pH 5.0
DNA loading buffer	40% (w/v) sucrose, 0.25% (w/v) bromophenol blue
His-tag buffer	100 mM Hepes, 200 mM KCl, 5 mM imidazole, pH 8.0
Immunofluorescence buffer (IF buffer)	PBS, 0.2% (v/v) fish skin gelatin, 0.5% (v/v) goat serum. Freshly made and filtered through a Nalgene 0.2μM vacuum type filter
Luria Broth (LB)	1% (w/v) tryptone, 0.5% (w/v) yeast extract, 1% (w/v) NaCl
Lysis buffer	20 mM Tris-HCl, 150 mM NaCl, 1% (w/v) $C_{12}E_8$ (Thesit), pH 7.4 proteinase inhibitors

Krebs Ringer phosphate (KRP)	128 mM NaCl, 4.7 mM KCl, 5 mM NaH_2PO_4, 1.25 mM $MgSO_4$, 1.25 mM $CaCl_2$, pH 7.4
Krebs Ringer MES buffer (KRM)	136 mM NaCl, 4.7 mM KCl, 1.25 mM $MgSO_4$, 10 mM MES, 25 mM glucose, pH 6.0
HES buffer	255 mM sucrose, 20 mM Hepes, 1 mM EDTA, pH 7.4
Phosphate buffered saline (PBS)	136 mM NaCl, 10 mM NaH_2PO_4, 2.5 mM KCl, 1.8 mM KH_2PO_4, pH 7.4
SDS-PAGE electrode buffer	25 mM Tris, 190 mM glycine, 0.1% (w/v) SDS
SDS-PAGE sample buffer	93 mM Tris-HCl pH 6.8, 1 mM sodium EDTA, 10% (v/v) glycerol, 2% (w/v) SDS, 0.002% (w/v) bromophenol blue, 20 mM dithiothrictol
1.3 x SDS sample buffer	120.9 mM Tris-HCl pH 6.8, 1.3 mM sodium EDTA, 13% (v/v) glycerol, 2.6% (w/v) SDS, 0.0026% (w/v) bromophenol blue, 6 M urea, 20 mM dithiothreitol
Super medium	1.5% tryptone, 2.5% yeast extract, 1% NaCl
TAE	40 mM Tris acetate, 1 mM EDTA pH 7.8
TBST	20 mM Tris-HCl, 150 mM NaCl, 0.08% (v/v) Tween-20, pH 7.4
Transfer buffer	25 mM Tris base, 192 mM glycine, 20% (v/v) methanol

2.2 Cell Culture

3T3-L1 cells for differentiation were grown in Falcon plastic ware for better adhesion. All other cells were grown in Iwaki plastic ware.

2.2.1 Growth of 3T3-L1 murine fibroblasts

Fibroblasts were cultured in DMEM, 10% (v/v) newborn calf serum and 100 U/ml penicillin and 100 μg/ml streptomycin (fibroblast media) at 10% CO_2 and 37°C. Cells for passaging were grown in 75 cm^2 flasks. Cells for experiments were grown in 10 cm dishes, 12-well or 6-well plates. Media was replaced every 2-3 days. Cells were passaged when they were 70-80% confluent. Cells for differentiation were grown 2-4 days post confluence and then differentiated into adipocytes.

2.2.2 Trypsinisation and passage of 3T3-L1 fibroblasts

One 75 cm^2 flask was usually split into roughly 6-10, 10 cm dishes. Media of sub-confluent fibroblasts was aspirated and the cells were washed twice with sterile PBS (section 2.1.5). Cells were then incubated with 2 ml trypsin/EDTA at 37 °C and 10% CO_2 for about 2 min. Cells were lifted by careful agitation and were resuspended in the required volume of fibroblast media (section 2.2.1). The cell suspension was split between 10 cm dishes, 12-well or 6-well plates and 75 cm^2 flasks with intermittent mixing of the cell suspension prior to dispersal.

2.2.3 Differentiation of 3T3-L1 fibroblasts

Differentiation media contained DMEM, 10% (v/v) foetal bovine serum (FBS), 100 U/ml penicillin and 100 µg/ml streptomycin, 0.25 µM dexamethasone, 0.5 mM isobutyl methyl xanthine (IBMX) and 1 µg/ml insulin, which were prepared as outlined below.

A stock solution of 2.5 mM dexamethasone (in ethanol) was diluted prior to differentiation in DMEM, 10% FBS, 100 U/ml penicillin and 100 µg/ml streptomycin to yield a 500x stock solution. An IBMX 500x solution was prepared freshly by dissolving 55 mg of IBMX in 1 ml of 1 M KOH. Insulin (1 mg/ml) was prepared in 0.01 M HCl. Dexamethasone and IBMX were then added to DMEM, 10% FBS, 100 U/ml penicillin and 100 µg/ml streptomycin media at 1x final concentration in the total volume required for differentiation. Insulin was added to 1 µg/ml . Fibroblasts between passages 4 and 12 were used for differentiation. The growth media of 2-4 day post confluent 3T3-L1 fibroblasts was aspirated and replaced with differentiation media. Cells were grown for 2 days in the same media and replaced the media with DMEM, 10% FBS, 100 U/ml penicillin and 100 µg/ml streptomycin, 1 µg/ml insulin. After another 2 days media was replaced with DMEM, 10% FBS, 100 U/ml penicillin and 100 µg/ml streptomycin media and changed every 2 days. Cells were used for experiments 8-12 days post differentiation.

2.2.4 Freezing and storage of cells

Fibroblasts grown to about 80% confluence were trypsinised as described in section 2.2.2. About 8 ml fibroblast media (section 2.2.1) per 75 cm^2 flask was added to

trypsinised cells and the cells were gently resuspended. The cells were subsequently centrifuged at 2000 x g for 4 min. The cell pellet was resuspended gently in 1 ml of fibroblast media containing 10% (v/v) DMSO. The cell suspension was transferred to a 1.8 ml polypropylene cryo-vial and placed at -80°C overnight and then stored in a liquid nitrogen vat.

2.2.5 Resurrection of cells

Cells stored at liquid nitrogen were rapidly thawed by incubating at 37°C. Cell clumps were dispersed by pipetting and were transferred to a flask containing previously equilibrated fibroblast media (section 2.2.1) at 37°C. Growth media were changed the following day to remove the DMSO.

2.2.6 Growth of HEK 293 cells

Human embryonic kidney (HEK) 293 cells were cultured in DMEM supplemented with 10% FCS, 2 mM L-glutamine and 100 U/ml penicillin and 100 µg/ml streptomycin at 5% CO_2 and 37°C. Media were replaced every 2-3 days. Cells were trypsinised and passaged around 80% confluence as described in section 2.2.2.

2.2.7 Growth of HeLa cells

Human cervical carcinoma cells were cultured in minimum essential medium supplemented with 10% FCS (v/v) (EU origin), 1% non-essential amino acids, 2 mM L-glutamine, 100 U/ml penicillin and 100 µg/ml streptomycin at 5% CO_2 and 37°C. Media were replaced every 2-3 days. Cells were trypsinised and passaged around 80% confluence as described in section 2.2.2.

Freezing and resurrection of HEK 293 or HeLa cells were performed as outlined in sections 2.2.4 and 2.2.5 with the use of appropriate cell culture media.

2.3 General Laboratory procedures

2.3.1 Preparation of 3T3-L1 adipocyte homogenate

Cells cultured in 10 cm plates were serum starved for 2 h and treated in separate groups according to the experimental condition. (e.g. ± insulin). At the end of treatment, plates were transferred to ice and cells were washed three times with ice-

cold HES buffer (see section 2.1.5). Cells were scraped in about 1-2 ml ice-cold HES buffer containing protease inhibitors per plate. Then the cells were homogenised with twenty hand strokes in a Teflon/ glass homogeniser.

2.3.2 Total membrane preparation

Cells cultured on 10 cm plates were either experimentally treated or incubated at 37°C in serum free DMEM for 2 h. Plates were transferred to ice and cell homogenates were obtained as described in section 2.3.1. The homogenate was centrifuged at 180,000 x g for 1 h at 4°C. The pellet from this spin was dissolved in HES buffer containing proteinase inhibitors. These total membrane fractions were snap frozen in liquid nitrogen and stored at -80°C prior to analysis.

2.3.3 Subcellular fractionation

All buffers and consumables were pre-chilled and all centrifugation steps were carried out at 4°C. Homogenates of 3T3-L1 adipocytes were transferred to pre-chilled Oakridge Beckman centrifuge tubes and centrifuged at 19,000 x g for 20 min in Beckman JA-20 rotor. The resulting pellet was resuspended in 1 ml ice-cold HES buffer (section 2.1.5) and layered onto 1 ml cushion of 1.2 M sucrose, 20 mM Hepes, 1 mM EDTA, pH 7.4. This was centrifuged at 100,000 x g for 1 h in a swing out rotor (Beckman TLS-55). A fraction enriched in plasma membranes was collected from the layer just above the sucrose cushion, using a pasteur pipette. The plasma membrane fraction was diluted 5-fold in 20 mM Hepes, 1 mM EDTA, pH 7.4 and centrifuged at 40,000 x g for 20 min in a fixed angle rotor (TLA-100).

The supernatant of the initial spin was centrifuged at 41,000 x g for 20 min, yielding a pellet referred as high-density microsomal fraction (HDM). The resulting supernatant was centrifuged at 180,000 x g for 1 h (in Beckman TLA-100 rotor), yielding a pellet referred as the low-density microsomal fraction (LDM). The supernatant of this spin contains the soluble proteins.

All membrane fractions were resuspended in HES buffer containing proteinase inhibitors. Fractions were snap frozen in liquid nitrogen and stored at -80°C prior to analysis.

2.3.4 Iodixanol gradients

Optiprep is a sterile solution of iodixanol (5,5'[(2-hydroxy-1-3propanediyl)-bis(acetylamino)]bis[2,3dyhydroxypropyl-2,4,6-triiodo-1,3-benzenecarboxamide].

Low-density microsomal (LDM) membranes were prepared as described (see section 2.3.3) and mixed with iodixanol to a final concentration of 14%. Total volumes were made up to 3.9 ml using HES buffer (see section 2.1.5) and were sealed in quick seal Beckman polyallomer tubes. Contents of the tube were mixed and spun at 295,000 x g in a near vertical rotor (Beckman, TLN100) for 1 h at 4°C. Acceleration from 0-5000 rpm during centrifugation was set to be 5 min and deceleration was set without brakes in order not to disturb the gradient. Fractions of 300 µl were collected from the bottom by piercing the tube. All fractions were snap frozen in liquid nitrogen and stored at –80°C prior to analysis.

2.3.5 Protein estimation

Protein concentration of various cell fractions was measured by the Bradford method (Bradford, 1976) using Biorad Coomassie Brilliant Blue reagent. Bovine serum albumin 1-5 µg was used as the standard. Sample volumes were used within the linear range of the standard curve. Assays were set up in duplicate, in 1 cm disposable cuvettes, according to manufacturer's instructions and absorbance was measured at 595 nm. Protein concentrations were calculated using the standard values.

2.3.6 SDS polyacrylamide gel electrophoresis (SDS-PAGE)

SDS Polyacrylamide gel electrophoresis was carried out using Bio-Rad mini-PROTEAN II gel apparatus. The percentage of acrylamide in a gel, ranged from 7.5%-15%, according to the molecular weight of the protein of interest.

The resolving gel was prepared using 30% acrylamide/bisacrylamide, 1.5 M Tris-HCl (pH 8.8) (to a final concentration of 375 mM), 10% (w/v) SDS (to a final concentration of 0.1%), polymerised with 10%(w/v) ammonium persulphate (to a final concentration of 0.1%) and TEMED (to a final concentration of 0.01%).

The stacking gel was prepared using 30% acrylamide/bisacrylamide, 1 M Tris-HCl (pH 6.8) (to a final concentration of 125 mM), 10% (w/v) SDS (to a final

concentration of 0.1%), polymerised with 10% (w/v) ammonium persulphate (to a final concentration of 0.1%) and TEMED (to a final concentration of 0.05%).

Protein samples were solubilised in sample buffer (93 mM Tris-HCl, pH 6.8, 1 mM sodium EDTA, 10% (w/v) glycerol, 2% (w/v) SDS, 0.002% (w/v) bromophenol blue 20 mM dithiothreitol (added immediately before boiling), and incubated in a boiling water bath for 3 min. Gels were immersed in SDS-PAGE electrode buffer (see section 2.1.5) and electrophoresed until the dye front had reached the desired position or until adequate separation of pre-stained molecular weight markers was achieved. A constant voltage of 80 volts was applied through the stacking gel, which was increased to 120 volts through the resolving gel.

2.3.7 Western blotting

After separation of the proteins as described earlier, gels were removed from the plates. A sandwiched arrangement of components, individually soaked in transfer buffer (see section 2.1.5), were made as follows from bottom to top: a sponge pad, a layer of Whatmann 3 mm filter paper, nitrocellulose paper (pore size 0.45 μm), polyacrylamide gel (electrophoresed to resolve proteins), a layer of Whatmann 3 mm filter paper, a sponge pad. The sandwich was placed in a cassette and slotted, bottom nearest to cathode, into a Bio-Rad mini trans-blot tank filled with transfer buffer. Transfer of proteins was performed at room temperature for 3 hours at a constant current of 250 mA or overnight at 40 mA. Efficiency of transfer was determined by staining the nitrocellulose membrane with Ponceau S solution prior to blocking.

2.3.8 Immunodetection of proteins

Following Western blotting, nitrocellulose membrane was incubated with 5% (w/v) dried non-fat milk (see section 2.1.1.) made up in TBST (see section 2.1.5) for 1 h to block non-specific binding sites. Primary antibodies were diluted in 1% (w/v) non-fat milk/ TBST at the appropriate dilution. Membrane was incubated with primary antibody of interest for 1 h on a shaking platform at room temperature. Membrane was washed five times over 1 h with TBST and incubated with the appropriate secondary antibody (HRP-linked Ig) at a 1:1000 dilution for 1 h at room temperature. Then the membrane was washed five times over 1 h with TBST.

2.3.9 Immunoblot analysis.

Immuno-labelled proteins on Western blots were visualised using HRP-conjugated secondary antibody and the ECL system (Amersham, UK). ECL detection reagents 1 and 2 were mixed 1:1 and the membrane was immersed for 1 min. Membrane was dried slightly and exposed to Konica X-ray film in a light-proof cassette. Multiple exposures of X-ray film were performed in order to ensure linearity of response to film to signal. The film was developed using an X-OMAT processor. Bands were quantified by densitometry using NIH image software. All immunoblot signals were quantified from linear regions of the protein titration curve.

2.3.10 Coomassie blue staining of SDS polyacrylamide gel

A 0.25% Coomassie blue stain solution was prepared by mixing 10% glacial acetic acid (v/v), with 90% methanol: H_2O (1:1 v/v) mixture and 0.25 g of Coomassie Brilliant Blue. The mixture was stirred well and filtered through Whatman number 1 filter paper. Following electrophoresis, SDS polyacrylamide gel was immersed in the stain for about 2 h and destained with the same acetic acid, methanol: H_2O mixture (without dye) described in this section. Destaining was continued from 2 h to overnight depending on the resolution required.

2.3.11 Endosome ablation

Ablation of the recycling endosomal system was carried out as described by Livingstone and co-workers (Livingstone *et al.*, 1996).

Cells were serum starved for 2 h at 37°C. During the last hour, transferrin-HRP conjugate was added to a final concentration of 20 μg/ml. The cell plates were then placed on ice, washed three times over a period of 10 min with ice-cold isotonic citric buffer (150 mM NaCl, 20 mM tri-sodium citrate, pH 5.0) and once with ice-cold PBS (see section 2.1.5). A freshly prepared solution of 3,3'-diaminobenzidine (2 mg/ml) was vortexed thoroughly, filtered through a 0.22 μm pore size filter and added to all plates of cells at 100 μg/ml. H_2O_2 was added (at a concentration of 0.02% v/v) to the ablation group (half of the cells) but not to the control group. The cells were incubated for 1 h at 4°C in the dark. The ablation reaction was terminated by washing the cells

with ice-cold PBS. Cell homogenates and LDM were prepared as described in section 2.3.3.

2.3.12 Immunoprecipitation (IP)

Preparation of cell lysate

Cells were washed three times in ice-cold Tris buffer (20 mM Tris-HCl, 150 mM NaCl, pH 7.4). Then ice-cold lysis buffer (see section 2.1.5) was added to cells (1ml/well of a 6-well plate). Cells were scraped off the plate and incubated on ice for 30 min with intermittent vortexing. Then the lysates were centrifuged in a microfuge at 14,000 x g for 20 min at 4°C. The pellets were discarded and the supernatants were used for IP.

Immunoprecipitation step

Supernatants obtained from previous step, were incubated with the appropriate antibodies (about 1.5 μg/ well) overnight, on a rotating wheel at 4°C. Control IPs were performed using mouse or rabbit random Igs.

Protein G Sepharose and Protein A Sepharose beads were mixed in 3:1 ratio to precipitate mouse antibodies, and Protein A Sepharose alone was used to precipitate rabbit antibodies. The beads were washed three times in lysis buffer and then 50% slurry of beads was made in the same buffer. About 30 μl of slurry was added to the lysate (previously incubated with antibody) of 1 well and incubated on a rotating wheel for 3-6 h at 4°C.

The immunoprecipitates were then centrifuged in a microfuge for 30 sec at 4°C. The supernatants were snap frozen and stored separately (unbound proteins). The pellets were washed two times in lysis buffer and then washed in the same buffer containing 0.1% Thesit (instead of 1%). Buffer was discarded and pellets were resuspended in 75 μl 1.3X SDS sample buffer (section 2.1.5). This suspension was incubated at room temperature for 20 min with occasional vortexing and then boiled for 3 min. Subsequently immunoprecipitates were centrifuged in a microfuge for 2 min at room temperature and the supernatants (the IPs) were snap frozen and stored at –80°C prior to use.

2.3.13 GLUT4 vesicle immunoadsorption

GLUT4 vesicle immunoadsorption was carried out as described by Morris *et al.* (Morris *et al.*, 1997).

Preparation of 3T3-L1 for immunoadsorption

3T3-L1 adipocytes were washed once with serum-free media and then incubated with serum-free media for 2 h at 37°C. The cells were then washed twice in ice-cold PBS, and HES buffer with protease inhibitors was added at a volume of 1 ml/10 cm plate. Cells were scraped off the plate and homogenised in a Teflon/ glass homogeniser with 10 strokes. Cells were further homogenised with 5 passages through a 25 gauge needle. Cell homogenates were centrifuged at 1500 x g for 10 min at 4°C and the supernatant was further centrifuged at 11,000 x g for 20 min at 4°C. The supernatant of 11,000 x g spin was used as the source of GLUT4 vesicles.

Preparation of adsorbant

Aliquot of pre-treated (see section 2.3.14) formaldehyde fixed *Staphylococcus aureous* adsorbant (Pansorbin cells, CN Bioscience) was centrifuged, at 14,000 x g for 90 sec at room temperature (1 ml aliquot can be used for four 10 cm plates). The supernatant was discarded and the cells were washed in PBS/BSA 1% BSA in PBS three times. Pipette tips used to resuspend the adsorbant cells were cut at the end to prevent damaging the cells. Pellet was then resuspended in 1% BSA in PBS (1 ml original volume of adsorbant in about 600 µl).

Antibodies (rabbit anti-GLUT4 or anti-rabbit Ig) were incubated with the adsorbant cell suspension, on a rotating wheel for 2 h at 4°C (about 7.5 µg antibodies/150 µl adsorbant/ 10 cm plate cell homogenate). At the end of this incubation, the adsorbant cells were collected by spinning at 14,000 x g in a microfuge at room temperature for 90 sec. Adsorbant cells were washed twice in HES buffer supplemented with 100 mM NaCl and resuspended in 100 µl of the same buffer.

Adsorption step

Aliquots of the 11,000 x g supernatant from 3T3-L1 cell homogenate were incubated with the adsorbant (100 µl) obtained after antibody binding step, for 2 h at 4°C on a rotating wheel.

Separation of post IP LDM

At the end of incubation adsorbant cells, were collected by centrifugation at 11,000 x g in the microfuge at 4°C for 2 min. The supernatant from this step was again subjected to centrifugation at 11,000 x g at 4°C for 10 min, then at 180,000 x g for 1 h at 4°C to pellet the LDM.

Separation of post IP GLUT4 vesicles

The adsorbant cell pellet obtained from the previous 11,000 x g spin (which carries bound GLUT4 vesicles) was washed three times in HES buffer containing 100 mM NaCl. All buffer was removed and the cells were resuspended in 100 µl solubilisation buffer (HES buffer, 100 mM NaCl, 0.5% Thesit) at 37°C and incubated for 10 min at room temperature. Then the mixture was microfuged for 2 min at room temperature and the supernatant (GLUT4 vesicle membrane proteins other than GLUT4) was collected. This supernatant was recentrifuged to remove all traces of adsorbant cells. The supernatant obtained was mixed with SDS sample buffer (section 2.1.5), snap frozen and stored prior to analysis.

Separation of GLUT4 from adsorbant

The adsorbant cell pellet (IP) obtained after adding solubilisation buffer was resuspended in 100 µl of 1.3 x SDS (section 2.1.5) and incubated for 10 min at room temperature. The mixture was spun at the end of incubation and the supernatant (the released GLUT4) was snap frozen and stored prior to analysis.

The LDM, vesicle proteins and IP (GLUT4) fractions obtained using anti GLUT4 and anti rabbit antibodies, were subjected to SDS-PAGE for analysis.

2.3.14 Pre-treatment of *S. aureous* adsorbant cells (Pansorbin cells, CN Bioscience)

The adsorbant cells (0.5 g) were subjected to a pre-treatment step to remove proteins that may be released upon the detergent treatment step of vesicle immunoadsorption (section 2.3.13).

Cells were centrifuged at 10,000 x g at room temperature for 10 min and the supernatant decanted. The cells were resuspended in wash buffer (50 mM Tris-HCl, 150 mM NaCl, 3% SDS (w/v), β mercaptoethanol (0.5% v/v), pH 7.4) and heated for 30 min at 95°C in a fume cupboard. After heating, cells were centrifuged at 10,000 x g for 10 min at room temperature and the supernatant was discarded. Cell pellets were washed twice in 50 mM Tris-HCl, 150 mM NaCl, pH 7.4 buffer by resuspension and centrifugation. Buffer was decanted and pellet was washed once in 20 mM Hepes, 150 mM KCl, 2 mM $MgSO_4.7H_2O$, pH 7.2. The pellet was resuspended in 5 ml of the same buffer (Hepes buffer), 0.02% NaN_3 was added and aliquots (0.5 ml) were snap frozen and stored at -80°C until use.

2.3.15 Biotinylation of IRAP

Biotinylation of cell surface IRAP was carried out as described (Garza and Birnbaum, 2000).

Cells grown in 6-well plates were serum starved for 2 h at 37°C. Insulin (100 nM) was added to 50% of the wells, during the last 30 min of incubation. Cells were gently washed three times in 2 ml/well ice-cold KRPB buffer (KRP (see section 2.1.5) with 20 mM Hepes, pH 7.4). Sulpho EZ-link NHS-LC biotin (1 mM) in KRPB (ice-cold) was added to each well and incubated at 4°C for 30 min on a shaking platform. Cells were then washed three times in ice-cold 25 mM ethanolamine prepared in 150 mM NaCl, 20 mM Tris-HCl, pH 7.4 buffer. The cells were then lysed in ice-cold lysis buffer (see section 2.1.5). Immunoprecipitation of IRAP from cell lysates was performed as described in section 2.3.12 using 1.5 µg IRAP antibody/lysate of a single well. Detection of biotinylated IRAP in immunoprecipitates was performed by SDS-PAGE followed by the use of Streptavidin-HRP (1 µg/ml) instead of primary and secondary antibodies during immuno-detection.

2.3.16 *In vivo* Phosphorylation

Cells were incubated in phosphate-free DMEM containing 0.25 mCi/ml $H_3{}^{32}PO_4$, for 2 h at 37°C. It has previously been established that under these conditions there is effective equilibrium between the added Pi and the ATP pool of the cells (Gibbs *et al.*, 1986). At the end of incubation, cells were washed three times in ice-cold buffer with phosphatase inhibitors (50 mM Hepes, 10 mM sodium pyrophosphate, 100 mM sodium fluoride, 2 mM EDTA, 2 mM sodium orthovandate, pH 7.4). Then the cells were lysed in the same buffer containing 2% Thesit (1 ml/well). Immunoprecipitations of the proteins of interest from cell lysates was carried out as described in section 2.3.12. Immunoprecipitates were subjected to SDS-PAGE, the gels were dried and the phosphorylation status of the protein examined by autoradiography.

2.4 Immunofluorescence and confocal microscopy

Cells for immunofluorescence were grown in 6-well plates containing glass coverslips of 13 mm/ 22 mm. Glass coverslips were collagen coated for the use of 3T3-L1 cells to ensure adherence of cells. Coverslips (flamed in ethanol briefly to ensure sterility), without collagen coating were used for other cell types (e.g. HeLa).

2.4.1 Collagen coating of cell culture plastic ware

Collagen coated plates were often used for permeabilisation experiments and plasma membrane lawn assays to enhance the adhesion of the cells to the plates. Plates containing glass coverslips were washed with a solution of collagen in acetic acid, to leave a thin coat of collagen. Plates were then dried in a sterile hood and irradiated with UV light. Prior to plating the cells, plates were washed once with DMEM to remove any traces of acetic acid.

2.4.2 Fixing of cells for immunofluorescence

Cells were washed three times in ice-cold PBS and fixed by incubating in ice-cold methanol at -20°C for 5 min. Methanol was aspirated and the cells washed again in PBS. Cells were either stored at 4°C in PBS containing 0.02% (w/v) NaN_3 or the staining process was continued.

As an alternative method of fixing, 4% *p*-formaldehyde in PBS was used at room temperature for 20 min.

2.4.3 Processing of cells for immunofluorescence

If the cells were fixed in *p*-formaldehyde, they were quenched with 50 mM NH_4Cl/PBS for 10 min and washed three times in PBS. Cells were permeabilised in 0.1% v/v Triton X-100 in PBS for 4 min and washed three times in PBS. Cells fixed in methanol were washed in PBS with no Triton permeabilisation step.

Thereafter, the processing of cells fixed by either of the methods was as follows. Cells were washed in fresh IF buffer (section 2.1.5), and were left in the second IF buffer wash for about 15 min. Meanwhile primary antibodies were diluted at 1:100-1:200 in IF buffer. Coverslips were then placed cells-down onto a drop (80 µl/ 22 mm coverslip) of primary antibody solution on parafilm. Incubation was carried out at room temperature for about 1 h. Coverslips were then washed three times in IF buffer and washed once in PBS. All steps with secondary antibody were performed in dark. Secondary antibodies labelled with fluorescent dyes were diluted at 1:200 in IF buffer and the coverslips were incubated for 1 h. Coverslips were washed in IF buffer for three times and then washed in PBS. The coverslips were then dried slightly and mounted onto a drop of Immu-mount (Shandon, Pittsburgh, USA) on glass slides, allowed to harden overnight and were stored in the dark until imaged by confocal microscopy.

2.4.4 Confocal microscopy

Mounted coverslips were analysed using a 63x oil immersion objective on a Zeiss Axiovert fluorescence microscope (Carl Zeiss, Germany) equipped with a Zeiss LSM410 laser confocal imaging system. Images were captured using either (or both) of 488 nm or 543 nm lasers with appropriate filter sets for collection of GFP/Alexa^{488}/FITC signals (band-pass 505-520 nm) or Alexa^{594}/ TRITC signals (long pass 590 nm). Data files were saved in .TIF format and analysed using adobe photoshop software.

2.4.5 Plasma membrane Lawn Assay

The plasma membrane lawn assay was carried out as described (Rodnick *et al.*, 1992) to generate highly purified plasma membrane fragments in order to determine the relative levels of different proteins at the cell surface.

3T3-L1 adipocytes cultured on collagen-coated plates were washed once with ice-cold buffer A (50 mM Hepes and 10 mM NaCl, pH 7.2) and then, twice with ice-cold buffer B (20 mM Hepes, 100 mM KCl, 2mM $CaCl_2$, 1 mM $MgCl_2$, protease inhibitors). Cells immersed in buffer B were sonicated using 0.8 mm tapered Dawa Ultrasonics probe at 50 watts for 3 sec to generate a lawn of plasma membrane fragments attached to the coverslip.

Lawns were washed three times with PBS and fixed using 4% *p*-formaldehyde, as described in section 2.4.2. After fixing, they were either stored or processed as described in 2.4.3 omitting the permeabilisation step.

Images were captured using confocal microscopy as described in 2.4.4. About eight different lawn areas were scanned and the intensity of signal was determined using Metamorph software (Universal imaging, Inc., West Chester, PA).

2.5 Transport assays

All transport assays were conducted in triplicate including triplicate non-specific counts for controls. Assays were conducted in 6-well plates unless otherwise mentioned.

2.5.1 Glucose transport assay

Cells were incubated in serum free medium for 2 h at 37°C. At the end incubation, plates were transferred to hot plates at 37°C to perform the transport assay. Cells were washed three times with 2 ml KRP buffer (see section 2.1.5) at 37°C per well, each time. Subsequently 950 µl of KRP, ± 100 nM insulin, ± 10 µM cytochalasin B was added to respective wells and incubated for 20 min. At the end of incubation, 50 µl of ^{3}H 2-deoxyglucose (DOG) (0.25 µCi per well, final concentration of DOG was 0.1 mM) was added and mixed. After 3 min of incubation, the contents of wells were

flipped out and the plates were dipped in ice-cold PBS in three consecutive beakers to wash the cells quickly. The plates were air dried for about 1 h and 1 ml of 1% Triton X-100 added to each well. Plates were left on a shaking platform for 1 h at room temperature. The permeabilised cells from each well were added to 4 ml of scintillation fluid in scintillation vials. Contents were mixed thoroughly and analysed by liquid scintillation spectrophotometry.

2.5.2 Reversal of GLUT4 translocation after insulin withdrawal

Cells were treated in the same manner as described in section 2.5.1 until incubation with KRP ± insulin. At the end of incubation, cells used to measure glucose uptake in basal and insulin-stimulated status, were treated exactly as described in section 2.5.1.

Cells used to measure the reinternalisation of GLUT4 were washed three times in KRM buffer (pH 6.0) (see section 2.1.5) at 37°C. Cells were incubated in KRM for different times (e.g. 5, 10, 15 and 30 min) with replacement of KRM buffer each 5 min to allow reinternalisation of GLUT4.

At the end of each time point, cells were washed once with KRP, 950 µl KRP (±10 µM cytochalasin B) was added and DOG uptake was performed for 3 min as described in section 2.5.1.

2.5.3 Surface transferrin receptor assay

3T3-L1 cells were incubated for 2 h at 37°C in serum free media, and ± 100 nM insulin, for the last 30 min. The cells were washed three times in ice-cold KRP containing 1 mg/ml BSA. The cells were then incubated with 1 ml ice-cold KRP/ BSA containing 3 nM ^{125}I transferrin ± 10 µM transferrin and incubated on ice for 2 h. These conditions have been shown to be sufficient for equilibrium binding of transferrin to TfR in these cells (Tanner and Lienhard, 1987). The cells were washed three times with KRP with 1 mg/ml BSA and solubilised in 1 M NaOH for 15 min on a shaking platform. The radioactivity associated with each well was determined using a gamma-counter.

2.5.4 Estimation of rate of transferrin internalisation

HeLa cells were incubated in serum-free media containing 1 mg/ml BSA, for 2 h at 37°C. ^{125}I transferrin (3 nM) ± 10 μM transferrin was added to the wells and incubated at 37°C for different times (e.g. 0, 5, 10, 30 and 60 min). At each time point, cells were rapidly washed three times in ice-cold citrate buffer (see section 2.1.5) to remove transferrin bound to surface receptors. The cells were then solubilised in 1 M NaOH (1 ml/well) and the radioactivity associated with each well determined.

2.5.5 Estimation of rate of externalisation of internalised transferrin

HeLa cells were incubated in serum free media containing 1 mg/ml BSA, for 2 h at 37°C. ^{125}I transferrin (3 nM) ± 10 μM transferrin was added to the wells and incubated at 37°C for 1 h. Plates were removed from incubator and washed three times in ice-cold citrate buffer (section 2.1.5) to remove cell surface-associated transferrin. The cells were then washed once in ice-cold KRP and returned to a hot plate at 37°C. Subsequently the cells were rapidly washed once in KRP at 37°C and incubated at 37°C, with 1ml of KRP for different times (0, 5, 10 and 30 min). After the defined time points cells were washed three times in KRP and solubilised in 1 M NaOH.

2.5.6 Secretion assay

The release of secretory proteins from 3T3-L1 adipocytes, such as adipsin and ACRP30 was measured as described by Kitagawa and co-workers (Kitagawa *et al.*, 1989).

Cells cultured on 10 cm plates were transferred onto hot plates at 37°C and washed twice with KRP buffer (section 2.1.5) at 37°C and then incubated in 10 ml KRP/BSA (10 μg/ ml) ± 1 μM insulin at 37°C. Aliquots (1 ml) of media were removed at defined times (e.g. 0, 2, 4, 12 and 30 min). Proteins were precipitated by adding 110 μl of 70% trichloroacetic acid and 20 μl of deoxycholate (as a carrier precipitant). The samples were incubated on ice for 10 min and centrifuged at 10,000 xg for 10 min in a microfuge. The protein pellets were resuspended in 50 μl 1xSDS-PAGE sample buffer (see section 2.1.5), snap frozen and stored at -80°C prior to analysis.

2.6 General Molecular biology

2.6.1 Polymerase chain reaction

Forward and reverse primers for the DNA sequence to be amplified were designed with the appropriate restriction sites. Plasmid DNA purified by using Qiagen miniprep kits was generally used as the template.

The following general recipe was used for the PCR. Thin walled tubes were used.

Nuclease free water	39 µl
10X cloned DNA polymerase buffer	5 µl
Purified plasmid DNA	1 µl (50-100 ng)
Forward primer	2.5 µl (250 ng)
Reverse primer	2.5 µl (250 ng)
dNTP	1 µl
Pfu Turbo DNA polymerase	1 µl
Total volume	50 µl

PCR was completed using following conditions.

94°C	2 min	
94°C	15 sec	25 cycles
55°C	30 sec	
68°C	2 min 15 sec	
68°C	2 min 15 sec	
4°C	Hold	

PCR product was subjected to Agarose gel electrophoresis to check for the correct product.

2.6.2 Agarose gel electrophoresis

Gels were made with 1% Agarose in TAE buffer (see section 2.1.5). Gels were usually run at 70 V and DNA bands were examined under UV light.

2.6.3 Purification of PCR product

PCR products were electrophoresed as described in 2.6.2. The band corresponding to the correct PCR product was identified under UV light and excised from the gel using a sterile scalpel blade with a minimal exposure to UV light.

PCR product was eluted from the gel using Qiagen gel purification kit according to the manufacturers instructions. The gel was dissolved by adding 500 µl solubilisation (QG) buffer in an eppendorf tube and incubating at 37°C. The tube was vortexed intermittently until the gel was completely dissolved. Isopropanol (200 µl) was then added to dissolved gel, and the solution was passed through the DNA binding mini column by centrifugation. The column containing the DNA was washed with 750 µl ethanol buffer and centrifgued to remove all contaminants and ethanol. Bound DNA was eluted with 50 µl elution buffer.

2.6.4 Restriction digestion

The plasmid or PCR product was cut with a pair of restriction enzymes either to identify the DNA with the expected restriction pattern or to ligate the DNA and plasmid. Two enzymes were selected based on compatibility in one buffer with 75-100 % efficiency in most cases.

Restriction mixture was prepared as follows.

DNA	5 µl (0.5-1.0 µg)
10x buffer	2 µl
Sterile water	11 µl
Restriction enzyme 1	1 µl
Restriction enzyme 2	1 µl

Samples were mixed by brief centrifugation and incubated at 37°C for 2 hours prior to analysis by electrophoresis or ligations.

2.6.5 TA cloning

Purified PCR products were cloned into pCRII vector by this method. The following protocol was used to add the A base overhangs on the insert DNA (the linearised pCRII TOPO vector has 3' T base overhangs).

Purified PCR product 50 µl

10x PCR+Mg buffer 5 µl

dNTPs 1 µl

Taq polymerase 1 µl

The mixture was incubated at 72°C for 20 min.

This product was then cloned into pCRII using TOPO TA cloning kit (Invitrogen) as follows:

Taq treated PCR product 1 µl

Nuclease free water 1 µl

pCRII TOPO vector 0.5 µl

This mixture was incubated for 5 min at room temperature. Stop reagent (0.5 µl) (from Invitrogen) was added to the mixture. The whole of the 3 µl mixture was added gently to TOPIO cells and incubated on ice for 30 min. Transformation was aided by warming the mixture at 42°C for 30 sec followed by cooling for 2 min on ice. Then 250 µl of SOC media (from Invitrogen) was added and incubated at 37°C for 1 hr before plating.

This mixture was plated on ampicilin (100 µg/ml), kanamycin (50 µg/ml) agar plates and incubated at 37°C overnight. About five colonies from each transformation were picked and grown separately overnight in LB medium (section 2.1.5) with ampicilin and kanamycin. Plasmid DNA were purified from each culture, digested with *Eco*R I and electrophoresed to check for the presence of an insert (inserts are cloned to a region of pCRII vector flanked by two *EcoR* I restriction sites) (see appendix).

2.6.6 Ligation

The insert and the cloning vector were digested separately with same set of restriction enzymes. Calf intestinal alkaline phosphatase (1 µl) was added to the digestion mixture

of the vector during last 10 min of incubation. Both digestion mixtures were eletrophoresed separately on agarose gels to identify and purify the restricted products. Correct bands were excised from the gel and purified as described in section 2.6.3. Restricted insert and vector (in the ratio of 3:1) were mixed with ligase buffer (2 µl) and ligase enzyme (1.5 µl). Total volume of the mixture was set to 20 µl. The mixture was incubated overnight at 14°C. Ligated product was transformed into competent *E. coli* DH5α as described in section 2.6.8, with the appropriate controls.

2.6.7 Preparation of competent *Escherichia coli* (DH5α)

Ten ml of sterile LB (see section 2.1.5) in a sterile universal tube was inoculated with *E. coli* (DH5α) from a glycerol stock and cultured overnight at 37°C with shaking at 250 rpm. Half of this culture was subcultured into 100 ml LB in a sterile 500 ml flask and further incubated at 37°C with shaking, until the optical density at 600 nm was 0.5 (typically about 3 h). The cells were then chilled on ice for 5 min and harvested by centrifugation in sterile 50 ml centrifuge tubes at 10,000 x g for 10 min at 4°C (in a Beckman benchtop centrifuge). The supernatant was discarded and the cells were gently resuspended in a total of 40 ml sterile buffer 1 (30 mM KAc, 100 mM $RbCl_2$, 10 mM $CaCl_2$, 50 mM $MnCl_2$, 15% (v/v) glycerol, pH 5.8) using a sterile pipette. The cells were incubated on ice for a further 5 min and were centrifuged as before. All traces of the supernatant were discarded and the cells were resuspended in a total of 4 ml sterile buffer 2 (10 mM MOPS, 75 mM $CaCl_2$, 10 mM $RbCl_2$, 15% (v/v) glycerol, pH 6.5). Following a further incubation of 15 min on ice, the cells were divided into 220 µl aliquots in pre-chilled sterile microfuge tubes and stored at -80°C until use.

2.6.8 Transformation of *Escherichia coli* cells

Competent cells, made as described in section 2.6.7, were thawed on ice and 50 µl was pipetted into sterile pre-chilled microcentrifuge tubes for each transformation. For each transformation, 5 µl of ligation reaction or 0.5 µl (50 ng) of purified plasmid DNA were added. The contents of the tube were gently mixed and incubated on ice for 15-30 min. The mixture was heat shocked in a water bath at 42°C for exactly 90 sec, and then chilled on ice for 1 min. LB (450 µl) was added to each tube and incubated at 37°C for 45 min. The supernatant was removed by centrifugation and cells were resuspended in

150 µl of LB. These cells were plated onto LB agar plates containing the appropriate antibiotic for the selection, and grown overnight on inverted plates, at 37°C.

Competent *E. coli* cells that had been obtained from commercial suppliers were transformed according to the protocols of the supplier.

2.6.9 Small scale DNA preparations (miniprep)

Bacterial colonies were picked from selective LB agar plates and transferred to 3 ml LB (containing appropriate antibiotic/s) in sterile universal tubes. These were incubated overnight at 37°C with shaking at 250 rpm. DNA purification was performed using a Qiagen miniprep kit, according to the manufacturers instructions. Briefly, the cells from 3 ml culture were collected by centrifugation for 5 min at 14,000 x g in microfuge. Cell pellets were resuspended in 250 µl buffer P1 (containing RNase A). Then 250 µl buffer P2 was added and the contents were mixed by inverting the tubes several times. These were left to incubate for 5 min at room temperature, after which time 350 µl buffer N3 was added and the tubes again mixed by inversion. The samples were then centrifuged for 10 min at 14,000 x g in a microfuge and the supernatants carefully decanted into Qiagen mini prep spin columns and spun at full speed for 1 min in microfuge. The flow through was discarded and 750 µl buffer PE (with ethanol) was added. (When the plasmid DNA was >10 kb, the column was washed with 500 µl buffer PB prior to addition of PE). The column was centrifuged again and flow through was discarded. The column was centrifuged again to remove all traces of PE buffer and the column was then placed in a sterile 1.5 ml microfuge tube. Buffer EB was warmed to 40°C (to 70°C if the plasmid is >10 kb) and 50 µl of it was pipetted into the centre of the column and incubated for 1 min. the DNA was then collected in the microcentrifuge tube by centrifugation for 1 min.

2.6.10 Large scale DNA preparations (maxiprep)

Large-scale DNA preparations were made using a Qiagen plasmid maxi kit, following the high copy plasmid protocol. Briefly, bacterial cultures of 100 ml were grown in 500 ml flasks, overnight at 37°C, with shaking (250 rpm) in LB with appropriate antibiotics. The cells were harvested by centrifugation at 10,000 x g for 10 min. The cells were resuspended in a total of 10 ml buffer P1 (containing RNase A) by pipetting.

Then 10 ml of buffer P2 was mixed with the cell suspension and left for 5 min to allow cell lysis. The reaction was neutralised by the addition of 10 ml of chilled buffer P3. The flocculent precipitate formed was removed by centrifugation at 10,000 x g for 30 min followed by filtration of supernatant through two layers of muslin. This supernatant was applied to a P100 Qiagen column pre-equilibrated with 10 ml buffer QBT and was allowed to drain under gravity. The column was washed with 30 ml buffer QC (with ethanol). The DNA was then eluted into a 50 ml sterile tube by the addition of 15 ml buffer QF. Isopropanol (10.5 ml) was added to DNA solution and mixed well. Precipitated DNA was collected by centrifugation at 10,000 x g for 30 min in a benchtop centrifuge. The supernatant was discarded and the pellet was washed in 4 ml 70% (v/v) ethanol. Ethanol was removed and the pellet air-dried prior to resuspend in 250 µl TE (10 mM Tris-HCl, 1 mM EDTA, pH 8.0). The DNA concentration was assessed spectrophotometrically.

2.6.11 Transfection of mammalian cells

HEK 293 cells were transfected using lipofectamine reagent (Life Technologies) according to manufacturers recommendations. Typically cells were seeded on 10 cm dishes on the day before, to obtain about 50% confluence on the day of transfection. DNA (10 µg) obtained from maxipreps (section 2.6.10) was diluted in 400 µl Optimem (Life Technologies) in a sterile tube. Lipofectamine (30 µl) were diluted in a separate 400 µl Optimem. The Lipofectamine/ Optimem mixture was added drop-wise to the DNA/ Optimem mixture and incubated for 30 min at room temperature. Meanwhile, the cells were rinsed in 10 ml serum-free medium at 37°C / 10 cm plate and incubated with 5.2 ml of Optimem for about 10 min at 37°C. At the end of 30 min incubation DNA Lipofectamine mixture was added to the cells incubated in Optimem. Then the cells were returned to the incubator at 37°C for 3-6 h, after which time 5 ml complete growth media containing 10% (v/v) FCS was added to give a final concentration of 5% FCS (slow growth was required, as these cells were grown for about 1 week after transfection). After overnight incubation, media was replaced with normal growth medium with 5% FCS (section 2.2.6).

2.6.12 DNA sequencing

The University of Glasgow Molecular Biology Support Unit performed all DNA sequencing using Big Dyes kits (PE biosystems) and an ABI Prism 377 sequencer. This was performed for all constructs that were produced following PCR steps to ensure that no undesirable mutations had been introduced.

2.7 Recombinant protein production in *E. coli*

Expression and purification of His-tagged proteins was performed as outlined ((Martin *et al.*, 1998)). An *E. coli* colony harbouring an appropriate plasmid was picked from a freshly grown selective LB agar plate and used to inoculate 10 ml of LB containing appropriate antibiotics. This was grown overnight at 37°C with shaking at 250 rpm. The following day, 1 L of super media (section 2.1.5) (in a 5 L flask) was inoculated with 10 ml culture. This was grown at 30°C with shaking until the optical density at 600 nm had reached about 0.5-0.6. Isopropyl-thio-β-D-galactopyranoside (IPTG) was then added to a final concentration of 0.5-1 mM to induce the culture for 5 h. The cells were then harvested in 250 ml tubes in a Beckman JA-14 rotor by centrifugation at 10,000 x g for 15 min. Then the cell pellets were resuspended in 40 ml His-tag buffer (100 mM Hepes, 200 mM KCl, 5 mM imidazole, pH 8.0), transferred to a 50 ml centrifuge tube and centrifuged at 10,000 x g in a benchtop centrifuge for 20 min. The supernatant was discarded and the cell pellet was stored at -20°C.

2.7 Recombinant protein purification

The final cell pellet obtained in section 2.7 was thawed and resuspended in 20 ml ice-cold His-tag buffer (section 2.7) (containing protease inhibitor cocktail and 1 mM PMSF). One ml of 10 mg/ml lysozyme in the same buffer was then added, the tube was inverted several times and vortexed to ensure proper mixing. The mixture was then incubated on ice for 30 min until the contents had become viscous due to cell lysis. The lysate was then sonicated (4 x 30 sec) using 0.8 mm tapered Dawa ultrasonics probe at 50 W with a 30 sec pause between sonications. The lysate was clarified by centrifugation for 15 min at 40,000 x g in a Beckman JA-20 rotor at 4°C. The clarified lysate was then transferred to a 50 ml centrifuge tube containing 2.5 ml of washed nickel NTA Agarose (Qiagen) beads. The tube was sealed with parafilm and placed on a roller mixer for 2 h at 4°C. Following centrifugation at 10,000 x g for 5

min in a benchtop centrifuge, the supernatant was removed and the beads were washed five times in 50 ml His-tag buffer. The beads were transferred to a column (5 or 10 ml syringe barrel plugged with a small disc of Whatman filter paper). His-tag elution buffer (His-tag buffer pH 7.0, containing 200 mM imidazole) (5 ml) was then added to the column and 0.5 ml fractions were collected from the bottom of the column. The protein concentrations of the fractions were determined as described in section 2.3.5. Fractions containing highest protein concentrations were pooled and dialysed into PBS using slide-a-lyzer dialysis cassettes (Pierce). The purity of the protein was assessed by SDS-PAGE followed by Coomassie staining of the gel (see sections 2.3.6 and 2.3.10).

2.9 Statistical analysis

Data were analysed by unpaired Student's *t* test and are shown as mean±SEM. All transport assays were performed in triplicate with appropriate blanks and all the experiments were repeated on a further two or more independent occasions.

Chapter 3

Studies on distribution of post-Golgi syntaxins in 3T3-L1 adipocytes

3.1 Introduction

Studies in mammalian synapses have revealed the pivotal role of SNARE proteins in synaptic vesicle exocytosis. Since then several SNAREs have been identified in non-neuronal tissues, which led to the suggestion that the SNARE complex formation is an essential step in all membrane fusion events (Bock *et al.*, 1996; Advani *et al.*, 1998; Prekeris *et al.*, 1998; Tang *et al.*, 1998c). Adipocytes express at least two R-SNAREs involved in endosomal recycling, cellubrevin (VAMP3) and VAMP2 both of which are present in GLUT4 vesicles (Volchuk *et al.*, 1995), (Volchuk *et al.*, 1996). Several studies have shown that, insulin-stimulated GLUT4 vesicle fusion with the plasma membrane (PM) requires specific interactions between the PM Q-SNAREs, syntaxin (STX) 4, SNAP-23 and the R-SNARE of GLUT4 vesicle VAMP2 (Cheatham *et al.*, 1996; Martin *et al.*, 1998; Kawanishi *et al.*, 2000). Cellubrevin is shown to mediate the GTPγS-sensitive endosomal GLUT4 trafficking pathway in insulin-sensitive cells (Millar *et al.*, 1999).

The intracellular trafficking of GLUT4, and its targeting to GLUT4 storage vesicle compartment (GSV) are poorly understood. It appears that entry into the GSV compartment requires special sorting events that probably occur in the endosome and/ or at TGN (Rea and James, 1997). The targeting of GLUT4 to GSVs is a prerequisite for its ability to translocate to the PM under the stimulation of insulin, with a 10-40 fold increase over basal levels. This contrasts with the to 2-3 fold increase at the PM of other recycling proteins such as the TfR (Bryant *et al.*, 2002).

All the studies carried out to date in regard to the involvement of SNAREs in GLUT4 trafficking have focused on the aspect of insulin-stimulated GLUT4 translocation to the PM. There are no reports documented on the involvement of SNAREs in intracellular GLUT4 trafficking events.

Several mammalian post-Golgi syntaxins have been identified. Among them, STX 6, STX 10, STX 11 and STX 16 are primarily localised to the TGN (Bock *et al.*, 1996;Tang *et al.*, 1998b; Valdez *et al.*, 1999; Mallard *et al.*, 2002, respectively) and syntaxins 7, 8, 12/13 are primarily localised to the endosomal compartment (Prekeris *et al.*, 1999b; Subramaniam *et al.*, 2000; Tang *et al.*, 1998c/ Prekeris *et al.*, 1998,

respectively). Some of these post-Golgi syntaxins localised to the TGN and endosomal system may have a role in trafficking of GLUT4 in adipose and muscle tissue.

This chapter focuses on the characterisation of post-Golgi syntaxins, STX 6, STX 8, STX 12 and STX 16 of 3T3-L1 adipocytes to identify their possible involvement in intracellular GLUT4 trafficking.

3.1.1 Syntaxin 6

STX 6 encodes a 255 amino acid, 29 kD protein, expressed in a variety of cell types, with high levels in brain, kidney and lung. STX 6 shows homology to yeast SNAREs, Pep12p and Tlg1p (Bock *et al.*, 1996; Bock *et al.*, 2001, respectively). Based on the primary structure organisation (N-terminal domain, SNARE domain and C-terminal transmembrane (TM) domain) and significant homology to several syntaxins in the SNARE motif, STX 6 was previously classified as a syntaxin family member. STX 6 also shares significant sequence homology with the C-terminal SNARE region of SNAP-25 (Bock *et al.*, 2001). A recent genome scale comparison of SNARE-motif sequences placed STX 6 SNARE motif in the Qc-SNARE/ SNAP-C family (Bock *et al.*, 2001), suggesting it is homologous to SNAP-23, -25 and -29.

STX 6 is predicted to contain two domains (H1 and H2), which can form coiled-coils. The twenty C-terminal amino acids are hydrophobic and form a membrane anchor. STX 6 H2 domain (SNARE domain) is adjacent to this hydrophobic segment and is predicted to adopt a 63 amino acid amphipathic ∝-helical structure. The cytoplasmic domain has two putative di-leucine domains (at amino acids 31-32 and 123-124) and a tyrosine based sorting motif (YGRL at 140-143). The H2 domain in concert with the tyrosine motif, act as retrieval signals from the PM to TGN and plays a major role in maintaining STX 6 in TGN (Watson and Pessin, 2000). The function of the H1 domain is not well characterised and studies indicate a role in α-SNAP binding (this is in contrast to other SNARE proteins where the C- terminal domain, including the SNARE domain is involved in ∝-SNAP binding).

STX 6 is primarily localised to the TGN, and to a lesser extent to small vesicles in the vicinity of endosome like structures (Bock *et al.*, 1997). Low, but significant levels of

STX 6 were found at the PM of 3T3-L1 adipocytes, under steady-state conditions (Watson and Pessin, 2000). In human resting neutrophils, STX 6 was primarily localised at the PM (Martin-Martin *et al.*, 2000). STX 6 is found in the post-Golgi immature secretory granules (derived from TGN) of PC12 cells (Wendler and Tooze, 2001), endocrine pancreatic cells and exocrine parotid cells (Klumperman *et al.*, 1998). Electron microscopic studies have shown the localisation of STX 6 with clathrin and AP1 complex in parotid cells (Klumperman *et al.*, 1998). It has been suggested that STX 6 functions in the maturation of immature secretory granules to mature secretory granules by facilitating membrane retrieval (Tooze *et al.*, 2001).

STX 6 is found to be associated with a variety of SNARE proteins. These include the R-SNARES: VAMP2/VAMP3 in rat brain (Bock *et al.*, 1997), VAMP3 in HeLa cells (Mallard *et al.*, 2002), VAMP4 in rat brain and HeLa cells (Steegmaier *et al.*, 1999; Mallard *et al.*, 2002 respectively), VAMP7 and VAMP8 (together with Qa-SNARE, STX 7 and Qb-SNARE, Vti1b), in B16 melanoma cells (Wade *et al.*, 2001).

STX 6 has also been found to interact with the Qa SNAREs: STX 4 (personal communication N Bryant), STX 7 in B16 melanoma cells (Wade *et al.*, 2001), STX 16 in HeLa cells (Mallard *et al.*, 2002; unpublished observation of Wendler and Tooze 2001). It has also been shown to interact with SNAP-25 homologues: SNAP-23 in neutrophils (Martin-Martin *et al.*, 2000), and SNAP-25 and SNAP-29 in PC12 cells (Wendler and Tooze, 2001).

STX 6 is suggested to mediate a TGN trafficking event, probably targeting vesicles to endosomes (Bock *et al.*, 1997; Simonsen *et al.*, 1999). STX 6 also has been identified as a component of the core machinery responsible for homotypic immature secretory granule fusion (Wendler and Tooze, 2001) and involved in regulated secretory pathway (Klumperman *et al.*, 1998). In human neutrophils, STX 6 mediates granule exocytosis (Martin-Martin *et al.*, 2000). Overexpression of the cytosolic domain of STX 6 was found to inhibit TGN38 trafficking to the TGN in CHO cells and suggested to be required in early endosome (EE)/ recycling endosome (RE) to TGN transport (Mallard *et al.*, 2002). Such data could be interpreted to imply a likely role in GLUT4 traffic to GSV, because GSVs are at least functionally similar to secretory granules.

3.1.2 Syntaxin 8

STX 8 is a broadly expressed protein of predicted size 27 kD. It is more abundant in heart, skeletal muscle, kidney, pancreas than in other tissues investigated (brain, placenta, liver, lung) (Thoreau *et al.*, 1999). The members of the t-SNARE family most closely related to STX 8 are mammalian STX 6 and yeast Vam7p (Thoreau *et al.*, 1999; Subramaniam *et al.*, 2000). Even though previously categorised as a syntaxin based on the primary structure, STX 8 SNARE motif is now categorised as a Qc-SNARE due to its structural similarity to C-terminal SNARE region of SNAP-25 (Bock *et al.*, 2001).

The rat cDNA predicts a 236 amino acid polypeptide (Subramaniam *et al.*, 2000). Two coiled-coil domains have been predicted in human STX 8, between residues 30 and 95 and 142 and 211 (SNARE domain) with a TM domain between residues 216 and 230 (Thoreau *et al.*, 1999). Three regions of rat STX 8 with potential coiled-coil domains, between residues 13 and 37, 44 and 68 and 166 & 204, and 18 amino acid TM domain have also been predicted (Subramaniam *et al.*, 2000).

STX 8 has been shown partially colocalised with TfR (EE/RE) and LAMP1 (LE/ lysosomal) in COS7 cells (Prekeris *et al.*, 1999b). STX 8 also partially overlaps with STX 6, a known TGN protein (their unpublished observation). Immunolocalisation studies in PC12 and COS7 cells demonstrated that STX 8 is present in TGN, EEs, LEs, and tubulovesicles dispersed throughout the cytoplasm or in the vicinity of endosomes. Quantitation of the distribution in PC12 cells showed approximately similar percentages of STX 8 in EE, LE and lysosomes. Another study has shown the preferential localisation of STX 8 in EE (Subramaniam *et al.*, 2000). They demonstrated the colocalisation of majority of STX 8 with Rab5 and rabaptin5 (EE markers) in NRK cells, using immunofluorescence microscopy and immunogold labelling. In their study, STX 8 was found to a lesser, but significant extent in LE, PM and coated pits.

Immunoprecipitation studies showed that STX 8 is associated with γ-SNAP, α-SNAP and Vti1-rp1 which is one of two mammalian homologues of yeast Vti1p which function in both retrograde intra-Golgi transport as well as several trafficking events in the endosomal pathway (Subramaniam *et al.*, 2000).

A role of STX 8 in trafficking from EEs to LE is supported by the effect of an anti-STX 8 antibody on epidermal growth factor receptor trafficking in SLO-permeabilized HeLa cells (Prekeris *et al.*, 1999b). Subramaniam and co-workers (2000) proposed that STX 8 might function in EE.

3.1.3 Syntaxin 12

STX 12 is a polypeptide of 272 amino acids with a fairly ubiquitous 39 kD protein. A putative TM region of 23 hydrophobic amino acids was identified in rat STX 12 cDNA (Tang *et al.*, 1998c). STX 12 is assumed to be identical to STX 13 (Jahn and Sudhof, 1999). STX 13 is a broadly expressed protein. Its expression is relatively high in brain, lung, spleen and pancreas. STX 13 displays high homology to STX 7 and Pep12p, putative endosomal SNAREs in mammals and yeast (Prekeris *et al.*, 1998a).

The effects of brefeldin A and wortmannin on STX 12 in NRK cells demonstrated its localisation to endosomes. Its compact perinuclear staining pattern suggested that STX 12 localises to LE (Tang *et al.*, 1998c). Prekeris *et al.*, showed the primary localisation of STX 13 in both tubular early and recycling endosomes where it is colocalised with TfR (Prekeris *et al.*, 1998). Immunofluorescence analysis of CHO, PC12, NRK, NIH3T3 cells, and electron microscopy of CHO cells combined with the effect of brefeldin A and nocadozole on supported this conclusion (Prekeris *et al.*, 1998). By contrast very little colocalisation was found with lgp120 (LE and lysosome marker). STX 13 also showed significant overlap with STX 6 (Prekeris *et al.*, 1998). In hippocampal neurons STX 13 was localised to tubular extensions of EE and tubulovesicular RE (Prekeris *et al.*, 1999a). Collectively, such data place STX 12/ 13 in the endosomal system, and thus these syntaxin isoforms may function in GLUT4 trafficking. STX 12 may function to receive vesicles either from TGN or EE or participate in recycling of surface receptors. (Tang *et al.*, 1998c). The effects of anti-STX 13 antibodies in permeabilised PC12 cells suggested that STX 13 plays a role in recycling of PM proteins via tubulovesicular RE (Prekeris *et al.*, 1998).

The cytosolic domain of STX 12 was able to bind to α-SNAP and SNAP-23/ syndet *in vitro* (Tang *et al.*, 1998c). Immunoprecipitation of STX 13 from rat brain showed its association with SNAP-25, VAMP2/ VAMP3 and β-SNAP (Prekeris *et al.*, 1998).

3.1.4 Syntaxin 16

Human STX 16 cDNA, encoding a 307 amino acid protein has been cloned (Tang *et al.*, 1998a). Several potential coiled-coil regions and a stretch of 21 hydrophobic amino acids at the C-terminus, a possible TM domain, were identified. The transcript was fairly ubiquitous but slightly enriched in heart and pancreas. Another group cloned three human syntaxin cDNAs, presumably originating from alternative splicing of the same transcript (Simonsen *et al.*, 1998). They are STX 16A and STX 16B, which are identical, except for an insertion of 21 amino acids in the latter, and STX 16C (115 amino acids) which is a truncated version of STX 16A, lacking C-terminal TM domain. The yeast SNARE Tlg2p shows sequence similarity with STX 16.

Tang and co-workers (1998) demonstrated that *Myc*-STX 16 has a perinuclear-staining pattern and colocalises with the Golgi marker, *lens culinaris agglutinin* and Golgi SNAREs GS28 and STX 5 in COS cells. They also showed that the effect of brefeldin A on the *Myc*-STX 16 labelling was similar to that of a Golgi protein (not to TGN). Colocalisation of STX 16 with Golgi marker β-COP and MPR (primarily TGN in BHK cells) was observed in BHK cells transfected *with Myc*-STX 16A and STX 16B (Simonsen *et al.*, 1998). Mallard and co-workers showed extensive colocalisation of STX 16 with TGN38, a TGN marker (Mallard *et al.*, 2002). STX 16C was found in the cytosol (Simonsen *et al.*, 1998). No colocalisation was found with Rab5, EEA1 (EE) and LAMP2 (LE/lysosomal) (Simonsen *et al.*, 1998).

The three STX 16 forms may have differential roles in intracellular trafficking (Simonsen *et al.*, 1998) but at present this remains unclear. Mallard and co-workers have proposed a role for STX 16 in the regulation of EE/ RE to TGN transport (Mallard *et al.*, 2002). They identified interactions between the TGN-localised putative Q-SNAREs syntaxin 6 (Qc-SNARE), syntaxin 16 (Qa-SNARE), and Vti1a (Qb-SNARE), and two early/recycling endosomal R-SNAREs, VAMP3/cellubrevin, and VAMP4 by immunoprecipitation studies in HeLa cells. They also found that overexpression of the cytosolic domain of STX 16 inhibited TGN38 trafficking to TGN in CHO cells. Such data suggest the hypothesis that STX 16 might function in the GLUT4 trafficking pathway.

3.2 Aims of this chapter:

The aims of this chapter were to identify the localisation of post-Golgi syntaxins, 6, 8, 12 and 16 relative to GLUT4 vesicles of 3T3-L1 adipocytes and to elucidate any possible role of syntaxins in GLUT4 targeting. Furthermore, we sought to identify the SNARE partners of those post-Golgi syntaxins as another means of identifying the role of these syntaxins in 3T3-L1 adipocytes.

In this study I have examined the subcellular localisation of post-Golgi syntaxins in 3T3-L1 adipocytes using different techniques. I also extended this study to assess whether these syntaxin isoforms localised in GLUT4 vesicles. Finally I attempted to identify the *in vivo* SNARE partners of these syntaxins using immunoprecipitation studies.

3.3 Results:

3.3.1 Production of polyclonal syntaxin antisera

Aliquots of anti-syntaxin antisera were obtained (section 2.1.3) to conduct the initial experiments in order to identify their presence in 3T3-L1 adipocytes. His-tagged recombinant syntaxins were produced in *E.coli* and used to prepare antiserum, to conduct further studies.

3.3.1.1 Generation of recombinant His-tagged syntaxins

The cytosolic domain (705 bp) encompassing amino acids 1 to 235 of STX 6 (rat) flanked by two restriction sites, *Bgl* II and *Hind* III, was subcloned directly from STX 6-pCRII (constructed as described in section 4.4.1.A), into the *BamH* I and *Hind* III sites of pQE30 (see appendix) as described in section 2.6.6. This vector introduces an N-terminal 6xHis-tag to the protein encoded by the insert. A fragment of 708 bp consisting of cytosolic domain (642 bp) encompassing amino acids 1 to 214 of STX 8 (rat) flanked by two restriction sites, *Bgl* II and *Kpn* 1, from STX 8-pCRII (constructed as described in section 4.4.1.A), was subcloned into *BamH* I and *Kpn* 1 sites of pQE30. STX 12 (mouse) cytosolic fragment (744 bp) encompassing amino acids 1 to 248 was amplified as described in section 2.6.1 using 5'-CAGGAGCTCATGTCCTACGGTCCCTTA-3' (*Sac1* site underlined) as forward primer and 5'-GAGGGTACC**CTA**CTTCTTGCGAGATTTTTT-3' as reverse primer (*Kpn* 1 site underlined and STOP codon in bold letters). The STX 12 insert was cloned

into *Sac* 1 and *Kpn* 1 sites of pQE30. The STX-pQE30 vectors were then transformed into competent *E.coli* (strain DH5α). The presence and correct orientation of the insert was verified by restriction digestion. The sequence of the STX 12-pQE30 was verified before proceeding. The STX-pQ30 vectors were transformed into competent *E.coli* strain M15 and selected for the presence of insert. M15 cells carrying the correct inserts were used to produce His-tagged STX 6, 8 and 12 as described in section 2.7. His-syntaxins were purified as described in section 2.8, and illustrated in figure 3.1.

3.3.1.2 Immunisation of animals and collection of sera

All antibody production was performed by Diagnostics Scotland under the direction of Dr. M. Chambers, Carluke, Lanarkshire, Scotland. Briefly, rabbits were immunised with 150 μg of His-Syntaxin 6, 8 and 12 respectively. A pre-immune serum sample was obtained before first inoculation. Three booster injections were given at four-week intervals, each time with approximately 150 μg of His-syntaxin. About 25 ml of serum was recovered two times after one week of first and second booster injections. The final bleed was an exsanguination.

All three His-tagged syntaxins were successfully produced and purified as shown in figure 3.1. Anti-His-syntaxin sera were able to recognise the particular syntaxin in 3T3-L1 adipocyte membranes, specifically (Figure 3.2). Anti-STX 6 serum produced some reaction with an area above 47.5 kD marker of the Western blots, above the size of STX 6. A dilution of 1:3000 was used with the antiserum for Western blots. For immunofluorescence dilutions of 1:200 were used.

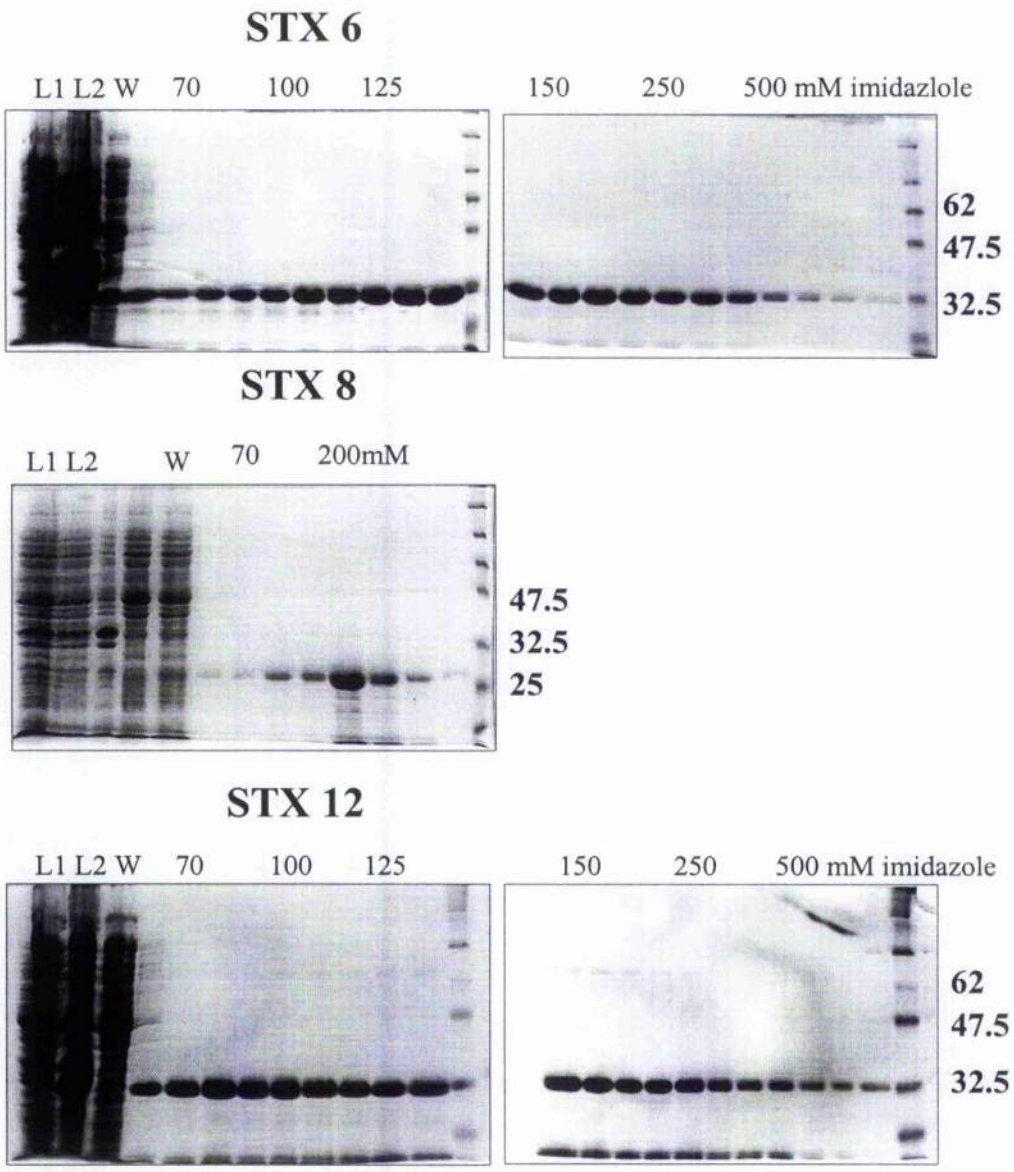

Figure 3.1 Purity of recombinant His-tagged syntaxins recovered from *E. coli* cell lysates

Cytosolic domains of syntaxins 6, 8 and 12 including His-tags were expressed in M15 *E. coli* cells. Expression of His-tagged syntaxins was induced for 5 hrs, by adding isopropyl-thio-β-D-galactopyranoside as described in section 2.7. His-syntaxins were purified from bacterial lysates. Ni-NTA Agarose, His-tag buffer and elution buffer containing imidazole was used for purification, as described in section 2.8. The purity of the protein eluted was assessed by SDS-PAGE followed by Coomassie staining of the gel (sections 2.3.6 and 2.3.10). The figure shows the assessment of purity of pre-induction lysate (L1), post-induction lysate (L2), flow through (W) and final fractions eluted using imidazole (70-500 mM). Positions of the broad range molecular weight markers between 62 and 25 kD are shown.

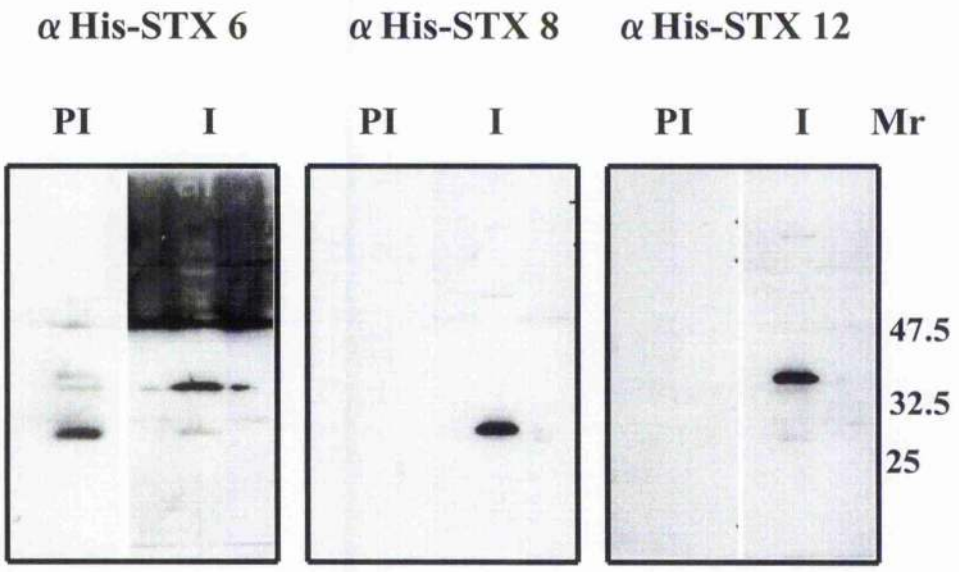

Figure 3. 2 Identification of syntaxins in 3T3-L1 adipocytes, using anti-His-syntaxin antisera (α-His STX)

Purified His-tagged syntaxins were used to immunise rabbits. Pre-immune serum and antiserum were obtained for each of His-syntaxin. The immunoblots show the use of pre-immune serum (PI) and antiserum (I) to identify corresponding syntaxin from homogenates of 3T3-L1 adipocytes. Antisera at 1:3000 dilutions were used as the primary antibodies in immuno detection. Positions of the broad range molecular weight markers (M_r) between 47.5 and 25 kD are shown.

3.3.2 Distribution of post-Golgi syntaxins in membrane fractions

Other than for STX 6 there were no reports which examined the distribution of post-Golgi syntaxins in adipocytes. Therefore as the first step of the localisation studies, I determined whether these syntaxins are present in 3T3-L1 adipocytes, and the membrane fractions within which they are localised. Subcellular fractionations of 3T3-L1 adipocytes collected with or without insulin stimulation were performed as described in section 2.3.3. Plasma membrane (PM), high-density microsome (HDM) and low-density microsome (LDM) fractions were obtained. The distribution of post-Golgi syntaxins in the fractions, were detected by Western blotting (2.3.7 and 2.3.8).

The three different membrane fractions showed the previously demonstrated distribution pattern of GLUT4 and IRAP under basal and insulin-stimulated conditions, i.e. elevation of PM GLUT4 and IRAP levels and depletion of LDM GLUT4 and IRAP levels, which are well established changes in response to insulin stimulation. All three subcellular fractions showed the presence of syntaxins 6, 8, 12 and 16 under both basal status and insulin-stimulated conditions (Figures 3.3 and 3.4). Surprisingly STX 6 and STX 16 consistently showed a similar distribution pattern to GLUT4 and IRAP under insulin stimulation. The increase of STX 6 and 16 in PM and corresponding decrease in LDM observed in response to insulin was significant. In contrast, there was no significant change observed in STX 8 and STX 12 distribution in response to insulin. It was apparent that the distribution of GLUT4, IRAP, STX 6 and STX 16 in PM in the basal state was low (<5%) compared to that of STX 8 and STX 12 (16% and 10% respectively). The insulin-stimulated translocation of STX 6 and STX 16 to the PM implicate them as potential components of GLUT4 vesicles. The data are quantified in figure 3.4 and table 3.1.

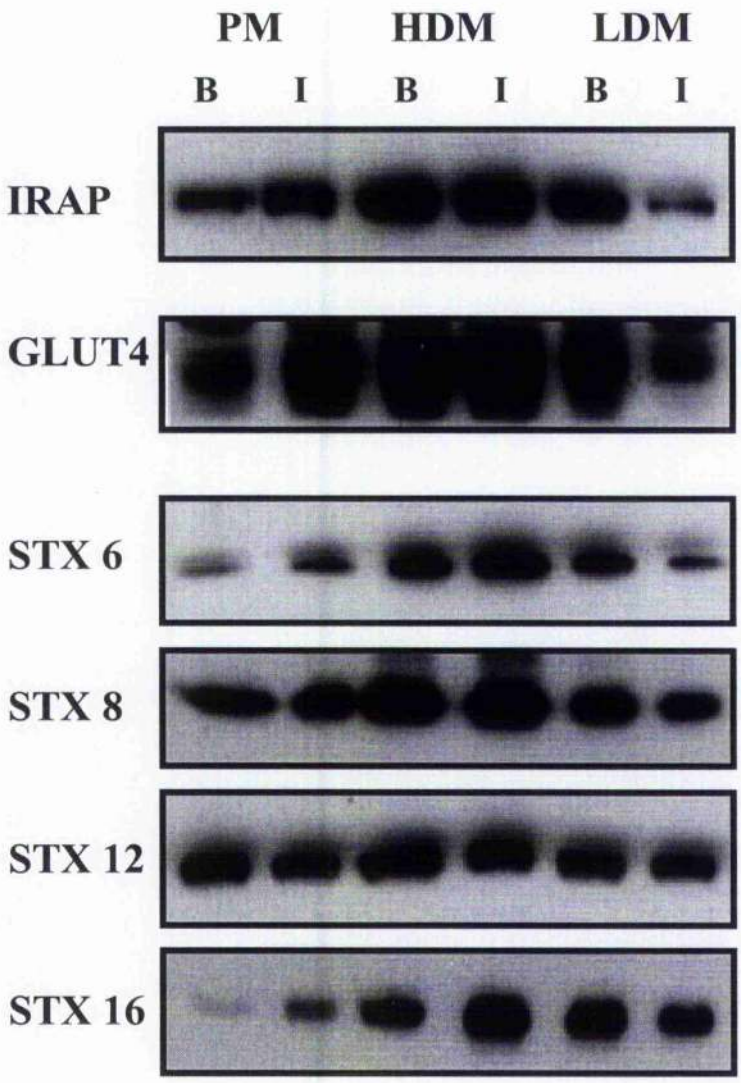

Figure 3.3 Distribution of post-Golgi syntaxins in subcellular fractions of 3T3-L1 adipocytes

3T3-L1 adipocytes were treated with (I) or without (B) 100 nM insulin for 30 minutes. Cells were homogenised and plasma membrane (PM), high-density microsome (HDM) and low-density microsome (LDM) fractions were separated as described in sections 2.3.1 and 2.3.3. SDS-PAGE was performed as described in section 2.3.6, using equal quantities of protein (15 μg) from each fraction. The distribution of proteins was identified using Western blotting (2.3.7) and immuno detection (2.3.8). The data shown is from a typical experiment repeated three further times with similar results.

Figure 3.4 Quantitation of post-Golgi syntaxins in subcellular fractions of 3T3-L1 adipocytes

Immunoblots similar to figure 3.3 were analysed quantitatively using NIH image software. All immunoblot signals were quantified from linear regions of the protein titration curve. The relative amount of each protein in all three fractions was measured, and for insulin-stimulated fractions was expressed as a % of its corresponding basal value. Figure shows the relative amounts of proteins, from a typical experiment repeated three more times with similar results. Mean ± SEM are shown. The insulin-stimulated changes in PM and LDM levels of STX 6 and STX 16 were significant ($p<0.05$) which followed a pattern similar to GLUT4 and IRAP.

Table 3.1 Calculation of total post-Golgi syntaxin quantity in subcellular fractions of 3T3-L1 adipocytes at basal condition

The quantities of proteins measured at basal condition (B) were used to calculate total protein content in each fraction. The amount of protein loaded in each well (15 μg) was representing 16.6% of total PM, 5% of total HDM and 2.7% of total LDM. These values represent similar experiments conducted four times.

Figure 3.4

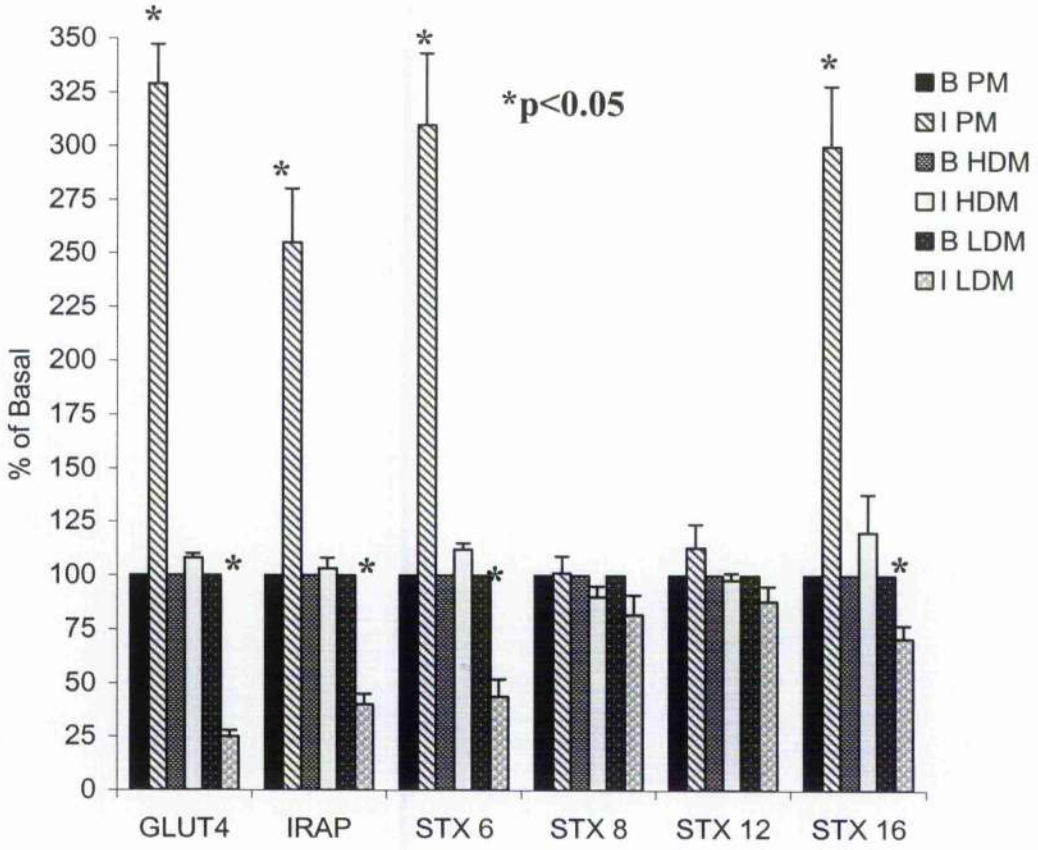

Table 3.1

protein	% in PM	% in HDM	% in LDM
GLUT4	3.6	42.8	53.6
IRAP	4	36.6	59.4
STX 6	1.5	37.9	60.6
STX 8	16.2	46.9	36.9
STX 12	9.9	36.9	53.2
STX 16	2	33	65

3.3.3 Distribution of post-Golgi syntaxins in iodixanol gradients

Iodixanol gradient centrifugation has been successfully used to resolve two distinct GLUT4 pools from LDM of 3T3-L1 adipocytes (Hashiramoto and James, 2000; Maier and Gould, 2000). Maier and Gould (2000) have found evidence to show that these two pools represent the GSV and endosomal TGN compartments.

In this study I used iodixanol gradient centrifugation to examine whether the post-Golgi syntaxins present in LDM show any similarity to the distribution of GLUT4 in this fraction. Therefore the LDM fractions from basal and insulin-stimulated cells were further separated as described in section 2.3.4. GLUT4 and IRAP were separated into two distinct pools by this method, as described by previous studies. The results clearly showed the depletion of GLUT4 and IRAP predominantly from the GSV pool (first peak) and to a lesser degree from the endosomal pool (second peak), under insulin stimulation in agreement with the work of Maier and Gould (2000) (Figure 3.5). All four post-Golgi syntaxins tested distributed in two peaks, which overlapped with those of GLUT4 and IRAP. Quantification of the data, revealed that all syntaxin isoforms showed a predominant depletion from the GSV peak, as in the case of GLUT4 and IRAP, under insulin stimulation (Figures 3.6). When the two peaks of syntaxins separated under basal state were compared, it was found that 40% of STX 6, 8 and 12 are in peak 1 and 60% are in peak 2. In contrast GLUT4 and IRAP showed around 60% of total in peak 1 and around 40% in peak 2. STX 16 showed a similar distribution to GLUT4 and IRAP, where around 65% of total was found in peak 1 and 35% was in peak 2.

Figure 3.5 Distribution of post-Golgi syntaxins of 3T3-L1 adipocytes in iodixanol gradients

3T3-L1 adipocytes were treated with (I) or without (B) 100 nM insulin for 30 minutes. LDM fractions were separated as described in section 2.3.3, and subjected to iodixanol gradient analysis as described in section 2.3.4. Fractions were collected from the bottom of the gradient (No: 1 to 13). SDS-PAGE was performed using 10% of each fraction. The distribution of proteins was identified using Western blotting and immuno detection. Peak 1 (fractions 2-5) represents GLUT4 storage vesicles (GSV) and peak 2 (last four fractions) represents endosome and TGN compartments. Figure shows blots of a typical experiment conducted three times.

Figure 3.5

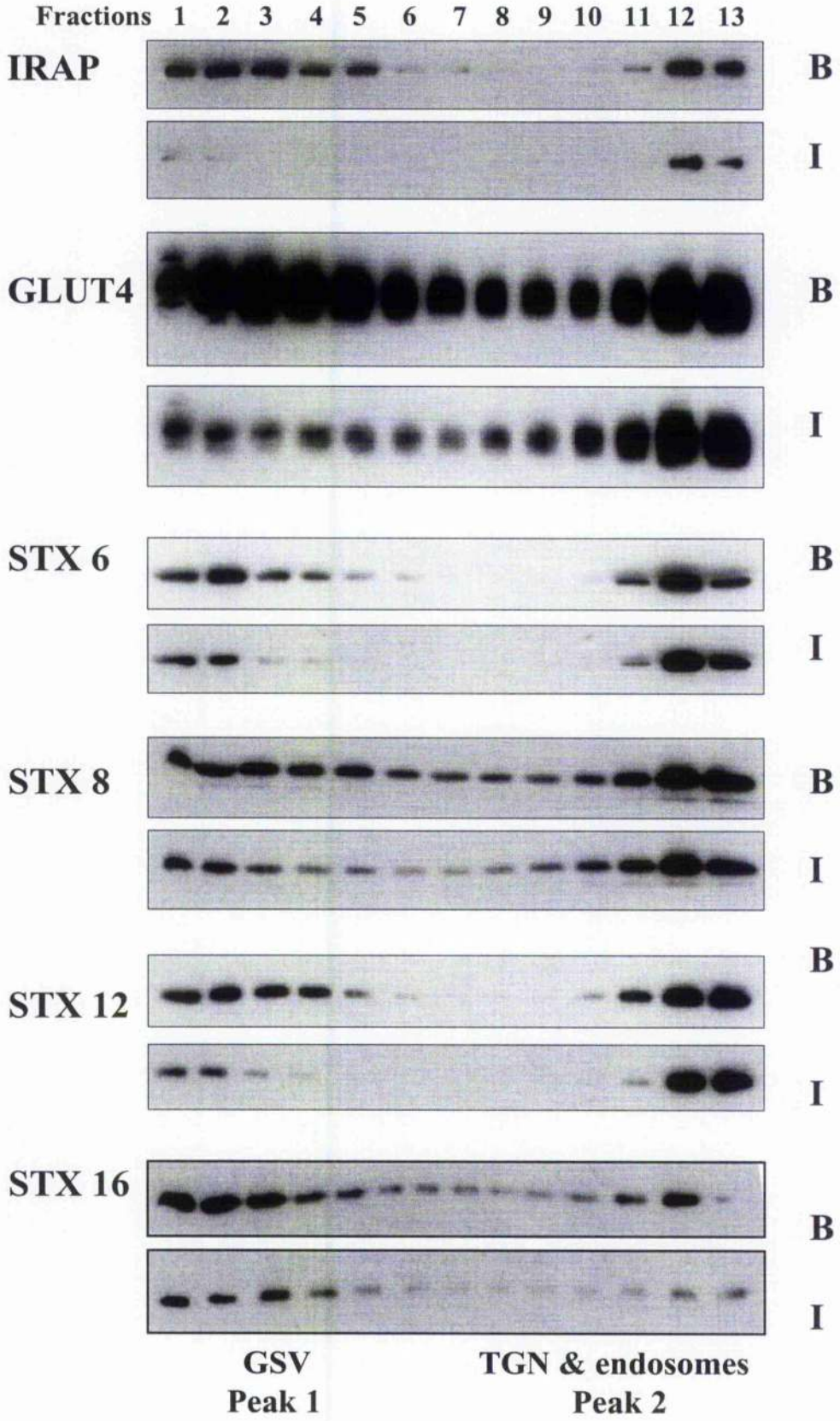
Fractions 1 2 3 4 5 6 7 8 9 10 11 12 13
IRAP
B
I
GLUT4
B
I
STX 6
B
I
STX 8
B
I
STX 12
B
I
STX 16
B
I
GSV
Peak 1
TGN & endosomes
Peak 2

Figure 3.6.A

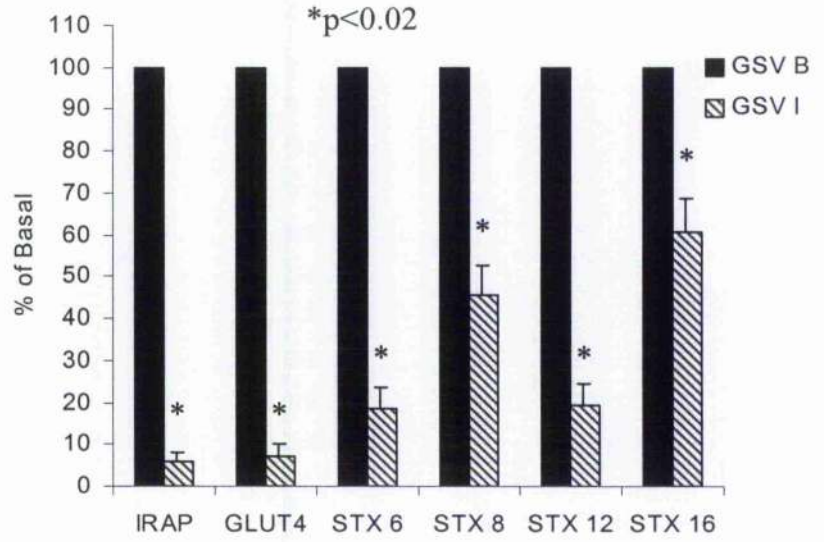

Figure 3.6.B

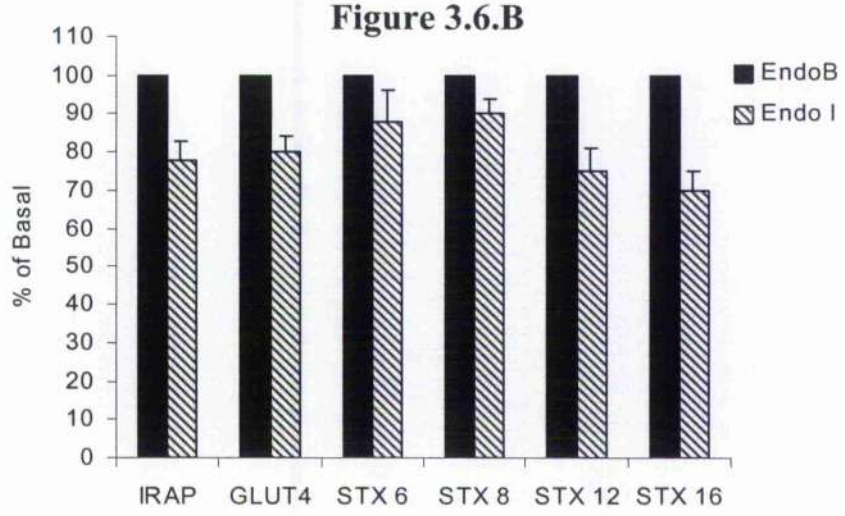

Figure 3.6 Quantitation of post-Golgi syntaxins of 3T3-L1 adipocytes, in iodixanol gradients

Blots similar to figure 3.5 were analysed quantitatively using NIH image software. The peaks corresponding to the two GLUT4 pools separated in presence (I) or absence of insulin (B) were analysed separately. Fractions No: 2-5 was considered as GSV (GSV) and the last four fractions were considered as endosome and TGN pool (Endo). Measurements of insulin-treated fractions, were expressed as % of its corresponding basal value. n=3.

Figure 3.6.A represents the quantities obtained at B (GSV B) and I (GSV I) in GSV fractions. All four syntaxins showed a reduction of the level in GSV pool in response to insulin, which was significantly higher than the reduction of these proteins in endosomal and TGN pool ($p<0.02$).

Figure 3.6.B represents the quantities obtained at B (Endo B) and I (Endo I) in endosome and TGN fractions.

3.3.4 GLUT4 vesicle immunoadsorption to detect the association of syntaxins with GLUT4 vesicles

To extend the results of iodixanol gradients, I attempted to purify GLUT4 vesicles from the two pools of GLUT4 resolved on the gradient. As this effort was not successful, GLUT4 vesicles were separated without prior fractionation on iodixanol gradients. Post nuclear fractions of 3T3-L1 adipocyte homogenates collected under basal conditions were used to isolate GLUT4 vesicles, using the method described in section 2.3.13. All procedures were conducted in parallel with non-specific antibodies to account for the possibility of non-specific recovery of proteins in the GLUT4 vesicle fraction. It was able to isolate more than 90% of GLUT4 vesicles of post-nuclear supernatant using this procedure (Figures 3.7 and 3.8). The results showed the presence of IRAP in GLUT4 vesicle fraction, a protein that is known to localise extensively in GLUT4 vesicles. All four post-Golgi syntaxins tested were present in GLUT4 vesicle fractions. STX 6 showed the highest recovery in GLUT4 vesicles with a corresponding reduction of the level in LDM separated after immunoadsorption. This data is quantified in figure 3.8.

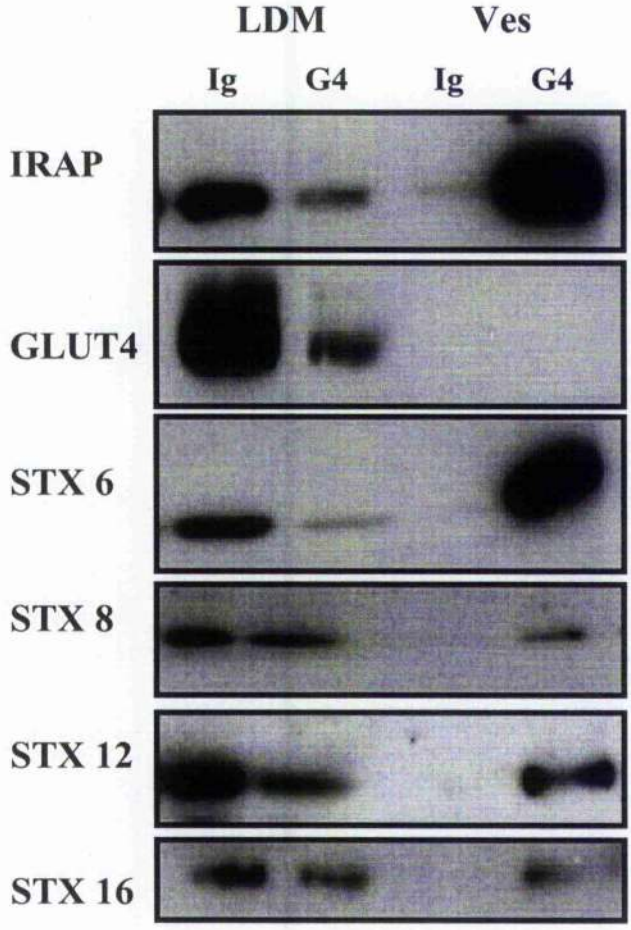

Figure 3.7 Detection of post-Golgi syntaxins in GLUT4 vesicles of 3T3-L1 adipocytes

GLUT4 vesicles were isolated from 3T3-L1 adipocyte post nuclear supernatants as described in section 2.3.13. About 7.5 μg anti-GLUT4 or anti-rabbit Ig / 10 cm plate cell homogenate was used. 1.9% of LDM and 5% of vesicles were used for the SDS-PAGE. Four lanes (as described below) of each immunoblot show the distribution of proteins. Immunoblots are from a typical experiment repeated three times with similar results.

From left to right:

LDM Ig: LDM recovered after immunoadsorption using anti- rabbit IgG

LDM G4: LDM recovered after immunoadsorption using anti-GLUT4

Ves Ig: vesicle fraction recovered after immunoadsorption using anti-rabbit Ig

Ves G4: vesicle fraction recovered after immunoadsorption using anti-GLUT4

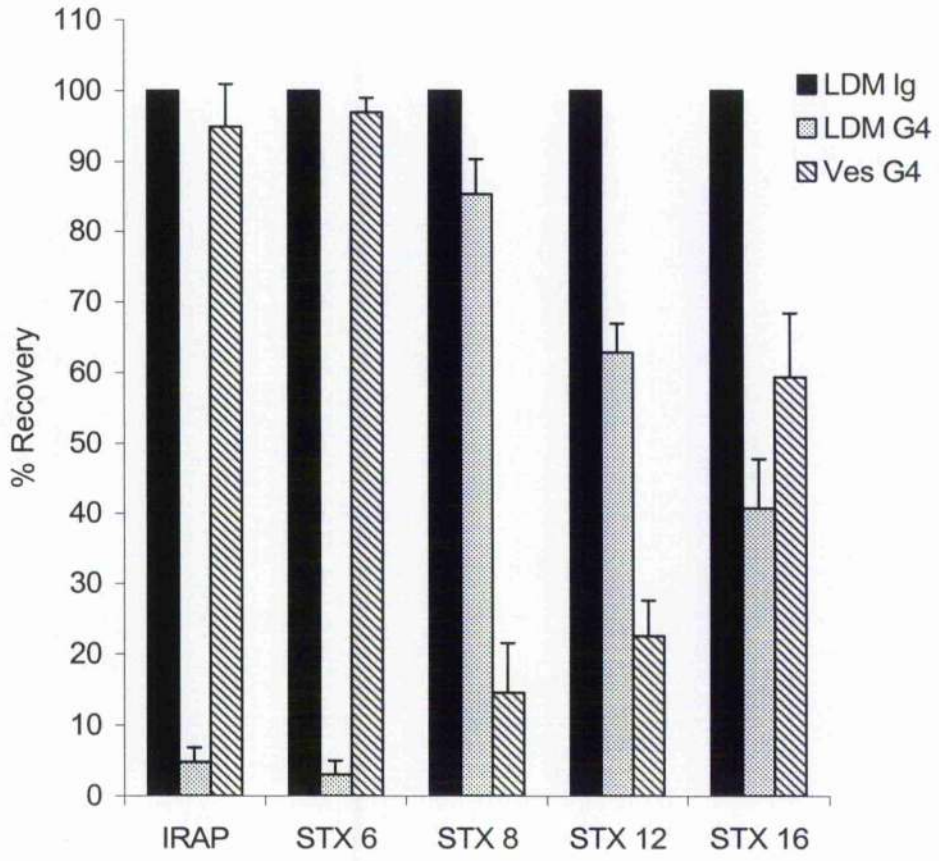

Figure 3.8 Recovery of post-Golgi syntaxins in GLUT4 vesicles of 3T3-L1 adipocytes

Blots similar to figure 3.7 were analysed quantitatively using NIH image software. Total measurement of LDM collected after immunoadsorption with anti-rabbit IgG (LDM Ig) was expressed as 100%. Recovery of proteins in LDM G4 and Ves G4 were expressed as % of LDM Ig. Measurements of vesicles obtained with anti-rabbit Ig (Ves Ig), were not plotted in the graph, as all those values were zero. Mean±SEM is shown. n=3.

LDM G4: LDM recovered after immunoadsorption using anti-GLUT4

Ves G4: vesicle fraction recovered after immunoadsorption using anti-GLUT4.

3.3.5 Indirect immunofluorescence to detect the association of syntaxins in GLUT4 vesicles

As another means of studying the colocalisation of post-Golgi syntaxins in GLUT4 vesicles, indirect immunofluroscence and confocal microscopy was carried out as described in chapter 2.4. STX 6 showed a perinuclear-staining pattern with a colocalisation with GLUT4 labeling. STX 8 and STX 12 labelling showed a more punctate pattern with a lower degree of colocalisation with IRAP labelling at perinuclear area. STX 12 labelling was mainly perinuclear and showed colocalisation with IRAP (Figure 3.9).

3.3.6 Effect of endosomal ablation on syntaxins

Endosomal ablation is a technique used extensively, to show the presence of an endosomal GLUT4 pool and the ablation resistant GSV pool in 3T3-L1 adipocytes (Livingstone *et al.*, 1996). To examine the distribution of post-Golgi syntaxins within the endosomes, endosomal ablation of 3T3-L1 adipocytes was conducted as described in section 2.3.11 and data of a typical experiment is shown in figure 3.10. The results showed the ablation of majority of the TfR, and nearly 50% GLUT4 and IRAP by this method, as described by previous studies (Livingstone *et al.*, 1996). This experiment further showed the ablation of STX 6, 8, and 12 by about 50% consistently (Figures 3.10 and 3.11).

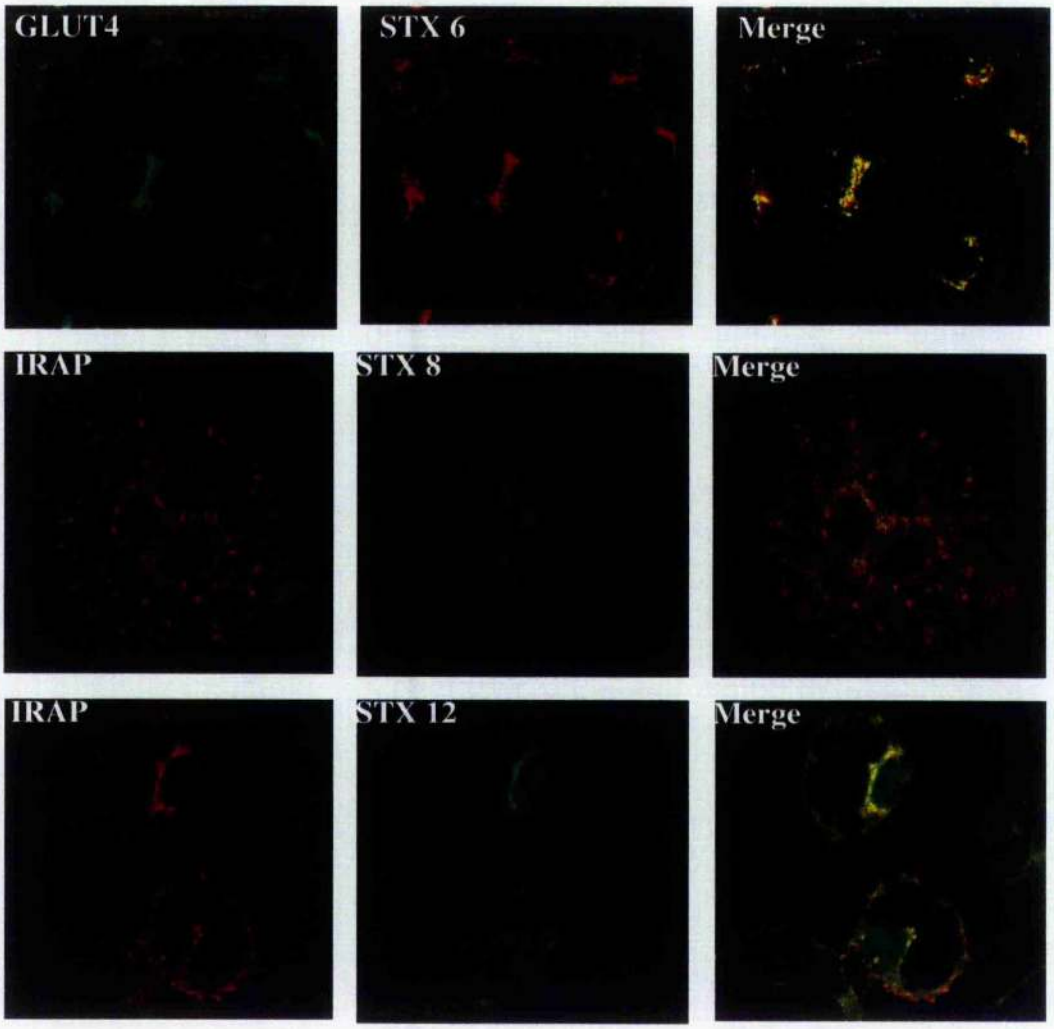

Figure 3.9 Localisation of post-Golgi syntaxins in GLUT4 vesicles of 3T3-L1 adipocytes, using immunofluorescence microscopy

3T3-L1 adipocytes grown on coverslips, were fixed with methanol and processed for immunofluorescence as described in section 2.4. All syntaxin antiserum were used at 1:200. Anti-GLUT4 and anti-IRAP antibodies were used at 1:100. STX 6 and IRAP are labelled with TRITC (red). GLUT4, STX 8 and STX 12 are labelled with FITC (green). Secondary antibodies were used at 1:200. Anti-STX 6 was monoclonal while anti-STX 8 and 12 were polyclonal. (Some of the staining of STX 8 and 12 might be non-specific). Figure shows representative images from three experiments conducted on separate occasions. Magnification of the three groups of cells are different (STX 6, 8 and 12).

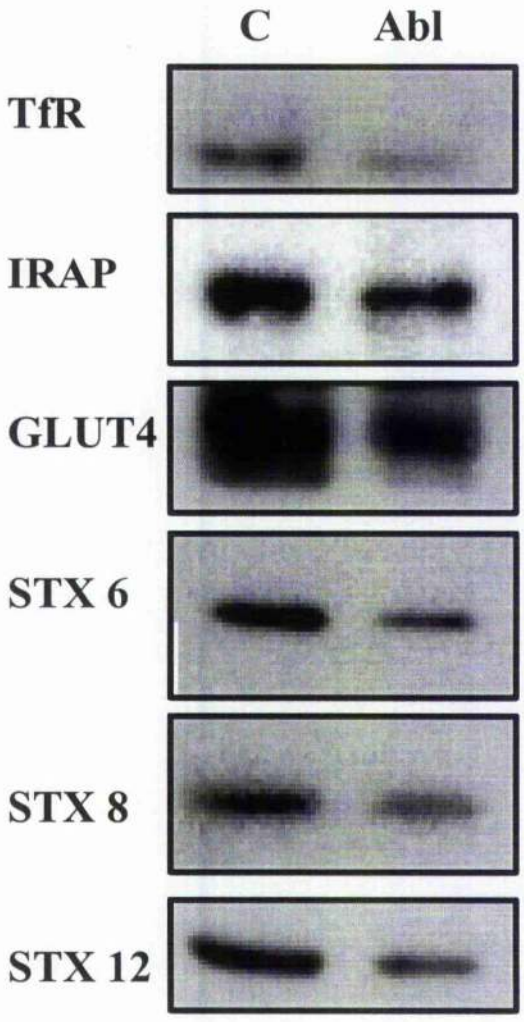

Figure 3.10 Effect of endosomal ablation on post-Golgi syntaxins of 3T3-L1 adipocytes

Endosomal ablation was performed as described in section 2.3.11. Cells were subsequently incubated for 1h at 4°C in the dark in the presence (ablated) or absence (control) of 0.02% v/v H_2O_2. LDM fractions were collected from the two groups and 30 μg protein from each was subjected to SDS-PAGE. Immunoblots show the effect of the endosomal ablation (Abl), on different proteins, compared to controls (C). Data from one experiment repeated two more times with similar results are shown.

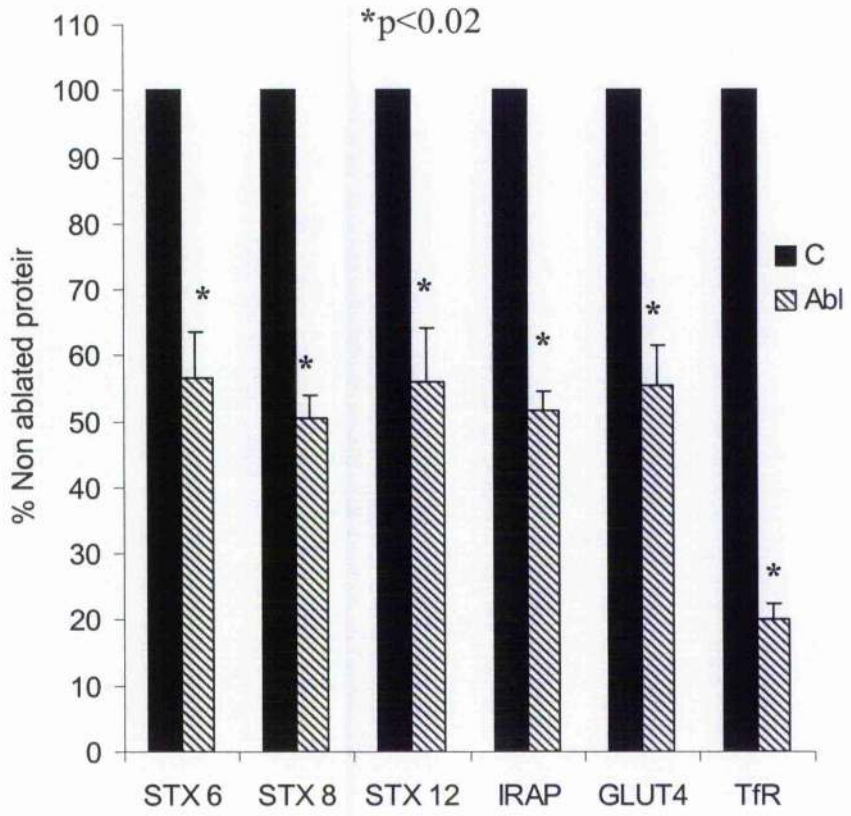

Figure 3.11 Quantitation of the non-ablated proteins recovered in LDM after endosomal ablation

Blots similar to figure 3.10 were analysed quantitatively using NIH image software. Measurements of non-ablated proteins in ablated group of LDM (Abl) were expressed considering the value of control (C) LDM as 100%. Mean±SEM is shown. Syntaxins 6, 8 and 12 showed a significant ablation under the experimental conditions used ($p<0.02$) n=3.

3.3.7 SNARE partners of syntaxin 6 in 3T3-L1 adipocytes

Immunoprecipitation of STX 6 was performed as described in section 2.3.12, to identify *in vivo* SNARE partners. All experiments were conducted along with appropriate controls, using random Ig. STX 6 showed immunoprecipitation of more than 90% of STX 6 from 3T3-L1 adipocyte lysates (Figure 3.12.A and B). Immunoprecipitation of STX 6 was not modulated by presence of *N*-ethylmaleimide. Some association of STX 6 with STX 4 was observed in presence of *N*-ethylmaleimide. STX 8 and STX 12 were associated with STX 6 to a small degree, which was not affected by *N*-ethylmaleimide. Very minor association of STX 6 with VAMP2 was observed. The fraction of STX 4, 8, 12 and VAMP2 associated with STX 6 appear to be low, as this was not accompanied by a reduction in the total STX 4, 8 or 12 content in the post-immunopreciptation supernatant (Figure 3.12.A).

Among the SNARE members examined for in immunoprecipitates, STX 6 showed association with STX 16 very clearly with a reduction of STX 16 in post-immunopreciptation supernatant (Figure 3.12.B).

Figure 3.12.A

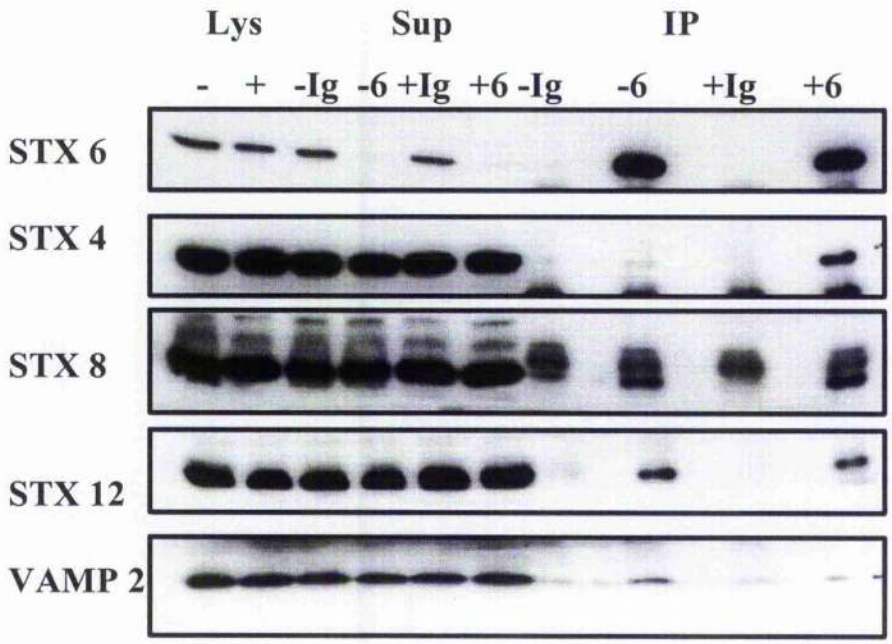

Figure 3.12.B

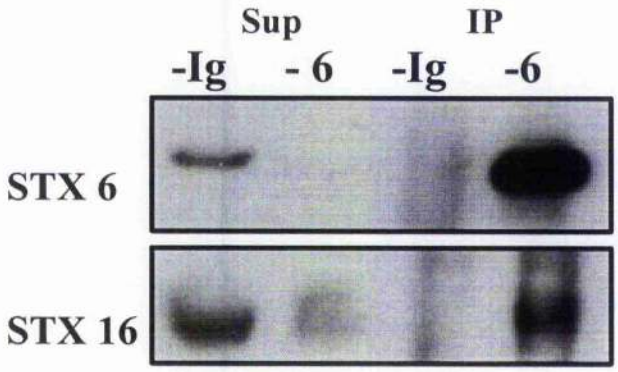

Figure 3.12 Detection of SNARE partners of STX 6 in 3T3-L1 adipocytes
Cells were incubated in presence (+) or absence (-) of 10 mM *N*-ethylmalemide for 20 min. STX 6 was immunoprecipitated from lysates (± 5 mM *N*-ethylmalemide) of 3T3-L1 adipocytes, as described in section 2.3.12. Anti-Syntaxin 6 (6) and anti-mouse Ig (Ig) were used at 7.5 µg/ 10 cm dish. Immunoblots show the protein distribution in fractions described below. These blots are from a typical experiment conducted three times.
Figure 3.12.A shows week association of certain SNAREs with STX 6
Figure 3.12.B shows strong association of STX 16 with STX 6
Lys: lysate taken before immunoprecipitation
Sup: supernatants collected after immunoprecipitation
IP : immunoprecipitates
For SDS-PAGE 2% of Lys, 2% of Sup and 10% of IP were used (10% equals $1/10^{th}$ of a 10 cm dish).

3.3.8 Identification of phosphorylated proteins associated with syntaxins

It has been reported that phosphorylation of SNARE proteins regulates SNARE protein interactions, as well as the availability of SNAREs to participate in membrane trafficking events (Gurunathan *et al.*, 2002). I sought to determine whether the post-Golgi syntaxins are phosphorylated, and to detect any *in vivo* association with other phosphorylated proteins. Labelling of 3T3-L1 adipocytes with ^{32}P was performed as described in section 2.3.16. None of STX 6, STX 8 and STX12 was phosphorylated (Figure 3.13.A). Furthermore, STX 8 and STX 12 did not show association with phosphorylated proteins. In contrast, the results show the association of STX 6 with a phosphorylated protein, under basal and insulin-stimulated conditions (Figure 3.13.A). Calculated molecular mass of this phosphorylated protein was approximately 42 kDa. In addition STX 16 immunoprecipitates contained a phophorylated protein under the same conditions, with a mass of approximately 42 kDa (Figure 3.13.B).

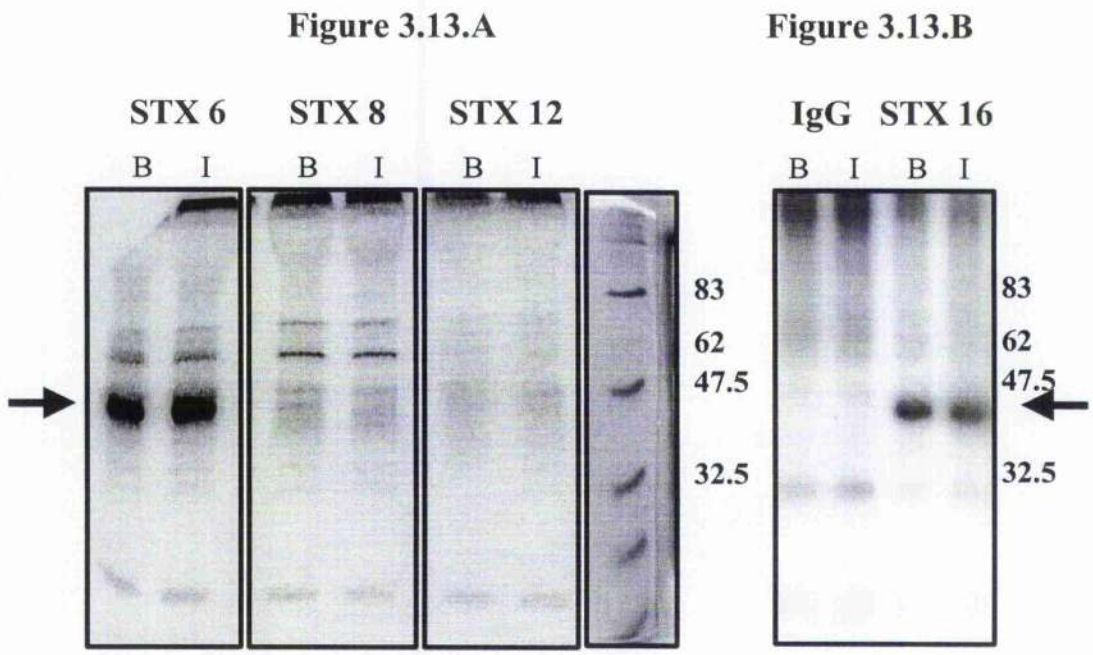

Figure 3.13 Detection of phosphorylated proteins present in immunoprecipitates of syntaxins obtained from 3T3-L1 adipocytes

Cells were incubated in phosphate-free DMEM containing 0.25 mCi/ml ^{32}Pi for 1 h. Subsequently cells were treated with (I) or without (B) 100 nM insulin for 15 min. Cells were prepared for immunoprecipitation, as described in section 2.3.16. Syntaxins were immunoprecipitated using anti-syntaxin 6, 8, 12 and 16. Immunoprecipitates (from about 2% of a 10 cm dish) were subjected to SDS-PAGE, the gels were dried and the phosphorylation status of the protein examined by autoradiography. Similar results were obtained in two repetitions of this experiment. Arrows show the phosphorylated proteins. Molecular weight standards are shown.

Figure 3.13.A shows the phosphorylated proteins in STX 6 immunoprecipitates

Figure 3.13.B shows the phosphorylated proteins in STX 16 immunoprecipitates

3.4 Discussion

The SNARE hypothesis predicts that the cellular function of a particular syntaxin as a Q-SNARE would be determined by its localisation. In this chapter, experiments have been described which identified the localisation of syntaxins, 6, 8, 12 and 16 in 3T3-L1 adipocytes by various approaches and compared their distribution in relation to GLUT4. In addition experiments were conducted to identify their *in vivo* SNARE partners in 3T3-L1 adipocytes. The aim was to identify the possible role of these syntaxins in GLUT4 trafficking.

Previous studies have identified three PM syntaxins, STX 2, 3 and 4 from primary rat adipocytes and cultured 3T3-L1 adipocytes (Olson *et al.*, 1997). In addition STX 6 is localised, mainly in perinuclear region but with a low, but significant, amount on the PM of 3T3-L1 adipocytes (Watson and Pessin, 2000). There are no reports describing the localisation of other post-Golgi syntaxins in adipocytes. Among the syntaxins characterised, STX 4 has been demonstrated to function as one of the Q-SNAREs involved in the insulin-stimulated fusion of GLUT4 vesicles with the PM (Volchuk *et al.*, 1996; Olson *et al.*, 1997). It is suggested that the targeting of GLUT4 into the insulin-sensitive GSV compartment requires a sorting event probably at the endosomes or at the TGN (Rea and James, 1997). Therefore this study aimed to characterise some of TGN and endosomal syntaxins in fat cells.

STX 6 had previously been localised to the TGN in 3T3-L1 adipocytes (Watson and Pessin, 2000). Although not characterised in adipocytes, STX 8 and STX 13 were identified as ubiquitously expressed proteins (Thoreau *et al.*, 1999; Prekeris *et al.*, 1998). STX 8, STX 12 and STX 13 were shown to be localised to the endosomal compartment (Subramaniam *et al.*, 2000; Tang *et al.*, 1998c; Prekeris *et al.*, 1998, respectively). As STX 12 has been suggested to be identical to STX 13 (Jahn and Sudhof, 1999), STX 8 and STX 12 were selected as endosomal syntaxins in this study. STX 16 has been shown to be localised to the TGN and recently it has been identified in a SNARE complex with STX 6 in HeLa cells (Mallard *et al.*, 2002). Therefore localisation of STX 16 in addition to STX 6, 8 and 12 was examined in this study.

Subcellular fractionation studies showed that all four syntaxins are indeed present in 3T3-L1 adipocytes and more than 80% of these proteins were present in intracellular

membranes, which contrasts with STX 2 and STX 4, in which the majority (67% of STX 4) was localised to PM (Volchuk *et al.*, 1996). This suggests that all four of these syntaxins may have a role in intracellular membrane trafficking. Movement of the syntaxins 6 and 16 to the PM in response to insulin with a high magnitude similar to GLUT4 and IRAP was observed in this study, with a corresponding decrease in LDM (Figure 3.3. and 3.4). Such data argue that at least a proportion of these post-Golgi SNAREs are present in GLUT4 vesicles and translocate to PM upon insulin stimulation. As the Western blotting was used, to analyse the quantities of syntaxins, subtle differences, which could occur on distribution of STX 8 and 12 in response to insulin may have passed undetected. In fact around a 2-fold increase in PM-associated M6PR and TfR occurred under insulin stimulation yet is barely detectable by Western blot analysis (Kandror, 1999).

Iodixanol gradient analysis has been shown to resolve intracellular GLUT4 into two distinct peaks, which have been characterised as GSV and endosomal/ TGN compartments (Hashiramoto and James, 2000; Maier and Gould, 2000). Iodixanol is an iodinated compound, which forms a self-generating gradient upon centrifugation. By this method membrane vesicles can be separated according to their density under iso-osmotic conditions. As the syntaxins tested in this study were present in the LDM fraction, their distribution in these gradients was examined. Some degree of overlap was found with all four syntaxins and the two peaks of GLUT4 suggesting that these syntaxins are present in both GSV and endosomal pools of GLUT4 vesicles at least to some extent (Figure 3.5). The observed reduction of syntaxins in the LDM under insulin stimulation, mainly from the first peak may be due to their presence in a more insulin-sensitive compartment such as GSVs (Figure 3.6). Maier and Gould (2000), showed that the first peak represents the GSV pool based on its high sensitivity to insulin and overlap with the GSV R-SNARE, VAMP2 (Maier and Gould, 2000). Overlap of syntaxins with these two peaks of GLUT4 and the similar pattern of their sensitivity to insulin suggests that syntaxins are localised in GSV and endosomal/TGN pools of GLUT4. Such data suggest STX 16 is present at high levels in the GSVs, STX 6 is in both GSVs and TGN and that STX 8/12, although present in GSV fraction, are more abundant in the endosomal pool.

Hashiramoto and James (2000) have shown that the distribution of STX 6 in iodixanol gradients, which is similar to the pattern observed in this study. However, the two peaks of STX 6 seen in our study are more distinct. This difference may be due to the use of slightly higher centrifugal force and a shorter centrifugation time in this study, giving rise to subtle differences in gradient formation. Hashiramoto and James, also have observed overlap of GLUT4 and IRAP with STX 6 in both peaks and suggested that STX 6 may localise to GLUT4 vesicles (Hashiramoto and James, 2000). However the possibility of syntaxins being localised to completely different compartments with similar densities to GLUT4 vesicles cannot be excluded by this approach.

To address this question further, GLUT4 vesicles were isolated using anti GLUT4 antibodies. Isolation of GLUT4 vesicles from the GSV pool of iodixanol gradients was not successful, possibly due to the presence of iodixanol. Therefore, post-nuclear supernatants were used as the starting material for these experiments. The data (Figure 3.7) strongly suggest that all four of these syntaxins are localised in GLUT4 vesicles but to very different extents. There is a high degree of localisation of STX 6 in GLUT4 vesicles, similar to that of IRAP, a protein, known to show extensive colocalisation with GLUT4 (Malide *et al.*, 1997; Martin *et al.*, 1997). This suggests that >90% of STX 6 and >50% of STX 16 present in post nuclear membranes are associated with GLUT4 vesicles (Figure 3.8). In contrast, only a small proportion of STX 8 and STX 12 seem to be associated with GLUT4 vesicles. As this experiment does not differentiate between the GSV and endosomal/ TGN pools these results alone do not provide evidence for the presence of the syntaxins in the GSV compartment. But, taken together with iodixanol gradient experiment results, it is possible to suggest that the two pools of syntaxins separated on iodixanol gradients actually represent the two pools of GLUT4.

The localisation of STX 6, 8 and 12 in GLUT4 vesicles is further supported by the indirect immunofluorescence studies conducted using anti-syntaxins and anti-GLUT4 or anti-IRAP antibodies (Figure 3.9). In agreement with the GLUT4 vesicle immunoadsorption data, the colocalisation of STX 6 with GLUT4 was very prominent. As shown by other studies, STX 6 showed a perinuclear labeling pattern of TGN localisation (Bock *et al.*, 1996, Watson and Pessin, 2000). STX 8 did not show a very

strong signal. STX 12 also showed a perinuclear staining pattern and colocalisation with IRAP labelling was detected.

The endosomal ablation approach was used to determine the proportion of syntaxins present in early and recycling endosomal system, where TfR trafficking occurs. This approach specifically ablates the early and recycling endosomal system without a significant ablation of TGN, LE, lysosomes and secretory pathways (Livingstone *et al.*, 1996). Ablation of only about 50% of syntaxins, which is similar to the proportion of GLUT4 susceptible to ablation, suggests that about 50% of syntaxins are localised in the EE and/ or RE. The other 50% of syntaxins present in LDM should be localised to ablation resistant compartments where the level of TfR is low or absent. One possibility is that they are localised in GSV compartment, but their presence in other compartments cannot be excluded.

Taken together these data on localisation of syntaxins strongly suggest that all four syntaxins present in the LDM compartment are localised to GLUT4 vesicles, at least to some degree. About 50% of these GLUT4-positive compartments are suggested to be EE and/ or RE. In the case of STX 6, our data suggest it most likely resides in specialised GSVs, and EE and/ or RE. Based on data of previous studies, which suggest about 10-20% of total GLUT4 is localised in TGN it is formally possible that the overlap of STX 6 and GLUT4 is restricted to TGN. However, as the recovery of STX 6 with the GLUT4 vesicles in this study was around 90% and some of STX 6 was separated into peak 1 of iodixanol gradient, these data suggest that a proportion of STX 6 is present in the GSV compartment.

It is suggested that SNARE proteins may have different localisations and different SNARE partners among different tissues. Immunoprecipitation of STX 6 from 3T3-L1 adipocytes confirmed that STX 16 is a SNARE partner of STX 6. STX 6 is described as a Qc-SNARE (Bock *et al.*, 2001). Binding with the Qa-SNARE STX 16 suggests, that STX 6 acts as a Qc-SNARE in 3T3-L1 adipocytes, at least in one trafficking event. We did not observe significant binding of STX 6 with R-SNARES VAMP2 and cellubrevin, even though these associations have been previously demonstrated in rat brain (Bock *et al.*, 1997) and HeLa cells (Mallard *et al.*, 2002). The reasons for this are not clear. The evidence of association of STX 6 with STX 16 in the present study

suggests that the putative SNARE complex may function in the regulation of EE to TGN transport as Mallard and co-workers proposed over similar observations in HeLa cells (Mallard *et al.*, 2002). To confirm this suggestion, the R-SNARE associated with STX 6 and STX 16 has to be identified. Association of STX 6 with VAMP4 has been previously demonstrated (Steegmaier *et al.*, 1999; Mallard *et al.*, 2002). VAMP7 and VAMP8 were identified with STX 6, in a SNARE complex from melanoma cells (Wade *et al.*, 2001). We could not study the association with VAMP4, VAMP 7 and VAMP 8 due to a lack of good antibodies. There was some association of STX 6 with a smaller fraction of total STX 4, 8 and 12, yet did not show any reduction of them in post IP supernatant. Steegmaier and co-workers have made an unpublished observation that STX 8 is colocalised partially with STX 6. Furthermore, significant overlap of STX 13 with STX 6 has been shown by light microscopy (Prekeris *et al.*, 1998). These observations support our data on the binding of STX 6 with STX 8 and 12. STX 4 showed binding with STX 6 only in the presence of *N*-ethylmaleimide, which prevents the dissociation of SNARE complex. As STX 6 has been shown to be associated with a variety of SNAREs (Wendler and Tooze, 2001) it is possible for it to have multiple partners in 3T3-L1 adipocytes also. Evidence regarding the SNARE partners of STX 8 and 12 could not be found due to difficulty in detecting proteins in the immunoprecipitates.

Protein phosphorylation is a common and important mechanism for regulating a variety of cellular processes. Numerous studies have shown that the phosphorylation regulates SNARE protein interactions, as well as the availability of SNAREs to participate in membrane trafficking events (Gurunathan *et al.*, 2002). Risinger and Bennett showed that STX 1, STX 3, STX 4 and SNAP-25 are phosphoylated by variety of serine/ threonine kinases (Risinger and Bennett, 1999). They have found that phosphorylation of STX 4 reduced its interaction with SNAP-25 while STX 1A enhanced its interaction with the synaptic vesicle protein synaptotagmin I. Another study showed that STX 4 was phosphorylated when human platelets are treated with physiologic agents such as thrombin, that induces secretion (Chung *et al.*, 2000). Phosphorylation of STX 4 was functionally important, because it decreased binary interactions of STX 4 with SNAP-23, both *in vitro* and *in vivo*. Phosphorylation of SNAP-25 in PC12 cells reduced the amount of syntaxin co-immunoprecipitated with SNAP-25, suggesting that the phosphorylation of SNAP-25 may be involved in protein

kinase C-mediated regulation of catecholamine release from PC12 cells (Shimazaki *et al.*, 1996).

In order to examine the possibility that post-Golgi syntaxins undergo phosphorylation immunoprecipitation experiments were conducted from cells incubated with ^{32}P. According to the results syntaxins 6, 8 and 12 are not phosphorylated under basal and insulin stimulation. However results showed that STX 6 interacts with a phosphoprotein under both conditions. Based on the molecular mass of the phosphoprotein I suggest it might be a syntaxin (Qa-SNARE). The molecular mass of 42 kDa is similar to molecular mass of STX 16, which showed interaction with STX 6 (Figure 3.12.A). Therefore an experiment was performed to determine whether STX 16 immunoprecipitate contains a phosphoprotein. The results showed that this is the case (Figure 3.12.B). Therefore it is possible to suggest that STX 16 undergoes phosphorylation to regulate interactions with STX 6. In the phosphorylated state it was able to bind with STX 6.

All the findings described in this chapter suggest the possibility that STX 6, 8, 12 and 16 may mediate some aspect of intracellular GLUT4 trafficking. STX 6 and 16 may have a more significant role in GLUT4 trafficking. In 3T3-L1 adipocytes STX 6 associates with STX 16 suggesting a role of the in EE to TGN with or without involving in GLUT4 trafficking. Attempts made to find out the functional role of STX 6, 8 and 12, in 3T3-L1 adipocytes are described in Chapter 5.

Chapter 4

Generation of recombinant adenoviruses to study the function of post-Golgi syntaxins in 3T3-L1 adipocytes

4.1 Introduction

4.1.1 Use of adenoviral vectors for gene transfer into mammalian cells

The modification of viruses for the delivery of exogenous genes was first reported in 1968, using the tobacco mosaic virus (Rogers and Pfuderer, 1968). Since adenoviruses (AdV) deliver their genome to the nucleus, and replicate with high efficiency, they became prime candidates for the delivery of foreign or mutant genes into cultured cells. The ability of adenoviral vectors to deliver and express genes at high yields in numerous mammalian cells has been well demonstrated over the last 15 yrs (reviewed in Russell, 2000). Indeed the use of AdV vectors is probably the most efficient gene transfer technique currently available to deliver the genes into mammalian cells (reviewed in Hitt *et al.*, 1997). This system is used efficiently, in both *in vivo* and *in vitro* systems and both dividing and terminally differentiated cells (Hitt *et al.*, 1997). Numerous studies have shown that a wide variety of cells and tissues of different species including humans, non-human primates, pigs, rodents, mice and rabbits can be infected by AdV (Hitt *et al.*, 1997).

In addition to its efficient infectivity, some other properties of the virus have made it an ideal vehicle for gene delivery. The genome of the AdV is relatively easy to manipulate by standard molecular biology techniques making it feasible to construct recombinant vectors. Recombinant AdV can be amplified and purified easily, generating high titer viral stocks in the range of 10^9-10^{12} plaque forming units (pfu)/ml. Furthermore, recombinant AdV infected mammalian cells express high levels of biologically active transgene products which are post-translationally modified correctly (Hitt *et al.*, 1997).

4.1.2 Adenoviruses

AdV are ubiquitous viruses that cause relatively mild upper respiratory tract infections (Collier and Oxford 2000). They were first isolated from human adenoids, and hence named adenoviruses. More than 100 different serotypes of AdV have been identified to date and about half of these are from humans. Among them human AdV serotypes 2 and 5 of subgroup C are most extensively characterised and used as vectors (Hitt *et al.*, 1997). All AdV serotypes generally share similar structural and biological features.

Adenoviruses are non-enveloped, DNA viruses. The virus particle consists of an outer protein shell (capsid) surrounding a double-stranded DNA chromosome of about 36 kb long. Adenovirus has an icosahedral (polyhedral with 20 facets) appearance and is about 70-100 nm in diameter. The viral capsid is made of 252 capsomeres, of which 240 are hexons and 12 are penton bases with a projecting fiber attached to each penton base (Benihoud *et al.*, 1999; Kovesdi *et al.*, 1997; Russell, 2000). The AdV genome codes for 20-30 polypeptides of which, 15 are structural proteins. The viral genome has inverted terminal repeats (ITR) on either end that have a role in viral replication. Near the left ITR there is the encapsidation signal, which is required for packaging of the virus (Figure 4.1.A and B).

Figure 4.1.A

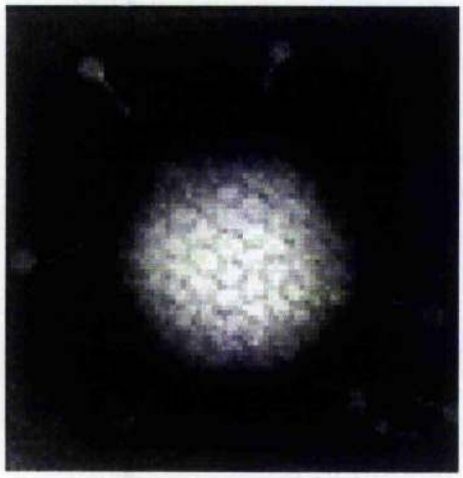

Figure 4.1.B

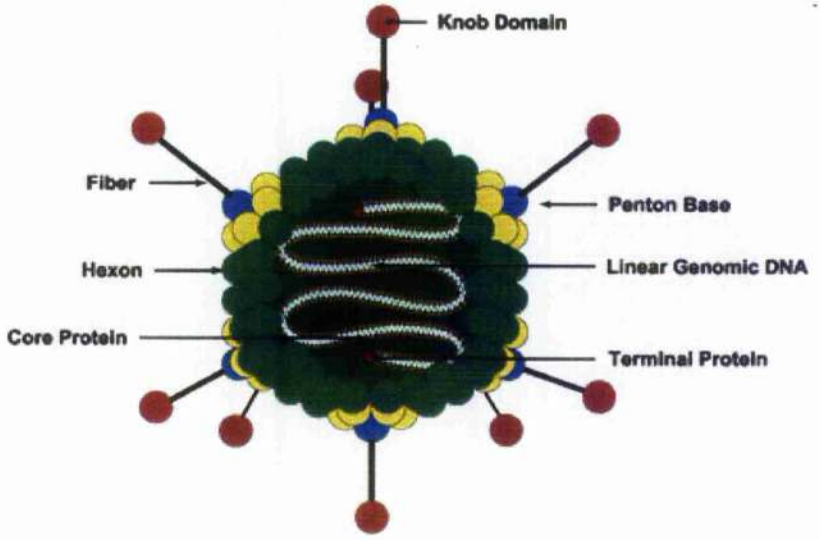

Figure 4.1.A Electron microscopic view of the human adenovirus (adapted from Virus Ultrastructure Electron Micrograph Images, Linda M Stannard, 1995, University of Capetown, Africa web page)

Figure 4.1.B Schematic view to show the structural components of adenovirus (adapted from Q-BIOgene adenovator application manual version 1.0)
Adenoviruses are non-enveloped icosahedral viruses. The capsid is composed of three major proteins: hexons, pentons and knobbed fibers attached to pentons. The viral genome is linear double strandard DNA, with terminal proteins attached to the 5'ends, which have inverted terminal repeats. The DNA is associated with core proteins (Russel, 2000).

4.1.3 Cycle of the adenovirus

The entry of subgroup C AdV into target cells is mediated by two cell-surface receptors. First, the knob of the viral fiber binds to the coxsackie adenoviral receptor (CAR) of the host cell. This is followed by the binding of the virus penton base (see figure 4.1.B), to α_v intergrin (the cellular receptor for extracellular matrix protein vitronectin), which facilitates internalisation of the virus through receptor-mediated endocytosis. The CAR receptor acts as a specific high-affinity receptor for both the coxsackie virus and subgroup C AdV. The virus escapes from the endosome by lysis of the endosomal membrane in a process mediated by penton base, to the cytosol (Curiel *et al.*, 1991). The virus then translocates to the nuclear pore complex, where the viral DNA is released into the nucleus and transcription begins, with both strands of the viral DNA transcribed. Nearly all the transcripts are spliced. Transcription of the AdV genome occurs in two phases, early and late. Early (E1-E4) genes are expressed within 6-8 hrs after infection and multiple mRNAs are produced from each of these regions. E1, E2 and E4 encode essential regulatory proteins involved in activation of viral and cellular promoters, DNA replication, cell cycle and apoptosis. E3 products help the virus evade host immunity. The late genes encode proteins required for packaging the viral genome (for review see Hitt *et al.*, 1997).

Viral DNA replication begins about 6-8 h post infection in permissive cells. Late regions of the viral genome start to express following the onset of viral DNA replication with the use of the major late promoter. Virus production is complete ~ 30-40 h post infection resulting in approximately 1000 viral particles per cell along with synthesis of a substantial excess of viral proteins and DNA that are not assembled into virions (Hitt *et al.*, 1997).

4.1.4 Adenoviral E1 gene

E1 gene is essential to initiate the AdV cycle and therefore it is deleted from adenoviral vectors to make the virus replication defective. The E1 proteins (which are coded by the E1 gene) have two major functions. One function is to turn on expression of all other AdV genes so that AdV proteins are made and virions can form. The other function is to deregulate the cell cycle of quiescent cells and drive the cells from G_0 into S phase, so that viral gene expression and DNA replication can occur efficiently.

4.1.5 Replication defective adenoviruses

Replication of the virus leads to the death of host cell and dissemination of virus. Therefore gene transfer should be carried out using highly attenuated AdV. E1-deleted AdV are replication defective unless E1 products are complemented. These deletions create space for the insertion of foreign DNA. In addition to creating room for DNA inserts, deleting E1 restricts the cytopathic effects of the recombinant AdV (Graham *et al.*, 1977). This replication incompetent AdV propagates only in cell types such as HEK 293 cells (human embryonic kidney cell line transformed by the E1 region of AdV serotype 5) (Graham *et al.*, 1977) and 911 cells (E1-transformed human embryonic retinal cells) that express E1 proteins. All other cell types susceptible to AdV infection will have a transient, non-cytopathic infection.

Genome sizes up to 105% of wild type can be packed in full length AdV, thus allowing the insertion of up to 1.8 to 2 kb foreign DNA. Larger inserts can be accommodated by deletion of E1/ E3 regions. Up to 3.5 kb of E1 can be deleted without affecting the growth of virus in 293 cells. E3 deletion provides about 3 kb space for insertion. Most AdV vectors are both E1 and E3 deleted (Hitt *et al.*, 1997).

Following the infection of non-permissive cells (in which the E1 gene products are not available), the target gene is transiently expressed at high levels since many cells receive multiple copies of the recombinant genome. The AdV genome is not replicated or actively transcribed, since the cell lacks the necessary transcription factors expressed by E1 genes. However, the target gene is expressed at high levels because it is independently controlled by a constitutive promoter.

4.1.6 Specificity, level and duration of expression of transgene in target cell

One of the factors that influence the ability of AdV to infect a particular cell is the presence of α_v intergrins, the cell surface receptors for the viral internalisation. Although they are widespread among most cell types, there are some exceptions such as lymphocytes (Hitt *et al.*, 1997). The level of expression of the transgene in AdV infected cell is influenced largely by the promoter driving the expression. The murine cytomegalovirus (CMV) immediate early promoter has been the strongest promoter used so far for *in vitro* expression in rodent cells (Hitt *et al.*, 1997). *In vitro*, transgene expression is often observed on the first day of infection, reaches a peak on day two to

three and is sustained for about one week. The level of protein decreases thereafter in non-dividing cells (Mackay, 2001). In dividing cells, duration of expression is shorter as the transgene is diluted out during mitosis, as the AdV does not integrate its genes into the host genome (Mackay, 2001).

4.2 Aims

To date, the efficiency of transfection of 3T3-L1 adipocytes has been at best poor. Hence, for expression of foreign or mutant genes, the options are either the time-consuming and inefficient process of making stable transformants or microinjection, which provides only small cell populations. Hence, to examine the role of STX 6, 8 and 12 in GLUT4 traffic, the aim of this chapter was to produce three different recombinant AdV carrying the DNA inserts for the cytosolic domains of STX 6, 8 and 12, and a control virus. Subsequently these will be amplified and purified to obtain adequate quantities of pure virus, to drive overexpression of truncated syntaxins in 3T3-L1 adipocytes.

4.3 Materials

Rat STX 6 cDNA was a kind gift of Dr. J. E. Pessin, University of Iowa, USA.

Rat STX 8 and mouse STX 12 cDNA were kind gifts of Drs Wanjin Hong and Bor Luen Tang, Institute of Molecular and Cell Biology, Singapore.

pAdEasy vector, pShuttle CMV and electro-competent BJ5183 cells were the kind gifts from Dr. Timothy Palmer, University of Glasgow.

Large-scale amplification of STX 6-AdV was performed once commercially by Q-BIOgene (France).

4.4 Methods and Results

4.4.1 Generation of recombinant adenoviruses.

This process involved three major steps, outlined in figure 4.2. These are,

4.4.1.A Cloning of the gene of interest into pShuttle-CMV vector

4.4.1.B Homologous recombination of pShuttle-CMV and the AdV backbone vector in *E. coli* strain BJ5183.

4.4.1.C Production of AdV particles in HEK 293 cells

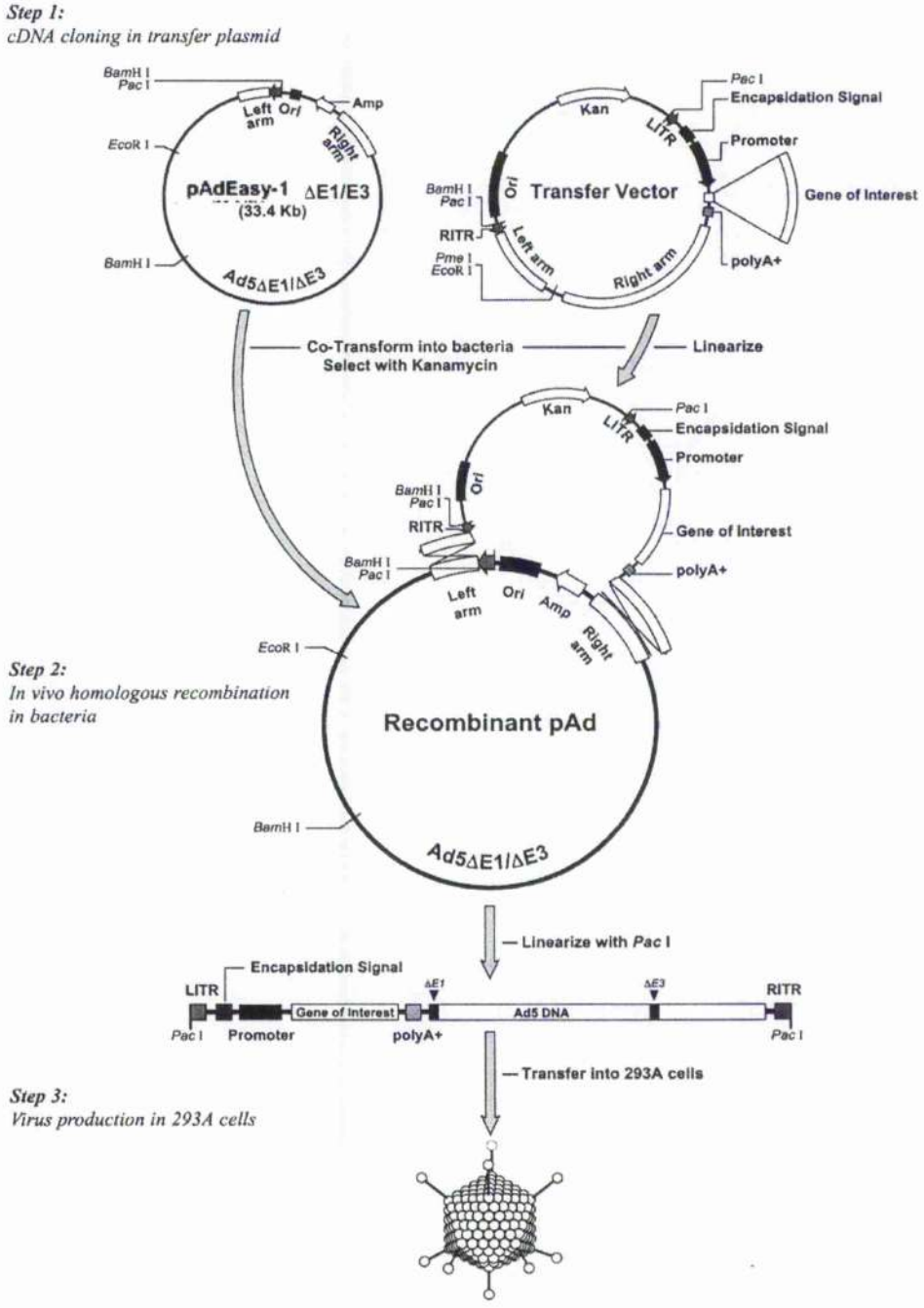

Figure 4.2 Three basic steps followed to generate recombinant adenoviruses (adapted from Q-BIOgene AdEasy protocol)

Step 1: Cloning of gene of interest into pShuttle-CMV

Step 2: Homologous recombination of pShuttle-CMV and AdV backbone vector (pAdEasy-1) in *E. coli*

Step 3: Production of AdV particles in HEK 293 cells

The method is described in sections 4.4.1.A, B and C.

4.4.1.A Cloning of genes of interest into pShuttle-CMV (Figure 4.2- Step 1)

Two methods have been used traditionally to insert the gene of interest to adenoviral genome. The first method was the direct ligation of insert into adenoviral genome, which is technically challenging due to large size of the genome (36 kb) and scarcity of restriction sites. The second and more widely used method involves cloning of the gene of interest into a shuttle vector and homologous recombination with adenoviral genome in a packaging cell line (HEK 293 cell). Recently, a more efficient and less time consuming method was described, where the homologous recombination occurs in *E. coli*, using its efficient recombination machinery (He *et al.*, 1998).

pShuttle-CMV vector

This vector contains a multiple cloning site for insertion of exogenous transgenes between cytomegalovirus (CMV) promoter and polyadenylation site (see appendix). Furthermore, there are adenoviral sequences (left and right arms) that allow homologous recombination with pAdEasy-1 adenoviral vector. Also, the sequence of pShuttle includes inverted terminal repeats and packaging signals. Artificially created *Pac* I sites surround both arms. The vector also contains a kanamycin resistance gene and the origin of replication from pBR322 (He *et al.*, 1998). pShuttle-CMV has a cloning capacity of 6.6 kb (AdEasy adenoviral vector system instruction manual-Stratagene, USA).

PCR of DNA encoding cytosolic domains of syntaxins 6, 8 and 12

Forward and reverse primers for the three inserts were designed including restriction sites appropriate for the multiple cloning site of pShuttle-CMV vector. Reverse primers were designed with a stop codon at the end of cytosolic domain of each syntaxin. The DNA stretch encoding the transmembrane domain was not included. The length of STX 6, 8 and 12 inserts were 705 bp (encompassing amino acids 1 to 235), 642 bp (encompassing amino acids 1 to 214) and 744 bp (encompassing amino acids 1 to 248) respectively.

STX 6 forward primer was, 5'-CCGAGATCTATGTCCATGGAGGACCCC-3' containing a *Bgl* II site (underlined). The reverse primer was 5'-GGCAAGCTT**TCA**CCACTGGCGCCGATCACTG-3' with a *Hind* III site (restriction site is underlined and the stop codon in bold).

STX 8 forward primer was, 5'-GACAGATCTATGGCCCAGACCCCTGG-3' containing *Bgl* II site (underlined). The reverse primer was 5'-TATTCTAGA**TCA**GGAAGCTGACTTTCTGTC-3' with a *Xba* I site (restriction site is underlined and the stop codon is in bold).

STX 12 forward primer was, 5'-CAGCTCGAGATGTCCTACGGTCCCTTA-3' containing a *Xho* I site (underlined). The reverse primer was 5'-GAGTCTAGA**CTA**CTTCTTGCGAGATTTTTT-3' with a *Xba* I site (restriction site is underlined and the stop codon in bold).

PCR amplification of these three DNA sequences was carried out as described in section 2.6.1 using cDNAs for rat STX 6, rat STX 8 and mouse STX 12 as templates. The PCR products were gel purified and TA cloned into pCRII vector (see appendix), as described in sections 2.6.3 and 2.6.5 respectively. Colonies were selected in presence of ampicillin and kanamycin and assayed for the presence of inserts by restricting with *EcoR* I (Figure 4.3.A). The sequences of the syntaxin-pCRII clones were verified before proceeding further. The inserts were then subcloned into pShuttle-CMV as described in sections 2.6.4 and 2.6.6, by restriction, purification and ligation of insert and pShuttle-CMV vector. Ligated product was transformed into *E. coli* DH5α as described in section 2.6.8. Colonies were selected in presence of kanamycin and assayed for the presence of an insert by restriction digestion (Figure 4.3.B). Plasmid DNA was purified as described in 2.6.9, and was used for the homologous recombination step.

Cloning of inserts into pShuttle-CMV did not present any problems except for the failure to detect the insert of STX 8 construct when using *Bgl* II and *Xba* I digestion. It was found that in the reverse primer, the *Xba* I site adjacent to the stop codon TCA has created a Dam methylation site (bold letters) (5'-TATTCTA**GATC**AGGAAGCTGACTTTCTGTC-3'). Therefore STX 8 had to be ligated directly into pShuttle omitting the ligation into pCRII. The presence of insert in pShuttle was confirmed by restriction with *Bgl* II and *EcoR* V (next available restriction site), instead of *Bgl* II and *Xba* I.

Figure 4.3.A

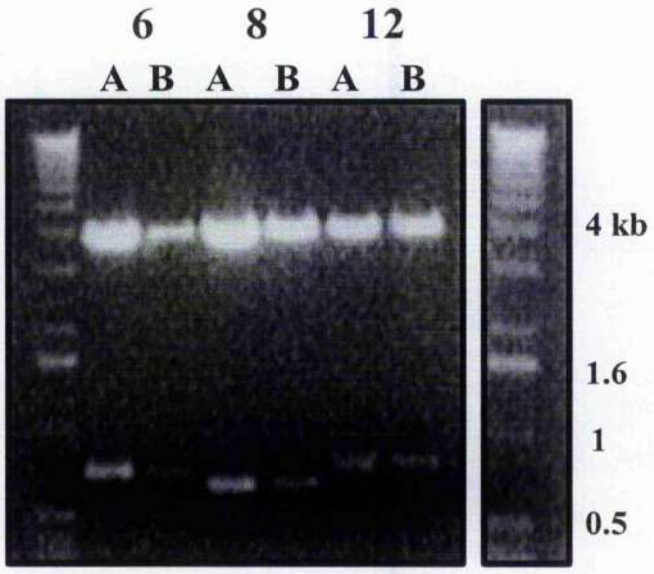

Figure 4.3.B

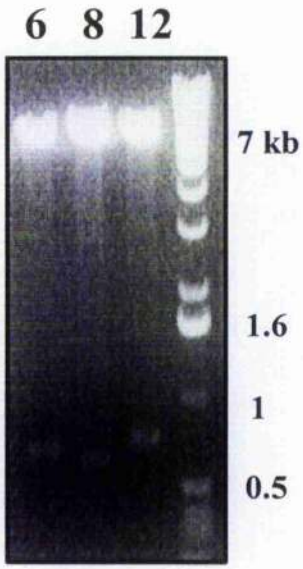

Figure 4.3.A Restriction of STX-pCRII with *EcoR* I to identify the presence of insert

Shown are typical restriction digests from the ligation of STX into pCRII, using *EcoR* I to liberate the insert. The STX 6, 8 and 12 inserts were of 705 bp, 642 bp and 744 bp respectively. The band at 4 kb represents the pCRII vector. The lane at further right shows the separation pattern of 1 kb DNA ladder. As shown, STX 6, 8 and 12 were present in both clones (A and B) shown here.

Figure 4.3.B Restriction of STX-pShuttle-CMV to identify the presence of insert

Shown are typical restriction digests from the ligation of STX into pShuttle-CMV, using restriction enzymes for the forward and reverse primer sites. The bands between 0.5 and 1 kb represent STX inserts, the band at 7 kb is pShuttle.

4.4.1.B Homologous recombination of pShuttle-CMV and adenoviral backbone vector in *E. coli* (Figure 4.2- Step 2)

The method described by He and co-workers (1998) was used. pAdEasy-1 is a 33.4 Kb plasmid, which contains all AdV serotype 5 sequences except nucleotides 1-3,533, the deletion of E1 gene, and nucleotides 28,130-30,820 the deletion of E3 gene. In this method homologous recombination between the shuttle vector and AdV genome is performed in *E. coli* strain BJ5183 (Genotype: *endA sbcBC recBC galK met thi-1 bioT hsdR* (Str^r)) as this strain has a high recombination capability and high transformation efficiency. During recombination, a new plasmid is generated with the expression cassette inserted into the E1 region of the adenovirus genome.

Before transfection of BJ5183 cells, pShuttle vector carrying the syntaxin DNA was linearised, using *Pme* I. As a control, pShuttle-CMV, without the insert was linearised. Linearised vectors were gel purified and the DNA extracted using phenol-chloroform, ethanol precipitated, and resuspended in 6 µl nuclease free water.

Co-transformation was conducted using the following amounts of linearised pShuttle vector, pAdEasy AdV plasmid and electro-competent BJ5183 cells:

Linearised pShuttle with/ without insert	Miniprep DNA from 3 ml culture (100-500 ng DNA is sufficient)
pAdEasy	1 µl (100ng/µl)
Electro-competent BJ5183 cells	20 µl /transfection

All three components were added to a 2 mm electroporation cuvette on ice and collected at the bottom of cuvette by gentle tapping. Electroporation was performed at 2,500V, 200 Ohms, and 25 µF for 1 sec in a Bio-Rad Gene Pulser Electroporator. The transformation mixture was resuspended in 500 µl LB (see section 2.1.5) and incubated at 37°C for 20 min. Each mixture was plated on three LB agar plates containing kanamycin and grown overnight at 37°C.

Colonies of two sizes could be identified following transformation. The smaller colonies tend to be those containing the pAdEasy recombinants (AdEasy adenoviral vector system instruction manual-Stratagene, USA). The recombination efficiency is

known to be more than 20%. Colonies carrying the recombinants were identified by growing them in presence of Kanamycin, purifying plasmid DNA and examining the pattern of DNA electrophoresis on a 0.8% Agarose gel. Plasmids carrying the AdV genome showed a band above the 12 kb marker which represents a species about 35 kb (Figure 4.4). Recombination was confirmed by restriction of DNA with *Pac* I, which generated a band at approximately 30 kb and another at either 3 kb or 4.5 kb (Figure 4.5). Finally, the presence of the inserts was confirmed by PCR using the recombinant AdV DNA as templates (Figure 4.5). The plasmid DNA of the correct recombinants was transformed into DH5α cells to produce high yields of plasmid DNA necessary for transfection of 293 cells. Large scale DNA preparation (maxi prep) was carried out as described in section 2.6.10.

Figure 4.4 Identification of presence of pAdEasy recombinants in purified DNA

Plasmid DNA was purified from the colonies obtained after the homologous recombination step, performed in BJ5183 cells. Purified DNA was electrophoresed on a 0.8% Agarose gel to identify a band representing pAdEasy (around 35 kb). The lane at further right shows the separation pattern of 1 kb DNA ladder.

* Indicates the correct recombinants of four different constructs.

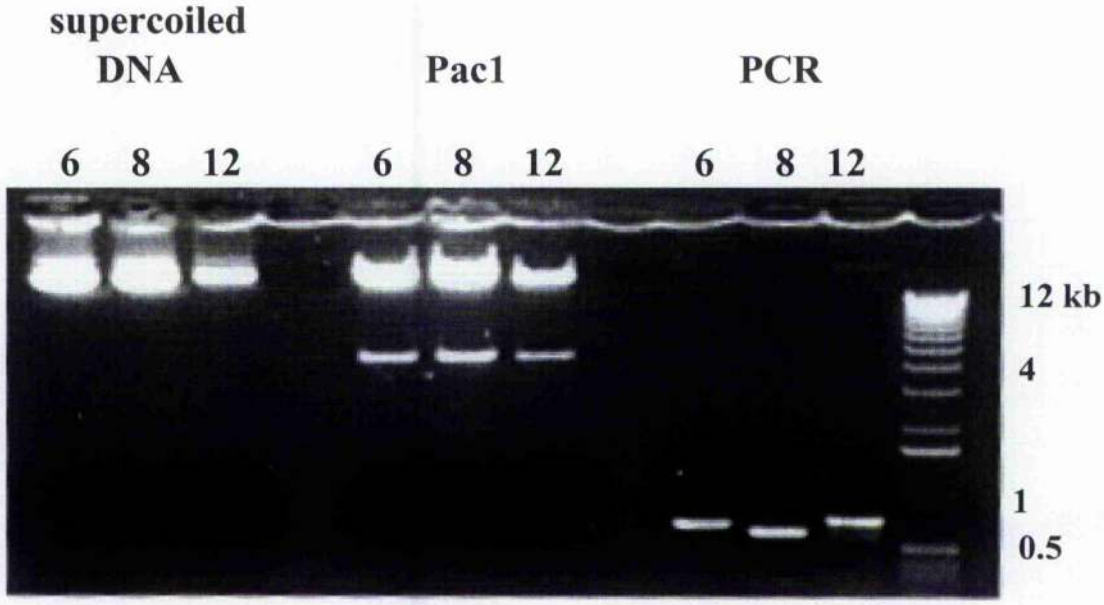

Figure 4.5 Confirmation of presence of pAdEasy recombinants in purified DNA

The first three lanes from the left, shows the size of supercoiled DNA (around 35 kb) indicating presence of pAdEasy. Three lanes in the middle show the 4.5 kb band on *Pac* I digestion of purified DNA which confirms the presence of pAdEasy. The three lanes at right show the confirmation of presence of the correct insert in the recombinants by PCR. STX DNA is found between 0.5-1 kb. The last lane shows markers of the 1 kb DNA ladder. 6, 8 and 12 refer to three respective syntaxin DNA (with or without pAdEasy).

4.4.1.C Production of adenoviral particles in HEK 293 cells (Figure 4.2-Step 3)

AdV plasmid was digested with *Pac* I to expose its inverted terminal repeats (ITRs), before transfection of the packaging cell line. HEK 293 cells between passages 40 to 60 were used. Transfection of HEK 293 cells grown on 10 cm plates was conducted as described in section 2.6.11, with 10 μg DNA used for each transfection. On the following day, transfection media was replaced by HEK cell media (section 2.2.6) with 5% FCS. The cells were then fed every third day with the same media without removing existing media. Feeding was continued until about 50% of the cells showed cytopathic effects (rounding of cells and formation of plaques) due to viral production. This process took about 5-7 days from the day of transfection. Gentle shaking of the plate lifted all cells off the plate at this stage. The cells were then harvested by centrifugation of the medium at 2000 x g for 10 min at room temperature. The medium was preserved as this contains about 10% of AdV at this stage. Cells were then resuspended in PBS, and lysed using Arklone P (Trichlorotriflurocthane) (ICI Ltd). An equal volume of Arklone P solution was added to the HEK cell suspension and mixed gently by inverting the tube for about 10 sec. The mixture was left at room temperature for 3 min and then centrifuged at 2000 x g for 10 min. The upper layer, containing virus was separated from cell debris (interface) and the Arklone P layer (bottom layer). Aliquots of this supernatant from three different syntaxin-pAdEasy constructs were used to test for the expression of truncated syntaxins. Both the supernatant from cell lysate and the growth media collected separately were used to infect more HEK cells and thus expand the clones.

4.4.2 Production of high titer viral stocks

The amplification of virus was carried out simply by infecting more HEK cells with the harvest of the initial transfection. Two 75 cm^2 (T-75) flasks of HEK cells at 50%-70% confluence were used for the infection at the first round. After about 3-5 days virus was harvested as described above, and this harvest was used to infect a second round of cells (two T-150 flasks). Finally, the harvest of two T-150 flasks was used to infect around twenty T-150 flasks with HEK cells at about 80% confluence. When more than 50% of cells infected at the final round were detached, the cells were collected with the growth medium. From this suspension, the cells were collected separately and resuspended in about 10 ml PBS (section 2.1.5). The supernatant was

discarded. The cells were then lysed to release the virus using Arklone P as described above.

The virus layer (up to about 8 ml) was loaded on a CsCl step gradient consisting of 1.44 g/ml (1.5 ml) and 1.33 g/ml (2.5 ml) solutions. The viruses were purified by centrifugation at 100,000 x g for 75 min at 8°C with the brakes off in a SW 40 rotor. The viral band could be seen as a discrete white band after centrifugation in the middle of the CsCl gradients, just below the defective capsid layer. The virus was aspirated from the side of the tube using a 21 guage needle, and dialysed overnight at 4°C in a Slide-A-Lyzer dialysis cassette (0.5- 3 ml). Virus stock buffer (10 mM Tris-HCl, 100 mM NaCl, 0.1% BSA, 10% glycerol, pH 8.0) was then added in 1:1 ratio to the virus. Aliquots of around 50 µl were stored at –80 °C until use.

In addition to the four different viruses made without a reporter gene such as green fluorescent protein (GFP), a stock of control virus containing pAdTrack-CMV (gene for GFP is included) instead of pShuttle-CMV obtained from Dr. Timothy Palmer, University of Glasgow was amplified in the same way as described above. This virus was used for the initial optimisation of infection conditions.

4.4.3 Titration of adenovirus by end-point dilution

The method described by Nicklin and Baker (1999) was used for titration of adenovirus stocks. We used the end-point dilution method (tissue culture infectivity dose in 50% of cells ($TCID_{50}$)), which gives more consistent results compared to methods such as plaque forming unit assay (AdEasy adenoviral vector system instruction manual-Stratagene, USA). HEK cells were seeded into 80 wells of a 96 well plate so that the cells were at 50-60% confluence the next day. Serial dilutions of virus were made in HEK cell media with 5% FCS at the time of infection, to obtain 10^{-2}, 10^{-4}, 10^{-6}, 10^{-7}, 10^{-8},10^{-9}, 10^{-10} and 10^{-11}dilutions. The media of the wells was removed and each lane of cells was infected with the viral dilutions (100 µl/ well) starting from 10^{-11} to 10^{-4} or 10^{-2} leaving first lane without virus. Media carrying the virus was replaced with HEK media with 5% FCS, after 18 h. Cells which did not show cytopathic effects (CPE), were fed every 3rd day. Wells that showed CPE were

marked during the period. After 10 days the proportion of wells which showed CPE in each lane were taken into account to calculate the titer.

e.g.;

10^{-4}: 10/10 10^{-6}: 10/10 10^{-7}: 10/10

10^{-8}: 9/10 10^{-9}: 3/10 10^{-10}: 0/10

10^{-11}: 0/10.

In this case 100% of the wells at dilution 10^{-7} are positive, and 0% of the wells at 10^{-10} are positive for CPE. Titer can be precisely determined using the KARBER statistical method (adapted from Q-BIOgene adenovator application manual version 1.0).

For infections performed using 100 µl of viral dilutions the $TCID_{50}$ is = $10^{1+d(S-0.5)}$

d = Log 10 of the dilution (=1 for a ten-fold dilution)

S = the sum of ratios (always starting from the first 10^{-1} dilution) = 7+0.9+0.3 = 8.2

(7 in above formula represents 10/10 positives from 10^{-1} to 10^{-7}).

$TCID_{50}$= $10^{1+1(8.2-0.5)}$ = $10^{8.7}$ (for 100 µl aliquot of virus)

$= 10^{9.7} \sim 5x10^9$/ml

1 $TCID_{50}$= 0.7 plaque forming units (pfu)

Therefore titer = 3.5x 10^9 pfu/ml

Titers of amplified recombinant AdV produced in this study were usually between 10^9 and 10^{10} pfu/ml.

4.5 Use of recombinant adenovirus in 3T3-L1 adipocytes

For the optimisation purposes infection of 3T3-L1 adipocytes was first conducted with GFP-AdV. Infection was conducted at different times of differentiation of 3T3-L1 cells. Multiplicities of infections (MOI) between 1:10 (10 pfu per adipocyte) and 1:200 were used, determined to be the most effective range to use (data not shown). Expression of GFP as an indicator of efficiency of infection, was visualised using a fluorescent microscope within first 2-3 days post infection. Infection between day 6-8 of differentiation at MOI 1:100 showed expression of GFP in about 70% of cells after 48 h (Figure 4.6.A). Efficiency of infection of 3T3-L1 was increased when DMEM, 0.5% BSA was used compared to normal FCS media or DMEM alone. Minimising the

volume of media during infection also increased the efficiency. No morphological change was observed in infected 3T3-L1 adipocytes compared to non-infected cells.

After optimisation of infection of 3T3-L1 adipocytes with GFP-AdV, STX-AdV was used to infect 3T3-L1 adipocytes. At Day 7 of differentiation, cells were washed in serum free DMEM (section 2.1.2) once, and DMEM containing 0.5% BSA added (1 ml/ well of a 6-well plate). 3T3-L1 adipocytes were infected with AdV by adding the virus to BSA media. The plates were swirled intermittently during first two hours to allow uniform contact of virus with the cells. Infected cells were incubated at 10% CO_2 and 37°C. After 24 h, viral media was removed and cells were fed with normal 10% FCS media. Two or three days after infection, cells were harvested and homogenised. These homogenates were tested for the expression of the truncated syntaxins by Western blotting.

All three viruses made to overexpress syntaxins were capable of overexpressing truncated versions of syntaxins in 3T3-L1 adipocytes (Figure 4.6.B). The labelling of fixed 3T3-L1 cells with anti syntaxin antibodies (results not shown) showed that at least 70% of 3T3-L1 cells were infected with MOI 1:100. Both STX 6 and STX 12 showed the apparent low molecular mass truncated syntaxins below the full-length syntaxins. But truncated STX 8 showed a band above the full-length STX 8. This may be due to a species difference as the truncated STX was of rat origin. A similar observation was made by Prekeris and co-workers in their study, where they found a slightly higher apparent molecular mass of STX 8 in NRK and PC12 cells which are of rat origin compared to that of tissues from other species tested (Prekeris *et al.*, 1999). With MOI 1:100, the level of overexpression achieved was 19-fold for STX 6 and, 2-fold in STX 8 compared to expression of full-length protein. At a MOI 1:50 STX 12-AdV gave 16-fold overexpression of STX 12 (Figure 4.7). The much lower fold increase associated with STX 8 may be partly due to the higher concentration of wild type STX 8 expressed in 3T3-L1 adipocytes (Figure 4.6.B).

Figure 4.6.A

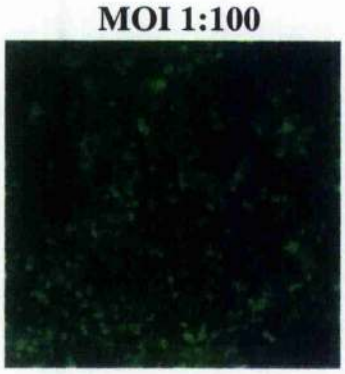

Figure 4.6.B

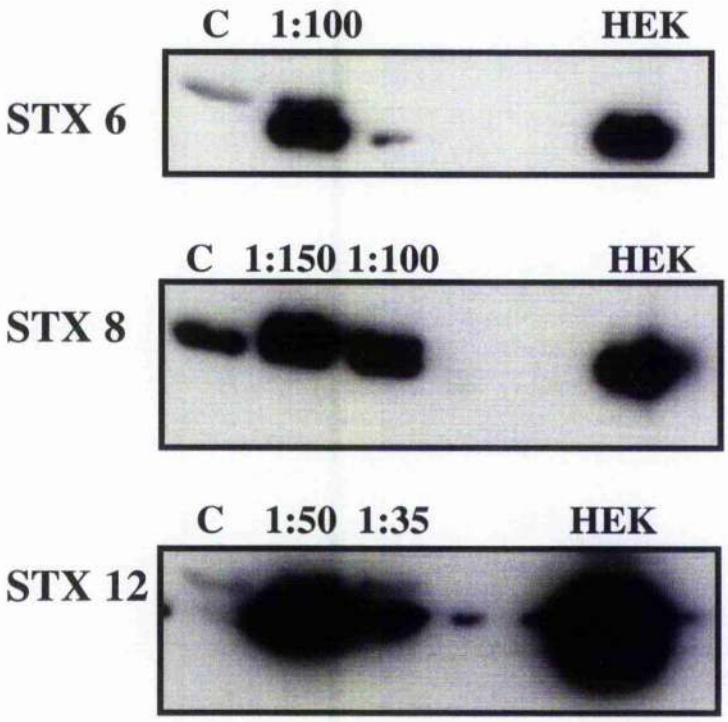

Figure 4.6.A Infection of 3T3-L1 adipocytes by GFP-AdV
MOI of 1:100 was used for the infection. Cells were observed under fluorescent microscope 48 h post infection, to identify GFP expression. A representative field is shown.

Figure 4.6.B Overexpression of syntaxins in 3T3-L1 adipocytes by STX-AdV
Cells were infected with the three different STX-AdV at the MOI as indicated in the figure. C: indicates full-length syntaxin expressed in non-infected (control) cells. The adjacent lanes show the overexpression of truncated STX in 3T3-L1 adipocytes at the indicated MOI. The lane labelled HEK indicates the overexpressed truncated STX identified from infected HEK 293 homogenates. Figure shows immunoblots from one experiment. Similar pattern was seen in all other experiments, which used AdV infected 3T3-L1 adipocytes.

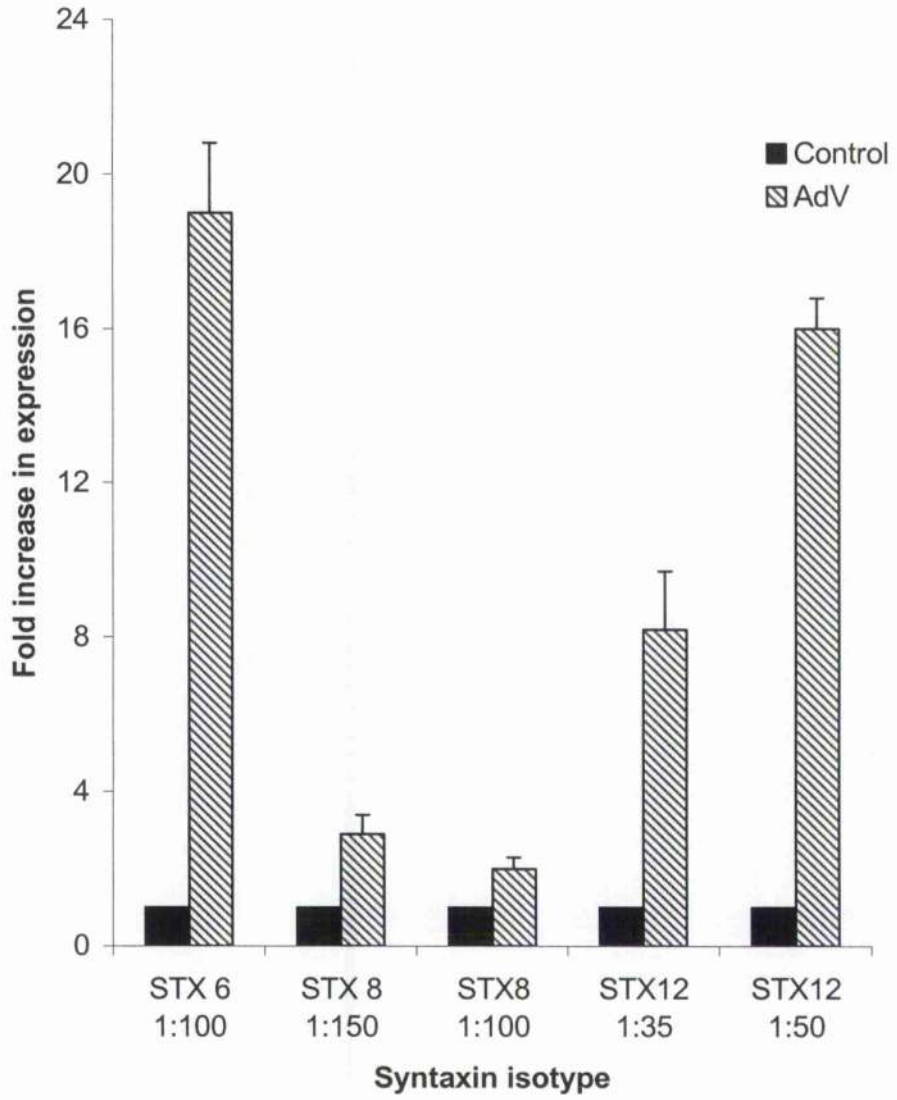

Figure 4.7 Quantitation of overexpression of syntaxins in 3T3-L1 adipocytes

A representative blot of overexpression of STX, as shown in figure 4.6.B was analysed quantitatively using NIH image software. Fold increase of overexpressed STX (AdV) was calculated, considering the quantity of non-infected control (Control) as one (Mean±SEM) (n=4).

Subcellular fractionation, of infected 3T3-L1 cells were carried out as described in section 2.3.3. PM, HDM, LDM and cytosolic fractions were examined for the presence of truncated syntaxins. Such experiments illustrated the extensive localisation of truncated syntaxins in the cytosol (Figure 4.8). The overexpressed syntaxins lack the hydrophobic TM domain necessary for its membrane anchoring, so would be expected to be cytosolic. Some incorporation of overexpressed STX 12 into PM, HDM and LDM was observed (Figure 4.8).

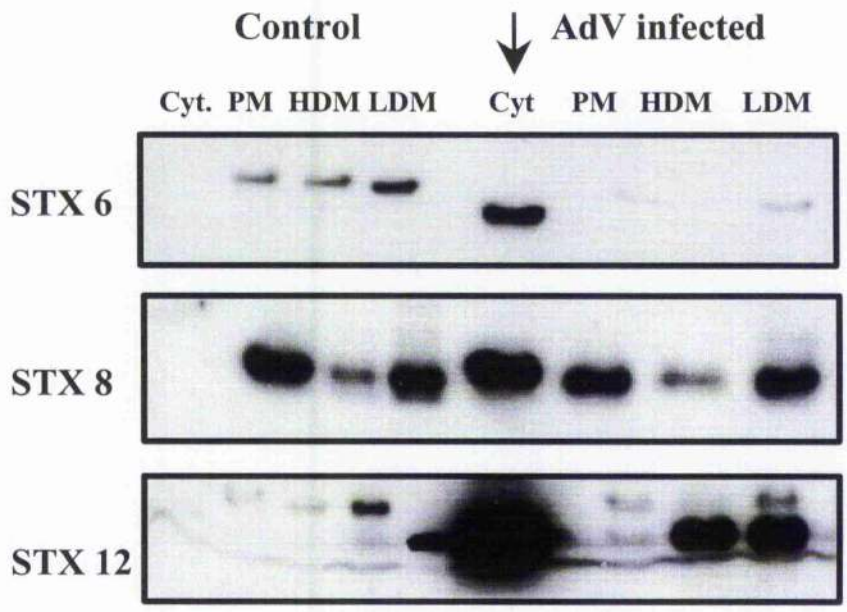

Figure 4.8 Subcellular fractionation of 3T3-L1 adipocytes infected with STX-AdV

PM, HDM, LDM and cytosolic fractions (Cyt.) were separated from 3T3-L1 adipocyte homogenates as described in section 2.3.3 on a small scale. Shown are those fractions from control and AdV infected cells immunoblotted with antibodies for each STX. Arrow shows the localisation of overexpressed STX in cytosolic fractions of infected cells.

4.6 Use of recombinant adenovirus in HeLa cells

HeLa cells grown on 6-well plates were infected with GFP-AdV at MOI 1:5, 1:10 and 1:15 in DMEM, DMEM, 0.5% BSA and normal HeLa medium (section 2.2.7). The next day the media containing virus was replaced with fresh HeLa cell medium. Expression of GFP was visualised using a fluorescent microscope 2-3 days post infection. Figure 4.9.A shows a typical result in which about 70% cells expressed GFP 48 h after infection at an MOI of 1:5. Almost 100% cells showed GFP fluorescence at MOI 1:10 and 1:15. At MOI 1:15 GFP signals were brighter.

HeLa cells were infected in normal HeLa media with STX 6-AdV at MOI 1:5, 1:10 and 1:25. Cell homogenates were checked for the expression of truncated STX 6 at different times post infection by Western blotting (7 h, 24 h and 48 h). Figure 4.9.B shows a typical result. Similar results were seen with STX 8 and STX 12 AdV infections. This demonstrates that the overexpression of STX 6 is time dependent and dose dependent. Our findings illustrated that MOI of 1:10 after 48 h infection gives almost 100% infection and overexpression of transgene without apparent cell toxicity.

Use of different media did not show a difference in efficiency of infection of HeLa cells. Therefore normal HeLa media was used. Increasing the volume of media at the time of infection showed a reduced infection rate. HeLa cells showed signs of cellular toxicity (cell rounding and detachment from the monolayer) on prolonged incubation (more than 2 days) after infection with virus at high MOI (>1:10).

Figure 4.9.A

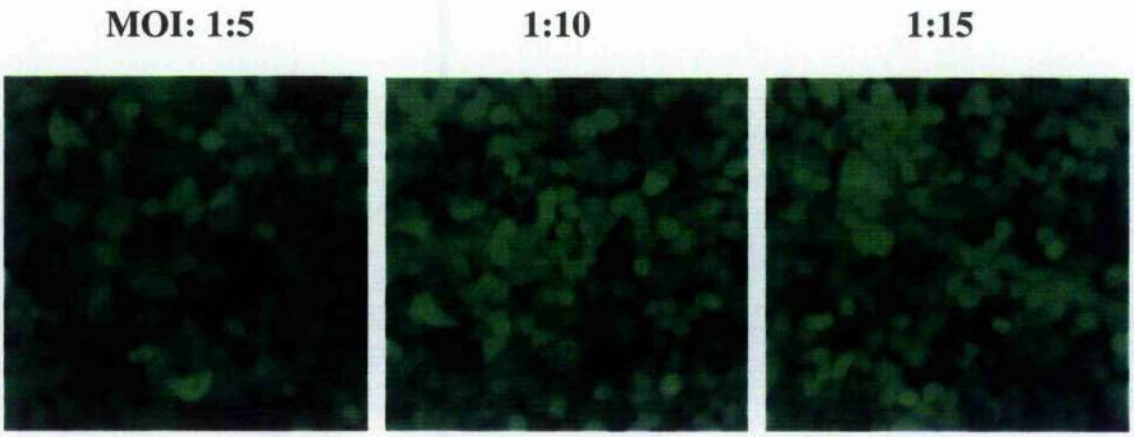

Figure 4.9.B

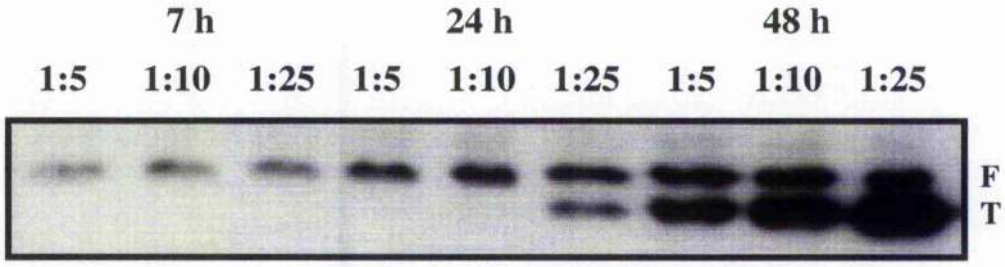

Figure 4.9.A Infection of HeLa cells by GFP-AdV

GFP-AdV was used at a MOI of 1:5, 1:10 and 1:15 to infect HeLa cells. Cells were observed under fluorescent microscope 48 h post infection, to identify GFP expression. Representative fields are shown.

Figure 4.9.B Overexpression of STX 6 in HeLa cells under different MOI, for different periods

Cells were infected with STX 6-AdV at MOI 1:5, 1:10 and 1:25. Cells were harvested and examined for the presence of truncated STX 6, at 7 h, 24 h and 48 h post infection by immunoblotting. Similar patterns were seen with STX 8 and 12. Figure shows a representative immunoblot of STX 6-AdV infected HeLa homogenates collected at 7, 24 and 48 h post infection. F-full length STX 6; T-truncated STX 6.

4.7 Discussion

Native trafficking of GLUT4 could be studied only in terminally differentiated adipocytes or myocytes, since these are the cells that express GLUT4 and they contain the cellular factors required for normal trafficking of GLUT4. This chapter described the construction of adenoviruses as a method to overexpress cytosolic domains of syntaxins in 3T3-L1 adipocytes, in order to study the function of their wild type counterparts. Standard transfection methods have only a very low efficiency in transferring genes into these highly differentiated cells (Gnudi *et al.*, 1997). Preparation and isolation of stable cell lines expressing the transgene, on the other hand is a very prolonged and expensive process. Also the transfection has to be done before differentiation, which might affect the normal differentiation process due to expression of transgene.

Adenoviral vectors have proved effective for gene transfer in differentiated cells and tissues for transient expression of gene of interest (Miyake *et al.*, 1996). Adenoviruses have been used successfully in 3T3-L1 adipocytes to transfer various genes. There are studies which have shown an efficiency of at least 80% infection of 3T3-L1 adipocytes at MOI 1:50 (Emoto *et al.*, 2001; Bose *et al.*, 2001),. Studies performed with adenoviruses produced by slightly different methods have shown the use of MOI ranging from 1:30 (Sakaue *et al.*, 1997), which gave more than 95% infection) to 1:1000 (Yang and Mueckler, 1999, Huppertz *et al.*, 2001).

In our study the method of He and co-workers (1998) was used mainly because it overcomes the requirement of repeated rounds of plaque purification to obtain homogeneous recombinant viruses. They found that at least 95% of the cells infected with GFP/lacZ virus made with this system expressed both transgenes.

During infection of 3T3-L1 adipocytes it was found that presence of serum at the time of infection reduced the efficiency of infection. This may be due to a competitive inhibition caused by the growth factors for the binding of viral particles to the cell surface receptors. Infection of 3T3-L1 adipocytes was much more difficult compared to infection of HeLa cells which needed about 20 times more virus (than for HeLa) to achieve the same infection rate. This low efficiency may be due to low availability of CAR receptors and/ or α_v intergrins in 3T3-L1 adipocytes. One problem encountered

regarding the infection of 3T3-L1 cells was the difficulty of detecting the actual percentage of cells expressing the truncated syntaxins. During adenovirus production pAdTrack-CMV could have been used instead of pShuttle-CMV, which provides the opportunity to track the infection, due to GFP expression. pAdTrack vector was not used in this case to eliminate the expression of an additional protein (GFP) with syntaxins. Incorporation of a tag sequence to the inserts would have been the best option, and with hindsight this was a mistake, but we were concerned about masking the critical SNARE domain by including extra residues. However the available data suggested that majority of 3T3-L1 adipocytes were infected at 1:100 MOI.

STX 6 and STX 12 constructs were able to overexpress the truncated syntaxins by more than 15 fold at 1:100 MOI. However, STX 8 overexpression was only about 2 fold at MOI 1:100 which could be partly due to presence of higher levels of native STX 8. Nevertheless, these could seem reasonable levels for experiments to attempt to perturb syntaxin function. Subcellular fractionation of infected 3T3-L1 adipocytes showed that the truncated syntaxins are localised in cytosol due to their lack of transmembrane domain. Our expectation was that these cytosolic syntaxins would act as dominant negative mutants against the wild type syntaxins found in the post-Golgi membranes. A fraction of STX 12 truncated protein seems to be incorporated into membranes, PM, HDM and LDM, which might be caused by association with some other SNAREs found in these membranes.

As expected the infection of HeLa cells were much more efficient compared to that of 3T3-L1 adipocytes, which showed 100% infection at MOI of 1:10. Therefore HeLa cells were used to study the effect of syntaxins on constitutive trafficking pathways such as TfR trafficking.

In summary, I was able to generate the four recombinant AdV and use them in 3T3-L1 adipocytes to overexpress transgenes in majority of cells without apparent cell toxicity. The four recombinant viruses were used in 3T3-L1 adipocytes and HeLa cells to identify the role of syntaxins 6, 8 and 12 on various forms of intracellular trafficking events, giving priority to GLUT4 trafficking of 3T3-L1 adipocytes. Chapter 5 describes the outcome of these experiments.

Chapter 5

Functional studies of post-Golgi syntaxins in 3T3-L1 adipocytes

5.1 Introduction

The initial characterisation studies of post-Golgi syntaxins, described in chapter 3, suggested that STX 6 and STX 16 are highly colocalised (more than 85% and 50% respectively) in GLUT4 vesicles, with a lesser degree of colocalisation of STX 8 and STX 12. To study the functional importance of these syntaxin isoforms, recombinant adenoviruses (AdV) were produced as described in chapter 4 to overexpress the soluble cytosolic domains of STX 6, 8 and 12 in 3T3-L1 adipocytes. Due to the lack of transmembrane domains in these mutants, competitive inhibition of wild type syntaxin function was expected by this approach. As STX 16 distribution in GLUT4 compartments was characterised at a later stage of this study, a recombinant AdV encoding cytosolic domain of STX 16 was not made.

The functional requirement of STX 4 in GLUT4 translocation to the PM upon insulin stimulation in both fat and muscle cells is well established (Cheatham *et al.*, 1996; Timmers *et al.*, 1996; Tellam *et al.*, 1997; Olson *et al.*, 1997; Macaulay *et al.*, 1997). However, to date there are no studies reporting the role of syntaxins of the endocytic pathway on GLUT4 traffic in insulin-sensitive tissues. Hence the main focus of this chapter was to study the endocytic pathway of GLUT4. Many trafficking events that occur in cells, for instance the transferrin receptor (TfR) follows the well-established constitutive recycling pathway, and the low-density lipoprotein (LDL) follows the pathway directed to lysosomes (reviewed in Mellman, 1996). Furthermore, adipsin and ACRP30 are secreted from 3T3-L1 adipocytes in a pathway not followed by GLUT4 (Millar *et al.*, 2000; Bogan and Lodish, 1999 respectively). Whether these two secreted proteins use a common pathway or not, is currently unknown.

5.2 Aims

The main aim of this chapter was to study the effect of inhibition of syntaxins on membrane trafficking in 3T3-L1 adipocytes. This included the exocytosis and endocytosis of GLUT4 and three other trafficking events, TfR and LDL trafficking and secretion of adipsin and ACRP30.

5.3 Results

All the experiments were performed two days after the cells were infected with four different adenoviruses that included the control (pSh) AdV and STX 6, STX 8 and STX 12 AdV. A group of control cells, which were not infected was included in most of the assays. A MOI of 1:50 or 1:100 was used to infect 3T3-L1 adipocytes (between day 6 and 8) unless otherwise specified. HeLa cells were infected at a MOI of 1:5 when the cells are nearly 50% confluent. Prior to each assay, cells were incubated in serum-free media for 2 h. Transport assays were conducted in 6-well or 12-well plates. Ms. Mairi Clarke performed the secretion assays described in this chapter.

5.3.1 Effect of inhibition of post-Golgi sytaxins on DOG transport of 3T3-L1 adipocytes

Deoxy glucose (DOG) uptake was assayed as described in section 2.5.1 in the presence or absence of 100 nM insulin in 3T3-L1 adipocytes infected with AdV. Results showed that all five groups of cells (non infected control, infected control (control AdV) and three groups infected with STX AdV) responded in a similar way in the presence of insulin leading to a marked increase in DOG transport (Figure 5.1). However the cells overexpressing STX 6 cytosolic domain consistently showed an approximately 2-fold increase in basal DOG transport, compared to basal values of other groups (Figure 5.1). To clarify this aspect further, the assay was repeated with adipocytes infected at MOIs of 1:25, 1:50 and 1:100 using control AdV and STX 6 AdV. A dose-dependent increase of basal DOG uptake was observed with the cells infected with STX 6 AdV compared to that of the control group (Figure 5.2). This increase was significant ($p<0.03$).

5.3.2 Distribution of GLUT4 in subcellular fractions of infected 3T3-L1 adipocytes

Subcellular fractionation was performed as described in section 2.3.3 using cells (10 cm plates) incubated in the presence or absence of insulin, which were infected or not infected with AdV. GLUT4 and IRAP distribution in the PM, LDM and HDM fractions obtained in each condition was studied using Western blotting and immuno-detection. Analysis of Western blots did not show any apparent difference in the distribution of GLUT4 and IRAP among the five different groups used (control, control AdV and three STX AdV) (results not shown).

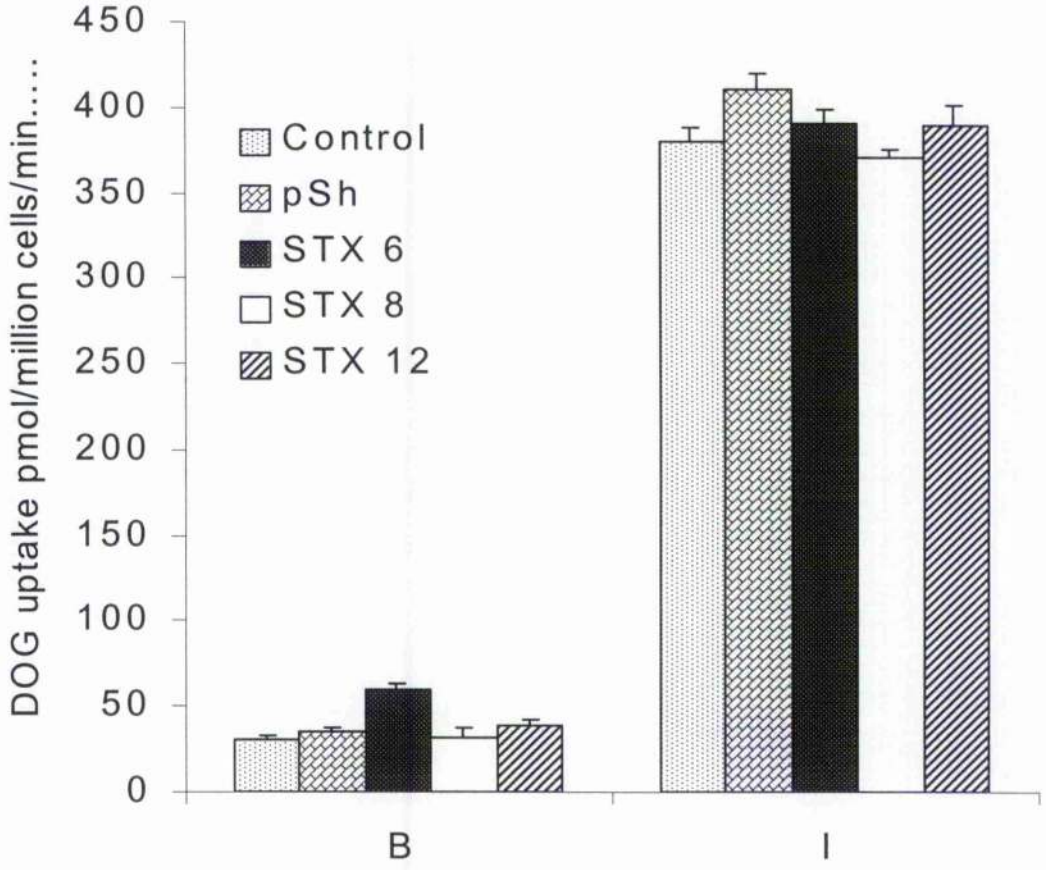

Figure 5.1 Effect of STX cytosolic domain overexpression in DOG transport of 3T3-L1 adipocytes

Adipocytes infected with control (pSh), STX 6, 8, 12 AdV at MOI 1:100 and non-infected adipocytes (control) were used. DOG transport was measured 48 h later at basal state or after stimulating with insulin (100 nM 20 min) as described in section 2.5.1. The data shown are mean±SEM of triplicate measurements from a typical experiment repeated four times.

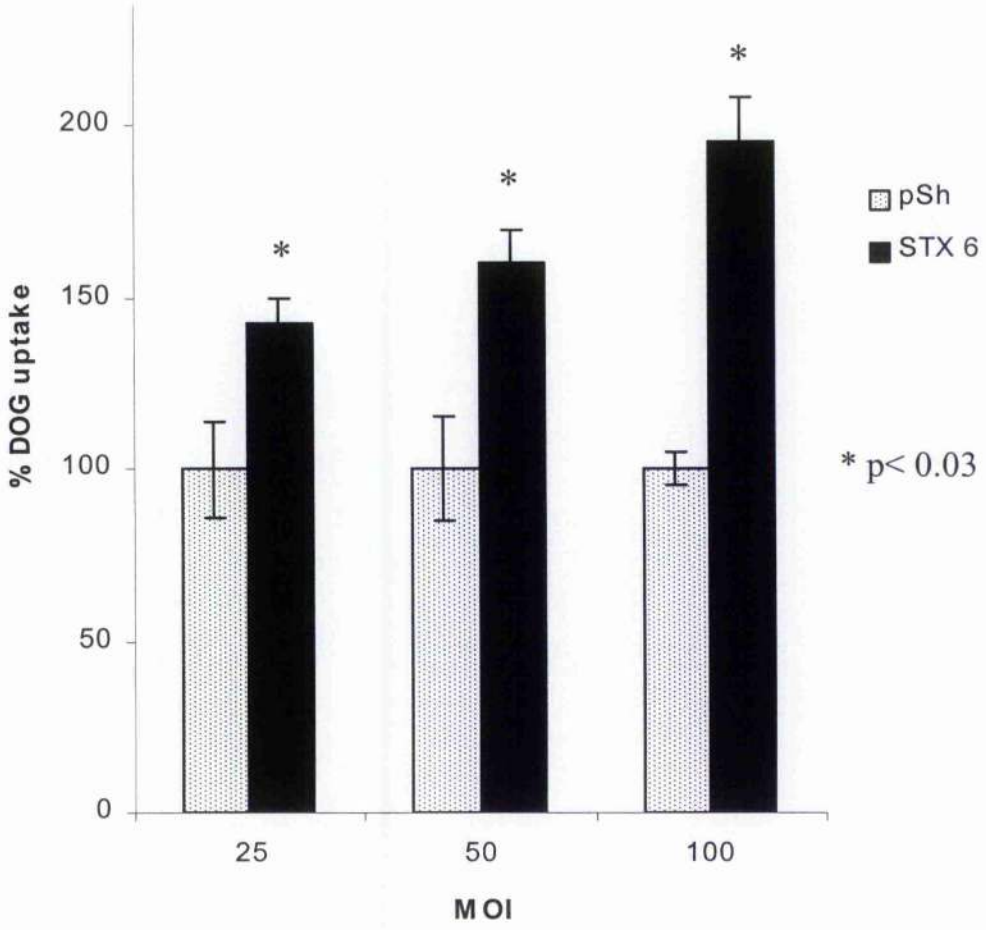

Figure 5.2 Effect of STX 6 cytosolic domain overexpression on basal DOG transport in 3T3-L1 adipocytes

Adipocytes infected with pSh AdV and STX 6 AdV at MOI of 1:25, 1:50 and 1:100 were assayed 48 h later. Basal DOG uptake was measured as described in section 2.5.1. Measurements of STX 6 AdV group were expressed as a % of corresponding values of pSh AdV. Mean±SEM of triplicate measurements from a typical experiment are shown (n=4). *statistically significant difference ($p<0.03$).

5.3.3 The distribution of GLUT4 in infected 3T3-L1 adipocytes.

Adipocytes (non-infected control, infected with either control AdV or STX 6 AdV or STX 8 AdV) were fixed to visualise the localisation of GLUT4 or IRAP by immunofluorescence confocal microscopy in the basal state (section 2.4). Non-infected and infected controls show typical perinuclear labelling of GLUT4 with a punctate pattern of labelling at the periphery of the cells. They also showed the compact perinuclear staining of STX 6. Cells infected with STX 8 showed a distribution of IRAP similar to GLUT4 distribution in control cells. In contrast cells infected with STX 6 AdV did not show the dense perinuclear-staining pattern of GLUT4. Instead the labelling was found in a punctate pattern (Figure 5.3). These cells did not show the typical perinuclear labelling of STX 6, presumably as a result of high levels of expression of soluble STX 6 cytoplasmic domain.

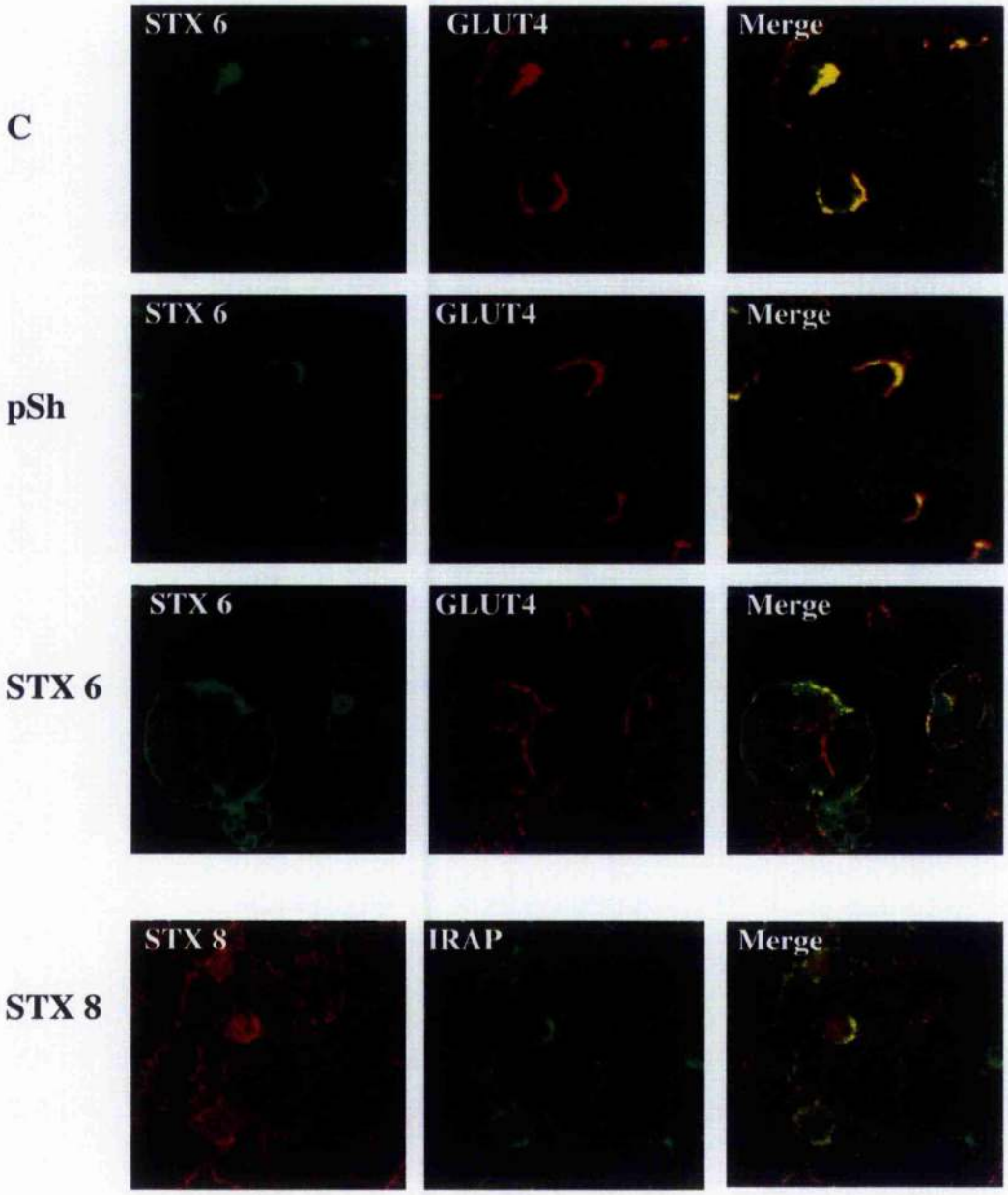

Figure 5.3 Effect of STX cytosolic domain overexpression on GLUT4 (or IRAP) distribution in 3T3-L1 adipocytes

Adipocytes grown on coverslips were either non-infected (C) or infected with pSh, STX 6 and STX 8 AdV for 48 h. Cells in the basal state were fixed with *p*-formaldehyde and prepared for confocal microscopic analysis (section 2.4). All syntaxin antiserum were used at 1:200. Anti-GLUT4 and anti-IRAP antibodies were used at 1:100. STX 6 and IRAP are labelled with FITC (green). GLUT4 and STX 8 are labelled with TRITC (red). (Anti-IRAP was used instead of anti-GLUT4 in cells labelled with anti-STX 8, as the latter two antibodies are from rabbit). Figure shows representative images from a typical experiment (n=3). The C, pSh, STX 6 and STX 8 indicated on left side of the figure represent the non infected cells (C) and cells infected with pSh AdV, STX 6 AdV and STX 8 AdV respectively.

5.3.4 Effect of inhibition of post-Golgi sytaxins on DOG transport of 3T3-L1 adipocytes after insulin withdrawal

To identify the effect of syntaxins on the endocytic pathway of GLUT4, the ability to return the DOG transport to basal levels after the withdrawal of insulin was examined. In this experiment, DOG uptake was measured at different times after insulin withdrawal, in the infected and non-infected 3T3-L1 adipocytes using the method described in section 2.5.2. Uptake of DOG was measured at insulin-stimulated state (0 min) and 10 min and 20 min after insulin withdrawal (Fig 5.4). The findings demonstrated that while DOG uptake in all five groups at 0 min was similar, STX 6 AdV resulted in a significantly higher ($p<0.05$) glucose uptake compared to the other groups of cells during the 10 and 20 min withdrawal periods, tested indicating a slowing down of the endocytic retrieval of GLUT4 in these cells. This delay prolonged the t½ of reversal of DOG transport to basal level from ~10 min to ~40 min. (Figure 5.4). In contrast cells expressing STX 8 and STX 12 domains showed normal reversal of DOG uptake.

5.3.5 Distribution of GLUT4 at PM and LDM fractions after insulin withdrawal of infected 3T3-L1 adipocytes

To further characterise the observations described in 5.3.4, adipocytes (grown on 10 cm plates) infected with AdV of pSh, STX 6, STX 8 were stimulated with insulin (100 nM) for 30 min and divided into four groups, insulin-stimulated (0 min), 10 min, 20 min and 60 min after insulin withdrawal. Insulin reversal was performed as described in section 2.5.2 and all groups were subjected to subcellular fractionation as described in section 2.3.3. Analysis of these membrane fractions prepared from cells infected with control virus and the cells expressing STX 8 cytosolic domain demonstrated a steady decrease of PM GLUT4 level with time after insulin withdrawal. The pattern of decrease was similar to that observed in previous studies (Holman *et al.*, 1994; Yang *et al.*, 1992). In contrast, cells expressing STX 6 cytosolic domain showed a high level of GLUT4 in the PM throughout the insulin withdrawal period examined (Figure 5.5.A). In support of these data, cells infected with control and STX 8 AdV demonstrated increasing levels of GLUT4 in the LDM fraction during the withdrawal period, whereas the return of GLUT4 and IRAP into LDM in STX 6 AdV infected cells was slower (Figure 5.5.B). This data supports and extends the finding of increased glucose uptake during insulin withdrawal providing compelling evidence in support for a role

of STX 6 in intracellular GLUT4 sequestration. These effects are specific since expression of STX 8 or STX 12 cytosolic domain was without effect.

5.3.6 Distribution of GLUT4 (from infected 3T3-L1 adipocytes) in iodixanol gradients

To examine whether STX 6 requires for the sorting of GLUT4 into the GSV compartment during insulin withdrawal, LDM fractions collected as described in section 5.3.5 were subjected to iodixanol gradient analysis (section 2.3.4) to resolve endosomal/ TGN and GSV pools of GLUT4. Analysis was conducted after 0,10, 20 and 60 min of insulin withdrawal. The data clearly show that in cells infected with STX 6 AdV, the extent of GLUT4 return into the GSV pool resolved by iodixanol gradient is impaired during insulin withdrawal (Figure 5.6.A). In contrast, the ability of GLUT4 to re-enter the GSV pool was not compromised in cells infected with STX 8 and STX 12 AdV, which followed a similar pattern to that of control AdV (Figure 5.6.A).

The distribution of IRAP in the same iodixanol gradient fractions was remarkably similar to GLUT4 with a marked decline in the rate of return of IRAP to the GSV fraction in cells infected with STX 6 (Figure 5.6.B) providing further evidence to support a role of STX 6 in GLUT4 traffic into GSV.

All fractions were analysed for STX 6 distribution which showed that the STX 6 level found in the fractions increase after insulin withdrawal with a rapid return in the endosomal/TGN pool and a slow and steady return into the GSV compartment similar to GLUT4. However, compared to the control AdV group and two other groups expressing STX 8 and 12 domains, accumulation of STX 6 in the GSV pool of cells infected with STX 6 AdV showed a delay (Figure 5.6.C). Based on this evidence it is clear that return of GLUT4 into the GSV occurs in parallel with a return of STX 6 into the same pool and GLUT4, IRAP and STX 6 retrieval into GSV is affected in the cells expressing the cytosolic fragment of STX 6.

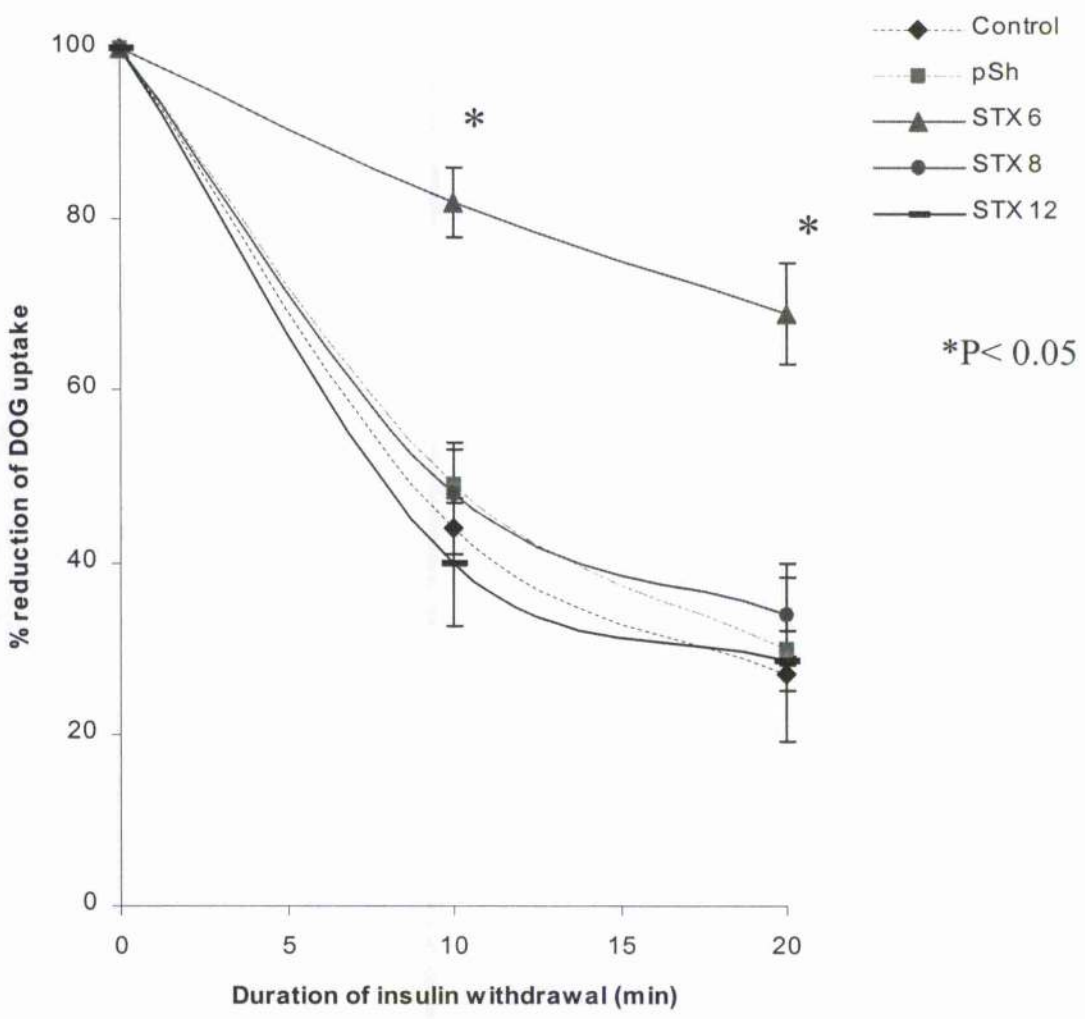

Figure 5.4 Effect of STX cytosolic domain overexpression on DOG uptake after insulin withdrawal

Assays were conducted as described in section 2.5.2, 48 h after infecting the 3T3-L1 adipocytes with pSh, STX 6, 8, and 12 AdV. A non-infected group of cells were used in parallel (control). The cells were stimulated with 100 nM insulin for 20 min and then either assayed immediately (0 min) or washed in KRM to induce reversal of glucose transport for 10 and 20 min. DOG uptake was measured at 10 and 20 min after insulin withdrawal and expressed as a % of the DOG uptake at 0 min. The graph shows the result of a typical experiment. Mean±SEM of triplicate measurements are shown (n=4). *statistically significant difference ($p<0.03$). The maximum rate of insulin-stimulated DOG uptake was similar between the groups (see figure 5.1).

Figure 5.5.A

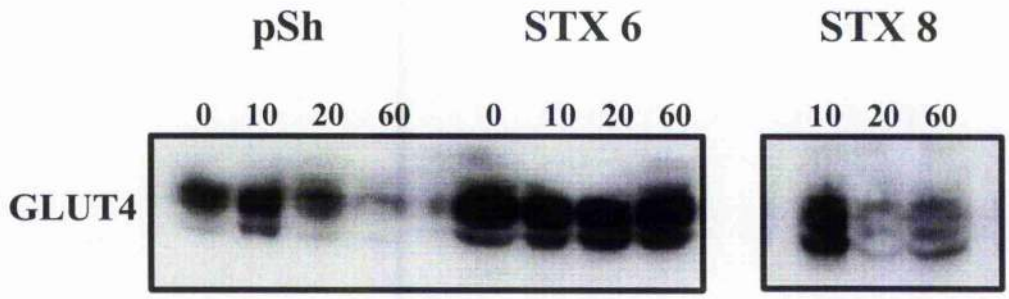

Figure 5.5.B

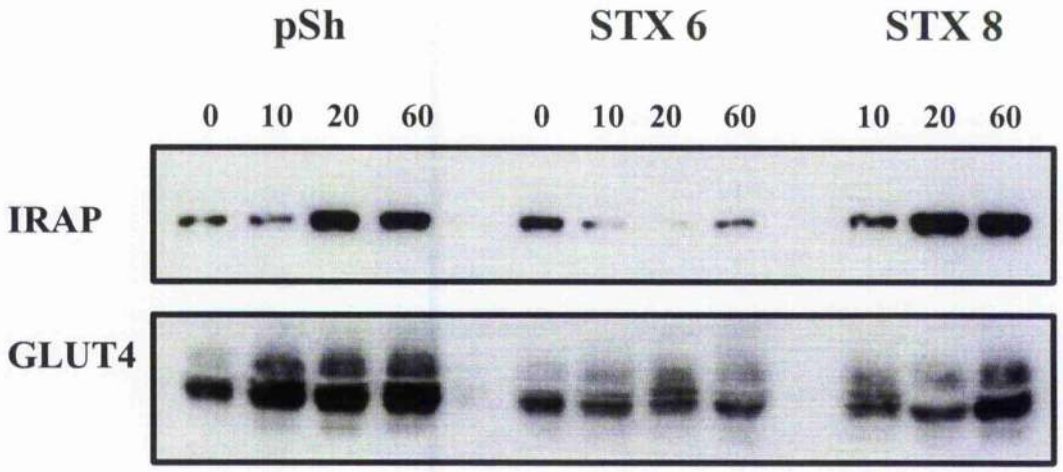

Figure 5.5 Effect of STX cytosolic domain overexpression on the subcellular distribution of GLUT4 after insulin withdrawal

Subcellular fractionation was performed (section 2.3.3) at different times of the insulin withdrawal (0, 10, 20 and 60 min) using cells infected with pSh, STX 6 or STX 8. (Insulin withdrawal was performed as described in figure 5.4). Labels at the top of the immunoblots indicate the AdV used and the duration of insulin withdrawal (min).

Figure 5.5.A shows the GLUT4 distribution in PM fractions collected.

Figure 5.5.B shows the distribution of IRAP and GLUT4 in LDM fractions.

Immunoblots are from a typical experiment repeated three times with similar results.

Figure 5.6.A Effect of STX cytosolic domain overexpression on GLUT4 distribution in iodixanol gradients after insulin withdrawal

3T3-L1 adipocytes infected with pSh, STX 6, 8 and 12 AdV were used 48 h after the infection. Following incubation for 2 h in serum-free media, cells were stimulated with insulin (100 nM) for 20 min. Cells were prepared for subcellular fractionation (section 2.3.3) immediately after (IW 0) or washed in KRM to induce reversal of glucose transport for 10, 20 and 60 min. LDMs were separated from each group(2.3.3) and subjected to iodixanol gradient analysis (section 2.3.4). Fractions were collected from the bottom of the gradient (No: 1 to 14). SDS-PAGE was performed using 10% of each fraction. Immunoblots show the distribution of GLUT4 in the gradients from a typical experiment performed three times. IW 0, 20 and 60: insulin withdrawal for 0, 20 and 60 min respectively. Labels at the left of the immunoblots indicate the AdV used. GSV and TGN/ endo represents the GSV, TGN/endosomal pools of GLUT4 separated by iodixanol gradient analysis.

Figure 5.6.A

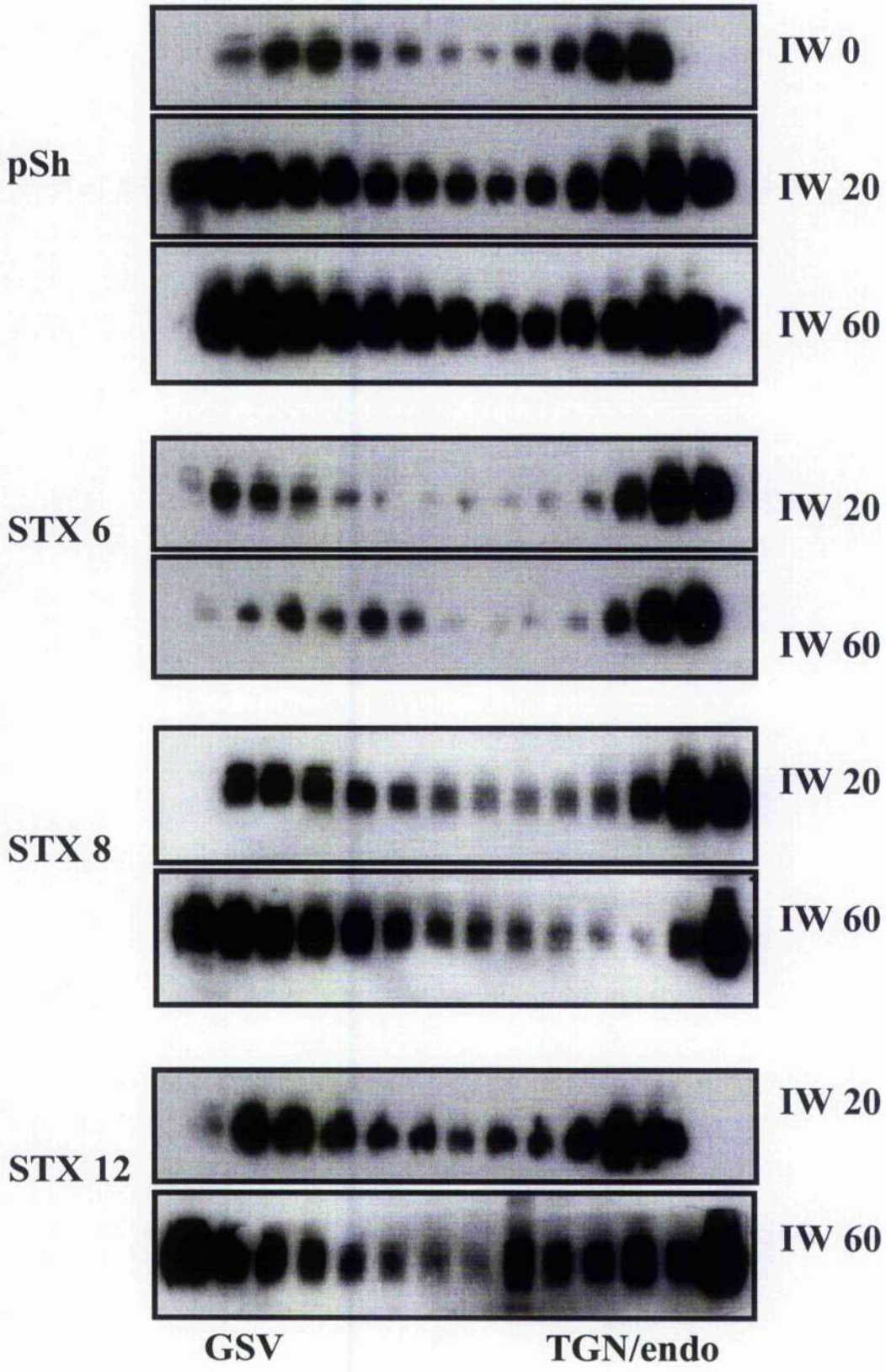
pSh
IW 0
IW 20
IW 60
STX 6
IW 20
IW 60
STX 8
IW 20
IW 60
STX 12
IW 20
IW 60
GSV
TGN/endo

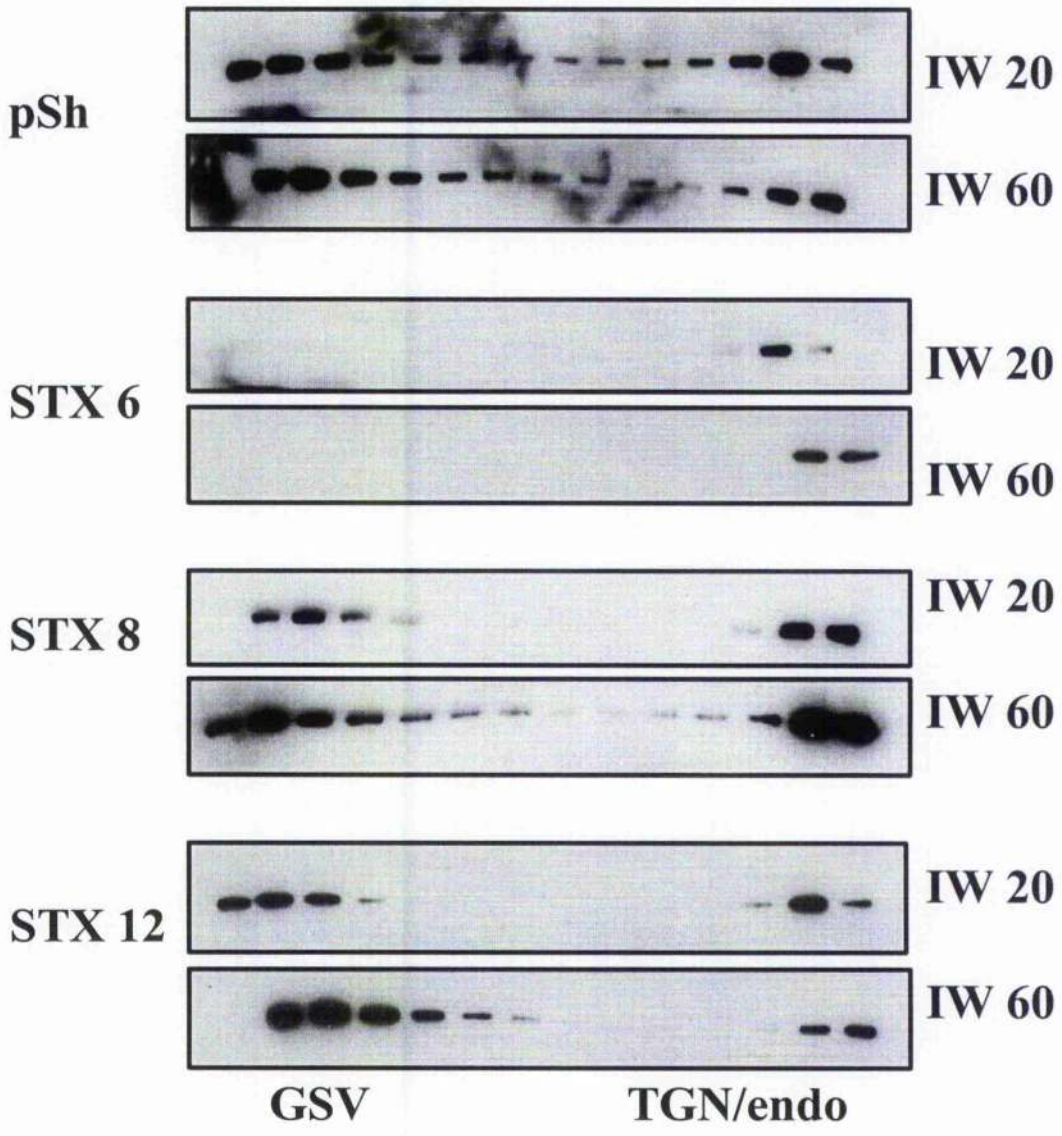

Figure 5.6.B Effect of STX cytosolic domain overexpression on IRAP distribution in iodixanol gradients after insulin withdrawal

The fractions collected after iodixanol gradient analysis as described in figure 5.6.A were analysed for IRAP distribution. The Data shown are from a typical experiment repeated two more times with similar results. IW 20 and 60: insulin withdrawal for 20 and 60 min respectively. Labels at the left of the immunoblots indicate the AdV used. GSV and TGN/ endo represents the GSV, TGN/endosomal pools of GLUT4 separated by iodixanol gradient analysis.

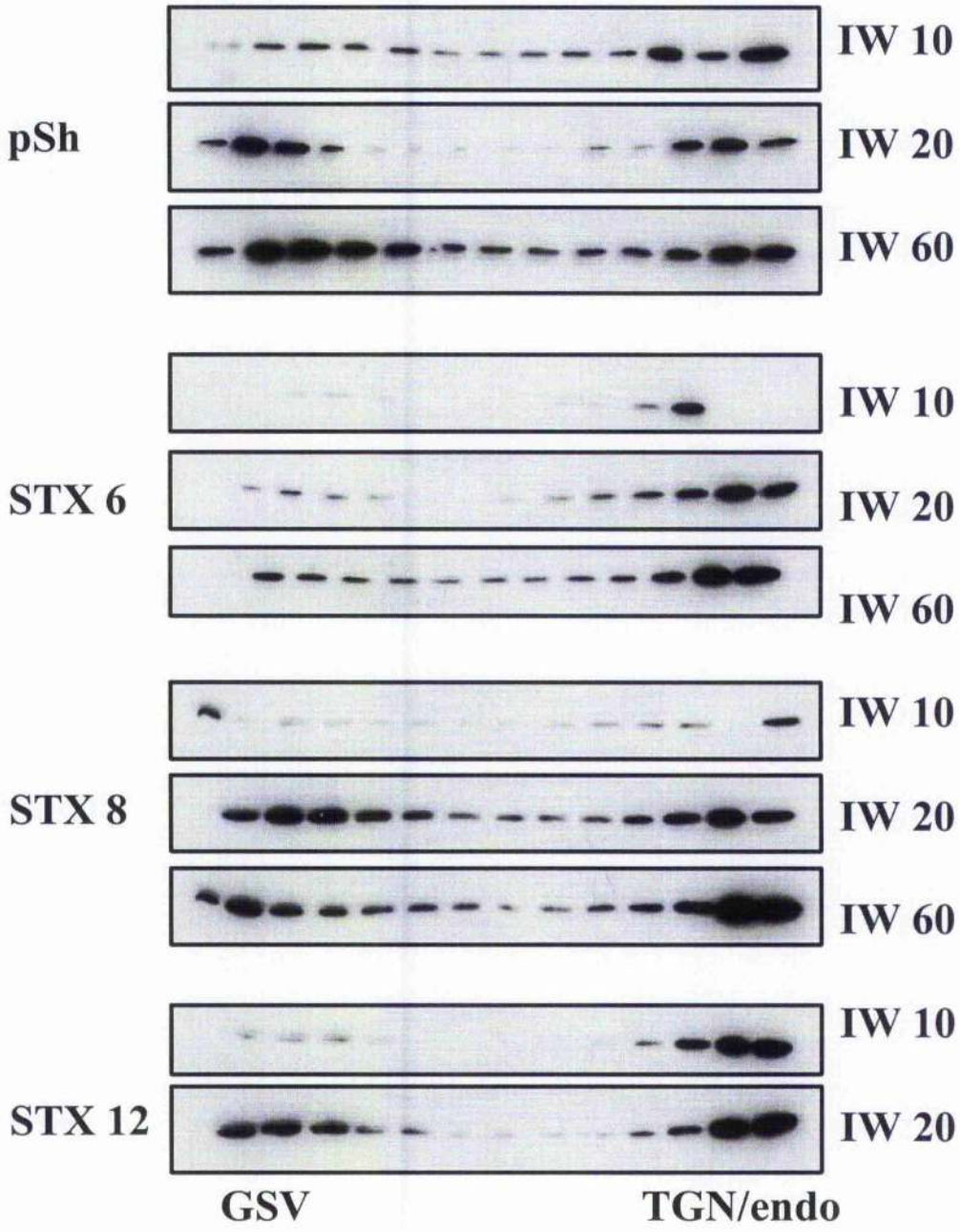

Figure 5.6.C Effect of STX cytosolic domain overexpression on STX 6 distribution in iodixanol gradients after insulin withdrawal

The fractions collected from iodixanol gradient analysis as described in figure 5.6.A were analysed for STX 6 distribution. The data shown are from a typical experiment repeated two more times with similar results. IW 20 and 60: insulin withdrawal for 20 and 60 min respectively. Labels at the left of the immunoblots indicate the AdV used. GSV and TGN/ endo represents the GSV, TGN/endosomal pools of GLUT4 separated by iodixanol gradient analysis.

5.3.7 Effect of inhibition of syntaxins on PM TfR level

To assess whether inhibition of syntaxins by overexpression of cytosolic domains in 3T3-L1 adipocytes has an impact on trafficking pathways other than GLUT4 trafficking three more trafficking events were examined. To ascertain whether there were effects on constitutive recycling, PM TfR level in the presence or absence of insulin (100 nM for 30 min) was measured as described in section 2.5.3. The findings identified that PM TfR level is increased by about 1.3 fold in the presence of insulin in all five groups of cells. Furthermore, infection with the AdV had no significant effect on the TfR levels observed under basal and insulin-stimulated conditions (Figure 5.7).

5.3.8 Effect of inhibition of syntaxins on transferrin internalisation

To study whether the TfR internalisation is affected in the cells expressing the syntaxin domains, transferrin internalisation assay was performed for 5, 10, 30 and 60 min at 37°C, according to section 2.5.4. For this experiment HeLa cells were used instead of 3T3-L1 adipocytes due to the requirement of very low MOI of AdV to carryout the infection efficiently. The results obtained from five groups of cells showed that the rate of internalisation in all groups changes with time in the same manner. Overexpression of STX 6, 8 and 12 had no effect on the pattern of internalisation compared to control AdV group (Figure 5.8)

5.3.9 Effect of inhibition of syntaxins on externalisation of internalised transferrin

The outward trafficking of transferrin for periods of 0, 5, 10 and 30 min in HeLa cells was studied according to the method described in section 2.5.5. Consistent with the above data no effect was found in the cells expressing cytoplasmic domains of STX 6, 8 or 12 compared to control AdV group (Figure 5.9).

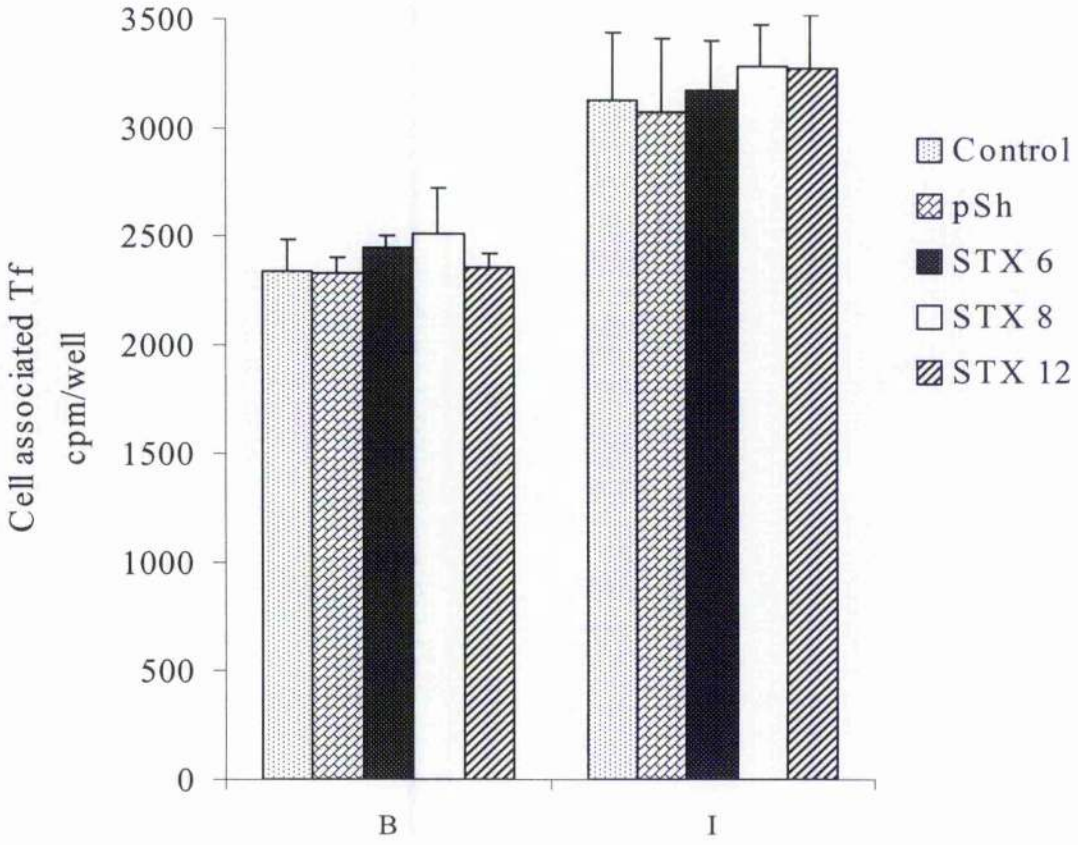

Figure 5.7 Effect of STX cytosolic domain overexpression on cell surface TfR level

Assays were conducted 48 h after infecting the 3T3-L1 adipocytes with pSh, STX 6, 8, and 12 AdV. Non-infected (control) group of cells were used in parallel. Cells were treated with (I) or without (B) 100 nM insulin for 30 min. Subsequently, cells were washed in ice-cold buffer and incubated with 3 nM ^{125}I transferrin ± 10 μM transferrin on ice for 2 h to measure cell surface TfR levels and continued as described (2.5.3). Figure shows results of a typical experiment conducted in triplicate (Mean ± SEM). Experiment was repeated two more times with similar results.

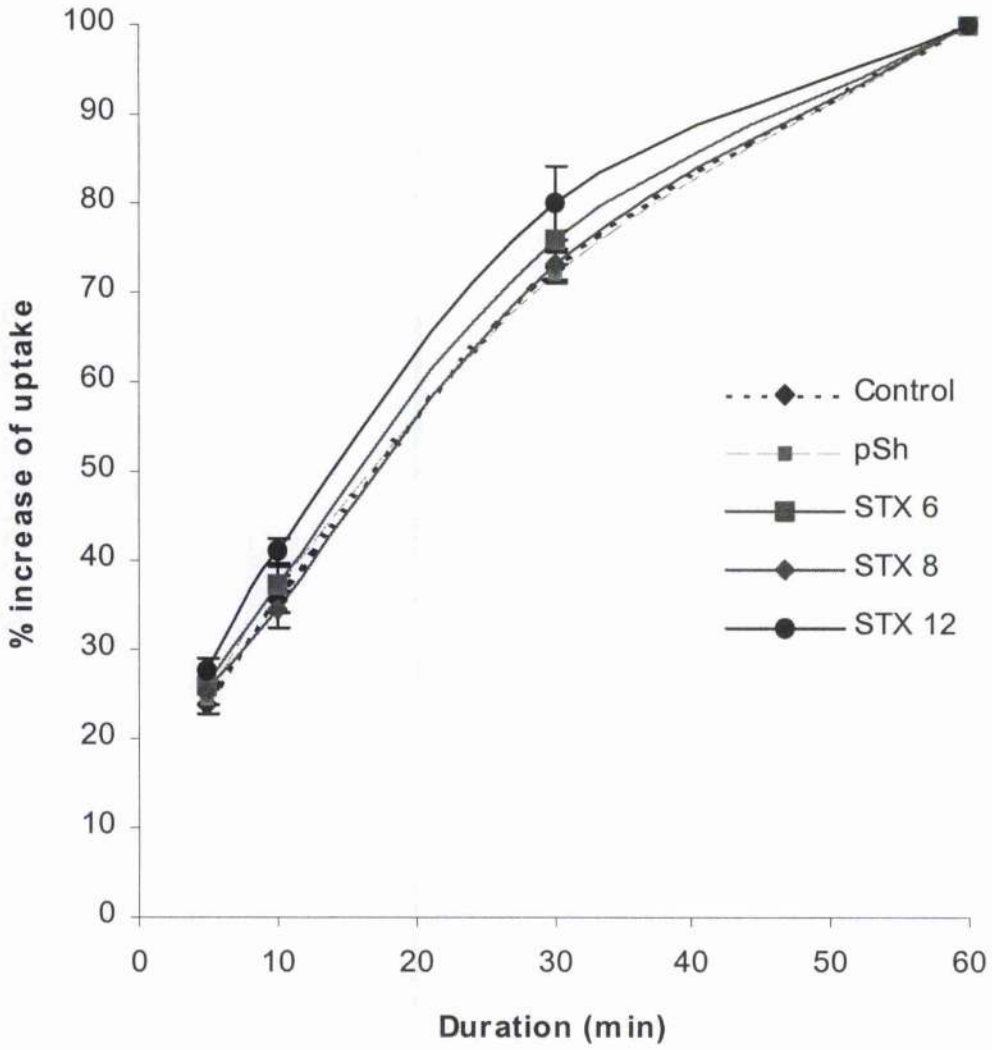

Figure 5.8 Effect of STX cytosolic domain overexpression on transferrin internalisation in HeLa cells

Tf internalisation assay was carried out for 5, 10, 30 and 60 min at 37°C (section 2.5.4) using HeLa cells infected at a MOI of 1:5 (pSh, STX 6, 8 and 12 AdV) or not infected (control) with AdV. Data express the transferrin uptake at different periods as a % of the uptake at 60 min. Mean ± SEM of triplicate measurements are shown (n=3).

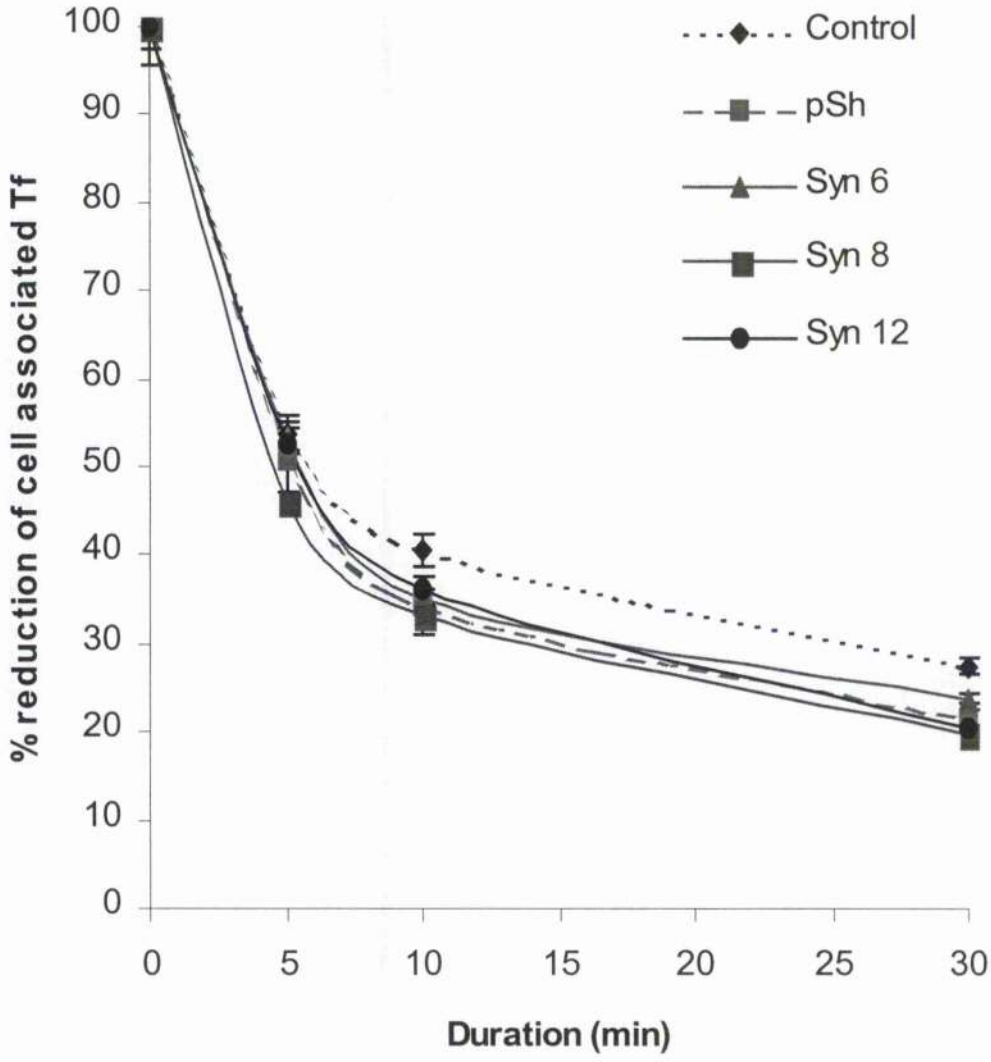

Figure 5.9 Effect of STX cytosolic domain overexpression on externalisation of internalised transferrin in HeLa cells

HeLa cells infected (pSh, STX 6, 8 and 12 AdV) or not infected (control) were used 48 h after infection. Assay was carried out as described in section 2.5.5. Briefly, transferrin was internalised for 1 h at 37°C and cells were washed to remove all cell surface-associated transferrin. Internalised transferrin was allowed to externalise for different periods (0, 5, 10 and 30 min) at 37°C, and cell-associated transferrin was measured after washing. Data at each point are shown as a % of cell associated transferrin at 0 min. Mean± SEM of triplicate measurements is shown. n=3.

5.3.10 Monitoring internalisation of surface bound transferrin in infected cells

To visualise the compartments accessed by TfR, HeLa cells (grown on coverslips) infected two days prior to the assay. Cells were incubated with transferrin Texas red (10 μg/ml) (Molecular probes) in ice-cold KRP buffer (section 2.1.5) with BSA (1mg/ml) for 1 h at 4°C. Surface-bound transferrin was allowed to internalise at 37°C for 0, 5, 10 and 30 min. After the incubation, coverslips were washed and fixed with methanol (2.4.2) and examined by confocal microscopy (2.4.4). The images collected from cells infected with different STX AdV did not show a clear difference in the pattern of transferrin distribution from two control groups (infected and non infected) (Figure 5.10).

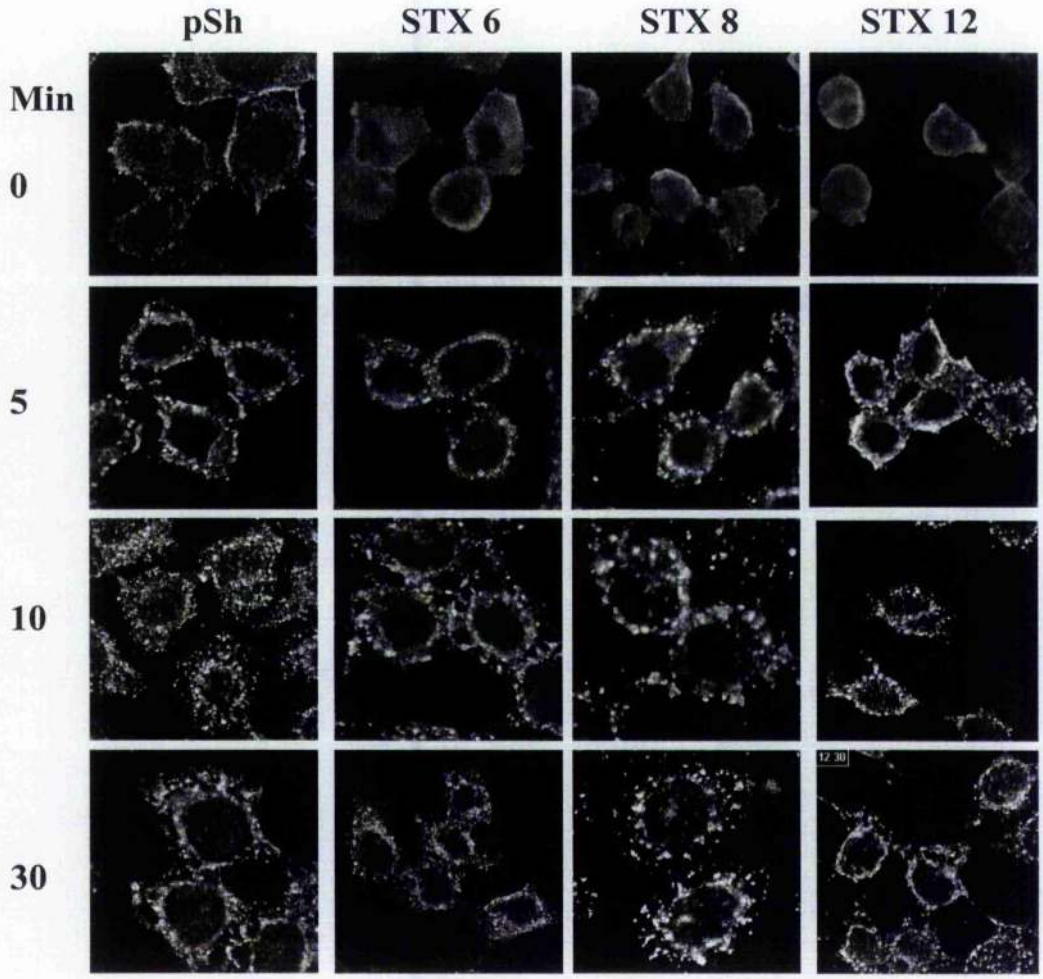

Figure 5.10 Effect of STX cytosolic domain overexpression on internalisation of cell surface associated transferrin

HeLa cells (grown on coverslips) infected with pSh, STX 6, 8 and 12 AdV at a MOI of 1:5 were used 48 h later. Cells were incubated with transferrin Texas red (10 μg/ml) for 1 h at 4°C in ice-cold KRP buffer (section 2.1.5) with BSA (1mg/ml). Cells were subsequently washed in ice-cold buffer and surface-bound transferrin was allowed to internalise at 37°C for periods of 0, 5, 10 and 30 min. At the end of the period cells were washed and fixed with methanol (2.4.2) and analysed by confocal microscopy (2.4.4). Figure shows representative images from a typical experiment (n=3). Labels at top of the image indicate the AdV used and at left indicate the duration of internalisation (min).

5.3.11 Effect of inhibition of syntaxins on LDL uptake of HeLa cells

In order to study the effect of inhibition of syntaxins on traffic towards lysosomes, LDL uptake was conducted in HeLa cells. Cells grown on coverslips were infected two days prior to assay. Cells were incubated in serum-free media for 2 h and washed once in warm KRP buffer. DiI LDL (10 μg/ml) (Molecular probes) (section 2.1.1) was added and incubated for 30 min at 37°C. Following incubation cells were washed once in warm KRP buffer and washed twice in cold KRP buffer. Coverslips were mounted in a coverslip holder and examined under confocal microscope as live cells.

The images collected from cells infected from STX 8 and 12 AdV revealed presence of LDL in both endosomal and perinuclear area. In contrast STX 6 showed a different pattern with a more peripheral distribution of LDL without perinuclear labelling in the cells, suggesting impaired lysosomal trafficking caused by inhibition of STX 6 function (Figure 5.11).

5.3.12 Effect of inhibition of syntaxins on secretion of adipsin and ACRP30

We next assayed the secretion of adipsin and ACRP30 from 3T3-L1 adipocytes expressing STX cytosolic domains. Cells grown on 10 cm plates were used in these assays. Secretion assays were conducted using five groups (non infected, control AdV and three STX AdV) as described in section 2.5.6 in the presence or absence of insulin (1 μM). The results obtained did not show any effect of inhibition of syntaxin 6, 8 or 12 on rate of secretion of these proteins (results not shown).

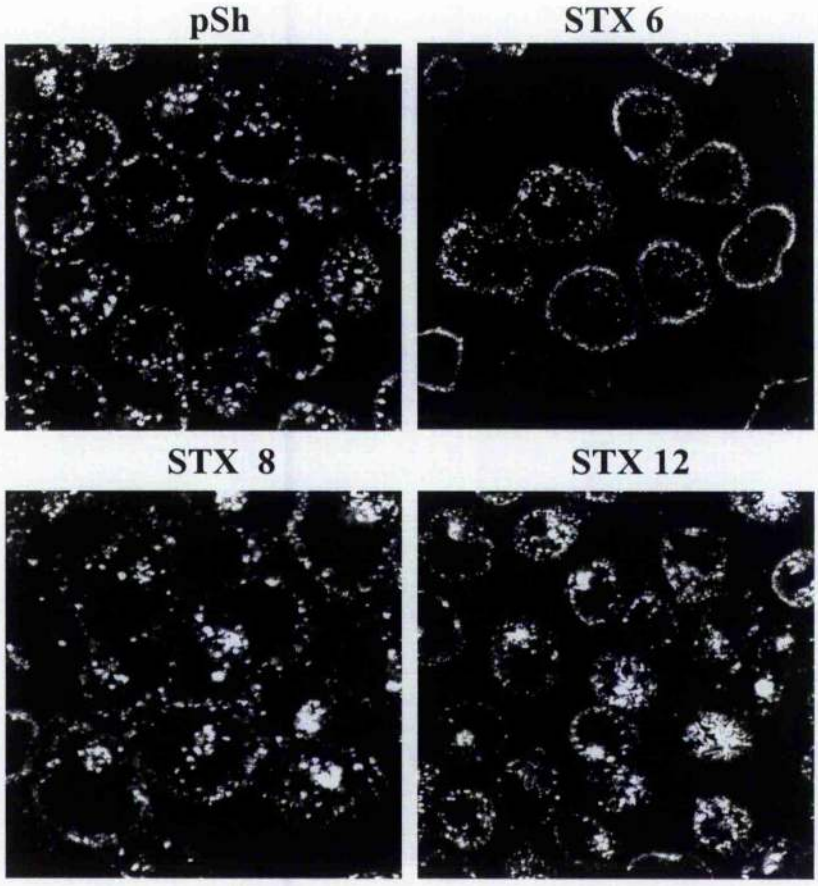

Figure 5.11 Effect of STX cytosolic domain overexpression on LDL uptake

HeLa cells (grown on coverslips) infected with pSh, STX 6, 8 and 12 AdV were used 48 h later. Cells were incubated with DiI LDL (10 μg/ml) for 30 min at 37°C, and washed subsequently. Images were captured using confocal microscopy from live cells immediately after removal of LDL. Shown are representative images from a typical experiment. Similar results were obtained in repeat experiments (n=3). Labels at top of the image indicate the AdV used.

5.4 Discussion

A group of recombinant AdV were produced and used to overexpress the cytosolic domains of post-Golgi syntaxins to explore their functional importance in trafficking pathways of 3T3-L1 adipocytes. As the syntaxins are membrane-anchored proteins with the majority of the polypeptide exposed to cytosol, the cytosolic domains are expected to function as inhibitors of the full-length syntaxins. Introduction of the cytosolic domain of VAMP2 and STX 4 either using microinjection (Cheatham *et al.*, 1996; Martin *et al.*, 1996; Macaulay *et al.*, 1997) or vaccinia virus (Olson *et al.*, 1997) has been successfully used previously to study the functional role of these SNAREs in GLUT4 translocation to the PM in response to insulin in adipocytes.

Various experiments have been performed to identify the role of these syntaxins 6, 8 and 12 in GLUT4 trafficking. As cytosolic domains of these syntaxins had no effect on DOG transport in the presence of insulin (Figure 5.1), it is suggested that these post-Golgi syntaxins either do not have a role in the exocytic pathway of GLUT4 or that involvement of these syntaxins in SNARE complexes in the presence of insulin is inhibited. In contrast basal DOG uptake was increased in a dose-dependent manner by about 2-fold (at MOI 1:100) in the presence of STX 6 domain (Figure 5.2). This effect was specific to the expression of the STX 6 domain, since expression of STX 8 and STX 12 cytosolic domains were without effect (Figure 5.1). This increase in the level of basal glucose uptake could be related to a slower endocytic rate or a longer time required for sequestration of GLUT4 away from the recycling pathway.

Subcellular fractionation of the five groups of adipocytes (two controls and three STX AdV) at basal state did not reveal a difference in the distribution of GLUT4 among the groups. This is not surprising as the modest increase of PM GLUT4 level under basal state is not sufficient to be differentiated from normal levels by Western blotting. However, confocal microscopic study of these cells (two controls, STX 6 AdV and STX 8 AdV groups) showed a difference in the distribution of GLUT4 in the cells expressing the inhibitory domain of STX 6 compared to controls. These data suggest a role of STX 6 in GLUT4 trafficking into intracellular compartments.

To examine the endocytic pathway of GLUT4 in more detail DOG transport after insulin withdrawal was measured to assess whether the reinternalisation of GLUT4

into intracellular compartments is delayed when STX 6 function is inhibited. The results showed a delay in the reversal of DOG transport prolonging the t½ from 10 min to 40 min in presence of STX 6 cytosolic domain compared to control AdV group (Figure 5.4). Again this effect was specific as STX 8 and STX 12 were without effect. These results were further supported by analysis of the subcellular distribution of GLUT4 after various periods of insulin withdrawal from 0 to 60 min, which showed high levels of GLUT4 retained at the PM even after 60 min of insulin withdrawal (Figure 5.5.A). In addition, GLUT4 level in the LDM of these cells (STX 6 AdV) remained low even 60 min after withdrawal of insulin (Figure 5.5.B). IRAP was found to follow the same distribution pattern of GLUT4 in support of impaired endocytosis or retention of these molecules (Figure 5.5.B). All these data support a role of STX 6 in endocytosis or sequestration of GLUT4 into the GSV compartment. However, the findings described above do not clarify whether STX 6 mediates GLUT4 movement to the GSV compartment.

Iodixanol gradient analysis of purified fractions LDM has been demonstrated to resolve the intracellular GLUT4 pool into GSV and endosomal/TGN pools (Hashiramoto and James, 2000; Maier and Gould, 2000). This approach was used in this study to analyse the LDM fractions purified from 3T3-L1 adipocytes during various periods of insulin withdrawal to examine whether the GSV and endosomal/TGN GLUT4 pools exhibit any difference in the presence or absence of the STX 6 cytosolic fragment. The results clearly showed that the return of GLUT4 to the GSV pool is specifically impaired in cells infected with STX 6 AdV (Figure 5.6.A). Further supporting evidence was obtained by the distribution pattern of IRAP among the fractions of iodixanol gradient analysis (Figure 5.6.B). These results suggest that STX 6 function is needed for the biogenesis of the GSV compartment. Trafficking along the enodosomal pathway appeared superficially normal based on the retrieval of GLUT4 into peak 2 of the gradient in the cells expressing STX 6 cytosolic domains. However, the resolution between endosomes and TGN is not sufficient here to understand whether GLUT4 reaches the TGN from endosomes in the cells expressing cytosolic domain of STX 6. Therefore it is suggested that STX 6 is needed in a sequestration step of GLUT4 from endosomes to the GSV either via the TGN or directly.

Several studies conducted on STX 6 suggested that it mediates a TGN trafficking event, (Bock *et al.*, 1997; Simonsen *et al.*, 1999). A more recent study however has found an impact of STX 6 inhibition (by vaccinia virus mediated overexpression of the cytosolic domain of STX 6), which inhibited TGN38 and B-subunit of Shiga toxin trafficking from early endosomes to the TGN in CHO cells (Mallard *et al.*, 2002). Based on the findings of Mallard and co-workers, the movement of GLUT4 from endosomes to GSV might be affected due to an inhibition of endosome to TGN traffic.

The pattern of STX 6 distribution in the iodixanol gradient fractions described above showed that STX 6 is also sequestered to the GSV pool in parallel with GLUT4, during the insulin withdrawal period. Similar to findings with the GLUT4 and IRAP, retrieval of STX 6 in pool 1 (GSV) in cells expressing STX 6 cytosolic domain was low (Figure 5.6.C). This latter finding suggests the vesicles carrying GLUT4 into the GSV compartment contain STX 6. This is supported by extensive localisation of STX 6 in GLUT4 vesicles and the relatively high increase in PM levels of STX 6 in response to insulin described in chapter 3. The results described in chapter 3 showed that STX 6 associates with STX 16 in 3T3-L1 adipocytes and that both syntaxins were highly localised in GLUT4 vesicles. Therefore we propose that the Qa-SNARE of this fusion event is STX 16. STX 6 (Bock *et al.*, 1997) and STX 16 (Mallard *et al.*, 2002) are predominantly localised to TGN, suggesting the possibility that sequestration of GLUT4 to GSV from endosomes goes via the TGN. In support of this hypothesis, a considerable proportion (10-20%) of GLUT4 was found to reside in the TGN of myocytes and adipocytes under basal conditions independent of the biosynthetic pathway (Slot *et al.*, 1991; Martin *et al.*, 1994; Slot *et al.*, 1997).

Although inhibition of STX 6 caused a marked difference in GLUT4 distribution in 3T3-L1 adipocytes after insulin withdrawal, there was no reflection of this difference on insulin-stimulated glucose transport. However, all the insulin-stimulated glucose transport assays were conducted only after stimulating the basal cells for about 20 min. Cells used for the assays were infected with AdV between day 6-8 of differentiation where a high level of GLUT4 are already produced and sorted into native compartments including GSV. Therefore the newly expressed STX 6 domains may have had a small effect on slowly recycling GLUT4 under the basal state, which could be reflected by the increased basal glucose transport rate. As the majority of GLUT4

could still be in the GSV in such a situation, any subtle reduction of insulin-stimulated glucose transport may not be detected. However, the confocal microscopic data obtained from basal cells of STX 6 AdV infected cells did show a difference in the distribution of GLUT4. Whether this localisation was just the recycling endosomal compartment or another subdomain of endosomal compartment, which is known to sequester GLUT4 in non-native cells (Zeigerer *et al.*, 2002) is not known.

In the studies focused on GLUT4 trafficking we were unable to find a detectable effect of inhibition of STX 8 and 12 functions. The findings of chapter 3 however, showed that about 25% of STX 12 is localised in GLUT4 vesicles even though STX 8 colocalisation was very marginal. Previous studies have proposed STX 12 to function in receiving vesicles either from the TGN or early endosomes or participating in recycling of surface receptors. (Tang *et al.*, 1998c; Prekeris *et al.*, 1998). It is possible that STX 12 may not have a role in GLUT4 trafficking even though it is present in some of the GLUT4 vesicles. Another possibility is that a subtle effect of STX 12 inhibition on GLUT4 trafficking may not have been within the detection limits of the assays used. A rare possibility is that the cytosolic fragment expressed was not effective in inhibiting STX 12.

The functional studies carried out with the STX 6, 8 and 12 were extended to three more trafficking events, TfR recycling (constitutive recycling), LDL trafficking (lysosomal pathway) and secretion of adipsin and ACRP30. PM TfR receptor levels in the absence or presence of insulin was measured using 3T3-L1 adipocytes (Figure 5.7). Three other assays were conducted in HeLa cells to minimise the quantity of AdV needed. Assays conducted in HeLa cells measured rates of internalisation and externalisation of transferrin, which represents the trafficking of TfR. Furthermore, internalisation of surface bound transferrin was monitored using transferring Texas red. Surprisingly, none of these assays reveal an effect of either STX 6 or 8 or 12 (Figures 5.7 to 5.10). As STX 12 is suggested to be a Q-SNARE involved in recycling of PM receptors (Tang *et al.*, 1998c; Prekeris *et al.*, 1998), was expected to have some impact on transferrin recycling. Before ruling out the functional role of these syntaxins in TfR recycling it will be necessary to conduct the different experiments performed in HeLa cells in 3T3-L1 adipocytes, as there is a possibility that rat/ mouse syntaxin cytosolic domains expressed by AdV were not effective against human syntaxins of

HeLa cells. However, STX 6 AdV infected cells caused a change in distribution of LDL in HeLa cells (Figure 5.11) giving evidence at least that rat STX 6 domain was effective against human STX 6.

LDL distribution after 30 min uptake in cells infected with control AdV showed peripheral and perinuclear distributions, which probably reflect early endosomal and lysosomal compartments respectively. Cells overexpressing STX 8 and STX 12 domains showed a similar pattern of LDL distribution, failing to identify a role of STX 8 and 12 in LDL trafficking. However, the presence of the STX 6 cytosolic domain resulted in a distinct staining pattern, which did not show the perinuclear labelling (Figure 5.11). Although this difference was obvious in the images it is difficult to believe that STX 6 has any role in the lysosomal pathway based on the available data concerning STX 6. There is a possibility that this apparent block or delay in the transport of LDL to lysosomes is an indirect effect of impaired early endosomal to TGN trafficking caused by inhibition of STX 6. It is possible in such a situation that maturation of early endosomes to late endosomes is delayed or impaired due to poor exit of proteins targeted to TGN. These aspects require further clarification, which could be achieved using various markers for different compartments. In a previous study STX 8 has been found to be distributed in early and late endosomes in PC12 and COS7 cells and anti-STX 8 antibody partially inhibited epidermal growth factor receptor trafficking into lysosomes in HeLa cells (Prekeris *et al.*, 1999b). Another study has shown that the majority of STX 8 is localised in early endosomes and other localisations including late endosomes, with a proposed role of STX 8 in early endosomes (Subramaniam *et al.*, 2000). However, the data obtained in this study did not show any detectable effect of STX 8 inhibition on LDL trafficking, which follows the same route as epidermal growth factor receptor. Future studies on the trafficking steps will need to include proteins such as TGN 38 and epidermal growth factor receptor whose trafficking was demonstrated to be affected by inhibition of STX 6 (Mallard *et al.*, 2002) and STX 8 (Prekeris *et al.*, 1999b) respectively.

Even though recent studies have shown that STX 6 is required for homotypic fusion of immature secretory granules derived from the TGN in PC12 cells (Wendler and Tooze, 2001) the data of this study do not show any evidence for the involvement of STX 6, 8 or 12 in secretion of adipsin or ACRP30 from 3T3-L1 adipocytes.

Failure to detect a role of STX 8 or STX 12 in any of the trafficking events examined may have been caused by an inefficiency of inhibiting full-length syntaxin central to syntaxins function as their participation in the formation of extremely stable SNARE complexes. Certain studies have suggested that transmembrane domains of syntaxin and VAMP are essential in membrane fusion (Grote *et al.*, 2000) and that they contribute to the overall stability of the SNARE complex (Poirier *et al.*, 1998). Lack of transmembrane domain in the cytosolic domain may have stop targeting STX 8 and 12 to the sites at which they can inhibit. Furthermore, proteins such as Munc 18c, which stabilise the closed conformation of syntaxin, may act on these inhibitory cytosolic domains as well leaving a proportion of full-length syntaxins in the open active state. Therefore the detectable impact of inhibition will be a balance of these inhibitory and indirect stimulatory effects, which could be a fraction of absolute impact.

Future studies are needed to investigate the role of STX 6 in GLUT4 trafficking to GSV more precisely and identify the other SNARE partners in this trafficking step. The putative Qa-SNARE is STX 16 as suggested by its association with STX 6 in 3T3-L1 adipocytes and extensive colocalisation with GLUT4 vesicles. The R-SNARE and Qb-SNAREs involved also have to be identified, possible candidates being VAMP4 and Vti1a, which are demonstrated to complex with STX 6 and STX 16 in HeLa cells (Mallard *et al.*, 2002).

Based on the findings here we propose that STX 6 is required for one or both of following steps of GLUT4 trafficking- early endosome to the TGN and/or TGN to the GSV. STX 6 in the TGN with its putative Q-SNAREs of TGN- STX 16 and Vti1a might complex with putative R-SNARE VAMP4 localised in GLUT4 vesicles exiting the early endosome. Supporting evidence for a role for STX 6 in endosome to TGN traffic has been published (Mallard *et al.*, 2002). Inhibition of STX 6 blocks the fusion of GLUT4 vesicles with the TGN preventing GLUT4 from being sequestered into the GSV compartment. STX 6 may also mediate formation of the GSV itself by participating in a homotypic fusion event in vesicles carrying GLUT4, which bud from TGN. In support of this idea STX 6 has been identified as a component of the core machinery involved in homotypic fusion of immature secretory granules prepared from PC12 cells (Wendler and Tooze, 2001). A model of the role of STX 6 in GLUT4 trafficking is illustrated in figure 5.12.

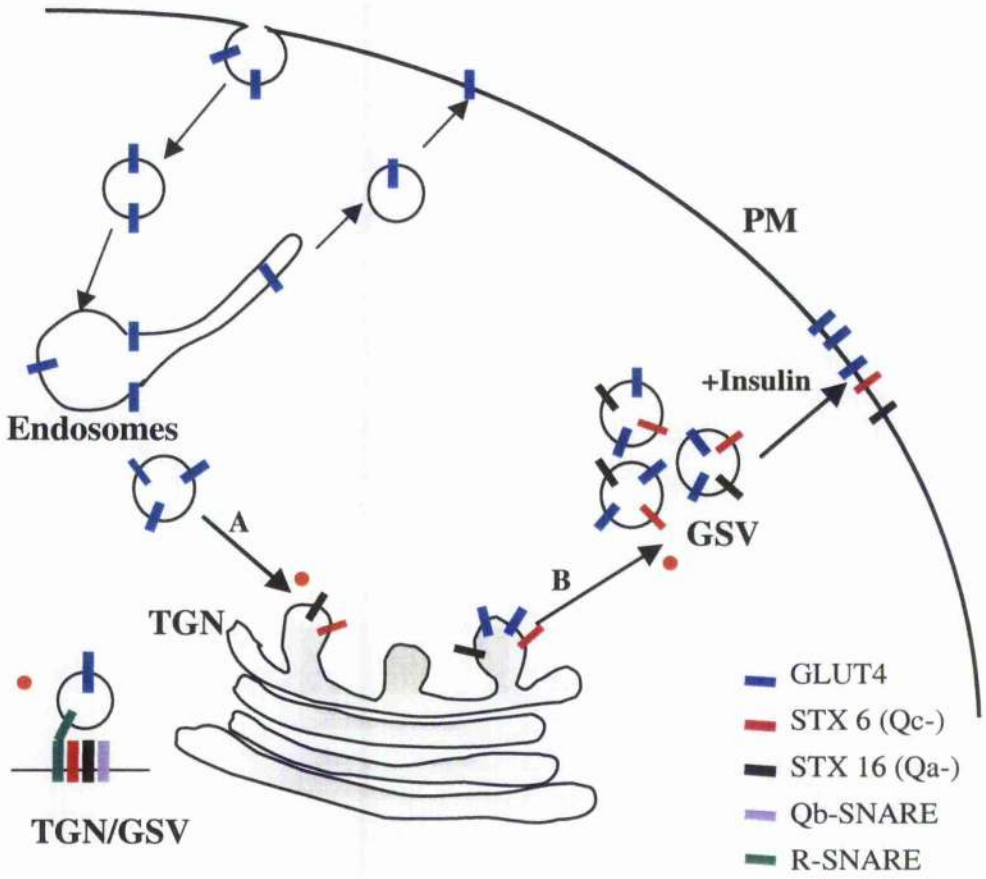

Figure 5.12 A possible model of the role of STX 6 in GLUT4 trafficking

The results described in this chapter strongly support a role of STX 6 in trafficking GLUT4 into the GSV compartment. The fusion step/s involved could be early endosome to TGN or the TGN to the GSV or both. We found evidence to suggest that STX 16 is the Qa-SNARE needed in this event (chapter 3). The Qb-SNARE and R-SNARE of this event are unknown. •Indicates the putative SNARE complex of this event. At basal state GLUT4 is sequestered to the TGN and subsequently to the GSV with the aid of STX 6. STX 6 is also moved to GSV with the GLUT4. STX 6 is increased at the PM with a corresponding depletion in the LDM after insulin stimulation in a similar manner to GLUT4 and IRAP. Data obtained in this study on STX 16 (chapter 3) suggest that STX 16 is also moved into GSV in the basal state and translocates to the PM in response to insulin.

Chapter 6

A study of the biogenesis of insulin-responsive GLUT4 compartment during differentiation of 3T3-L1 cells

6.1 Introduction

6.1.1 Biogenesis of GSV compartment in 3T3-L1 cells

Insulin stimulation results in an acute increase in glucose transport in fat and muscle cells by increasing the PM GLUT4 content by between 10-40 fold. It has been shown that this huge response of GLUT4 to insulin compared to the marginal elevation of constitutively recycling proteins such as TfR at the PM is due to the localisation of GLUT4 in a specialised insulin-responsive compartment. Even though the existence of such a compartment has been suggested by different approaches (Section 1.3.1) the biogenesis and nature of this compartment remain poorly understood (Reviewed in Bryant *et al.*, 2002).

In 1975 it was demonstrated that confluent 3T3-L1 cells could be hormonally induced to differentiate into adipocytes (Green and Kehinde, 1975). During differentiation, their morphology changes from fibroblastic to a spherical shape, with dramatic changes in cytoskeletal components, type of extracellular matrix components, protein expression, and with the accumulation of fat droplets. These changes are believed to be influenced by the expression of two transcription factors (CCAAT/ enhancer binding protein α and peroxisome proliferator-activated receptor-γ), which activate adipocyte specific genes (Gregoire *et al.*, 1998; Wu *et al.*, 1998b). During late phases of differentiation, 3T3-L1 adipocytes increase lipogenesis and acquire sensitivity to insulin (Gregoire *et al.*, 1998). At this stage GLUT4 (Garcia and Birnbaum 1989), insulin receptors (Reed *et al.*, 1977; Rubin *et al.*, 1978) and insulin receptor substrate, IRS-1 (Rice and Garner, 1994) expression is increased. GLUT4 is usually only detectable after day 4 post differentiation (Kaestner *et al.*, 1989; Garcia and Birnbaum, 1989).

Even though GLUT4 expression is restricted to fat and muscle, insulin-regulated amino peptidase (IRAP), which is extensively colocalised with GLUT4 (see section 1.5), is expressed in many tissues. This suggests the possibility that a similar insulin-sensitive compartment exists in tissues other than fat and muscle. On the other hand, this compartment may exist only in insulin-sensitive tissues and the trafficking of IRAP in other cells may be distinct. Hence, the behaviour of IRAP in adipocyte and non-adipocyte cells may offer some clues to the biogenesis of the GLUT4 compartment. GLUT4 is not an ideal marker to address the biogenesis of the

specialised compartment, as it is detectable only around day 4 of differentiation of 3T3-L1 adipocytes (Kaestner *et al.*, 1989; Garcia and Birnbaum, 1989) and thus it is unclear whether GLUT4 is required for the formation of the compartment. In adipocytes IRAP is largely localised in GLUT4 vesicles (Ross *et al.*, 1996). Furthermore, the trafficking of IRAP in adipocytes under basal and insulin-stimulated states is similar to that of GLUT4 (Ross *et al.*, 1997; Martin *et al.*, 1997; Garza and Birnbaum, 2000) and is the only other protein known to traffic identically to GLUT4 (Kandror and Pilch, 1994; Ross *et al.*, 1996). Therefore IRAP can be used as an independent marker for GLUT4 compartments.

Studies regarding the existence of an insulin-responsive compartment in tissues other than fat and muscle have had conflicting results. Intracellular sequestration of GLUT4 was observed when expressed in cells that do not express GLUT4, such as 3T3-L1 fibroblasts, HepG2 cells (Haney *et al.*, 1991), CHO cells (Asano *et al.*, 1992; Piper *et al.*, 1992), NIH-3T3 cells (Hudson *et al.*, 1992), COS-7 cells (Czech *et al.*, 1993) and PC12 cells (Verhey *et al.*, 1993). However, intracellular GLUT4 did not show a pronounced response to insulin (Haney *et al.*, 1991; Hudson *et al.*, 1992). A study conducted to assess response of IRAP to insulin in confluent 3T3-L1 fibroblasts (prior to differentiation) and mature 3T3-L1 adipocytes showed the fold increase in PM IRAP on insulin stimulation was increased from 1.8 to 8-fold following differentiation (Ross *et al.*, 1998). Ross and co-workers (1998) also showed that there is no difference in the insulin-response towards translocation of TfR into PM, between fibroblasts and adipocytes. Such data argue for the formation of an insulin-sensitive compartment after differentiation of 3T3-L1 cells.

In contrast to the above findings, there is evidence for the insulin-responsive translocation of GLUT4 in cells other than differentiated fat and muscle cells such as 3T3-L1 fibroblasts and CHO cells. Dobson and co-workers used a GFP-GLUT4 chimera to study the effect of insulin on GLUT4 transport in CHO cells and found an increase in translocation in response to insulin (Dobson *et al.*, 1996). Two other groups used epitope tagged GLUT4 and a sensitive quantitative method to detect PM GLUT4 immunologically in 3T3-L1 fibroblasts, NIH 3T3 cells (Ishii *et al.*, 1995) and CHO cells (Kanai *et al.*, 1993; Ishii *et al.*, 1995) and found that insulin increased GLUT4 in PM by ~3-fold. Epitope tagged GLUT1 showed PM translocation to a lesser degree

(~1.5-fold) in the study of Ishi and co-workers. The presence of GLUT4 in a highly insulin-responsive compartment was observed in undifferentiated 3T3-L1 preadipocytes and CHO cells cultured similarly to 3T3-L1 adipocytes, using a GFP-GLUT4 chimera (Bogan *et al.*, 2001). These authors reported significant insulin-stimulated GLUT4 translocation throughout the differentiation from day 0. In their study they also showed that this insulin-responsiveness is not common to every cell as NIH 3T3 cells failed to respond.

The existence of a specialised insulin-regulated trafficking pathway in 3T3-L1 and CHO fibroblasts cells has been shown by another approach using IRAP and GLUT4 targeting domains fused to transferrin-binding domain of the TfR (Lampson *et al.*, 2000). In these studies insulin stimulated, translocation of GLUT4 and IRAP reporters into the PM in confluent 3T3-L1 fibroblasts (which are ready for differentiation) by ~3.6 and ~3.3-fold respectively. They also showed that native TfR was increased in PM only by 1.2-fold under similar conditions. Furthermore, they showed similarly high translocation of GLUT4 and IRAP reporters in CHO cells, when stimulated with insulin. Such data argue that insulin regulated trafficking pathway exists even in cells not expressing GLUT4.

Several studies have demonstrated that GLUT4 is sorted away from TfR when expressed in cells other than fat and muscle. A TfR negative intracellular pool of GLUT4 has been identified in PC12 cells stably transfected with GLUT4 by velocity sedimentation analysis and confocal microscopy (Herman *et al.*, 1994). In another study, it was found that epitope-tagged GLUT4 expressed in CHO cells was enriched in small vesicles, which are not enriched in TfR (Shibasaki *et al.*, 1992). Finally, in CHO cells stably expressing GLUT4, the transporter was segregated from endogenous TfR immediately upon endocytosis (Wei *et al.*, 1998). These studies suggested that the cells other than mature adipose and muscle also have the necessary machinery for retention of GLUT4 under basal state and translocation in response to insulin. However, they do not address the question of whether the retention of GLUT4 in the intracellular membranes of these cells is in a compartment similar to the GSVs in fat cells.

GSV biogenesis

In an effort to study the time at which 3T3-L1 cells become insulin-sensitive, El Jack and co-workers (1999) used a range of approaches to show that an insulin-sensitive intracellular compartment formed before the expression of detectable levels of GLUT4. Insulin-responsive compartment containing GLUT1 and TfR was present as early as day 3 (before expression of GLUT4) post differentiation. They further showed that insulin mobilised GLUT1 from this compartment. Moreover, they showed that basal glucose transport falls and cell surface TfR levels diminished markedly after day 3. IRAP distribution and response to insulin was found to be identical to that of GLUT1 at this time. Targeting of GLUT4 to the same compartment occurred upon its expression by day 5. Based upon this data, El Jack and co-workers argue that development of this compartment results from the expression of yet unknown genes, and it precedes and may be independent of expression of GLUT4 (El Jack *et al.*, 1999). They also contend that this is the bona fide insulin-sensitive compartment.

By contrast previous studies from our lab support the idea that GSV compartment is formed after the expression of GLUT4 (Maier V. Ph. D. thesis 2001; Baker, *et al.*, 2000 personal communication). Maier in her study showed that IRAP in differentiating 3T3-L1cells is highly susceptible to endosomal ablation at day 1 and 3 but resistant at day 5. This lead to the suggestion that IRAP is extensively localised with TfR in recycling endosomal system on day 3, but by day 5 most of it is sorted away from TfR possibly to GSV compartment. This idea is further supported by the work of Baker co-workers 2000 who showed the presence of IRAP almost totally in the endosomal pool (peak 2) of iodixanol gradients of 3T3-L1 cells 1 and 4 days post-differentiation, suggesting that the GSV compartment is not formed by day 4 of differentiation.

The study presented in this chapter aimed to address the question of the time of formation of GSV in 3T3-L1 cells by examining at the insulin-response during differentiation process. In this regard two proteins, which are expressed from fibroblast stage, IRAP and TfR were used instead of GLUT4 to monitor the insulin response. PM IRAP and TfR levels were measured in presence or absence of insulin during various stages of differentiation of 3T3-L1 cells, using a cell surface biotinylation approach and ^{125}I transferrin binding respectively.

6.1.2 Expression of post-Golgi syntaxins during differentiation of 3T3-L1 cells

Insulin-stimulated translocation of GLUT4 vesicles to PM in 3T3-L1 adipocytes is a process mediated by SNARE complex formation (described in section 1.14). Studies conducted to determine the pattern of expression of different SNAREs during differentiation of 3T3-L1 cells have found altered expression levels of some of these SNAREs. Increased relative expression of cellubrevin (Volchuk *et al.*, 1995), and STX 4 (Torrejon-Escribano *et al.*, 2002), a Q-SNARE involved in GLUT4 translocation was identified during differentiation. Using non-differentiated fibroblasts, 3T3-L1 cells at day 2 of differentiation and fully differentiated adipocytes in their study, Torrejon-Escribano and co-workers observed that cellubrevin is increased by day 2 and STX 4 is increased after day 2. In addition, expression of SNAP-23, the other Q-SNARE mediating GLUT4 translocation was not changed during differentiation (Wong *et al.*, 1997), but its distribution changed from an intracellular to PM localisation (Torrejon-Escribano *et al.*, 2002). These results indicated that certain changes in expression and distribution of SNAREs involved in GLUT4 translocation in mature adipocytes occur in parallel to achievement of insulin-stimulated GLUT4 translocation. Here I describe how the expression of post-Golgi STX 6, 8 and 12 changes from non-differentiated fibroblast to fully differentiated 3T3-L1 adipocyte and analyse the pattern of their distribution in iodixanol gradients during this process.

6.2 Aims

As the GSV compartment is highly insulin-sensitive, the aim of this study was to determine the kinetics of increased insulin-sensitivity during differentiation of 3T3-L1 cells, to identify the time of biogenesis of GSV. To achieve this, the response of IRAP and TfR to insulin was measured during the course of differentiation. In addition, distribution of STX 6, 8 and 12 in iodixanol gradients during differentiation of 3T3-L1 cells was studied with a view to identifying whether these syntaxins play a role in the changing patterns of membrane trafficking which accompany differentiation.

6.3 Results

6.3.1 Effect of insulin on the level of IRAP translocation to PM during differentiation of 3T3-L1 cells

3T3-L1 cells during differentiation at day-1 (day before differentiation), 0, 2, 4, 6 and 8 were treated with (I) or without (B) 100 nM insulin for 30 min at 37°C. Then the

cells were maintained at 4°C and subjected to cell surface biotinylation as described in section 2.3.15. The amount of biotinylated IRAP obtained represents the quantity of IRAP translocated to PM under each condition. Following biotinylation, cell lysates were prepared in lysis buffer (section 2.1.5) and IRAP was immunoprecipitated (section 2.3.12). Immunoprecipitates were used to detect the total IRAP and biotinylated IRAP content obtained under B and I states during differentiation, as described in section 2.3.15, using either an anti-IRAP antibody or HRP-linked streptavidin.

The data showed (Figure 6.1) that the total IRAP content immunoprecipitaed under B and I conditions was similar. However, the expression of IRAP increased during differentiation (Figure 6.1) in agreement with previous studies (Ross *et al.*, 1996) and was increased markedly by day 2. Out of three experiments conducted, one showed an increased biotinylation of IRAP under insulin stimulation from day 4. The other two showed increased biotinylation in insulin-stimulated cells from day 2. These data show that there is an increased insulin-sensitivity of IRAP translocation to PM by day 4, and suggest that the cells probably acquire the machinery for this between day 2 and 4 (Figure 6.1). No response of IRAP to insulin was seen in confluent 3T3-L1 fibroblasts (day -1) or in fibroblasts a few hours after differentiation (day 0). The amount of biotinylated IRAP under basal condition, was more or less similar throughout the differentiation (when used IRAP from equal amount of cells in Western blots) even though the total IRAP expression was increased markedly by day 2. Such data is consistent with increased sequestration of IRAP from day 2 to day 8.

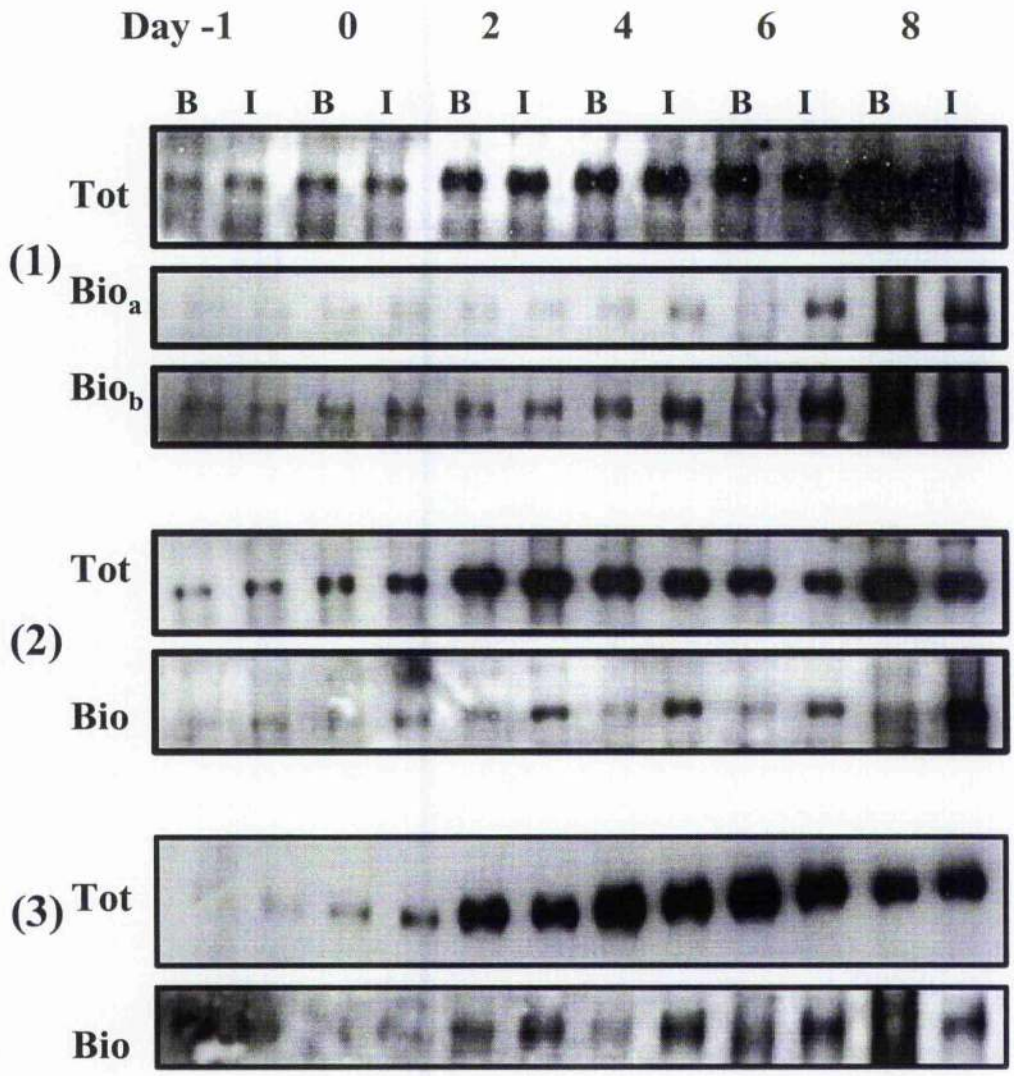

Figure 6.1 Effect of insulin on IRAP translocation into PM during differentiation of 3T3-L1 cells

3T3-L1 cells were treated with (I) or without (B) 100 nM insulin for 30 min, at day -1 (day prior to differentiation), 0, 2, 4, 6 and 8 of differentiation. Then the cells were subjected to cell surface biotinylation as described in section 2.3.15. IRAP was immunoprecipitated (section 2.3.12) and the immunoprecipitates were subjected to Western blotting (2.3.7) and immunodetection (section 2.3.15) to find the total IRAP (Tot) using the immunoprecipitates from ~$1.8x10^5$ cells and biotinylated IRAP (Bio) using the immunoprecipitates from ~$3.6x10^5$ cells of each fraction. (1), (2) and (3) represent independently performed experiments. Bio_a and Bio_b of (1), represent two different exposures of the same blot.

6.3.2 Expression of TfR during differentiation of 3T3-L1 cells

Homogenates collected from 3T3-L1 cells during differentiation (day -1, 0, 2, 4, 6 and 8) were subjected to Western blotting to detect the expression of TfR. Total protein content of homogenates were measured as described in section 2.3.5. Equal fractions of cell homogenates were subjected to Western blotting to detect the amount of TfR expressed during differentiation. (Equal protein quantity was not used in this case, as the difference between total protein concentrations obtained before and after differentiation was very high (Figure 6.2.A).

Total protein content of 3T3-L1 cells was increased extensively during differentiation. Peak amount was found at day 6 where it was around 10-fold higher than that of day 0 (Figure 6.2.A). Western blots showed that the total TfR content was increased during differentiation, following a fairly similar pattern to the total protein content. Peak TfR level was found between day 4 and 6 with a reduction towards day 8 (Figure 6.2.B).

Figure 6.2.A

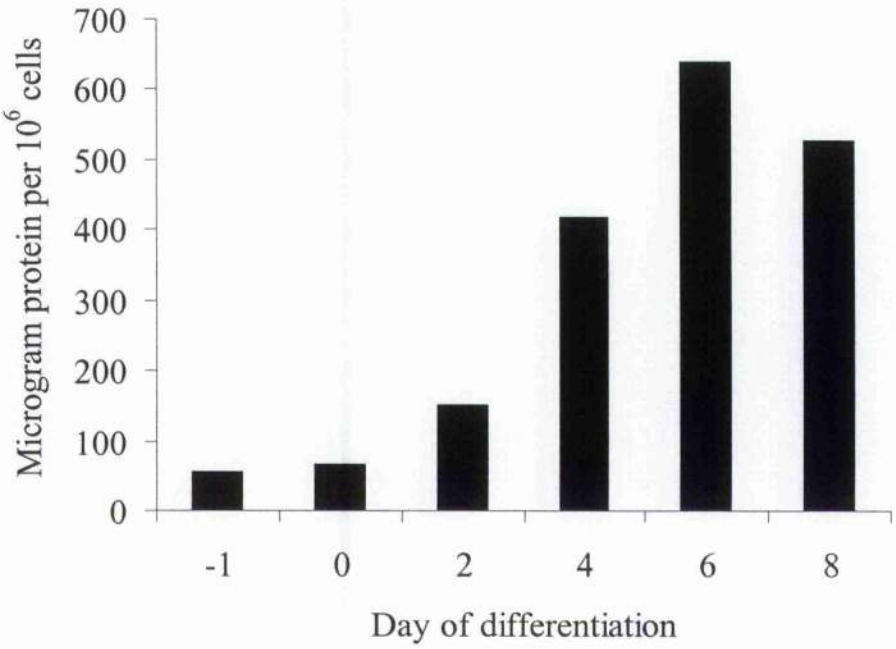

Figure 6.2 .B

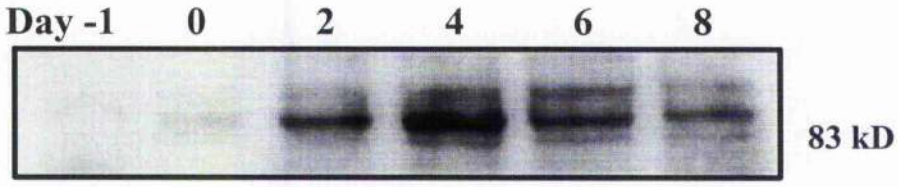

Figure 6.2.A Total protein content of 3T3-L1 cells during differentiation
Homogenates of 3T3-L1 cells were collected at day -1 (day prior to differentiation) 0, 2, 4, 6 and 8 of differentiation. Total protein content of the homogenates was measured as described in section 2.3.5. The graph shows change in the total protein content (per 10^6 cells) during differentiation from a representative experiment (n=3).

Figure 6.2.B Expression of TfR during differentiation of 3T3-L1 cells
Homogenates collected as described in figure 6.2.A were subjected to Western blotting to detect the difference in expression of TfR during differentiation. Equal proportions of the homogenates ($3x10^4$ cells) were tested. Figure shows the results of a representative experiment (n=3).

6.3.3 Effect of insulin on PM TfR level during differentiation of 3T3-L1 cells

TfR is a ubiquitous constitutively recycling protein, which shows about 1.5-fold increase at the PM on insulin stimulation of fully differentiated adipocytes (Ross *et al.*, 1998). The effect of insulin on cell surface TfR during differentiation was detected using the method described in section 2.5.3. 3T3-L1 cells were used from day before differentiation (-1) to day 8 after differentiation, and incubated ± 100 nM insulin at 37°C for 30 min prior to assay.

Figure 6.3 shows that there is around 1.3-fold increase of TfR in response to insulin even before differentiation of 3T3-L1 cells. The fold increase from day -1 to day 4 was similar. A slight increase of insulin-responsiveness was observed on day 6 and day 8 where the fold increase was around 1.5. This experiment also showed that TfR levels at the PM are increased by about four times from day 0 to day 2. The pattern of the quantity of TfR at the PM on each day is very similar to the expression pattern of TfR (Figure 6.2.B).

6.3.4 Transferrin uptake after insulin withdrawal of 3T3-L1 cells

The 3T3-L1 cells during the differentiation (day -1, 0, 2, 4, 6 and 8) were incubated with or without 100 nM insulin for 30 min and transferrin uptake for 5 min or 30 min was measured at 37°C immediately after insulin withdrawal (as in section 2.5.4). Results (Figure 6.4.A) show, that the increased TfR at PM following insulin-stimulation is not returned to its basal level 5 min after withdrawal (except at day 0) where the difference between transferrin uptake at basal and insulin groups is obvious. Figure 6.4.B shows basal level of equilibrium is returning after 30 min of withdrawal even though it is not complete in most groups. Comparing the figures 6.4.A and 6.4.B it is apparent that return into basal equilibrium status is faster at day 0 and day 4.

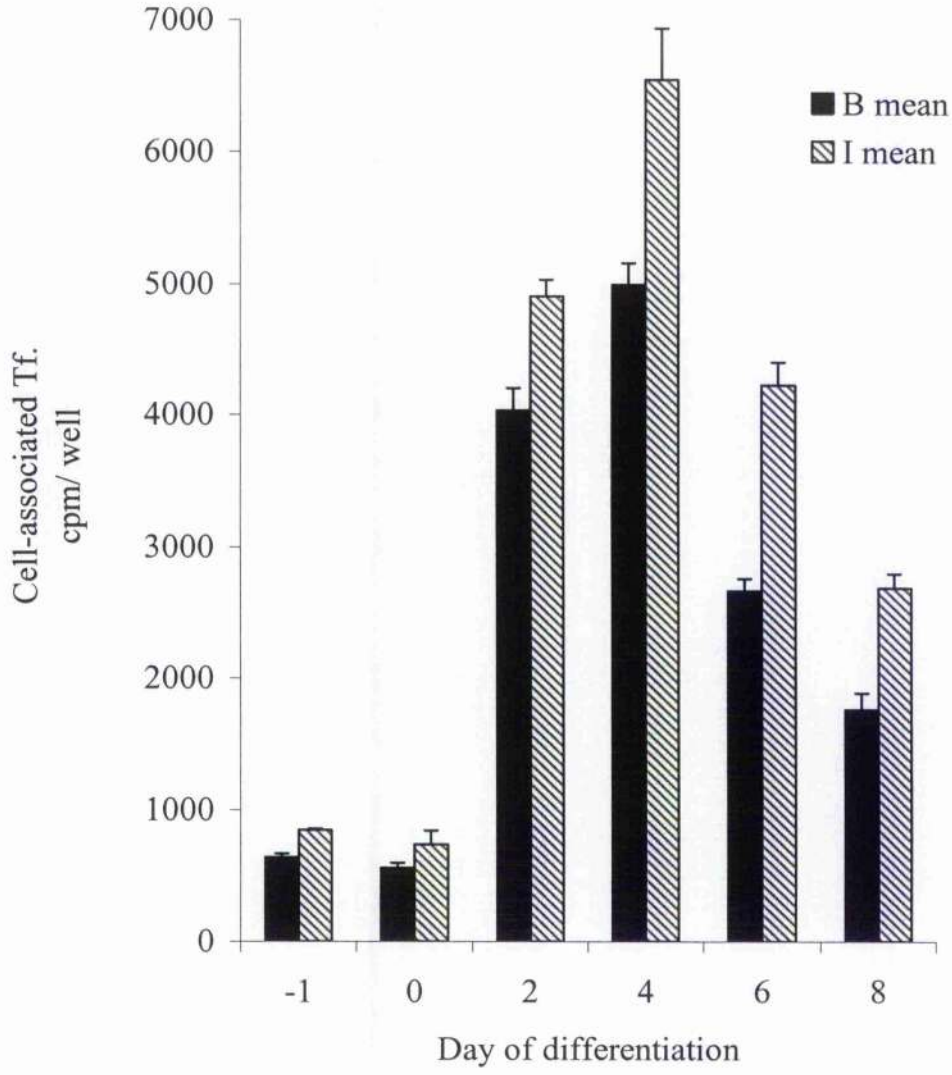

Figure 6.3 Effect of insulin on TfR level at PM during differentiation of 3T3-L1 cells

3T3-L1 cells were treated with (I) or without (B) 100 nM insulin for 30 minutes at day-1 (day prior to differentiation) 0, 2, 4, 6 and 8 of differentiation. Cells were washed in ice-cold buffer and incubated with 3 nM ^{125}I transferrin ± 10 μM transferrin on ice for 2 h, to measure cell surface TfR levels (2.5.3). Figure shows results of a typical experiment conducted in triplicate. Mean ± SEM are shown. n=3.

Figure 6.4.A

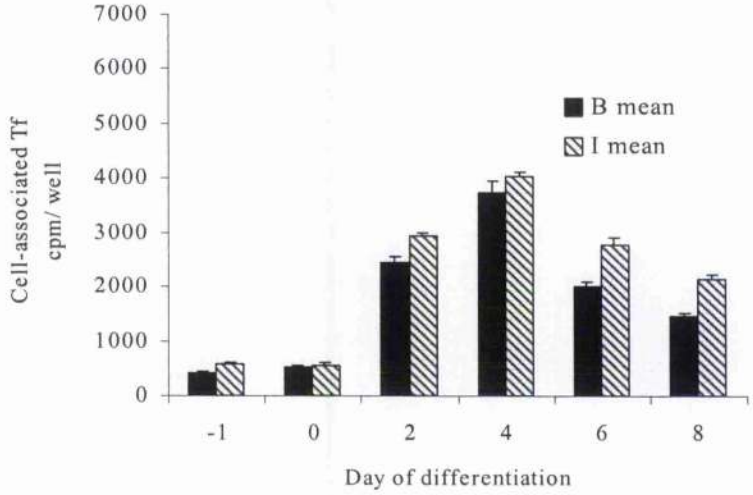

Figure 6.4.B

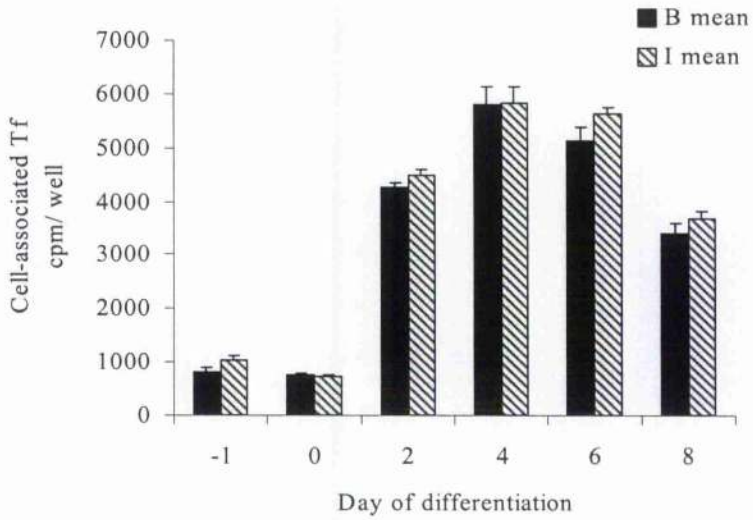

Figure 6.4.A Transferrin uptake for 5 min after insulin withdrawal from differentiating 3T3-L1 cells

3T3-L1 cells at day-1 (day prior to differentiation) 0, 2, 4, 6 and 8 of differentiation, were treated with (I) or without (B) 100nM insulin for 30 minutes. Cells were washed and incubated with 3 nM ^{125}I transferrin ± 10 μM transferrin for 5 min at 37°C. The uptake of ^{125}I transferrin was detected as described in section 2.5.4. Figure shows results of a typical experiment conducted in triplicate. Mean ± SEM are shown. n=3.

Figure 6.4.B Transferrin uptake for 30 min after insulin withdrawal from differentiating 3T3-L1 cells

This experiment was conducted in the same manner as described in figure 6.4.A legend except that the incubation with ^{125}I transferrin ± 10 μM transferrin was extended for 30 min. Uptake of ^{125}I transferrin was measured at the end of experiment. Shown is a representative experiment conducted in triplicate. Mean ± SEM are shown. n=3.

6.3.5 Distribution of post-Golgi syntaxins on iodixanol gradients during differentiation of 3T3-L1 cells

LDM collected from 3T3-L1 cells of day 2, 4, 6 and 8 of differentiation were separated on iodixanol gradients as described in section 2.3.4. Equal proportions of each fraction were subjected to Western blotting to identify the distribution of GLUT4, STX 6, 8 and 12 in iodixanol gradients during differentiation.

The results showed that GLUT4 is not apparent in the gradients at day 2 and 4 as previously reported (Maier V, thesis 2001). In contrast GLUT4 is expressed extensively, and distributed in two peaks of the iodixanol gradient, by day 6 and maintained at day 8 (Figure 6.5.A). Data shows that increased amount of syntaxins 6, 8 and 12 are present in iodixanol gradients towards the maturity of adipocytes (Figures 6.5.B, 6.6.A and 6.6.B). STX 6 was detected on day 2 in the peak 2, which represents the endosomal/TGN pool. By day 4 STX 6 showed its distribution in both peaks 1 and 2 with the majority (~60%) being in peak 2 (TGN/endosomal pool) thereafter throughout the differentiation (Figure 6.5.B). Distribution of STX 6 in the gradient is markedly increased by day 6. In contrast, STX 8 distribution was observed in both peaks throughout the differentiation with an increase in total amount present in LDM towards maturity (day 2 to 8) (Figure 6.6.A). STX 12 was almost undetectable at day 2 with apparent distribution at day 4 and much higher levels produced by day 6. At day 8, level of STX 12 was slightly reduced (Figure 6.6.B). Examination of these data show that the change of STX 6 and STX 12 levels in the gradients during differentiation follows a pattern similar to that of GLUT4.

Figure 6.5.A

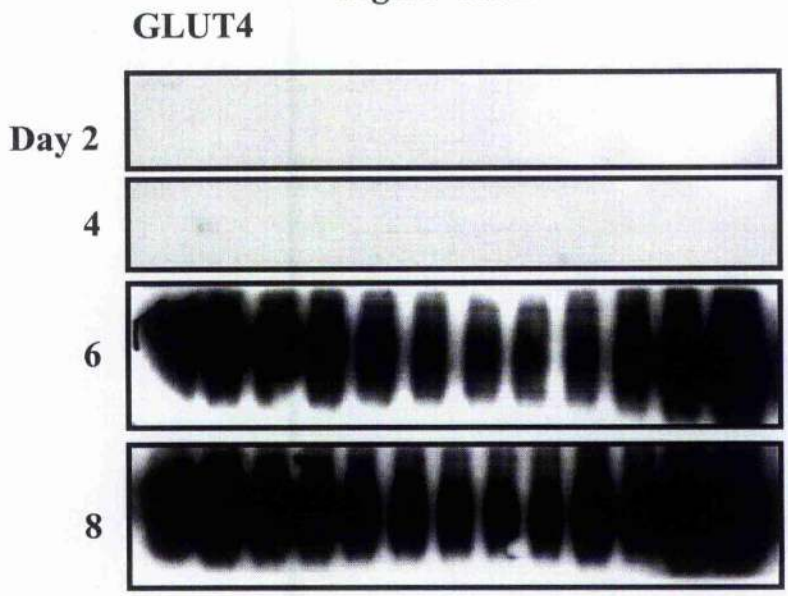

Figure 6.5.B

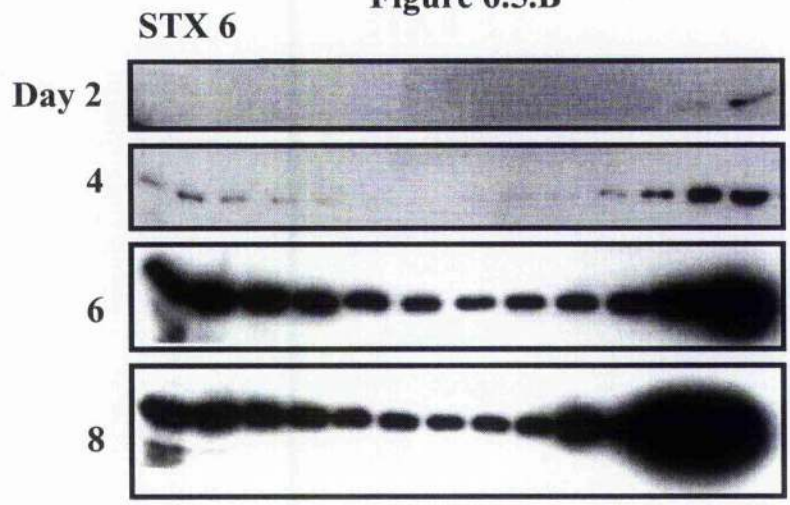

Figure 6.5.A Separation of LDM GLUT4 collected from 3T3-L1 cells during differentiation, on iodixanol gradients

LDM were collected as described in section 2.3.3, from 3T3-L1 cells at day 2, 4, 6 and 8 of differentiation and subjected to iodixanol gradient centrifugation as described in section 2.3.4. The distribution of GLUT4 in iodixanol fractions, was detected by Western blotting. A set of representative immunoblots is shown (n=3).

Figure 6.5.B Separation of LDM STX 6 collected from 3T3-L1 cells during differentiation, on iodixanol gradients

Distribution of STX 6 in 3T3-L1 cells during differentiation was detected by Western blotting, of the iodixanol fractions collected as described in figure 6.5.A legend. A representative immunoblot is shown (n=3).

Figure 6.6.A

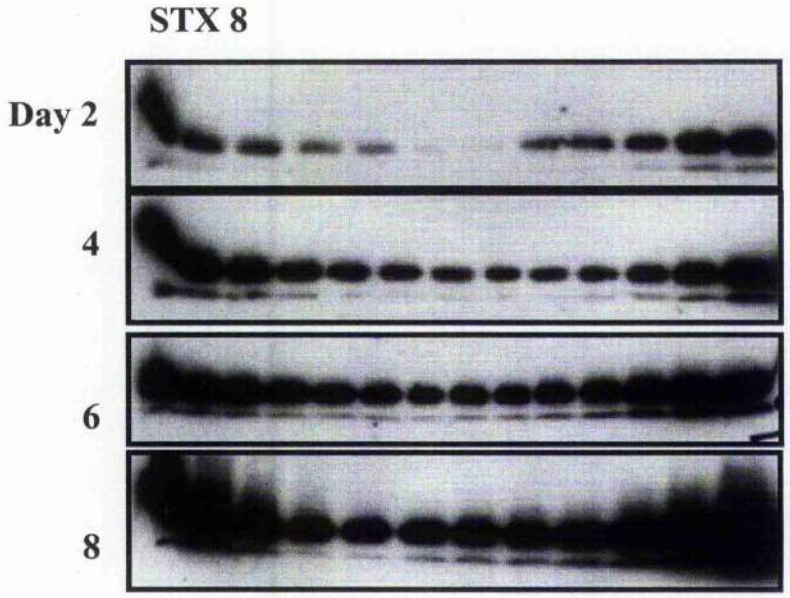

Figure 6.6.B

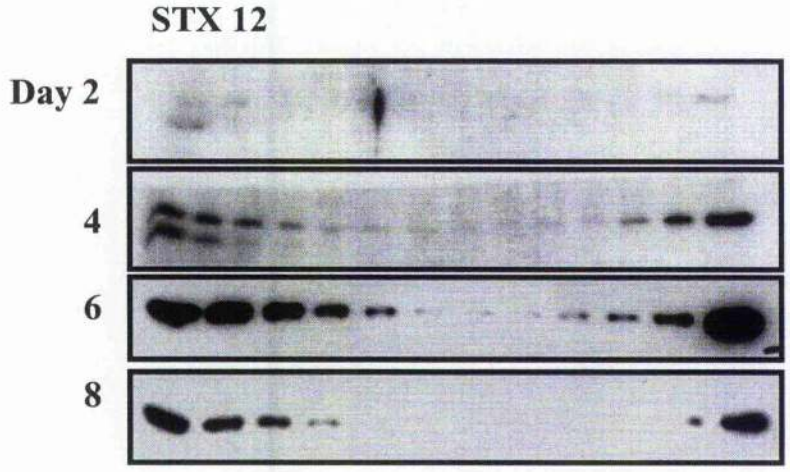

Figure 6.6.A Separation of LDM STX 8 collected from 3T3-L1 cells during differentiation, on iodixanol gradients
Distribution of STX 8 in 3T3-L1 cells during differentiation was detected by Western blotting using the iodixanol fraction collected as described in figure 6.5.A legend. Shown is the typical pattern of distribution (n=3).

Figure 6.6.B Separation of LDM STX 12 collected from 3T3-L1 during differentiation, on iodixanol gradients
Distribution of STX 12 in 3T3-L1 cells during differentiation was detected by Western blotting of the iodixanol fraction collected as described in figure 6.5.A legend. A set of representative immunoblots is shown (n=3).

6.4 Discussion

The ability of insulin to dramatically increase glucose uptake into fat and muscle tissues is suggested to be due to the presence of an insulin-responsive GLUT4 compartment (GSV) in these tissues, which is mobilised to the PM (Yang and Holman, 1993). However, the nature and the biogenesis of this compartment are poorly understood. Various studies have been conducted to identify whether exogenously expressed GLUT4 is retained intracellularly in tissues that do not express GLUT4 and whether these tissues are insulin-responsive. All these studies have shown the intracellular retention of GLUT4 and IRAP, yet none of these studies have shown whether this retention is in a bona fide GSV compartment. Several studies have shown in both fat cells and other cells that this intracellular retention is mediated by the presence of specific motifs in GLUT4 (FQQI and LL) (Piper *et al.*, 1993; Garippa *et al.*, 1996) and IRAP (LL motifs) (Keller *et al.*, 1995).

As regards the insulin-responsiveness of these cells there are conflicting results. Evidence for insulin-stimulated GLUT4 translocation in 3T3-L1 fibroblasts and cells other than fat and muscle came from studies which used more sensitive quantitative methods (Kanai *et al.*, 1993; Ishii *et al.*, 1995; Dobson *et al.*, 1996; Lampson *et al.*, 2000). It is also hypothesised that the insulin-responsiveness is gained in 3T3-L1 cells during some stage of differentiation. Evidence is there to support that this compartment is formed before expression of GLUT4 (El Jack *et al.*, 1999) and after expression of GLUT4 (our lab). In this study we aimed to determine the time of formation of the GSV compartment in 3T3-L1 cells by looking at the responsiveness of IRAP and TfR to insulin during differentiation.

IRAP is a protein, which is known to traffic identically to GLUT4 in mature 3T3-L1 adipocytes under basal and insulin-stimulated conditions (Ross *et al.*, 1997; Martin *et al.*, 1997; Garza and Birnbaum, 2000). Whereas IRAP is expressed in both the fibroblast and the differentiating adipocyte, GLUT4 is expressed at detectable levels only around day 4 of differentiation (Kaestner *et al.*, 1989; Garcia and Birnbaum, 1989). Therefore, in this study IRAP was used as a marker to assay the insulin-responsiveness of 3T3-L1 cells throughout the differentiation without complicating the system by ectopic expression of GLUT4 or a relevant reporter. The effect of insulin on

TfR trafficking was assayed in parallel to determine whether IRAP traffics differently to constitutively recycling TfR during differentiation of 3T3-L1 cells.

The amount of cell surface IRAP under different conditions was measured by biotinylation of cell surface proteins followed by immunoprecipitation of IRAP as described in previous studies (Garza and Birnbaum, 2000). In this method, proteins at the cell surface are biotinylated on exposed lysine residues with the membrane impermeant biotin reagent. IRAP is a good candidate for biotinylation as it has 45 lysine residues in its extracellular domain (Kaestner *et al.*, 1989; Keller *et al.*, 1995). The results of this experiment demonstrated that total cellular expression of IRAP is markedly increased from day 2 (Figure 6.1), in agreement with previous reports. Ross and co-workers (1996) showed an increase in IRAP content of 6-fold between day 2 and 4 of differentiation of 3T3-L1 cells. In addition, our study showed marked increase in TfR expression from day 2 (Figure 6.2.B).

The level of TfR in PM in the basal state is increased in parallel with increased expression (Figure 6.3). This indicates that the proportion of sequestration of TfR is not increased with the higher expression of TfR. In contrast to TfR, the total IRAP on PM in the basal state is unchanged from day -1 to 8. These findings strongly suggest that there is a mechanism to sequester more IRAP in differentiating adipocytes by sorting it away from TfR, which is obvious from day 2 onwards in this experiment. Furthermore, the results of cell surface TfR assays under basal and insulin-stimulated conditions suggest that the recycling endosomal compartment is insulin-responsive to almost the same extent in fibroblasts and throughout the differentiation of 3T3-L1 cells. A similar observation is made in the study of Ross and co-workers where no difference in the response of TfR to insulin between 3T3-L1 fibroblasts and adipocytes was detected (Ross *et al.*, 1998). Based on this result we suggest that there is a basal level of insulin-response present in 3T3-L1 fibroblasts (possibly it is a common feature present in many cells). However, IRAP showed high insulin-responsiveness only after differentiation, which probably occurs around day 2 and definitely by day 4. Whether this insulin-responsive compartment present in early stages of differentiation (before expression of detectable levels of GLUT4), is the actual GSV or another subdomain of endosomal system is not revealed by the findings of this study.

However, our data suggest that IRAP is targeted to a separate slow recycling intracellular compartment perhaps as early as day 2 but certainly by day 4 and before the expression of GLUT4. Our study does not provide evidence as on to whether this compartment is present before day 2. It is possible that the existence of this separate compartment becomes apparent only when there is a high level of IRAP produced, that is by day 2. Similarly the detection of insulin-responsiveness of this compartment before day 2, using the proteins produced at low levels at that time may not reveal the actual response by the cell surface biotinylation method. In the studies where the insulin-response was seen from confluent 3T3-L1 fibroblasts and cells such as CHO more sensitive assays were used and reporter molecules for GLUT4 or IRAP which produced a high level of expression of these proteins from the beginning of differentiation (Kanai *et al.*, 1993; Ishii *et al.*, 1995; Lampson *et al.*, 2000; Bogan *et al.*, 2001). Kanai and co-workers were unable to show this insulin-response when they used measurement of glucose uptake, Western blotting of subcellular fractions or immunofluorescence microscopy. At present, our methodologies do not allow for definitive conclusions.

The findings of El Jack and co-workers (1999) support the idea that a new insulin-responsive compartment is formed on day 3 of differentiation. They have observed a "narrowing-down" of the GLUT1 peak (identified by sucrose velocity gradient) and depletion of GLUT1 from this peak upon insulin-stimulation. But their suggestion that this peak represent the specialised GSV compartment based on its almost complete overlap with GLUT4 peak at day 9 is highly debatable. Many studies have shown that GLUT1 is only partially colocalised with GLUT4 (Calderhead *et al.*, 1990; Rodnick *et al.*, 1992; Livingstone *et al.*, 1996). The reason behind this discrepancy may be due to the inability of separation of GLUT4 into discrete pools by the use of sucrose gradient velocity gradients.

Previous studies from our lab support the idea that the specialised GSV compartment is formed by day 5 post-differentiation, concomitant with the time of GLUT4 expression. In the study of Maier it was found that IRAP was highly susceptible to endosomal ablation on day 3 (Maier, Ph.D. thesis 2001). Moreover, Baker *et al.*, in their personal communication showed that IRAP is not found in peak 1 of iodixanol gradient on day 4 and almost all were distributed in peak 2 (Baker *et al.*, 2000). Both

of these studies showed that IRAP is in endosomal structures at day 3 or 4 of differentiation. Taking these previous findings together with the findings of the present study it is possible to speculate that the "insulin-responsive" compartment identified here at days 2 to 4 is a subdomain of the endosomal system, which is not as completely segregated from endosomes as GSV. Perhaps this is not a completely "mature" GSV compartment. Therefore this compartment is susceptible to endosomal ablation and separated into peak 2 in iodixanol gradients. But it is not the same constitutively recycling compartment where TfR traffics, so the IRAP is sequestered into this before GLUT4 is expressed and also insulin accelerates the exocytosis of this compartment. The complete formation of the GSV compartment may then occur around day 5 either influenced by expression of GLUT4 or some other proteins or by combination of both.

Many studies have shown that highest insulin-response is achieved during late phase of differentiation of 3T3-L1 (Ross *et al.*, 1998). In agreement, in the majority of biotinylation experiments conducted in this study, the magnitude of IRAP translocation in insulin-stimulation was highest at day 6 and 8 (Figure 6.1). Achievement of this maximal response may be a result of localisation to a fully mature GSV compartment.

The findings obtained in this study support the recent model of Zeigerer and co-workers to describe trafficking of IRAP in 3T3-L1 during differentiation of 3T3-L1 cells (Zeigerer *et al.*, 2002). They found evidence that ~50% of GLUT4 is sorted from endosomal compartment to a specialised compartment in 3T3-L1 adipocytes, which are in dynamic communication with one another and with PM. They used reporters for GLUT4 and IRAP and a compartment-specific fluorescence-quenching assay in live cells in this study. They proposed that in differentiated and undifferentiated cells, IRAP and GLUT4 are sorted away from TfR within the endosomal recycling compartment to form separate vesicles which are slowly recycled to PM. Furthermore, they showed that IRAP and GLUT4 are targeted to a highly insulin-responsive specialised compartment which is found only in cells such as mature adipocytes and muscle cells (Figure 6.7).

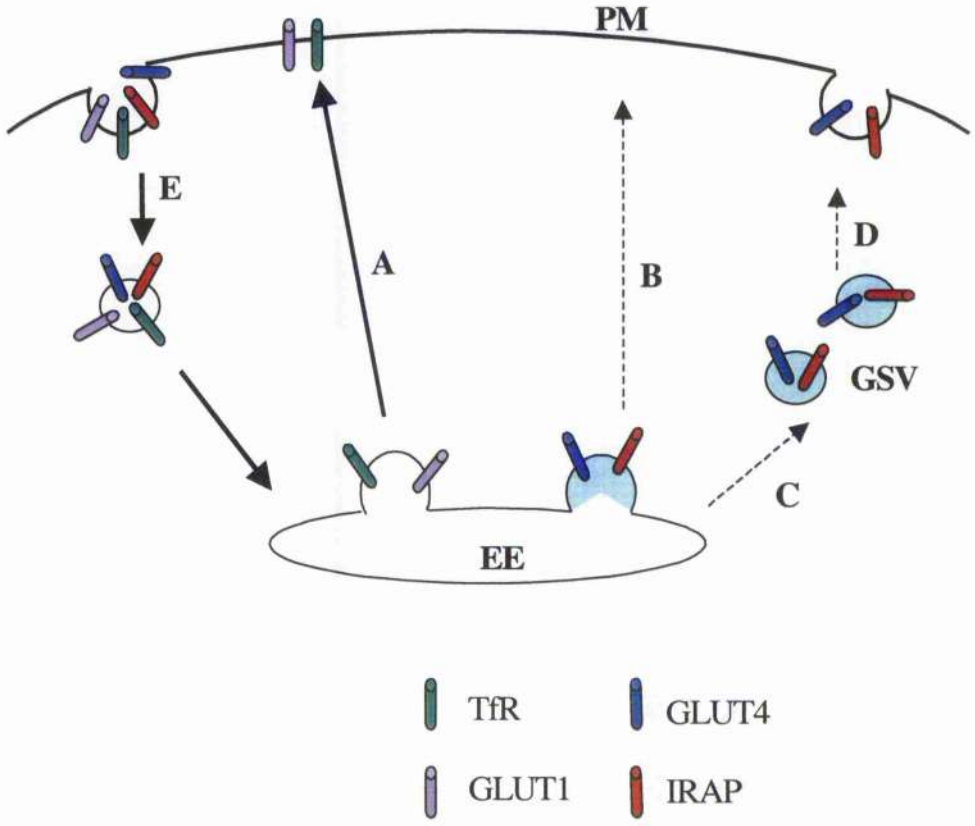

Figure 6.7 A model to describe a possible mode of IRAP trafficking in 3T3-L1 cells during early and late differentiation, under basal state (Adapted from Zeigerer *et al.*, 2002)

Membrane proteins localised into PM are recycled through constitutive recycling pathway (E) into endosomal system. There, the GLUT4 and IRAP are sorted from constitutively recycling proteins such as TfR and GLUT1 to a subdomain of the endosomal system. These sorted GLUT4 and IRAP proteins move into PM by a slow recycling pathway (B) common to differentiated and undifferentiated cells. Proteins such as TfR and GLUT1 recycle back to PM rapidly by a separate recycling pathway (A). At early stages of differentiation (e.g. until day 4) 3T3-L1 cells follow the pathway B to recycle IRAP and exogenous GLUT4 into PM. This slow recycling pathway (B) is more sensitive to insulin compared to that of constitutive pathway (A). IRAP and GLUT4 are sequestered from early endosomal (EE) compartment to specialised insulin-responsive GSV compartment (C) when it forms at a later stage of differentiation (e.g. day 5). GLUT4 and IRAP are slowly moved into PM from GSV (D) a process, which accelerates extensively in response to insulin.

The increased level of STX 6, 8 and 12 distribution in iodixanol gradients observed in this study suggests that these syntaxins have a more functional role upon differentiation. Among these syntaxins, expression of STX 6 and 12 at early differentiation (day 2) was almost negligible. This suggests the possibility that STX 6 and 12 may have a new functional role or a massive increase in their participation in membrane fusion in differentiating 3T3-L1 adipocytes. Iodixanol gradient profiles of STX 6 and 12 show the quantity of these proteins increased extensively from day 4 to day 6 in both peak 1 and 2 of the gradient, which suggests a possible role of STX 6 and 12 in a fusion step prevalent from day 4 to 6. Based on the identification of functional importance of STX 6 in intracellular GLUT4 sorting (Chapter 5), it is possible to speculate that the changes observed in the gradient profile of STX 6 which was similar to that of GLUT4, represents the increase demand for STX 6 for the extensive sorting of GLUT4 into GSV. STX 8 and 12 being endosomal SNAREs, might mediate the trafficking of proteins, which themselves show an increase (e.g. TfR). Appearance of STX 8 in peak 1 which is identified to be representing GSV in mature adipocytes (Hashiramoto and James, 2000; Maier and Gould, 2000) of the iodixanol gradient as early as day 2 of differentiation raises the question whether this compartment is the same GSV compartment where GLUT4 is sequestered or another of similar density.

Conclusions

Conclusions

A major physiological role of insulin is to increase glucose transport into fat and muscle tissues, which is vital for blood glucose homeostasis. This effect is brought about by the movement of an intracellularly localised glucose transporter GLUT4 to the PM. The majority (>90%) of GLUT4 is sequestered intracellularly in the basal state and is localised within small vesicles and tubular vesicular structures clustered around endosomes, the TGN and close to the PM. In addition, GLUT4 is localised to the TGN, early and recycling endosomes (Slot *et al.*, 1991; Gould 1997). Several studies have found evidence to show that the majority of GLUT4 is localised to a specialised storage compartment (GSV), which is highly insulin-responsive (Livingstone *et al.*, 1996; Malide *et al.*, 2000). Even though the process of GLUT4 translocation into the PM of fat and muscle cells is well documented, the molecular mechanisms involved in intracellular trafficking are poorly defined.

Recent studies have identified SNARE proteins, syntaxins, VAMPs and SNAP-25 homologues as central mediators involved in membrane fusion events (Jahn and Sudhof, 1999; Brunger, 2001). Numerous studies have shown that insulin-stimulated GLUT4 trafficking to the PM is mediated by the Q-SNAREs, STX 4 and SNAP-23 and the R-SNARE, VAMP2 (Macaulay *et al.*, 1997; Macaulay *et al.*, 1997; Martin *et al.*, 1998; St Denis *et al.*, 1999). However, the involvement of SNAREs in the intracellular trafficking of GLUT4 has yet to be defined. The aim of this study was to examine the role of post-Golgi syntaxins that are known to localise to the TGN and endosomal membranes, in intracellular GLUT4 trafficking in 3T3-L1 adipocytes.

The work conducted to characterise the post-Golgi syntaxins in 3T3-L1 adipocytes in this study showed extensive colocalisation of STX 6 and STX 16 with GLUT4 vesicles. Furthermore, the data suggested that both of these syntaxins were present in GSV and endosomal/TGN pools separated by iodixanol gradient centrifugation. In contrast, the colocalisation of STX 8 and 12 with GLUT4 vesicles was significantly low. Interestingly, the data also showed that STX 6 and STX 16 translocate to the PM in response to insulin to a similar degree compared to GLUT4, which supports the evidence describing colocalisation with GLUT4. These data provided evidence for the potential involvement of STX 6 and STX 16 in trafficking of GLUT4.

I extended this work to determine the functional role of STX 6, 8 and 12 in 3T3-L1 adipocytes. Since the characterisation of STX 16 was conducted in a later part of the study I was unable to include it for the functional studies even though the findings suggested that STX 16 could be a potential mediator in GLUT4 trafficking. Future studies to characterise the functional role of STX 16 could utilise similar approaches (adenoviral transfection).

In order to study the function of the syntaxins, an approach to over-express their cytosolic domains which could thereby act as inhibitors of the full-length syntaxins has been utilised. This approach has been used effectively in previous studies examining the functional role of STX 4 in GLUT4 trafficking to the PM in response to insulin (Cheatham *et al.*, 1996; Olson *et al.*, 1997; Macaulay *et al.*, 1997). Since standard transfection methods have only a very low efficiency in transferring genes into 3T3-L1 adipocytes, it was decided to produce recombinant AdV, which has been successfully used previously in 3T3-L1 adipocytes to transfer various genes (Sakaue *et al.*, 1997; Emoto *et al.*, 2001; Bose *et al.*, 2001).

The functional data obtained by using AdV to overexpress cytosolic domains of syntaxins provided compelling evidence to suggest that STX 6 is necessary for the sequestration of GLUT4 away from recycling endocytic pathway after insulin withdrawal. Extension of this study further revealed that STX 6 is, in fact, required to sequester GLUT4 to the GSV compartment after insulin withdrawal. In contrast, STX 8 and 12 had no detectable effects on the intracellular sequestration of GLUT4, providing evidence that the role of STX 6 identified in this thesis is specific.

However, expression of STX 6 did not have any effect on insulin-stimulated glucose transport in adipocytes when conducted without prior insulin withdrawal. This finding does not support the requirement of STX 6 in moving GLUT4 to the GSV. To clarify this aspect, it will be necessary to assay glucose transport (in the absence and presence of insulin) carried out at different periods after insulin withdrawal. It is possible that the activity of full-length STX 6 exceeds the competition with its cytosolic domain in making the putative SNARE complex over the time. Future studies utilising other approaches such as the use of anti-syntaxin antibodies or Fab fragments, and post-

transcriptional gene silencing by RNA interference (Elbashir *et al.*, 2001) could be performed to identify the reproducibility of these findings.

In addition to a role for STX 6 in trafficking of GLUT4 to GSV, the findings suggest that STX 6 accumulates in the GSV after the insulin withdrawal, which occurs in parallel with GLUT4. This finding suggests that STX 6 is present in vesicles carrying the GLUT4 to GSV. Similarly, STX 6 has been identified from M6PR and AP-1-positive immature secretory granules of the regulated secretory pathway of exocrine and endocrine pancreatic cells (Klumperman *et al.*, 1998). Therefore, GLUT4 and STX 6 might be incorporated into the vesicles carrying proteins destined for secretion and sorted away from this route to form the GSV prior to the maturation of secretory granules. To further investigate this possibility, immunoelectron microscopic studies would allow the identification of the presence of GLUT4 and STX 6 in immature secretory granules of 3T3-L1 adipocytes. There are supporting evidence for the presence of GLUT4 in immature secretory granules (containing atrial natriuretic factor) in atrial cardiomyocytes (Slot *et al.*, 1997). Furthermore, GLUT4 in adipocytes has been shown to localise with AP-1 positive clathrin-coated vesicles in the vicinity of the TGN (Martin *et al.*, 2000b).

STX 6 is known to mediate homotypic fusion of immature secretory granules in a cell-free fusion assay (Wendler *et al.*, 2001). However, the data described in this thesis, obtained by analysing the proteins secreted into the medium, did not show the involvement of either STX 6, 8 or 12 in the secretion of adipsin or ACRP30 from 3T3-L1 adipocytes, which argues against a role for STX 6 in homotypic fusion of secretory granules in adipocytes. A different approach such as immuno electron microscopy is necessary to investigate this pathway further.

Even though STX 6 has been suggested to act as a promiscuous SNARE (Wendler and Tooze 2001) due to its association with multiple SNARE partners, we could only find a significant association of STX 6 with STX 16 (no association with STX 12, STX 8, VAMP2, VAMP3 and SNAP-23). VAMP4 has been found to associate with STX 6 in rat brain (Steegmaier *et al.*, 1999) and HeLa cells (Mallard *et al.*, 2002) and it could be the R-SNARE of the SNARE complex involved with STX 6 in 3T3-L1 adipocytes. The present work was unable to detect VAMP4 in STX 6 immunoprecipitates due to

lack of good antibodies. Similar to STX 6, VAMP4 has been detected in immature secretory granules and was found to sort away before their maturation (Eaton *et al.*, 2000). Further studies are required to identify the R-SNARE of the STX 6 SNARE complex.

The strong association of STX 16 with STX 6 and the insulin-responsive translocation of STX 6 and 16 to the PM identified in this study suggests that the Qa-SNARE of the SNARE complex involved in this event is STX 16. This association further indicates that STX 16 has a role in GLUT4 trafficking, hence functional studies are essential to clarify this issue. The findings of this study further suggested that STX 16 associated with STX 6 is phosphorylated. The possibility of regulation of STX 16 association with STX 6 by phosphorylation has to be investigated using *in vivo* immunoprecipitation studies.

Furthermore, the association of STX 6 with STX 16 in this study supports the suggestion of Bock and co-workers (2001) that STX 6 acts as a Qc-SNARE instead of Qa-SNARE. In addition, it raises the possibility that four SNARE molecules are involved in this SNARE complex instead of three in neuronal exocytic complexes as identified previously (Antonin *et al.*, 2002; Xu *et al.*, 2000; Fukuda *et al.*, 2000).

The experiments conducted to identify the effects of STX 6, 8 and 12 inhibition on TfR trafficking were largely carried out in HeLa cells. To minimise the requirement for AdV, the use of 3T3-L1 adipocytes for these assays was reduced. However, failure to identify any effect of STX 6, 8 or 12 in these events raised the possibility that rat or mouse syntaxins were ineffective against the human homologues expressed by HeLa cells. Comparison of rat and human STX 8 amino acid sequences revealed that 14 amino acids are different in the N-terminal domain and 3 are different within the SNARE domain. As the human STX 12 sequence is not published, the differences found between mouse and human STX 12 were not determined. However, we are aware that rat STX 6 cytosolic domain interfered with human STX 6 based on its effect on LDL, which indicated a block of early endosome to late endosome trafficking. Supporting the hypothesis that rat/mouse STX 8 and 12 sequences do not interfere with human sequences (from HeLa and HEK cells) is data that comes from the use of anti-STX 8 and anti-STX 12 produced against rat/mouse syntaxin cytosolic domains.

In contrast anti-STX 6 against rat STX 6 cytosolic domain recognised human STX 6. Overlooking these previous findings and the need to use the AdV sparingly may have led me to the use of an inappropriate cultured cell line for the study. Therefore investigation of role of STX 8 and 12 in TfR trafficking is required in 3T3-L1 adipocytes.

STX 6 function in GLUT4 movement to the GSV could occur either in the early endosomes and/or the TGN. This is an area for future investigations, and would provide further evidence for the site of STX 6 action and the potential role of the TGN in GLUT4 trafficking to the GSV. The retention of LDL at a compartment similar to early endosomes in the presence of STX 6 cytosolic domain raises the possibility that STX 6 being mediates early endosome to GSV or early endosome to TGN trafficking. However, the data suggests that STX 6 reaches the GSV in parallel to GLUT4 following insulin withdrawal.

Additionally, I sought to examine the biogenesis of the insulin-sensitive compartment during the differentiation of 3T3-L1 cells to understand whether this compartment is present in early stages of differentiation. Studies conducted previously have provided conflicting results in this regard. The data presented in this study provides evidence to support the presence of an insulin-responsive compartment in 3T3-L1 cells by day 4 of differentiation, which suggests that biogenesis of a compartment similar to the GSV occurs before the expression of detectable levels of GLUT4. However, these results suggested that the insulin-responsive compartment is a subdomain of the endosomal compartment, which sequesters IRAP away from the endosomal recycling pathway, and is not identical to the GSV compartment present in mature adipocytes. Previous studies from our lab suggested that biogenesis of the GSV compartment occurs at the time of detectable GLUT4 expression (day 5). Further studies are needed to characterise this possibility and the post-transcriptional gene silencing by RNA interference (Elbashir *et al.*, 2001) would be an ideal approach.

Furthermore, the expression of STX 6, 8 and 12 during differentiation of 3T3-L1 cells was studied and all three syntaxins showed increased expression towards the latter part of differentiation. Of the syntaxins studied, STX 6 showed a very similar expression pattern to GLUT4 which supports the proposed role of STX 6 in GLUT4 trafficking.

In summary, this study provides the first documented evidence for the involvement of SNAREs in intracellular GLUT4 trafficking. Furthermore, we provide the first functional data on STX 6, 8 and 12 from an insulin-sensitive tissue. Strong evidence from this study suggests that STX 6 function is required for the sequestration of GLUT4 away from the recycling endosomal pathway to the GSV compartment, which is a prerequisite for the ability of GLUT4 to accumulate at the PM in a regulated manner. Furthermore, STX 6 acts as a Qc-SNARE in the 3T3-L1 adipocytes as previously classified (Bock et al., 2001). Based on the role of the highly regulated GLUT4 trafficking pathway and the specific association with SNARE partners, I propose that STX 6 is not a promiscuous SNARE as it has been suggested to be.

References

Advani,R.J., Bae,H.R., Bock,J.B., Chao,D.S., Doung,Y.C., Prekeris,R., Yoo,J.S., Scheller,R.H. (1998). Seven novel mammalian SNARE proteins localize to distinct membrane compartments. J.Biol.Chem. *273*, 10317-10324.

Al Hasani,H., Kunamneni,R.K., Dawson,K., Hinck,C.S., Muller-Wieland,D., Cushman,S.W. (2002). Roles of the N- and C-termini of GLUT4 in endocytosis. J.Cell Sci. *115*, 131-140.

Aledo,J.C., Lavoie,L., Volchuk,A., Keller,S.R., Klip,A., Hundal,H.S. (1997). Identification and characterization of two distinct intracellular GLUT4 pools in rat skeletal muscle: evidence for an endosomal and an insulin- sensitive GLUT4 compartment. Biochem.J. *325 (Pt 3)*, 727-732.

Antonin,W., Fasshauer,D., Becker,S., Jahn,R., Schneider,T.R. (2002). Crystal structure of the endosomal SNARE complex reveals common structural principles of all SNAREs. Nat.Struct.Biol. *9*, 107-111.

Araki,S., Tamori,Y., Kawanishi,M., Shinoda,H., Masugi,J., Mori,H., Niki,T., Okazawa,H., Kubota,T., Kasuga,M. (1997). Inhibition of the binding of SNAP-23 to syntaxin 4 by Munc18c. Biochem.Biophys.Res.Commun. *234*, 257-262.

Asano,T., Takata,K., Katagiri,H., Tsukuda,K., Lin,J.L., Ishihara,H., Inukai,K., Hirano,H., Yazaki,Y., Oka,Y. (1992). Domains responsible for the differential targeting of glucose transporter isoforms. J.Biol.Chem. *267*, 19636-19641.

Barlowe,C. (2000). Traffic COPs of the early secretory pathway. Traffic. *1*, 371-377.

Barr,V.A., Malide,D., Zarnowski,M.J., Taylor,S.I., Cushman,S.W. (1997). Insulin stimulates both leptin secretion and production by rat white adipose tissue. Endocrinology *138*, 4463-4472.

Barrett,M.P., Walmsley,A.R., Gould,G.W. (1999). Structure and function of facilitative sugar transporters. Curr.Opin.Cell Biol. *11*, 496-502.

Becherer,K.A., Rieder,S.E., Emr,S.D., Jones,E.W. (1996). Novel syntaxin homologue, Pep12p, required for the sorting of lumenal hydrolases to the lysosome-like vacuole in yeast. Mol.Biol.Cell *7*, 579-594.

Bell,G.I., Burant,C.F., Takeda,J., Gould,G.W. (1993). Structure and function of mammalian facilitative sugar transporters. J.Biol.Chem. *268*, 19161-19164.

Benihoud,K., Yeh,P., Perricaudet,M. (1999). Adenovirus vectors for gene delivery. Curr.Opin.Biotechnol. *10*, 440-447.

Bennett,M.K., Calakos,N., Scheller,R.H. (1992). Syntaxin: a synaptic protein implicated in docking of synaptic vesicles at presynaptic active zones. Science *257*, 255-259.

Bennett,M.K., Garcia-Arraras,J.E., Elferink,L.A., Peterson,K., Fleming,A.M., Hazuka,C.D., Scheller,R.H. (1993). The syntaxin family of vesicular transport receptors. Cell *74*, 863-873.

Bock,J.B., Klumperman,J., Davanger,S., Scheller,R.H. (1997). Syntaxin 6 functions in trans-Golgi network vesicle trafficking. Mol.Biol.Cell *8*, 1261-1271.

Bock,J.B., Lin,R.C., Scheller,R.H. (1996). A new syntaxin family member implicated in targeting of intracellular transport vesicles. J.Biol.Chem. *271*, 17961-17965.

Bock,J.B., Matern,H.T., Peden,A.A., Scheller,R.H. (2001). A genomic perspective on membrane compartment organization. Nature *409*, 839-841.

Boehm,M., Bonifacino,J.S. (2001). Adaptins: the final recount. Mol.Biol.Cell *12*, 2907-2920.

Boehm,M., Bonifacino,J.S. (2002). Genetic analyses of adaptin function from yeast to mammals. Gene *286*, 175-186.

Bogan,J.S., Lodish,H.F. (1999). Two compartments for insulin-stimulated exocytosis in 3T3-L1 adipocytes defined by endogenous ACRP30 and GLUT4. J.Cell Biol. *146*, 609-620.

Bogan,J.S., McKee,A.E., Lodish,H.F. (2001). Insulin-responsive compartments containing GLUT4 in 3T3-L1 and CHO cells: regulation by amino acid concentrations. Mol.Cell Biol. *21*, 4785-4806.

Bortoluzzi,M.N., Cormont,M., Gautier,N., Van Obberghen,E., Marchand-Brustel,Y. (1996). GTPase activating protein activity for Rab4 is enriched in the plasma membrane of 3T3-L1 adipocytes. Possible involvement in the regulation of Rab4 subcellular localization. Diabetologia *39*, 899-906.

Bos,K., Wraight,C., Stanley,K.K. (1993). TGN38 is maintained in the trans-Golgi network by a tyrosine-containing motif in the cytoplasmic domain. EMBO J. *12*, 2219-2228.

Bose,A., Cherniack,A.D., Langille,S.E., Nicoloro,S.M., Buxton,J.M., Park,J.G., Chawla,A., Czech,M.P. (2001). G(alpha)11 signaling through ARF6 regulates F-actin mobilization and GLUT4 glucose transporter translocation to the plasma membrane. Mol.Cell Biol. *21*, 5262-5275.

Bradford,M.M. (1976). A rapid and sensitive method for the quantitation of microgram quantities of protein utilizing the principle of protein-dye binding. Anal.Biochem. *72*, 248-254.

Brant,A.M., Jess,T.J., Milligan,G., Brown,C.M., Gould,G.W. (1993). Immunological analysis of glucose transporters expressed in different regions of the rat brain and central nervous system. Biochem.Biophys.Res.Commun. *192*, 1297-1302.

Brooks,C.C., Scherer,P.E., Cleveland,K., Whittemore,J.L., Lodish,H.F., Cheatham,B. (2000). Pantophysin is a phosphoprotein component of adipocyte transport vesicles and associates with GLUT4-containing vesicles. J.Biol.Chem. *275*, 2029-2036.

Brown,W.J., DeWald,D.B., Emr,S.D., Plutner,H., Balch,W.E. (1995). Role for phosphatidylinositol 3-kinase in the sorting and transport of newly synthesized lysosomal enzymes in mammalian cells. J.Cell Biol. *130*, 781-796.

Brunger,A.T. (2000). Structural insights into the molecular mechanism of Ca(2+)-dependent exocytosis. Curr.Opin.Neurobiol. *10*, 293-302.

Brunger,A.T. (2001). Structure of proteins involved in synaptic vesicle fusion in neurons. Annu.Rev.Biophys.Biomol.Struct. *30*, 157-171.

Bryant,N.J., Govers,R., James,D.E. (2002). Regulated transport of the glucose transporter GLUT4. Nat.Rev.Mol.Cell Biol. *3*, 267-277.

Cain,C.C., Trimble,W.S., Lienhard,G.E. (1992). Members of the VAMP family of synaptic vesicle proteins are components of glucose transporter-containing vesicles from rat adipocytes. J.Biol.Chem. *267*, 11681-11684.

Calderhead,D.M., Kitagawa,K., Tanner,L.I., Holman,G.D., Lienhard,G.E. (1990). Insulin regulation of the two glucose transporters in 3T3-L1 adipocytes. J.Biol.Chem. *265*, 13801-13808.

Chamberlain,L.H., Graham,M.E., Kane,S., Jackson,J.L., Maier,V.H., Burgoyne,R.D., Gould,G.W. (2001). The synaptic vesicle protein, cysteine-string protein, is associated with the plasma membrane in 3T3-L1 adipocytes and interacts with syntaxin 4. J.Cell Sci. *114*, 445-455.

Charron,M.J., Brosius,F.C., III, Alper,S.L., Lodish,H.F. (1989). A glucose transport protein expressed predominately in insulin- responsive tissues. Proc.Natl.Acad.Sci.U.S.A *86*, 2535-2539.

Cheatham,B. (2000). GLUT4 and company: SNAREing roles in insulin-regulated glucose uptake. Trends Endocrinol.Metab *11*, 356-361.

Cheatham,B., Volchuk,A., Kahn,C.R., Wang,L., Rhodes,C.J., Klip,A. (1996). Insulin-stimulated translocation of GLUT4 glucose transporters requires SNARE-complex proteins. Proc.Natl.Acad.Sci.U.S.A *93*, 15169-15173.

Chen,Y.A., Scheller,R.H. (2001). SNARE-mediated membrane fusion. Nat.Rev.Mol.Cell Biol. *2*, 98-106.

Chung,S.H., Polgar,J., Reed,G.L. (2000). Protein kinase C phosphorylation of syntaxin 4 in thrombin-activated human platelets. J.Biol.Chem. *275*, 25286-25291.

Ciaraldi,T.P., Kolterman,O.G., Scarlett,J.A., Kao,M., Olefsky,J.M. (1982). Role of glucose transport in the postreceptor defect of non-insulin- dependent diabetes mellitus. Diabetes *31*, 1016-1022.

Clary,D.O., Griff,I.C., Rothman,J.E. (1990). SNAPs, a family of NSF attachment proteins involved in intracellular membrane fusion in animals and yeast. Cell *61*, 709-721.

Collier,L., Oxford, J. (2000). Human virology 2nd edition, Oxford University press, Oxford.

Corvera,S., D'Arrigo,A., Stenmark,H. (1999). Phosphoinositides in membrane traffic. Curr.Opin.Cell Biol. *11*, 460-465.

Curiel,D.T., Agarwal,S., Wagner,E., Cotten,M. (1991). Adenovirus enhancement of transferrin-polylysine-mediated gene delivery. Proc.Natl.Acad.Sci.U.S.A *88*, 8850-8854.

Cushman,S.W., Wardzala,L.J. (1980). Potential mechanism of insulin action on glucose transport in the isolated rat adipose cell. Apparent translocation of intracellular transport systems to the plasma membrane. J.Biol.Chem. *255*, 4758-4762.

Czech,M.P., Chawla,A., Woon,C.W., Buxton,J., Armoni,M., Tang,W., Joly,M., Corvera,S. (1993). Exofacial epitope-tagged glucose transporter chimeras reveal COOH- terminal sequences governing cellular localization. J.Cell Biol. *123*, 127-135.

Czech,M.P., Corvera,S. (1999). Signaling mechanisms that regulate glucose transport. J.Biol.Chem. *274*, 1865-1868.

Daro,E., van der,S.P., Galli,T., Mellman,I. (1996). Rab4 and cellubrevin define different early endosome populations on the pathway of transferrin receptor recycling. Proc.Natl.Acad.Sci.U.S.A *93*, 9559-9564.

Darsow,T., Burd,C.G., Emr,S.D. (1998). Acidic di-leucine motif essential for AP-3-dependent sorting and restriction of the functional specificity of the Vam3p vacuolar t-SNARE. J.Cell Biol. *142*, 913-922.

Darsow,T., Rieder,S.E., Emr,S.D. (1997). A multispecificity syntaxin homologue, Vam3p, essential for autophagic and biosynthetic protein transport to the vacuole. J.Cell Biol. *138*, 517-529.

Dascher,C., Matteson,J., Balch,W.E. (1994). Syntaxin 5 regulates endoplasmic reticulum to Golgi transport. J.Biol.Chem. *269*, 29363-29366.

Davidson,H.W. (1995). Wortmannin causes mistargeting of procathepsin D. evidence for the involvement of a phosphatidylinositol 3-kinase in vesicular transport to lysosomes. J.Cell Biol. *130*, 797-805.

Davis,C.G., van Driel,I.R., Russell,D.W., Brown,M.S., Goldstein,J.L. (1987). The low density lipoprotein receptor. Identification of amino acids in cytoplasmic domain required for rapid endocytosis. J.Biol.Chem. *262*, 4075-4082.

de Wit,H., Lichtenstein,Y., Kelly,R.B., Geuze,H.J., Klumperman,J., van der,S.P. (2001). Rab4 regulates formation of synaptic-like microvesicles from early endosomes in PC12 cells. Mol.Biol.Cell *12*, 3703-3715.

Dobson,S.P., Livingstone,C., Gould,G.W., Tavare,J.M. (1996). Dynamics of insulin-stimulated translocation of GLUT4 in single living cells visualised using green fluorescent protein. FEBS Lett. *393*, 179-184.

Dohm,G.L., Tapscott,E.B., Pories,W.J., Dabbs,D.J., Flickinger,E.G., Meelheim,D., Fushiki,T., Atkinson,S.M., Elton,C.W., Caro,J.F. (1988). An in vitro human muscle preparation suitable for metabolic studies. Decreased insulin stimulation of glucose transport in muscle from morbidly obese and diabetic subjects. J.Clin.Invest *82*, 486-494.

Donaldson,J.G., Lippincott-Schwartz,J. (2000). Sorting and signaling at the Golgi complex. Cell *101*, 693-696.

Dresbach,T., Burns,M.E., O'Connor,V., DeBello,W.M., Betz,H., Augustine,G.J. (1998). A neuronal Sec1 homolog regulates neurotransmitter release at the squid giant synapse. J.Neurosci. *18*, 2923-2932.

Eaton,B.A., Haugwitz,M., Lau,D., Moore,H.P. (2000). Biogenesis of regulated exocytotic carriers in neuroendocrine cells. J.Neurosci. *20*, 7334-7344.

Elbashir,S.M., Harborth,J., Lendeckel,W., Yalcin,A., Weber,K., Tuschl,T. (2001). Duplexes of 21-nucleotide RNAs mediate RNA interference in cultured mammalian cells. Nature *411*, 494-498.

El Jack,A.K., Kandror,K.V., Pilch,P.F. (1999). The formation of an insulin-responsive vesicular cargo compartment is an early event in 3T3-L1 adipocyte differentiation. Mol.Biol.Cell *10*, 1581-1594.

Emoto,M., Langille,S.E., Czech,M.P. (2001). A role for kinesin in insulin-stimulated GLUT4 glucose transporter translocation in 3t3-L1 adipocytes. J.Biol.Chem. *276*, 10677-10682.

Fasshauer,D., Otto,H., Eliason,W.K., Jahn,R., Brunger,A.T. (1997). Structural changes are associated with soluble N-ethylmaleimide- sensitive fusion protein attachment protein receptor complex formation. J.Biol.Chem. *272*, 28036-28041.

Fasshauer,D., Sutton,R.B., Brunger,A.T., Jahn,R. (1998). Conserved structural features of the synaptic fusion complex: SNARE proteins reclassified as Q- and R-SNAREs. Proc.Natl.Acad.Sci.U.S.A *95*, 15781-15786.

Ferro-Novick,S., Jahn,R. (1994). Vesicle fusion from yeast to man. Nature *370*, 191-193.

Fiebig,K.M., Rice,L.M., Pollock,E., Brunger,A.T. (1999). Folding intermediates of SNARE complex assembly. Nat.Struct.Biol. *6* , 117-123.

Fleming,K.G., Hohl,T.M., Yu,R.C., Muller,S.A., Wolpensinger,B., Engel,A., Engelhardt,H., Brunger,A.T., Sollner,T.H., Hanson,P.I. (1998). A revised model for the oligomeric state of the N-ethylmaleimide- sensitive fusion protein, NSF. J.Biol.Chem. *273*, 15675-15681.

Foster,L.J., Klip,A. (2000). Mechanism and regulation of GLUT-4 vesicle fusion in muscle and fat cells. Am.J.Physiol Cell Physiol *279*, C877-C890.

Foster,L.J., Weir,M.L., Lim,D.Y., Liu,Z., Trimble,W.S., Klip,A. (2000). A functional role for VAP-33 in insulin-stimulated GLUT4 traffic. Traffic. *1*, 512-521.

Foster,L.J., Yaworsky,K., Trimble,W.S., Klip,A. (1999). SNAP23 promotes insulin-dependent glucose uptake in 3T3-L1 adipocytes: possible interaction with cytoskeleton. Am.J.Physiol *276*, C1108-C1114.

Foster,L.J., Yeung,B., Mohtashami,M., Ross,K., Trimble,W.S., Klip,A. (1998). Binary interactions of the SNARE proteins syntaxin-4, SNAP23, and VAMP- 2 and their regulation by phosphorylation. Biochemistry *37*, 11089-11096.

Fujimoto,W.Y. (2000). The importance of insulin resistance in the pathogenesis of type 2 diabetes mellitus. Am.J.Med. *108 Suppl 6a*, 9S-14S.

Fujita,Y., Sasaki,T., Fukui,K., Kotani,H., Kimura,T., Hata,Y., Sudhof,T.C., Scheller,R.H., Takai,Y. (1996). Phosphorylation of Munc-18/n-Sec1/rbSec1 by protein kinase C: its implication in regulating the interaction of Munc-18/n-Sec1/rbSec1 with syntaxin. J.Biol.Chem. *271*, 7265-7268.

Fukuda,M. (1991). Lysosomal membrane glycoproteins. Structure, biosynthesis, and intracellular trafficking. J.Biol.Chem. *266* , 21327-21330.

Fukuda,R., McNew,J.A., Weber,T., Parlati,F., Engel,T., Nickel,W., Rothman,J.E., Sollner,T.H. (2000). Functional architecture of an intracellular membrane t-SNARE. Nature *407*, 198-202.

Garcia,d.H., Birnbaum,M.J. (1989). The acquisition of increased insulin-responsive hexose transport in 3T3- L1 adipocytes correlates with expression of a novel transporter gene. J.Biol.Chem. *264*, 19994-19999.

Garippa,R.J., Johnson,A., Park,J., Petrush,R.L., McGraw,T.E. (1996). The carboxyl terminus of GLUT4 contains a serine-leucine-leucine sequence that functions as a potent internalization motif in Chinese hamster ovary cells. J.Biol.Chem. *271*, 20660-20668.

Garippa,R.J., Judge,T.W., James,D.E., McGraw,T.E. (1994). The amino terminus of GLUT4 functions as an internalization motif but not an intracellular retention signal when substituted for the transferrin receptor cytoplasmic domain. J.Cell Biol. *124*, 705-715.

Garvey,W.T., Huecksteadt,T.P., Matthaei,S., Olefsky,J.M. (1988). Role of glucose transporters in the cellular insulin resistance of type II non-insulin-dependent diabetes mellitus. J.Clin.Invest *81*, 1528-1536.

Garvey,W.T., Maianu,L., Hancock,J.A., Golichowski,A.M., Baron,A. (1992). Gene expression of GLUT4 in skeletal muscle from insulin-resistant patients with obesity, IGT, GDM, and NIDDM. Diabetes *41*, 465-475.

Garvey,W.T., Maianu,L., Huecksteadt,T.P., Birnbaum,M.J., Molina,J.M., Ciaraldi,T.P. (1991). Pretranslational suppression of a glucose transporter protein causes insulin resistance in adipocytes from patients with non-insulin- dependent diabetes mellitus and obesity. J.Clin.Invest *87*, 1072-1081.

Garvey,W.T., Maianu,L., Zhu,J.H., Brechtel-Hook,G., Wallace,P., Baron,A.D. (1998). Evidence for defects in the trafficking and translocation of GLUT4 glucose

transporters in skeletal muscle as a cause of human insulin resistance. J.Clin.Invest *101*, 2377-2386.

Garza,L.A., Birnbaum,M.J. (2000). Insulin-responsive aminopeptidase trafficking in 3T3-L1 adipocytes. J.Biol.Chem. *275*, 2560-2567.

Gerst,J.E. (1999). SNAREs and SNARE regulators in membrane fusion and exocytosis. Cell Mol.Life Sci. *55*, 707-734.

Gibbs,E.M., Allard,W.J., Lienhard,G.E. (1986). The glucose transporter in 3T3-L1 adipocytes is phosphorylated in response to phorbol ester but not in response to insulin. J.Biol.Chem. *261*, 16597-16603.

Gnudi,L., Frevert,E.U., Houseknecht,K.L., Erhardt,P., Kahn,B.B. (1997). Adenovirus-mediated gene transfer of dominant negative ras(asn17) in 3T3L1 adipocytes does not alter insulin-stimulated P13-kinase activity or glucose transport. Mol.Endocrinol. *11*, 67-76.

Goodyear,L.J., Giorgino,F., Sherman,L.A., Carey,J., Smith,R.J., Dohm,G.L. (1995). Insulin receptor phosphorylation, insulin receptor substrate-1 phosphorylation, and phosphatidylinositol 3-kinase activity are decreased in intact skeletal muscle strips from obese subjects. J.Clin.Invest *95*, 2195-2204.

Gotte,M., von Mollard,G.F. (1998). A new beat for the SNARE drum. Trends Cell Biol. *8*, 215-218.

Gould, G.W. (1997). Facilitative glucose transporters. R.G. Landes Company Austin, Texas, U.S.A.

Gould,G.W., Holman,G.D. (1993). The glucose transporter family: structure, function and tissue-specific expression. Biochem.J. *295 (Pt 2)*, 329-341.

Graham,F.L., Smiley,J., Russell,W.C., Nairn,R. (1977). Characteristics of a human cell line transformed by DNA from human adenovirus type 5. J.Gen.Virol. *36*, 59-74.

Green,H., Kehinde,O. (1975). An established preadipose cell line and its differentiation in culture. II. Factors affecting the adipose conversion. Cell *5*, 19-27.

Gregoire,F.M., Smas,C.M., Sul,H.S. (1998). Understanding adipocyte differentiation. Physiol Rev. *78*, 783-809.

Grote,E., Baba,M., Ohsumi,Y., Novick,P.J. (2000). Geranylgeranylated SNAREs are dominant inhibitors of membrane fusion. J.Cell Biol. *151*, 453-466.

Gruenberg,J., Maxfield,F.R. (1995). Membrane transport in the endocytic pathway. Curr.Opin.Cell Biol. *7*, 552-563.

Gurunathan,S., Marash,M., Weinberger,A., Gerst,J.E. (2002). t-SNARE Phosphorylation Regulates Endocytosis in Yeast. Mol.Biol.Cell *13*, 1594-1607.

Haney,P.M., Slot,J.W., Piper,R.C., James,D.E., Mueckler,M. (1991). Intracellular targeting of the insulin-regulatable glucose transporter (GLUT4) is isoform specific and independent of cell type. J.Cell Biol. *114*, 689-699.

Hashiramoto,M., James,D.E. (2000). Characterization of insulin-responsive GLUT4 storage vesicles isolated from 3T3-L1 adipocytes. Mol.Cell Biol. *20*, 416-427.

Hatsuzawa,K., Hirose,H., Tani,K., Yamamoto,A., Scheller,R.H., Tagaya,M. (2000). Syntaxin 18, a SNAP receptor that functions in the endoplasmic reticulum, intermediate compartment, and cis-Golgi vesicle trafficking. J.Biol.Chem. *275*, 13713-13720.

Hay,J.C. (2001). SNARE complex structure and function. Exp.Cell Res. *271*, 10-21.

Hay,J.C., Scheller,R.H. (1997). SNAREs and NSF in targeted membrane fusion. Curr.Opin.Cell Biol. *9*, 505-512.

Hayashi,T., McMahon,H., Yamasaki,S., Binz,T., Hata,Y., Sudhof,T.C., Niemann,H. (1994). Synaptic vesicle membrane fusion complex: action of clostridial neurotoxins on assembly. EMBO J. *13*, 5051-5061.

Hayashi,T., Yamasaki,S., Nauenburg,S., Binz,T., Niemann,H. (1995). Disassembly of the reconstituted synaptic vesicle membrane fusion complex in vitro. EMBO J. *14*, 2317-2325.

He,T.C., Zhou,S., da Costa,L.T., Yu,J., Kinzler,K.W., Vogelstein,B. (1998). A simplified system for generating recombinant adenoviruses. Proc.Natl.Acad.Sci.U.S.A *95*, 2509-2514.

Heilker,R., Manning-Krieg,U., Zuber,J.F., Spiess,M. (1996). In vitro binding of clathrin adaptors to sorting signals correlates with endocytosis and basolateral sorting. EMBO J. *15*, 2893-2899.

Herbst,J.J., Ross,S.A., Scott,H.M., Bobin,S.A., Morris,N.J., Lienhard,G.E., Keller,S.R. (1997). Insulin stimulates cell surface aminopeptidase activity toward vasopressin in adipocytes. Am.J.Physiol *272*, E600-E606.

Herman,G.A., Bonzelius,F., Cieutat,A.M., Kelly,R.B. (1994). A distinct class of intracellular storage vesicles, identified by expression of the glucose transporter GLUT4. Proc.Natl.Acad.Sci.U.S.A *91*, 12750-12754.

Hess,D.T., Slater,T.M., Wilson,M.C., Skene,J.H. (1992). The 25 kDa synaptosomal-associated protein SNAP-25 is the major methionine-rich polypeptide in rapid axonal transport and a major substrate for palmitoylation in adult CNS. J.Neurosci. *12*, 4634-4641.

Hirst,J., Bright,N.A., Rous,B., Robinson,M.S. (1999). Characterization of a fourth adaptor-related protein complex. Mol.Biol.Cell *10*, 2787-2802.

Hirst,J., Futter,C.E., Hopkins,C.R. (1998). The kinetics of mannose 6-phosphate receptor trafficking in the endocytic pathway in HEp-2 cells: the receptor enters and

rapidly leaves multivesicular endosomes without accumulating in a prelysosomal compartment. Mol.Biol.Cell *9*, 809-816.

Hitt,M.M., Addison,C.L., Graham,F.L. (1997). Human adenovirus vectors for gene transfer into mammalian cells. Adv.Pharmacol. *40*, 137-206.

Hodel,A. (1998). SNAP-25. Int.J.Biochem.Cell Biol. *30*, 1069-1073.

Holman,G.D., Kasuga,M. (1997). From receptor to transporter: insulin signalling to glucose transport. Diabetologia *40*, 991-1003.

Holman,G.D., Lo,L.L., Cushman,S.W. (1994). Insulin-stimulated GLUT4 glucose transporter recycling. A problem in membrane protein subcellular trafficking through multiple pools. J.Biol.Chem. *269*, 17516-17524.

Holman,G.D., Sandoval,I.V. (2001). Moving the insulin-regulated glucose transporter GLUT4 into and out of storage. Trends Cell Biol. *11*, 173-179.

Hu,E., Liang,P., Spiegelman,B.M. (1996). AdipoQ is a novel adipose-specific gene dysregulated in obesity. J.Biol.Chem. *271*, 10697-10703.

Hudson,A.W., Ruiz,M., Birnbaum,M.J. (1992). Isoform-specific subcellular targeting of glucose transporters in mouse fibroblasts. J.Cell Biol. *116*, 785-797.

Huizing,M., Sarangarajan,R., Strovel,E., Zhao,Y., Gahl,W.A., Boissy,R.E. (2001). AP-3 mediates tyrosinase but not TRP-1 trafficking in human melanocytes. Mol.Biol.Cell *12*, 2075-2085.

Humphrey,J.S., Peters,P.J., Yuan,L.C., Bonifacino,J.S. (1993). Localization of TGN38 to the trans-Golgi network: involvement of a cytoplasmic tyrosine-containing sequence. J.Cell Biol. *120*, 1123-1135.

Hunziker,W., Fumey,C. (1994). A di-leucine motif mediates endocytosis and basolateral sorting of macrophage IgG Fc receptors in MDCK cells. EMBO J. *13*, 2963-2967.

Huppertz,C., Fischer,B.M., Kim,Y.B., Kotani,K., Vidal-Puig,A., Slicker,L.J., Sloop,K.W., Lowell,B.B., Kahn,B.B. (2001). Uncoupling protein 3 (UCP3) stimulates glucose uptake in muscle cells through a phosphoinositide 3-kinase-dependent mechanism. J.Biol.Chem. *276*, 12520-12529.

Inoue,A., Obata,K., Akagawa,K. (1992). Cloning and sequence analysis of cDNA for a neuronal cell membrane antigen, HPC-1. J.Biol.Chem. *267*, 10613-10619.

Ishii,K., Hayashi,H., Todaka,M., Kamohara,S., Kanai,F., Jinnouchi,H., Wang,L., Ebina,Y. (1995). Possible domains responsible for intracellular targeting and insulin-dependent translocation of glucose transporter type 4. Biochem.J. *309 (Pt 3)*, 813-823.

Jahn,R., Niemann,H. (1994). Molecular mechanisms of clostridial neurotoxins. Ann.N.Y.Acad.Sci. *733*, 245-255.

Jahn,R., Sudhof,T.C. (1999). Membrane fusion and exocytosis. Annu.Rev.Biochem. *68*, 863-911.

James,D.E., Strube,M., Mueckler,M. (1989). Molecular cloning and characterization of an insulin-regulatable glucose transporter. Nature *338*, 83-87.

Jing,S.Q., Spencer,T., Miller,K., Hopkins,C., Trowbridge,I.S. (1990). Role of the human transferrin receptor cytoplasmic domain in endocytosis: localization of a specific signal sequence for internalization. J.Cell Biol. *110*, 283-294.

Joost,H.G., Bell,G.I., Best,J.D., Birnbaum,M.J., Charron,M.J., Chen,Y.T., Doege,H., James,D.E., Lodish,H.F., Moley,K.H., Moley,J.F., Mueckler,M., Rogers,S., Schurmann,A., Seino,S., Thorens,B. (2002). Nomenclature of the GLUT/SLC2A family of sugar/polyol transport facilitators. Am.J.Physiol Endocrinol.Metab *282*, E974-E976.

Kaestner,K.H., Christy,R.J., McLenithan,J.C., Braiterman,L.T., Cornelius,P., Pekala,P.H., Lane,M.D. (1989). Sequence, tissue distribution, and differential expression of mRNA for a putative insulin-responsive glucose transporter in mouse 3T3-L1 adipocytes. Proc.Natl.Acad.Sci.U.S.A *86* , 3150-3154.

Kanai,F., Nishioka,Y., Hayashi,H., Kamohara,S., Todaka,M., Ebina,Y. (1993). Direct demonstration of insulin-induced GLUT4 translocation to the surface of intact cells by insertion of a c-myc epitope into an exofacial GLUT4 domain. J.Biol.Chem. *268*, 14523-14526.

Kandror,K.V. (1999). Insulin regulation of protein traffic in rat adipose cells. J.Biol.Chem. *274*, 25210-25217.

Kandror,K.V., Pilch,P.F. (1994). gp160, a tissue-specific marker for insulin-activated glucose transport. Proc.Natl.Acad.Sci.U.S.A *91*, 8017-8021.

Kasai,K., Akagawa,K. (2001). Roles of the cytoplasmic and transmembrane domains of syntaxins in intracellular localization and trafficking. J.Cell Sci. *114*, 3115-3124.

Kawanishi,M., Tamori,Y., Okazawa,H., Araki,S., Shinoda,H., Kasuga,M. (2000). Role of SNAP23 in insulin-induced translocation of GLUT4 in 3T3-L1 adipocytes. Mediation of complex formation between syntaxin4 and VAMP2. J.Biol.Chem. *275*, 8240-8247.

Keller,P., Simons,K. (1997). Post-Golgi biosynthetic trafficking. J.Cell Sci. *110 (Pt 24)*, 3001-3009.

Keller,S.R., Scott,H.M., Mastick,C.C., Aebersold,R., Lienhard,G.E. (1995). Cloning and characterization of a novel insulin-regulated membrane aminopeptidase from Glut4 vesicles. J.Biol.Chem. *270*, 23612-23618.

Kelley,D.E., Mintun,M.A., Watkins,S.C., Simoneau,J.A., Jadali,F., Fredrickson,A., Beattie,J., Theriault,R. (1996). The effect of non-insulin-dependent diabetes mellitus and obesity on glucose transport and phosphorylation in skeletal muscle. J.Clin.Invest *97*, 2705-2713.

Khan,A.H., Thurmond,D.C., Yang,C., Ceresa,B.P., Sigmund,C.D., Pessin,J.E. (2001). Munc18c regulates insulin-stimulated glut4 translocation to the transverse tubules in skeletal muscle. J.Biol.Chem. *276*, 4063-4069.

King,P.A., Horton,E.D., Hirshman,M.F., Horton,E.S. (1992). Insulin resistance in obese Zucker rat (fa/fa) skeletal muscle is associated with a failure of glucose transporter translocation. J.Clin.Invest *90*, 1568-1575.

Kirchhausen,T. (2000). Clathrin. Annu.Rev.Biochem. *69*, 699-727.

Kirchhausen,T. (2002). Clathrin adaptors really adapt. Cell *109*, 413-416.

Kitagawa,K., Rosen,B.S., Spiegelman,B.M., Lienhard,G.E., Tanner,L.I. (1989). Insulin stimulates the acute release of adipsin from 3T3-L1 adipocytes. Biochim.Biophys.Acta *1014*, 83-89.

Klip,A., Ramlal,T., Bilan,P.J., Cartee,G.D., Gulve,E.A., Holloszy,J.O. (1990). Recruitment of GLUT-4 glucose transporters by insulin in diabetic rat skeletal muscle. Biochem.Biophys.Res.Commun. *172*, 728-736.

Klumperman,J., Kuliawat,R., Griffith,J.M., Geuze,H.J., Arvan,P. (1998). Mannose 6-phosphate receptors are sorted from immature secretory granules via adaptor protein AP-1, clathrin, and syntaxin 6-positive vesicles. J.Cell Biol. *141*, 359-371.

Kovesdi,I., Brough,D.E., Bruder,J.T., Wickham,T.J. (1997). Adenoviral vectors for gene transfer. Curr.Opin.Biotechnol. *8*, 583-589.

Lachaal,M., Rampal,A.L., Lee,W., Shi,Y., Jung,C.Y. (1996). GLUT1 transmembrane glucose pathway. Affinity labeling with a transportable D-glucose diazirine. J.Biol.Chem. *271*, 5225-5230.

Lampson,M.A., Racz,A., Cushman,S.W., McGraw,T.E. (2000). Demonstration of insulin-responsive trafficking of GLUT4 and vpTR in fibroblasts. J.Cell Sci. *113 (Pt 22)*, 4065-4076.

Lemmon,S.K. (2001). Clathrin uncoating: Auxilin comes to life. Curr.Biol. *11*, R49-R52.

Lemmon,S.K., Traub,L.M. (2000). Sorting in the endosomal system in yeast and animal cells. Curr.Opin.Cell Biol. *12*, 457-466.

Letourneur,F., Klausner,R.D. (1992). A novel di-leucine motif and a tyrosine-based motif independently mediate lysosomal targeting and endocytosis of CD3 chains. Cell *69*, 1143-1157.

Lin,R.C., Scheller,R.H. (2000). Mechanisms of synaptic vesicle exocytosis. Annu.Rev.Cell Dev.Biol. *16*, 19-49.

Livingstone,C., James,D.E., Rice,J.E., Hanpeter,D., Gould,G.W. (1996). Compartment ablation analysis of the insulin-responsive glucose transporter (GLUT4) in 3T3-L1 adipocytes. Biochem.J. *315 (Pt 2)*, 487-495.

Lodish,H., Berk,A., Zipursky,L., Baltimore,D., Darnell,J. (1999). Molecular Cell Biology 4th edition, Freeman and Company, New York.

Luzio,J.P., Mullock,B.M., Pryor,P.R., Lindsay,M.R., James,D.E., Piper,R.C. (2001). Relationship between endosomes and lysosomes. Biochem.Soc.Trans. *29*, 476-480.

Macaulay,S., Grusovin,J., Stoichevska,V., Ryan,J., Castelli,L., Ward,C. (2002). Cellular munc18c levels can modulate glucose transport rate and GLUT4 translocation in 3T3L1 cells. FEBS Lett. *528*, 154.

Macaulay,S.L., Hewish,D.R., Gough,K.H., Stoichevska,V., MacPherson,S.F., Jagadish,M., Ward,C.W. (1997). Functional studies in 3T3L1 cells support a role for SNARE proteins in insulin stimulation of GLUT4 translocation. Biochem.J. *324 (Pt 1)*, 217-224.

Maianu,L., Keller,S.R., Garvey,W.T. (2001). Adipocytes exhibit abnormal subcellular distribution and translocation of vesicles containing glucose transporter 4 and insulin-regulated aminopeptidase in type 2 diabetes mellitus: implications regarding defects in vesicle trafficking. J.Clin.Endocrinol.Metab *86*, 5450-5456.

Maier,V.H., Gould,G.W. (2000). Long-term insulin treatment of 3T3-L1 adipocytes results in mis- targeting of GLUT4: implications for insulin-stimulated glucose transport. Diabetologia *43*, 1273-1281.

Malide,D., Ramm,G., Cushman,S.W., Slot,J.W. (2000). Immunoelectron microscopic evidence that GLUT4 translocation explains the stimulation of glucose transport in isolated rat white adipose cells. J.Cell Sci. *113 Pt 23*, 4203-4210.

Malide,D., St Denis,J.F., Keller,S.R., Cushman,S.W. (1997). Vp165 and GLUT4 share similar vesicle pools along their trafficking pathways in rat adipose cells. FEBS Lett. *409*, 461-468.

Mallard,F., Tang,B.L., Galli,T., Tenza,D., Saint-Pol,A., Yue,X., Antony,C., Hong,W., Goud,B., Johannes,L. (2002). Early/recycling endosomes-to-TGN transport involves two SNARE complexes and a Rab6 isoform. J.Cell Biol. *156*, 653-664.

Martin,L.B., Shewan,A., Millar,C.A., Gould,G.W., James,D.E. (1998). Vesicle-associated membrane protein 2 plays a specific role in the insulin-dependent trafficking of the facilitative glucose transporter GLUT4 in 3T3-L1 adipocytes. J.Biol.Chem. *273*, 1444-1452.

Martin,S., Millar,C.A., Lyttle,C.T., Meerloo,T., Marsh,B.J., Gould,G.W., James,D.E. (2000a). Effects of insulin on intracellular GLUT4 vesicles in adipocytes: evidence for a secretory mode of regulation. J.Cell Sci. *113 Pt 19*, 3427-3438.

Martin,S., Ramm,G., Lyttle,C.T., Meerloo,T., Stoorvogel,W., James,D.E. (2000b). Biogenesis of insulin-responsive GLUT4 vesicles is independent of brefeldin A-sensitive trafficking. Traffic. *1*, 652-660.

Martin,S., Reaves,B., Banting,G., Gould,G.W. (1994). Analysis of the co-localization of the insulin-responsive glucose transporter (GLUT4) and the trans Golgi network marker TGN38 within 3T3- L1 adipocytes. Biochem.J. *300 (Pt 3)*, 743-749.

Martin,S., Rice,J.E., Gould,G.W., Keller,S.R., Slot,J.W., James,D.E. (1997). The glucose transporter GLUT4 and the aminopeptidase vp165 colocalise in tubulo-vesicular elements in adipocytes and cardiomyocytes. J.Cell Sci. *110 (Pt 18)*, 2281-2291.

Martin,S., Tellam,J., Livingstone,C., Slot,J.W., Gould,G.W., James,D.E. (1996). The glucose transporter (GLUT-4) and vesicle-associated membrane protein-2 (VAMP-2) are segregated from recycling endosomes in insulin- sensitive cells. J.Cell Biol. *134*, 625-635.

Martinez-Arca,S., Lalioti,V.S., Sandoval,I.V. (2000). Intracellular targeting and retention of the glucose transporter GLUT4 by the perinuclear storage compartment involves distinct carboxyl-tail motifs. J.Cell Sci. *113 (Pt 10)*, 1705-1715.

Martin-Martin,B., Nabokina,S.M., Blasi,J., Lazo,P.A., Mollinedo,F. (2000). Involvement of SNAP-23 and syntaxin 6 in human neutrophil exocytosis. Blood *96*, 2574-2583.

Matsuoka,K., Morimitsu,Y., Uchida,K., Schekman,R. (1998). Coat assembly directs v-SNARE concentration into synthetic COPII vesicles. Mol.Cell *2*, 703-708.

Mayor,S., Presley,J.F., Maxfield,F.R. (1993). Sorting of membrane components from endosomes and subsequent recycling to the cell surface occurs by a bulk flow process. J.Cell Biol. *121*, 1257-1269.

McMahon,H.T., Ushkaryov,Y.A., Edelmann,L., Link,E., Binz,T., Niemann,H., Jahn,R., Sudhof,T.C. (1993). Cellubrevin is a ubiquitous tetanus-toxin substrate homologous to a putative synaptic vesicle fusion protein. Nature *364*, 346-349.

McNew,J.A., Parlati,F., Fukuda,R., Johnston,R.J., Paz,K., Paumet,F., Sollner,T.H., Rothman,J.E. (2000). Compartmental specificity of cellular membrane fusion encoded in SNARE proteins. Nature *407*, 153-159.

McNew,J.A., Sogaard,M., Lampen,N.M., Machida,S., Ye,R.R., Lacomis,L., Tempst,P., Rothman,J.E., Sollner,T.H. (1997). Ykt6p, a prenylated SNARE essential for endoplasmic reticulum-Golgi transport. J.Biol.Chem. *272*, 17776-17783.

Mellman,I. (1996). Endocytosis and molecular sorting. Annu.Rev.Cell Dev.Biol. *12*, 575-625.

Melvin,D.R., Marsh,B.J., Walmsley,A.R., James,D.E., Gould,G.W. (1999). Analysis of amino and carboxy terminal GLUT-4 targeting motifs in 3T3- L1 adipocytes using an endosomal ablation technique. Biochemistry *38*, 1456-1462.

Millar,C.A., Meerloo,T., Martin,S., Hickson,G.R., Shimwell,N.J., Wakelam,M.J., James,D.E., Gould,G.W. (2000). Adipsin and the glucose transporter GLUT4 traffic to the cell surface via independent pathways in adipocytes. Traffic. *1*, 141-151.

Millar,C.A., Shewan,A., Hickson,G.R., James,D.E., Gould,G.W. (1999). Differential regulation of secretory compartments containing the insulin-responsive glucose transporter 4 in 3T3-L1 adipocytes. Mol.Biol.Cell *10*, 3675-3688.

Min,J., Okada,S., Kanzaki,M., Elmendorf,J.S., Coker,K.J., Ceresa,B.P., Syu,L.J., Noda,Y., Saltiel,A.R., Pessin,J.E. (1999). Synip: a novel insulin-regulated syntaxin 4-binding protein mediating GLUT4 translocation in adipocytes. Mol.Cell *3*, 751-760.

Misura,K.M., Scheller,R.H., Weis,W.I. (2000). Three-dimensional structure of the neuronal-Sec1-syntaxin 1a complex. Nature *404*, 355-362.

Miyake,S., Makimura,M., Kanegae,Y., Harada,S., Sato,Y., Takamori,K., Tokuda,C., Saito,I. (1996). Efficient generation of recombinant adenoviruses using adenovirus DNA- terminal protein complex and a cosmid bearing the full-length virus genome. Proc.Natl.Acad.Sci.U.S.A *93*, 1320-1324.

Morris,N.J., Ducret,A., Aebersold,R., Ross,S.A., Keller,S.R., Lienhard,G.E. (1997). Membrane amine oxidase cloning and identification as a major protein in the adipocyte plasma membrane. J.Biol.Chem. *272*, 9388-9392.

Mukherjee,S., Ghosh,R.N., Maxfield,F.R. (1997). Endocytosis. Physiol Rev. *77*, 759-803.

Nelson,B.A., Robinson,K.A., Buse,M.G. (2002). Insulin acutely regulates Munc18-c subcellular trafficking: altered response in insulin-resistant 3T3-L1 adipocytes. J.Biol.Chem. *277*, 3809-3812.

Nicklin SA, Baker AH. (1999). Simple methods for preparing recombinant adenoviruses for high efficiency transduction of vascular cells.In: Baker AH, ed. Vascular Disease: Molecular Biology and Gene Transfer Protocols (Methods in Molecular Medicine). Humana Press, New York.

Novick,P., Zerial,M. (1997). The diversity of Rab proteins in vesicle transport. Curr.Opin.Cell Biol. *9*, 496-504.

Olson,A.L., Knight,J.B., Pessin,J.E. (1997). Syntaxin 4, VAMP2, and/or VAMP3/cellubrevin are functional target membrane and vesicle SNAP receptors for insulin-stimulated GLUT4 translocation in adipocytes. Mol.Cell Biol. *17*, 2425-2435.

Oyler,G.A., Higgins,G.A., Hart,R.A., Battenberg,E., Billingsley,M., Bloom,F.E., Wilson,M.C. (1989). The identification of a novel synaptosomal-associated protein, SNAP-25, differentially expressed by neuronal subpopulations. J.Cell Biol. *109*, 3039-3052.

Paek,I., Orci,L., Ravazzola,M., Erdjument-Bromage,H., Amherdt,M., Tempst,P., Sollner,T.H., Rothman,J.E. (1997). ERS-24, a mammalian v-SNARE implicated in vesicle traffic between the ER and the Golgi. J.Cell Biol. *137*, 1017-1028.

Palacios,S., Lalioti,V., Martinez-Arca,S., Chattopadhyay,S., Sandoval,I.V. (2001). Recycling of the insulin-sensitive glucose transporter GLUT4. Access of surface internalized GLUT4 molecules to the perinuclear storage compartment is mediated by the Phe5-Gln6-Gln7-Ile8 motif. J.Biol.Chem. *276*, 3371-3383.

Peake,P.W., O'Grady,S., Pussell,B.A., Charlesworth,J.A. (1997). Detection and quantification of the control proteins of the alternative pathway of complement in 3T3-L1 adipocytes. Eur.J.Clin.Invest *27*, 922-927.

Pedersen,O., Bak,J.F., Andersen,P.H., Lund,S., Moller,D.E., Flier,J.S., Kahn,B.B. (1990). Evidence against altered expression of GLUT1 or GLUT4 in skeletal muscle of patients with obesity or NIDDM. Diabetes *39*, 865-870.

Pessin,J.E., Saltiel,A.R. (2000). Signaling pathways in insulin action: molecular targets of insulin resistance. J.Clin.Invest *106*, 165-169.

Pessin,J.E., Thurmond,D.C., Elmendorf,J.S., Coker,K.J., Okada,S. (1999). Molecular basis of insulin-stimulated GLUT4 vesicle trafficking. Location! Location! Location! J.Biol.Chem. *274*, 2593-2596.

Pevsner,J., Hsu,S.C., Scheller,R.H. (1994). n-Sec1: a neural-specific syntaxin-binding protein. Proc.Natl.Acad.Sci.U.S.A *91*, 1445-1449.

Piper,R.C., Tai,C., Kulesza,P., Pang,S., Warnock,D., Baenziger,J., Slot,J.W., Geuze,H.J., Puri,C., James,D.E. (1993). GLUT-4 NH2 terminus contains a phenylalanine-based targeting motif that regulates intracellular sequestration. J.Cell Biol. *121*, 1221-1232.

Piper,R.C., Tai,C., Slot,J.W., Hahn,C.S., Rice,C.M., Huang,H., James,D.E. (1992). The efficient intracellular sequestration of the insulin-regulatable glucose transporter (GLUT-4) is conferred by the NH2 terminus. J.Cell Biol. *117*, 729-743.

Ploug,T., van Deurs,B., Ai,H., Cushman,S.W., Ralston,E. (1998). Analysis of GLUT4 distribution in whole skeletal muscle fibers: identification of distinct storage compartments that are recruited by insulin and muscle contractions. J.Cell Biol. *142*, 1429-1446.

Poirier,M.A., Hao,J.C., Malkus,P.N., Chan,C., Moore,M.F., King,D.S., Bennett,M.K. (1998). Protease resistance of syntaxin.SNAP-25.VAMP complexes. Implications for assembly and structure. J.Biol.Chem. *273*, 11370-11377.

Prekeris,R., Foletti,D.L., Scheller,R.H. (1999a). Dynamics of tubulovesicular recycling endosomes in hippocampal neurons. J.Neurosci. *19*, 10324-10337.

Prekeris,R., Klumperman,J., Chen,Y.A., Scheller,R.H. (1998). Syntaxin 13 mediates cycling of plasma membrane proteins via tubulovesicular recycling endosomes. J.Cell Biol. *143*, 957-971.

Prekeris,R., Yang,B., Oorschot,V., Klumperman,J., Scheller,R.H. (1999b). Differential roles of syntaxin 7 and syntaxin 8 in endosomal trafficking. Mol.Biol.Cell *10*, 3891-3908.

Ramm,G., Slot,J.W., James,D.E., Stoorvogel,W. (2000). Insulin recruits GLUT4 from specialized VAMP2-carrying vesicles as well as from the dynamic endosomal/trans-Golgi network in rat adipocytes. Mol.Biol.Cell *11*, 4079-4091.

Rea,S., James,D.E. (1997). Moving GLUT4: the biogenesis and trafficking of GLUT4 storage vesicles. Diabetes *46*, 1667-1677.

Rea,S., Martin,L.B., McIntosh,S., Macaulay,S.L., Ramsdale,T., Baldini,G., James,D.E. (1998). Syndet, an adipocyte target SNARE involved in the insulin-induced translocation of GLUT4 to the cell surface. J.Biol.Chem. *273*, 18784-18792.

Reaven,G.M. (1995). Pathophysiology of insulin resistance in human disease. Physiol Rev. *75*, 473-486.

Reed,B.C., Kaufmann,S.H., Mackall,J.C., Student,A.K., Lane,M.D. (1977). Alterations in insulin binding accompanying differentiation of 3T3-L1 preadipocytes. Proc.Natl.Acad.Sci.U.S.A *74*, 4876-4880.

Rice,K.M., Garner,C.W. (1994). Correlation of the insulin receptor substrate-1 with insulin-responsive deoxyglucose transport in 3T3-L1 adipocytes. Biochem.Biophys.Res.Commun. *198*, 523-530.

Risinger,C., Bennett,M.K. (1999). Differential phosphorylation of syntaxin and synaptosome-associated protein of 25 kDa (SNAP-25) isoforms. J.Neurochem. *72*, 614-624.

Robinson,M.S., Bonifacino,J.S. (2001). Adaptor-related proteins. Curr.Opin.Cell Biol. *13*, 444-453.

Robinson,M.S., Watts,C., Zerial,M. (1996). Membrane dynamics in endocytosis. Cell *84*, 13-21.

Rodnick,K.J., Slot,J.W., Studelska,D.R., Hanpeter,D.E., Robinson,L.J., Geuze,H.J., James,D.E. (1992). Immunocytochemical and biochemical studies of GLUT4 in rat skeletal muscle. J.Biol.Chem. *267*, 6278-6285.

Rogers,S., Pfuderer,P. (1968). Use of viruses as carriers of added genetic information. Nature *219*, 749-751.

Roh,C., Roduit,R., Thorens,B., Fried,S., Kandror,K.V. (2001). Lipoprotein lipase and leptin are accumulated in different secretory compartments in rat adipocytes. J.Biol.Chem. *276*, 35990-35994.

Roh,C., Thoidis,G., Farmer,S.R., Kandror,K.V. (2000). Identification and characterization of leptin-containing intracellular compartment in rat adipose cells. Am.J.Physiol Endocrinol.Metab *279*, E893-E899.

Rosen,B.S., Cook,K.S., Yaglom,J., Groves,D.L., Volanakis,J.E., Damm,D., White,T., Spiegelman,B.M. (1989). Adipsin and complement factor D activity: an immune-related defect in obesity. Science *244*, 1483-1487.

Ross,S.A., Herbst,J.J., Keller,S.R., Lienhard,G.E. (1997). Trafficking kinetics of the insulin-regulated membrane aminopeptidase in 3T3-L1 adipocytes. Biochem.Biophys.Res.Commun. *239*, 247-251.

Ross,S.A., Keller,S.R., Lienhard,G.E. (1998). Increased intracellular sequestration of the insulin-regulated aminopeptidase upon differentiation of 3T3-L1 cells. Biochem.J. *330 (Pt 2)*, 1003-1008.

Ross,S.A., Scott,H.M., Morris,N.J., Leung,W.Y., Mao,F., Lienhard,G.E., Keller,S.R. (1996). Characterization of the insulin-regulated membrane aminopeptidase in 3T3-L1 adipocytes. J.Biol.Chem. *271*, 3328-3332.

Rothman,J.E., Warren,G. (1994). Implications of the SNARE hypothesis for intracellular membrane topology and dynamics. Curr.Biol. *4*, 220-233.

Rubin,C.S., Hirsch,A., Fung,C., Rosen,O.M. (1978). Development of hormone receptors and hormonal responsiveness in vitro. Insulin receptors and insulin sensitivity in the preadipocyte and adipocyte forms of 3T3-L1 cells. J.Biol.Chem. *253*, 7570-7578.

Russell,W.C. (2000). Update on adenovirus and its vectors. J.Gen.Virol. *81*, 2573-2604.

Rutledge,E.A., Gaston,I., Root,B.J., McGraw,T.E., Enns,C.A. (1998). The transferrin receptor cytoplasmic domain determines its rate of transport through the biosynthetic pathway and its susceptibility to cleavage early in the pathway. J.Biol.Chem. *273*, 12169-12175.

Sakaue,H., Ogawa,W., Takata,M., Kuroda,S., Kotani,K., Matsumoto,M., Sakaue,M., Nishio,S., Ueno,H., Kasuga,M. (1997). Phosphoinositide 3-kinase is required for insulin-induced but not for growth hormone- or hyperosmolarity-induced glucose uptake in 3T3-L1 adipocytes. Mol.Endocrinol. *11*, 1552-1562.

Scales,S.J., Chen,Y.A., Yoo,B.Y., Patel,S.M., Doung,Y.C., Scheller,R.H. (2000). SNAREs contribute to the specificity of membrane fusion. Neuron *26*, 457-464.

Scales,S.J., Yoo,B.Y., Scheller,R.H. (2001). The ionic layer is required for efficient dissociation of the SNARE complex by alpha-SNAP and NSF. Proc.Natl.Acad.Sci.U.S.A *98*, 14262-14267.

Shepherd,P.R., Kahn,B.B. (1999). Glucose transporters and insulin action--implications for insulin resistance and diabetes mellitus. N.Engl.J.Med. *341*, 248-257.

Shibasaki,Y., Asano,T., Lin,J.L., Tsukuda,K., Katagiri,H., Ishihara,H., Yazaki,Y., Oka,Y. (1992). Two glucose transporter isoforms are sorted differentially and are expressed in distinct cellular compartments. Biochem.J. *281 (Pt 3)*, 829-834.

Shimazaki,Y., Nishiki,T., Omori,A., Sekiguchi,M., Kamata,Y., Kozaki,S., Takahashi,M. (1996). Phosphorylation of 25-kDa synaptosome-associated protein. Possible involvement in protein kinase C-mediated regulation of neurotransmitter release. J.Biol.Chem. *271*, 14548-14553.

Simonsen,A., Bremnes,B., Ronning,E., Aasland,R., Stenmark,H. (1998). Syntaxin-16, a putative Golgi t-SNARE. Eur.J.Cell Biol. *75*, 223-231.

Simonsen,A., Gaullier,J.M., D'Arrigo,A., Stenmark,H. (1999). The Rab5 effector EEA1 interacts directly with syntaxin-6. J.Biol.Chem. *274*, 28857-28860.

Simpson,F., Bright,N.A., West,M.A., Newman,L.S., Darnell,R.B., Robinson,M.S. (1996). A novel adaptor-related protein complex. J.Cell Biol. *133*, 749-760.

Simpson,F., Whitehead,J.P., James,D.E. (2001). GLUT4-at the cross roads between membrane trafficking and signal transduction. Traffic. *2*, 2-11.

Slot,J.W., Garruti,G., Martin,S., Oorschot,V., Posthuma,G., Kraegen,E.W., Laybutt,R., Thibault,G., James,D.E. (1997). Glucose transporter (GLUT-4) is targeted to secretory granules in rat atrial cardiomyocytes. J.Cell Biol. *137*, 1243-1254.

Slot,J.W., Geuze,H.J., Gigengack,S., James,D.E., Lienhard,G.E. (1991a). Translocation of the glucose transporter GLUT4 in cardiac myocytes of the rat. Proc.Natl.Acad.Sci.U.S.A *88*, 7815-7819.

Slot,J.W., Geuze,H.J., Gigengack,S., Lienhard,G.E., James,D.E. (1991b). Immuno-localization of the insulin regulatable glucose transporter in brown adipose tissue of the rat. J.Cell Biol. *113*, 123-135.

Sollner,T., Whiteheart,S.W., Brunner,M., Erdjument-Bromage,H., Geromanos,S., Tempst,P., Rothman,J.E. (1993). SNAP receptors implicated in vesicle targeting and fusion. Nature *362*, 318-324.

Springer,S., Spang,A., Schekman,R. (1999). A primer on vesicle budding. Cell *97*, 145-148.

St Denis,J.F., Cabaniols,J.P., Cushman,S.W., Roche,P.A. (1999). SNAP-23 participates in SNARE complex assembly in rat adipose cells. Biochem.J. *338 (Pt 3)*, 709-715.

Steegmaier,M., Klumperman,J., Foletti,D.L., Yoo,J.S., Scheller,R.H. (1999). Vesicle-associated membrane protein 4 is implicated in trans-Golgi network vesicle trafficking. Mol.Biol.Cell *10*, 1957-1972.

Steegmaier,M., Oorschot,V., Klumperman,J., Scheller,R.H. (2000). Syntaxin 17 is abundant in steroidogenic cells and implicated in smooth endoplasmic reticulum membrane dynamics. Mol.Biol.Cell *11*, 2719-2731.

Steegmaier,M., Yang,B., Yoo,J.S., Huang,B., Shen,M., Yu,S., Luo,Y., Scheller,R.H. (1998). Three novel proteins of the syntaxin/SNAP-25 family. J.Biol.Chem. *273*, 34171-34179.

Steinmark,H., Olkkonen,V.M. (2001). The Rab GTPase family. Genome Biol. *2*, REVIEWS3007.

Stoorvogel,W., Oorschot,V., Geuze,H.J. (1996). A novel class of clathrin-coated vesicles budding from endosomes. J.Cell Biol. *132*, 21-33.

Subramaniam,V.N., Loh,E., Horstmann,H., Habermann,A., Xu,Y., Coe,J., Griffiths,G., Hong,W. (2000). Preferential association of syntaxin 8 with the early endosome. J.Cell Sci. *113 (Pt 6)*, 997-1008.

Sudlow,A.W., McFerran,B.W., Bodill,H., Barnard,R.J., Morgan,A., Burgoyne,R.D. (1996). Similar effects of alpha- and beta-SNAP on Ca(2+)-regulated exocytosis. FEBS Lett. *393*, 185-188.

Sumitani,S., Ramlal,T., Liu,Z., Klip,A. (1995). Expression of syntaxin 4 in rat skeletal muscle and rat skeletal muscle cells in culture. Biochem.Biophys.Res.Commun. *213*, 462-468.

Sutton,R.B., Fasshauer,D., Jahn,R., Brunger,A.T. (1998). Crystal structure of a SNARE complex involved in synaptic exocytosis at 2.4 A resolution. Nature *395*, 347-353.

Suzuki,K., Kono,T. (1980). Evidence that insulin causes translocation of glucose transport activity to the plasma membrane from an intracellular storage site. Proc.Natl.Acad.Sci.U.S.A *77*, 2542-2545.

Tamori,Y., Kawanishi,M., Niki,T., Shinoda,H., Araki,S., Okazawa,H., Kasuga,M. (1998). Inhibition of insulin-induced GLUT4 translocation by Munc18c through interaction with syntaxin4 in 3T3-L1 adipocytes. J.Biol.Chem. *273*, 19740-19746.

Tang,B.L., Hong,W. (1999). A possible role of di-leucine-based motifs in targeting and sorting of the syntaxin family of proteins. FEBS Lett. *446*, 211-212.

Tang,B.L., Low,D.Y., Lee,S.S., Tan,A.E., Hong,W. (1998a). Molecular cloning and localization of human syntaxin 16, a member of the syntaxin family of SNARE proteins. Biochem.Biophys.Res.Commun. *242*, 673-679.

Tang,B.L., Low,D.Y., Tan,A.E., Hong,W. (1998b). Syntaxin 10: a member of the syntaxin family localized to the trans- Golgi network. Biochem.Biophys.Res.Commun. *242*, 345-350.

Tang,B.L., Tan,A.E., Lim,L.K., Lee,S.S., Low,D.Y., Hong,W. (1998c). Syntaxin 12, a member of the syntaxin family localized to the endosome. J.Biol.Chem. *273*, 6944-6950.

Tanner,L.I., Lienhard,G.E. (1987). Insulin elicits a redistribution of transferrin receptors in 3T3-L1 adipocytes through an increase in the rate constant for receptor externalization. J.Biol.Chem. *262*, 8975-8980.

Tellam,J.T., Macaulay,S.L., McIntosh,S., Hewish,D.R., Ward,C.W., James,D.E. (1997). Characterization of Munc-18c and syntaxin-4 in 3T3-L1 adipocytes. Putative role in insulin-dependent movement of GLUT-4. J.Biol.Chem. *272*, 6179-6186.

Teng,F.Y., Wang,Y., Tang,B.L. (2001). The syntaxins. Genome Biol. *2*, REVIEWS3012.

Thoreau,V., Berges,T., Callebaut,I., Guillier-Gencik,Z., Gressin,L., Bernheim,A., Karst,F., Mornon,J.P., Kitzis,A., Chomel,J.C. (1999). Molecular cloning, expression analysis, and chromosomal localization of human syntaxin 8 (STX8). Biochem.Biophys.Res.Commun. *257*, 577-583.

Thurmond,D.C., Ceresa,B.P., Okada,S., Elmendorf,J.S., Coker,K., Pessin,J.E. (1998). Regulation of insulin-stimulated GLUT4 translocation by Munc18c in 3T3L1 adipocytes. J.Biol.Chem. *273*, 33876-33883.

Timmers,K.I., Clark,A.E., Omatsu-Kanbe,M., Whiteheart,S.W., Bennett,M.K., Holman,G.D., Cushman,S.W. (1996). Identification of SNAP receptors in rat adipose cell membrane fractions and in SNARE complexes co-immunoprecipitated with epitope-tagged N- ethylmaleimide-sensitive fusion protein. Biochem.J. *320 (Pt 2)*, 429-436.

Tooze,S.A., Martens,G.J., Huttner,W.B. (2001). Secretory granule biogenesis: rafting to the SNARE. Trends Cell Biol. *11*, 116-122.

Torrejon-Escribano,B., Gomez,d.A., I, Blasi,J. (2002). SNARE expression and distribution during 3T3-L1 adipocyte differentiation. FEBS Lett. *512*, 275-281.

Traub,L.M., Kornfeld,S. (1997). The trans-Golgi network: a late secretory sorting station. Curr.Opin.Cell Biol. *9*, 527-533.

Trayhurn,P., Beattie,J.H. (2001). Physiological role of adipose tissue: white adipose tissue as an endocrine and secretory organ. Proc.Nutr.Soc. *60*, 329-339.

Trimble,W.S., Cowan,D.M., Scheller,R.H. (1988). VAMP-1: a synaptic vesicle-associated integral membrane protein. Proc.Natl.Acad.Sci.U.S.A *85*, 4538-4542.

Valdez,A.C., Cabaniols,J.P., Brown,M.J., Roche,P.A. (1999). Syntaxin 11 is associated with SNAP-23 on late endosomes and the trans- Golgi network. J.Cell Sci. *112 (Pt 6)*, 845-854.

Verhage,M., Maia,A.S., Plomp,J.J., Brussaard,A.B., Heeroma,J.H., Vermeer,H., Toonen,R.F., Hammer,R.E., van den Berg,T.K., Missler,M., Geuze,H.J., Sudhof,T.C. (2000). Synaptic assembly of the brain in the absence of neurotransmitter secretion. Science *287*, 864-869.

Verhey,K.J., Hausdorff,S.F., Birnbaum,M.J. (1993). Identification of the carboxy terminus as important for the isoform- specific subcellular targeting of glucose transporter proteins. J.Cell Biol. *123*, 137-147.

Volchuk,A., Mitsumoto,Y., He,L., Liu,Z., Habermann,E., Trimble,W., Klip,A. (1994). Expression of vesicle-associated membrane protein 2 (VAMP- 2)/synaptobrevin II and cellubrevin in rat skeletal muscle and in a muscle cell line. Biochem.J. *304 (Pt 1)*, 139-145.

Volchuk,A., Sargeant,R., Sumitani,S., Liu,Z., He,L., Klip,A. (1995). Cellubrevin is a resident protein of insulin-sensitive GLUT4 glucose transporter vesicles in 3T3-L1 adipocytes. J.Biol.Chem. *270*, 8233-8240.

Volchuk,A., Wang,Q., Ewart,H.S., Liu,Z., He,L., Bennett,M.K., Klip,A. (1996). Syntaxin 4 in 3T3-L1 adipocytes: regulation by insulin and participation in insulin-dependent glucose transport. Mol.Biol.Cell *7*, 1075-1082.

von Mollard,G.F., Nothwehr,S.F., Stevens,T.H. (1997). The yeast v-SNARE Vti1p mediates two vesicle transport pathways through interactions with the t-SNAREs Sed5p and Pep12p. J.Cell Biol. *137*, 1511-1524.

Wade,N., Bryant,N.J., Connolly,L.M., Simpson,R.J., Luzio,J.P., Piper,R.C., James,D.E. (2001). Syntaxin 7 complexes with mouse Vps10p tail interactor 1b, syntaxin 6, vesicle-associated membrane protein (VAMP)8, and VAMP7 in b16 melanoma cells. J.Biol.Chem. *276*, 19820-19827.

Wang,G., Witkin,J.W., Hao,G., Bankaitis,V.A., Scherer,P.E., Baldini,G. (1997). Syndet is a novel SNAP-25 related protein expressed in many tissues. J.Cell Sci. *110 (Pt 4)*, 505-513.

Waters,M.G., Hughson,F.M. (2000). Membrane tethering and fusion in the secretory and endocytic pathways. Traffic. *1*, 588-597.

Watson,R.T., Pessin,J.E. (2000). Functional cooperation of two independent targeting domains in syntaxin 6 is required for its efficient localization in the trans-golgi network of 3T3L1 adipocytes. J.Biol.Chem. *275*, 1261-1268.

Watson,R.T., Pessin,J.E. (2001). Subcellular compartmentalization and trafficking of the insulin- responsive glucose transporter, GLUT4. Exp.Cell Res. *271*, 75-83.

Weber,T., Zemelman,B.V., McNew,J.A., Westermann,B., Gmachl,M., Parlati,F., Sollner,T.H., Rothman,J.E. (1998). SNAREpins: minimal machinery for membrane fusion. Cell *92*, 759-772.

Wei,M.L., Bonzelius,F., Scully,R.M., Kelly,R.B., Herman,G.A. (1998). GLUT4 and transferrin receptor are differentially sorted along the endocytic pathway in CHO cells. J.Cell Biol. *140*, 565-575.

Weimbs,T., Low,S.H., Chapin,S.J., Mostov,K.E., Bucher,P., Hofmann,K. (1997). A conserved domain is present in different families of vesicular fusion proteins: a new superfamily. Proc.Natl.Acad.Sci.U.S.A *94*, 3046-3051.

Wendler,F., Tooze,S. (2001). Syntaxin 6: the promiscuous behaviour of a SNARE protein. Traffic. *2*, 606-611.

White,M.F. (1998). The IRS-signalling system: a network of docking proteins that mediate insulin action. Mol.Cell Biochem. *182*, 3-11.

Whiteheart,S.W., Griff,I.C., Brunner,M., Clary,D.O., Mayer,T., Buhrow,S.A., Rothman,J.E. (1993). SNAP family of NSF attachment proteins includes a brain-specific isoform. Nature *362*, 353-355.

Wilson,D.W., Wilcox,C.A., Flynn,G.C., Chen,E., Kuang,W.J., Henzel,W.J., Block,M.R., Ullrich,A., Rothman,J.E. (1989). A fusion protein required for vesicle-mediated transport in both mammalian cells and yeast. Nature *339*, 355-359.

Wong,P.P., Daneman,N., Volchuk,A., Lassam,N., Wilson,M.C., Klip,A., Trimble,W.S. (1997). Tissue distribution of SNAP-23 and its subcellular localization in 3T3- L1 cells. Biochem.Biophys.Res.Commun. *230*, 64-68.

Wong,S.H., Xu,Y., Zhang,T., Hong,W. (1998). Syntaxin 7, a novel syntaxin member associated with the early endosomal compartment. J.Biol.Chem. *273*, 375-380.

Woodman,P.G. (2000). Biogenesis of the sorting endosome: the role of Rab5. Traffic. *1*, 695-701.

Wu,M.N., Littleton,J.T., Bhat,M.A., Prokop,A., Bellen,H.J. (1998a). ROP, the Drosophila Sec1 homolog, interacts with syntaxin and regulates neurotransmitter release in a dosage-dependent manner. EMBO J. *17* , 127-139.

Wu,Z., Xie,Y., Morrison,R.F., Bucher,N.L., Farmer,S.R. (1998b). PPARgamma induces the insulin-dependent glucose transporter GLUT4 in the absence of C/EBPalpha during the conversion of 3T3 fibroblasts into adipocytes. J.Clin.Invest *101*, 22-32.

Xu,D., Joglekar,A.P., Williams,A.L., Hay,J.C. (2000). Subunit structure of a mammalian ER/Golgi SNARE complex. J.Biol.Chem. *275*, 39631-39639.

Yamauchi,T., Kamon,J., Waki,H., Terauchi,Y., Kubota,N., Hara,K., Mori,Y., Ide,T., Murakami,K., Tsuboyama-Kasaoka,N., Ezaki,O., Akanuma,Y., Gavrilova,O., Vinson,C., Reitman,M.L., Kagechika,H., Shudo,K., Yoda,M., Nakano,Y., Tobe,K., Nagai,R., Kimura,S., Tomita,M., Froguel,P., Kadowaki,T. (2001). The fat-derived hormone adiponectin reverses insulin resistance associated with both lipoatrophy and obesity. Nat.Med. *7*, 941-946.

Yang,B., Gonzalez,L., Jr., Prekeris,R., Steegmaier,M., Advani,R.J., Scheller,R.H. (1999). SNARE interactions are not selective. Implications for membrane fusion specificity. J.Biol.Chem. *274*, 5649-5653.

Yang,C., Coker,K.J., Kim,J.K., Mora,S., Thurmond,D.C., Davis,A.C., Yang,B., Williamson,R.A., Shulman,G.I., Pessin,J.E. (2001). Syntaxin 4 heterozygous knockout mice develop muscle insulin resistance. J.Clin.Invest *107*, 1311-1318.

Yang,C.Z., Mueckler,M. (1999). ADP-ribosylation factor 6 (ARF6) defines two insulin-regulated secretory pathways in adipocytes. J.Biol.Chem. *274*, 25297-25300.

Yang,J., Clark,A.E., Harrison,R., Kozka,I.J., Holman,G.D. (1992). Trafficking of glucose transporters in 3T3-L1 cells. Inhibition of trafficking by phenylarsine oxide implicates a slow dissociation of transporters from trafficking proteins. Biochem.J. *281 (Pt 3)*, 809-817.

Yang,J., Holman,G.D. (1993). Comparison of GLUT4 and GLUT1 subcellular trafficking in basal and insulin-stimulated 3T3-L1 cells. J.Biol.Chem. *268*, 4600-4603.

Zeigerer,A., Lampson,M.A., Karylowski,O., Sabatini,D.D., Adesnik,M., Ren,M., McGraw,T.E. (2002). GLUT4 Retention in Adipocytes Requires Two Intracellular Insulin- regulated Transport Steps. Mol.Biol.Cell *13*, 2421-2435.

Zeng,Q., Subramaniam,V.N., Wong,S.H., Tang,B.L., Parton,R.G., Rea,S., James,D.E., Hong,W. (1998). A novel synaptobrevin/VAMP homologous protein (VAMP5) is increased during in vitro myogenesis and present in the plasma membrane. Mol.Biol.Cell *9*, 2423-2437.

Zerial,M., McBride,H. (2001). Rab proteins as membrane organizers. Nat.Rev.Mol.Cell Biol. *2*, 107-117.

Zierath,J.R., He,L., Guma,A., Odegoard,W.E., Klip,A., Wallberg-Henriksson,H. (1996). Insulin action on glucose transport and plasma membrane GLUT4 content in skeletal muscle from patients with NIDDM. Diabetologia *39*, 1180-1189.

Appendix

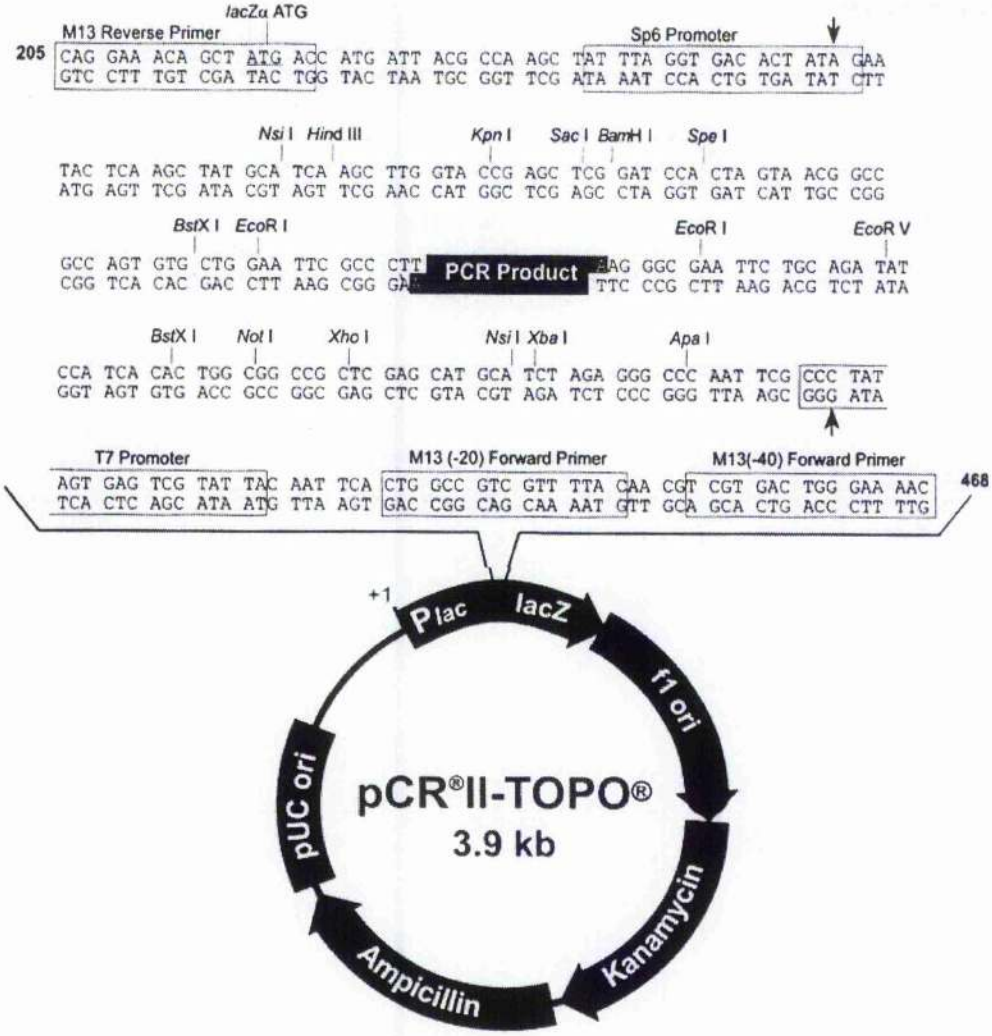

pCRII vector for TA cloning

The PCR product is cloned into the cloning site located in between two *EcoR* I sites of the vector (shown in the figure) by TA cloning. Prior to cloning PCR product is subjected to *Taq* polymerase amplification to add a single deoxyadenosine (A) to its 3' ends. The linearised vector contains overhanging 3' deoxythymidine (T) residues to allow the PCR insert to ligate efficiently with the vector. Multiple cloning sites are found between the bases 269-299.

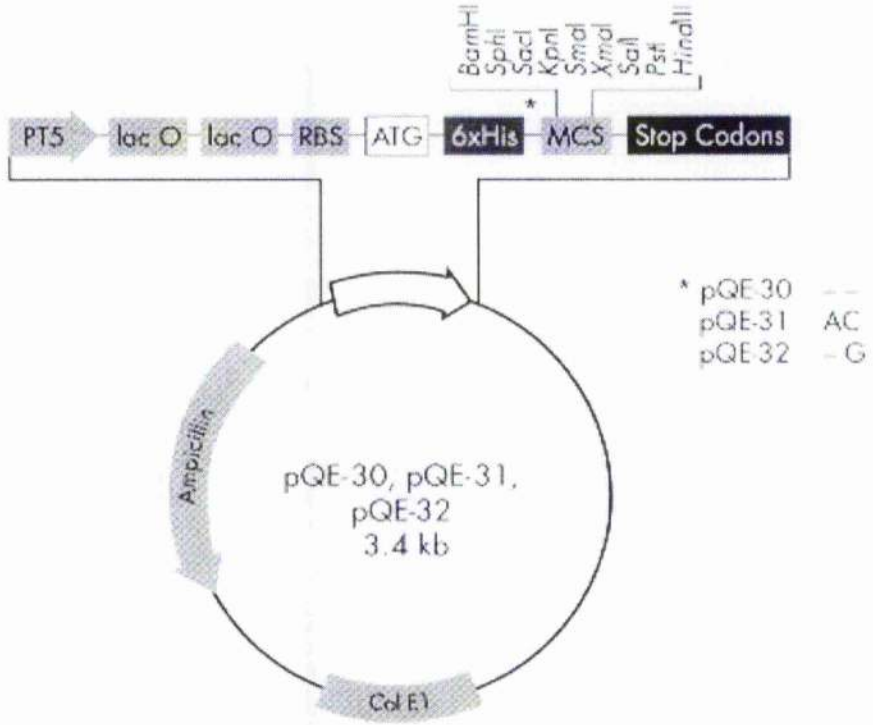

pQE-30 vector for N-terminal 6xHis tag constructs

This vector is used to add N-terminal 6xHis tag to the recombinant protein in order to purify it efficiently using Ni-NTA. After ligating the insert with pQE-30 vector it is transformed into M15 cells or other host strain carrying the pREP4 repressor plasmid to ensure production of lac repressor protein. (Lac repressor binds to operator sequence and tightly regulates the recombinant protein expression. The inducing agent IPTG binds to lac repressor and inactivates it.)

PT5- T5 promoter; lac O- lac operator; RBS- ribosome-binding site; ATG- start codon; 6xHis- 6xHis tag sequence; MCS- multiple cloning site (restriction sites are indicated); Stop codon; Col E1- Col E1 origin of replication; Ampicillin- ampicillin resistance gene.

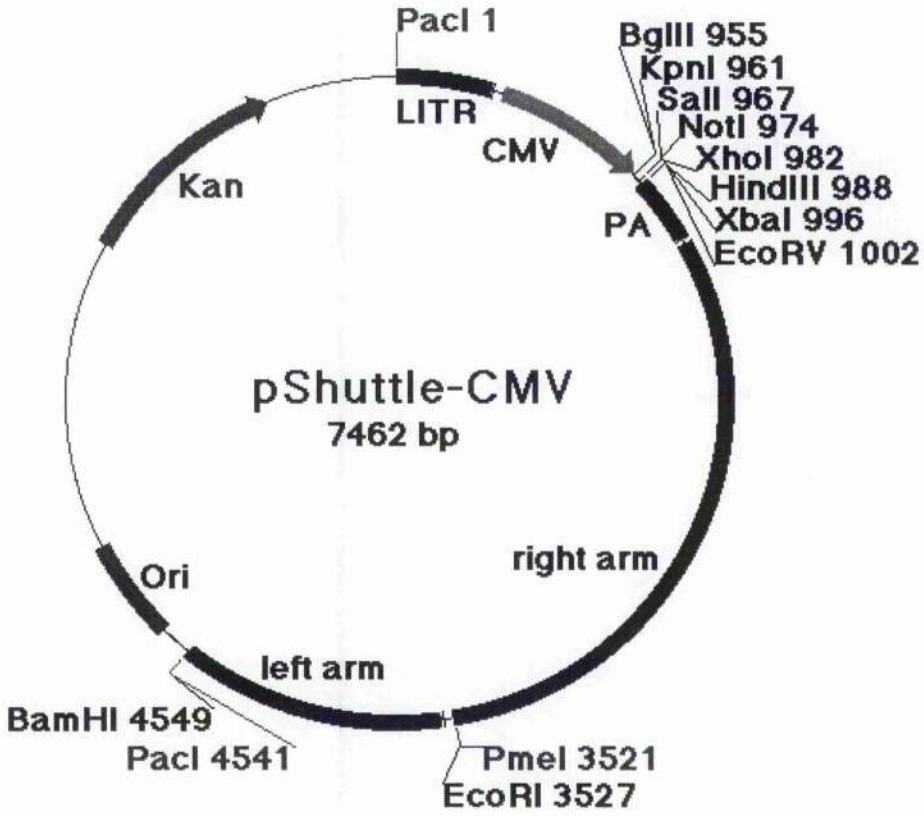

pShuttle-CMV vector

pShuttle-CMV is used as the transfer vector to incorporate the DNA insert into adenoviral backbone. Insert is cloned into multiple cloning site (in between CMV promoter and polyadenylation signal (PA)) sequence of pShuttle-CMV and the cassette is subsequently cloned into pAdEasy (adenoviral vector) by homologous recombination. There are two regions which are homologous to adenoviral sequence which allow the homologous recombination (left arm and right arm). Expression of the gene of interest will be under the control of CMV promoter.

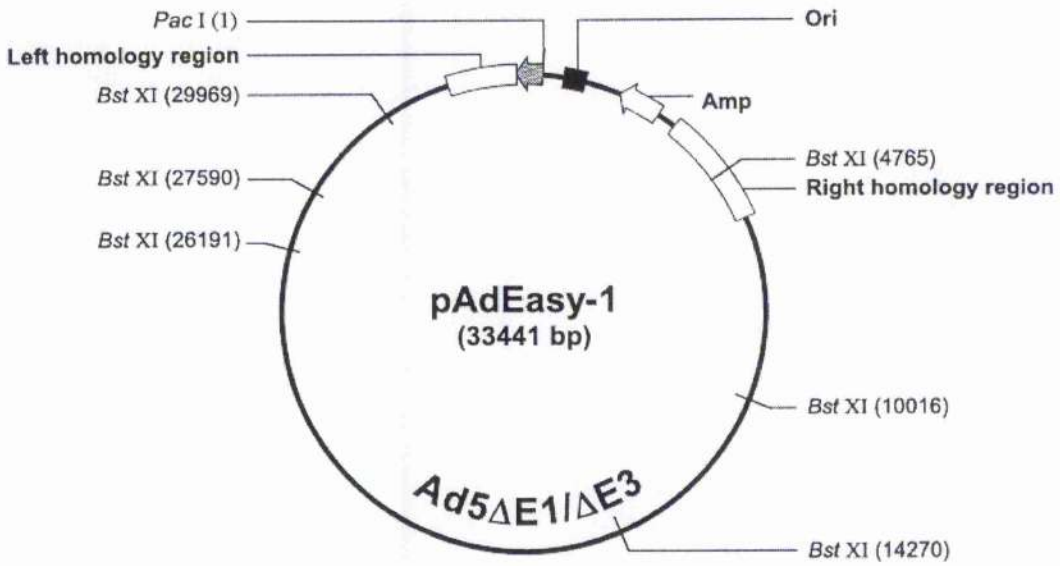

pAdEasy-1

pAdEasy-1 is a 33.4 kb plasmid containing the adenovirus serotype 5 (Ad5) genome with deletions in E1 and E3 regions. The pShuttle-CMV carrying the gene of interest is cloned into the E1 region of pAdEasy by homologous recombination. The pShuttle-CMV carries two homologous regions (arms) which have similar sequences to AdV left and right homology regions to allow homologous recombination. Adenovirus expressing the desired gene product is produced upon transfection of the recombinant plasmid into HEK 293 cells.